The Development of Small Molecule Inhibitors
for Fibrosis Drug Discovery

Lisa Margaret Miller

November 2016

The Development of Small Molecule Inhibitors

for Fibrosis Drug Discovery

Thesis submitted to the University of Strathclyde in fulfilment of the

requirements for the degree of Doctor of Philosophy

By

Lisa Margaret Miller

2016

Declaration of Copyright

This thesis is a result of the author's original research. It has been composed by the author and has not been previously submitted for examination which has led to the award of a degree.

The copyright of this thesis belongs to the author under the terms of the United Kingdom Copyright Acts as qualified by University of Strathclyde Regulation 3.50. Due acknowledgement must always be made of the use of any material contained in, or derived from, this thesis.

Signed:

Date: November 2016

Publication List

1. Structure-activity Relationships of Small Molecule Autotaxin Inhibitors with a Discrete Binding Mode.

   Lisa M. Miller, Willem-Jan Keune, Diana Castagna, Louise C. Young, Emma L. Duffy, Frances Potjewyd, Fernando Salgado-Polo, Paloma E. Garcia, Dima Semaan, John M. Pritchard, Anastassis Perrakis, Simon J. F. Macdonald, Craig Jamieson, and Allan J. B. Watson

   J. Med. Chem., **2017**, *60*, 722–748.

2. The Emergence of Small Molecule Non-RGD-mimetic Inhibitors for RGD Integrins

   Lisa M. Miller, John M. Pritchard, Simon J. F. Macdonald, Craig Jamieson, and Allan J. B. Watson

   DOI: 10.1021/acs.jmedchem.6b01711

3. A Quantitative Assessment of Reaction Variable on Racemisation During Amide Coupling of α-Amino Acids

   Diana Castagna, Lisa M. Miller, Amy A. Ott, Craig Jamieson, and Allan J. B. Watson

   Manuscript in preparation.

4. PF-8380 Structure-activity Relationships and the Development of Novel Autotaxin Inhibitors

   Frances Potjewyd, Emma L. Duffy, Willem-Jan Keune, Jennifer Clark, Louise C. Young, Susana Wood, Diana Castagna, Lisa M. Miller, John M. Pritchard, Simon J. F. Macdonald, Anastassis Perrakis, Allan. J. B. Watson, and Craig Jamieson

   Manuscript in preparation.

Abstract

Fibrotic diseases can be attributed to approximately 45% of deaths within western developed countries. This category of disease can affect nearly every tissue in the body, predominantly liver, kidney, and lung. The severity of fibrotic diseases is widely recognised but currently there is no accepted effective disease modifying treatment. There have been a number of potential drug targets identified in recent years, including the enzyme autotaxin (ATX) and the RGD integrins, which are known to play a key role in the pathogenesis. In collaboration with GlaxoSmithKline, the projects detailed in this report were aimed to develop small molecule inhibitors with druglike physicochemical properties for fibrosis drug discovery.

Chapter 1 focusses on the secreted enzyme ATX, which is responsible for the hydrolysis of lysophosphatidylcholine (LPC) to the bioactive lysophosphatidic acid (LPA) and choline. The ATX-LPA signalling pathway is implicated in cell survival, migration, and proliferation; thus, the inhibition of ATX is a recognised therapeutic target for a number of diseases including fibrotic diseases, cancer, and inflammation, amongst others. Many of the developed synthetic inhibitors for ATX have resembled the lipid chemotype of the native ligand; however, a small number of inhibitors have been described that deviate from this common scaffold. Herein, Chapter 1 details the structure-activity relationship (SAR) exploration of a previously reported small molecule ATX inhibitor through the design, synthesis, and biological evaluation of a series of analogues. Furthermore, using enzyme kinetics studies it is shown that

analogues of this chemotype are noncompetitive inhibitors, and using a crystal structure with ATX the discrete binding mode was confirmed. This work has provided valuable insight into the binding of this chemotype, which could aid the design of novel ATX inhibitors with non-lipid-like scaffolds.

Chapter 2 describes a lead-optimisation project targeting the RGD subfamily of the integrin receptors. The RGD integrins are recognised therapeutic targets for thrombosis, fibrosis, and cancer, amongst others. Current inhibitors are designed to mimic the tripeptide sequence of the natural ligands (arginine-glycine-aspartic acid); however, the RGD-mimetic antagonists for one particular RGD integrin ($\alpha_{IIb}\beta_3$) have been shown to cause partial agonism, leading to the opposite pharmacological effect. The challenge of obtaining oral activity and synthetic tractability with RGD-mimetic molecules, along with the issues relating to pharmacology, has left integrin-therapeutics in need of a new strategy. Recently, a new generation of inhibitor has emerged that lacks the RGD-mimetic. The work detailed herein aimed to build on this emerging area, with the design, synthesis, and biological evaluation of novel small molecule inhibitors targeting the $\alpha_v\beta_3$ integrin. These compounds are shown to be accessed via synthetically divergent routes, allowing for the quick exploration of a diverse set of potential lead compounds. Initial efforts led to the identification of four promising lead-like inhibitors with pIC_{50} values ranging from 4.1-5.5 for the target integrin $\alpha_v\beta_3$. Unfortunately, the initial hit compound, that the subsequent compound design stemmed from, was later determined to be a false positive, and as a result work on the project ceased. Thus, Chapter 2 details a project that was mis-led due to false positive assay results.

Acknowledgements

First and foremost I would like to thank my supervisor Dr Allan Watson for his insight and support throughout my PhD. I would also like to express my appreciation to my second supervisor Dr Craig Jamieson for his invaluable guidance in the biological areas of the projects. I would like to acknowledge the other members of the original Team Fibrosis: Diana Castagna, Emma Duffy, and Frances Potjewyd for their comradery throughout the ATX work. In addition, I would like to thank the other members of the Watson and Jamieson lab groups, past and present, for the limitless entertainment in the lab.

Furthermore, I would like to thank Dr Willem-Jan Keune at the Netherlands Cancer Institute for the time and effort that went into the running of the ATX assays, as well as his assistance during my placement at NKI. I would also like to thank Craig Irving for his help throughout my research. I am grateful to GSK for their funding in this collaborative project, and would like to acknowledge Dr Simon Macdonald and John Pritchard for their contributions.

Finally, I would like to thank Christian Stevenson as well as my friends and family for their invaluable support and encouragement throughout my research.

Abbreviations

ABTS	2,2'-Azinobis(3-ethylbenzothiazoline-6-sulfonic acid
AcO	Acetate
ADMET	Absorption, distribution, metabolism, excretion, and toxicity
Aq.	Aqueous
Ar	Aryl
ATX	Autotaxin
Bis-pNPP	Bis(p-nitrophenyl) phosphate
Bn	Benzyl
Bpin	Pinacol boronic ester
Boc	*tert*-Butyloxycarbonyl
CSD	Cambridge Structural Database
DCM	Dichloromethane
DIAD	Diisopropyl azodicarboxylate
DIPEA	*N,N*-Diisopropylethylamine
DMAP	4-Dimethylaminopyridine
DMSO	Dimethyl sulfoxide
Dppf	1,1'-Bis(diphenylphosphino)ferrocene
ECM	Extracellular martix
EDG	Endothelial differentiation G-protein-coupled
ENPP	Ectonucleotide pyrophosphatase and phosphodiesterase
Eq	Equation
Equiv.	Equivalent(s)
Et	Ethyl
EU	European Union
FDA	Food and Drug Administration
FRET	Förster fluorescence resonance energy transfer
FTIR	Fourier transformed infra-red
GPCR	G-protein-coupled receptor
GSK	GlaxoSmithKline
HAC	Heavy atom count
hATX	Human autotaxin

HBA	Hydrogen bond acceptor
HBD	Hydrogen bond donator
hERG	Human ether-a-go-go related gene
HPLC	High-performance/high-pressure liquid chromatography
HpH	High pH
HRP	Horseradish peroxidase
HTS	High-throughput screening
HVA	Homovanillic acid
ILD	Interstitial lung disease
IPA	Isopropyl alcohol
IPF	Idiopathic pulmonary fibrosis
*i*Pr	Isopropyl
LCMS	Liquid chromatography-mass spectrometry
LE	Ligand efficiency
LEI	Ligand efficiency index
LIDIA	Ligand display for interaction and analysis
LLE	Ligand lipophilicity efficiency
LogP	Partition coefficient
LPA	Lysophosphatidic acid
LPC	Lysophosphatidylcholine
LpH	Low pH
m	*Meta*
m-CPBA	*m*-Chloroperbenzoic acid
Me	Methyl
MIDA	Metal-ion-dependent adhesion site
MTBE	Methyl *tert*-butyl ether
MTS	Medium-throughput screening
MW	Molecular weight
NMR	Nuclear magnetic resonance
NT	Not tested
NUC	Nuclease-like domain
o	*Ortho*
p	*Para*

PAINS	Pan-assay interference compounds
PDE	Phosphodiesterase
PFI	Property forecast index
Ph	Phenyl
*p*NP-TMP	Thymidine 5'-mono-phosphate *p*-nitrophenyl ester
ppm	Parts per million
PPTS	Pyridinium *p*-toluenesulfonate
PSA	Polar surface area
rATX	Rat autotaxin
RGD	Arginine-glycine-aspartic acid
RT	Room temperature
SAR	Structure-activity relationship
Sat.	Saturated
SCX	Strong cation exchange
SIPBS	Strathclyde Institute of Pharmacy and Biomolecular Science
SMB	Somatomedin B
T	Temperature
t	Time
*t*Bu	*tert*-Butyl
tert	Tertiary
TFA	Trifluoroacetic acid
TG-*m*TMP	TokyoGreen *m*-thymidine monophosphate
TGF-β	Transforming growth factor β1
THF	Tetrahydrofuran
TLC	Thin layer chromatography
Ts	Tosyl
UV	Ultraviolet

Table of Contents

List of Figures, Schemes, and Tables

Chapter 1

Structure-activity Relationships of Small Molecule Autotaxin Inhibitors with a
Discrete Binding Site

This chapter is based on the published manuscript [ref 73]

1 Chapter 1: Structure-activity Relationships of Small Molecule Autotaxin Inhibitors with a Discrete Binding Site

1.1 Introduction

1.1.1 Fibrotic Disease

Fibrotic diseases are estimated to attribute to 45% of deaths within western developed countries.[1] The severity of this disease category is widely recognised but currently there is no accepted effective disease modifying treatment.[2] Fibrosis effects nearly every tissue in the body; the term "fibrosis" is used to describe a build-up of excess fibrous connective tissue, either within an organ or tissue, as a reparative response. The cells responsible for the production of this connective tissue are fibroblasts and myofibroblasts.[3] Once activated, these cells will synthesise the extracellular matrix and collagen, which are vital components in wound healing, required to repair the structural framework of cells. The normal healing process can evolve into a progressively irreversible fibrotic response if the tissue injury is severe or repetitive or if the tissue repair response becomes dysregulated.[2] An example of a fibrotic disease with a devastating prognosis is that associated with the lung: idiopathic pulmonary fibrosis (IPF), the most common interstitial lung disease (ILD).[4] IPF has a high mortality rate of 50% within 3-5 years after diagnosis and the number of cases diagnosed is increasing each year.[5] Currently the estimated disease prevalence in the European Union (EU) is 120,000 and an additional 40,000 new cases are diagnosed each year.[6] These numbers highlight the growing need for new therapeutic treatments in fibrotic diseases such as IPF.

1.1.2   Autotaxin

Autotaxin (ATX) is a secreted glycoprotein phosphodiesterase belonging to the ectonucleotide pyrophosphatase and phosphodiesterase family (ENPP). ATX is around 100 kDa in size and was first isolated from melanoma cells in 1992.[7] It functions as a lysophospholipase D, mediating the hydrolysis of lysophosphatidylcholine (LPC) **1.1** to the ubiquitous bioactive lipid mediator lysophosphatidic acid (LPA) **1.2** and choline **1.3** (Scheme 1.1).[8]

Scheme 1.1. ATX-mediated hydrolysis of LPC releasing LPA. R group = fatty acid chain with varying degrees of unsaturation.
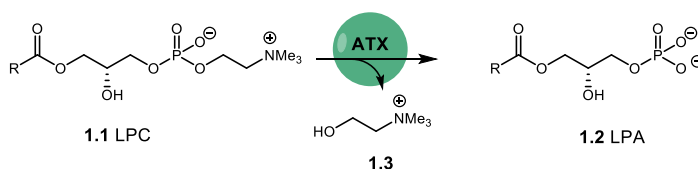
LPA **1.2** is the simplest glycerophospholipid; however, the length and saturation of the phospholipid chain can vary. In terms of stereochemistry, it is the L-(*R*)-enantiomer that is observed *in vivo*, but both the natural isomer and the unnatural D-(*S*)-enantiomer display equal activity when tested in bioassays.[9] Phospholipid **1.2** acts on the LPA receptors; a series of G-protein coupled receptors (GPCRs), of which six have been identified to date, termed LPA$_{1-6}$, with an additional three pending the publication of evidence to verify their categorisation (GPR87, P2Y10, and GPR35).[10] Upon binding, a series of intracellular signaling pathways are invoked which could result in a range of cellular functions including differentiation, migration, proliferation, and survival.[11] Dysregulation of the ATX-LPA signaling pathway is implicated in a variety of disease states and could lead to the development of several diseases including vascularisation diseases, autoimmune diseases, cancer,

fibrotic diseases, inflammation, and neurodegeneration, amongst others (Scheme 1.2).[12-17] Accordingly, the use of ATX inhibitors has been and continues to be an attractive strategy for therapeutic intervention.[18]

Scheme 1.2. Disease states via LPA action on the GPCRs LPA$_{1-6}$. R group = fatty acid chain with varying degrees of unsaturation.

1.2
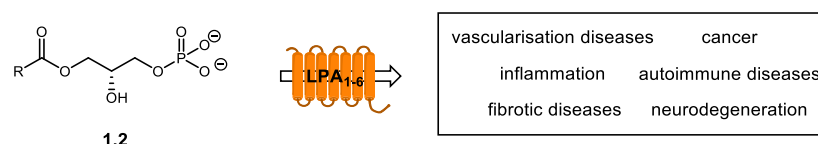
1.1.3 Autotaxin Morphology

The structure of ATX has been studied extensively and the morphology of the active site is well known. The importance of the two zinc ions located in the active site was first reported by Gijsbers *et al*. in 2003.[19] This work identified that these two ions, along with a threonine (T209) residue, were responsible for the enzymatic activity. In 2011, the solved crystal structure of ATX was published simultaneously by two groups, these reports furthered the understanding of active site by ascertaining a hydrophobic pocket which accommodates the long alkyl chain of LPA **1.2**.[20, 21] The active site is accessed via a tunnel which is believed to assist in the selectivity of ATX.[22] As well as the phosphodiesterase (PDE) domain where the catalytic site resides, ATX consists of two N-terminal somatomedin B (SMB) domains, a nuclease-like domain (NUC), and a lasso domain (Figure 1.1a).[22] The principle domain arrangement of two SMB domaine, a PDE domain, and a NUC domain is shared throughout the ENPP1-3 members of the ENPP family. The other four members of this enzyme family, ENPP4-7, only have a PDE domain in common.[23, 24]
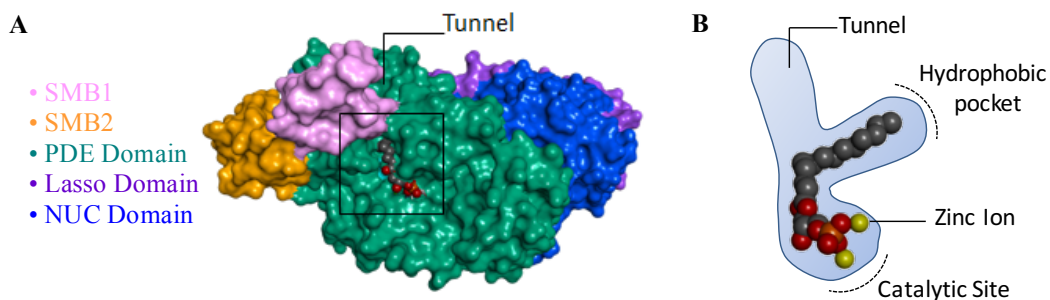
Figure 1.1. Structural features of ATX. **(a)** ATX domains colour coded with the catalytic site highlighted. Image created with ATX-LPA cocrystal (PDB 3NKN) using Discovery Studio Visualiser.[25] **(b)** Key features of the ATX active site "T-junction" with LPA **1.2** bound.

Analysis of crystal structures helped to identify these domains and revealed the high conservation of this arrangement between species, suggesting that the conformation plays a vital role in the enzyme activity.[24] As state previously, the catalytic site is accessed via a tunnel which runs between the hydrophobic pocket and SMB1, forming a "T-junction" with the catalytic site (Figure 1.1b). The tunnel is hypothesised to bind the LPA **1.2** produced and hold it in place for transport to the activated GPCRs by ATX.[21, 24] Although this shuttle mechanism has yet to be proven experimentally, the low concentration of LPA **1.2** found in the plasma does support this hypothesis of localised production. Furthermore, a β3 integrin produced on the cell surface interacts with the SMB2 domain which may induce a conformational change in the enzyme.[21] A conformational change could then assist in the release of LPA **1.2** at the target receptor. This idea of localised production of LPA **1.2** is further supported by a flat surface around the channel entrance which would allow for the close interfacing of the enzyme with the target receptor.

1.1.4 ATX Inhibition Assays
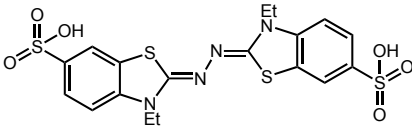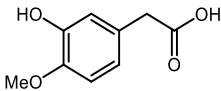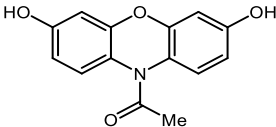
There are a number of *in vitro* assays that are currently used to evaluate ATX activity; these can be divided into two categories based on the type of substrate the assay utilises (Table 1.2). The first category employs the natural ligand **1.1** and the second uses unnatural ATX substrates. As depicted in Scheme 1, ATX hydrolyses **1.1** into **1.2** and **1.3**, thus the enzyme activity can be determined by quantitative measurement of these products using liquid chromatography-tandem mass spectrometry (LCMS),[26] radiometry,[27] colorimetry,[28] or fluorimetry.[19] An example of a more classical method employs ^{14}C labelled LPC **1.2** which when hydrolysed produces a ^{14}C LPA **1.1**.[29] This radiolabelled product can then be isolated and the enzyme activity quantified using radiometry. This assay has the advantage of high sensitivity but is not amenable to high-throughput screening (HTS) which is often required in the early stages of drug discovery. Another assay better suited to the demands of HTS employs LCMS for the fast and accurate measurement of LPA **1.2** produced.[30] Using LCMS the ATX incubation mixture can be assayed and the LC will separate the LPA **1.2** from LPC **1.1** which are then detected by tandem MS. This process can be automated to streamline the screening of large compound libraries against ATX. Of assays based on **1.1**, a commonly used method measures the production of **1.3** using an enzyme-coupled colorimetric assay[28] – choline oxidase converts **1.3** into betaine (**1.4**) and hydrogen peroxide, and then horseradish peroxidase (HRP) utilises the hydrogen peroxide to oxidise a colouring substrate into its chromophoric state (Scheme 1.3).

Scheme 1.3. ATX-mediated choline release assay for ATX inhibition. R group = fatty acid chain with varying degrees of unsaturation.
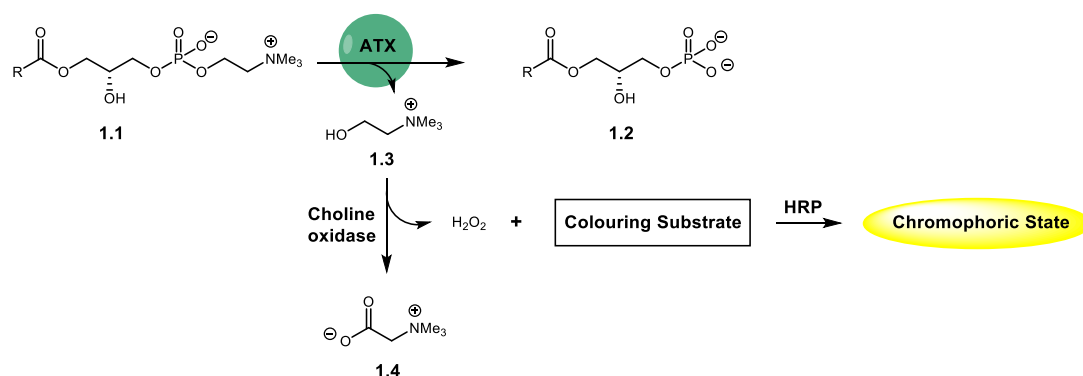
Three exemplar colouring substrates used in this assay and the modes of detection are detailed in Table 1.1. The choline release assay is a high throughput assay and suited to the demands of HTS; however, there is a risk of false positives associated with this assay as the molecules under analysis may inhibit the enzymes used in the colouring reactions.[31] Thus, it is important to use control reactions to reveal any interference. Accordingly, assays that employ synthetic substrates can appear to be advantageous over the LPC choline release assay as they do not require the use of these additional enzymes. There are a number of unnatural substrates widely used, including thymidine 5'-mono-phosphate p-nitrophenyl ester (pNP-TMP) (**1.5**),[8] the Förster resonance energy transfer (FRET) ligand CPF4 (**1.6**),[32] the fluorogenic substrate 3 (FS-3) (**1.7**),[33] and the fluorescence probe TokyoGreen m-thymidine monophosphate (TG-mTMP) (**1.8**).[34] CPF4 (**1.6**) produces fluorescence prior to hydrolysis due to FRET. After hydrolysis the FRET pair is separated and thus the fluorescence is quenched, providing a sensitive readout for ATX activity. Whereas FS-3 (**1.7**) consists of an intramolecular quencher which is removed during hydrolysis and thus the product becomes fluorescent.

Table 1.1. HRP colouring substrates.

Substrate	Structure	Detection
2,2'-azinobis(3-ethylbenzothiazoline-6-sulfonic acid (ABTS) (**1.9**)		Absorbance
Homovanillic acid (HVA) (**1.10**)		Fluorescence
Amplex® red (**1.11**)		Fluorescence

A particularly widely used method employs the unnatural substrate bis(*p*-nitrophenyl) phosphate (bis-*p*NPP) (**1.12**).[35] ATX catalyses the hydrolysis of **1.12** to release 4-nitrophenol **1.13** which, with an absorbance of 405 nm, is readily detected using colorimetry (Scheme 1.4). The popularity of this assay can be attributed to the low cost of this substrate and the direct readout the assay provides.[35] Table 1.2 provides a summary of the substrates for ATX-activity assays detailed in this section.
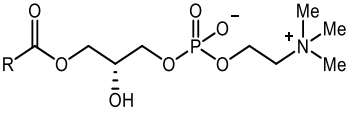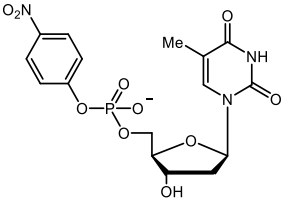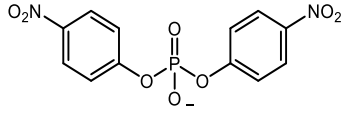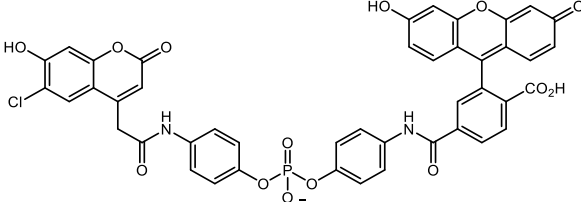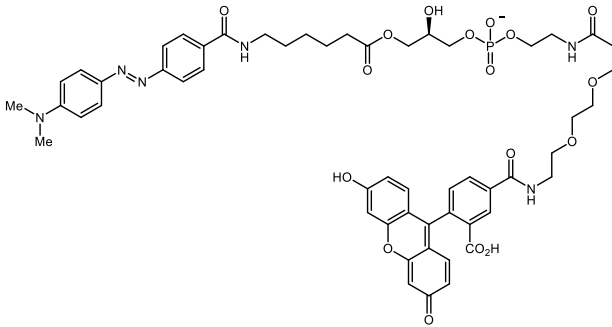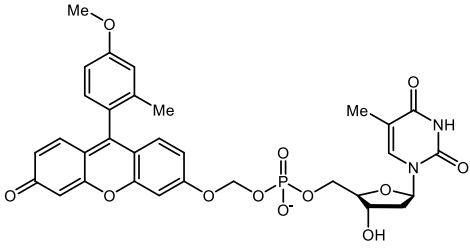
Scheme 1.4. ATX-mediated hydrolysis of bis-*p*NPP **1.12** releasing 4-nitrophenol **1.13**.
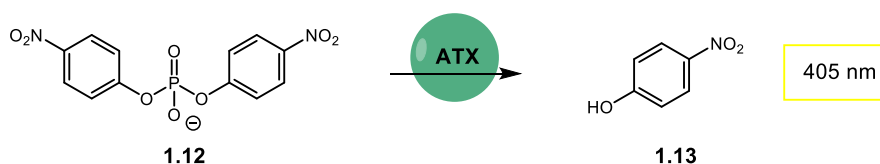
Table 1.2. Summary of ATX activity assays. R group = fatty acid chain with varying degrees of unsaturation.

Substrate	Structure	Analysis
LPC (**1.1**)		LCMS,[26] radiometry,[27] colorimetry,[28] fluorimetry[19]
pNP-TMP (**1.5**)[8]		Absorbance
Bis-*p*NPP (**1.12**)[35]		Absorbance
CPF4 (**1.6**)[32]		FRET
FS-3 (**1.7**)[33]		Fluorescence
TG-*m*TMP (**1.8**)[34]		Fluorescence

1.1.5 Inhibitors of Autotaxin

The first synthetic ATX inhibitors were reported in a 2006 patent detailing the use of the lipid-like compounds to treat cancer.[36] The majority of early ATX inhibitors were analogues of the natural substrate LPC **1.1** or the product LPA **1.2**, thus they resembled lipids with a long lipophilic chain and a polar terminal group (Figure 1.2). Inhibitor **1.14** was the most effective ATX inhibitor reported in this initial patent, reported to have an IC_{50} of 252 nM (Bis-*p*NPP assay).[36] Another study into anticancer treatments reported an α-substituted methylene phosphonate **1.15** analogue of LPA **1.2** as an effective ATX inhibitor with an IC_{50} of 22 nM (FS3 assay).[37] Servier's inhibitor S32826 **1.16** is also an example of a lipid-like ATX inhibitor, with an IC_{50} of 5.6 nM (LPC choline release assay) it was shown to be effective, however the anilinic amide bond resulted in an undesirably short half-life and as a result this compound was not suitable for use in animal models.[38] Although the lipid-like inhibitors exhibited nanomolar potency, their physicochemical properties were not ideal for *in vivo* applications. The high lipophilicity and low solubility of these compounds caused issues in testing,[39] and could have caused further difficulties in later stages of drug development such as formulation.

1.14
252 nM[a]

1.15
22 nM[b]

1.16
5.6 nM[c]
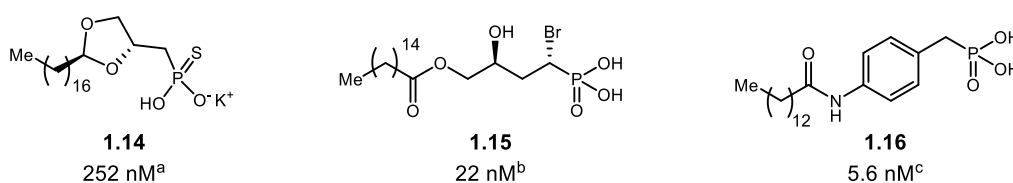
Figure 1.2. Lipid-like ATX inhibitors. [a]Bis-*p*NPP assay. [b]FS3 assay. [c]LPC choline release assay.

Another class of lipid-like inhibitors featuring a piperidine or piperazine motif were discovered by Pfizer and Merck KGA using compound library screening for ATX inhibitors (Figure 1.3). Inhibitor PF-8380 (**1.17**) was reported by Pfizer[40] to have a

low nanomolar IC_{50} of 1.7 nM whereas the Merck KGA compound **1.18** was quoted as have <1 μM activity (both using the LPC choline release assay).[41] Compound **1.17** has been reported to cause a >95% reduction of LPA **1.2** found in the air sac and plasma of rats *in vivo*, when administered at an oral dose of 30 mg/kg.[40] Although this is a very potent ATX inhibitor, at the time of this report no further progress of this compound had been published. Another ATX inhibitor reported by Merck, compound **1.19** (<1 μM IC_{50}, LPC choline release assay), included the benzoxazolidinone motif present in **1.17** but the core and tail structures varied.[42] The boronic acid based inhibitor HA155 (**1.20**) was reported to be a nanomolar inhibitor of ATX but still resembled the lipid-like chemotype. The cocrystal of **1.20** with ATX found that inhibitors of this particular class formed a reversible covalent bond between the boronic acid and the catalytic threonine (T209).[21]
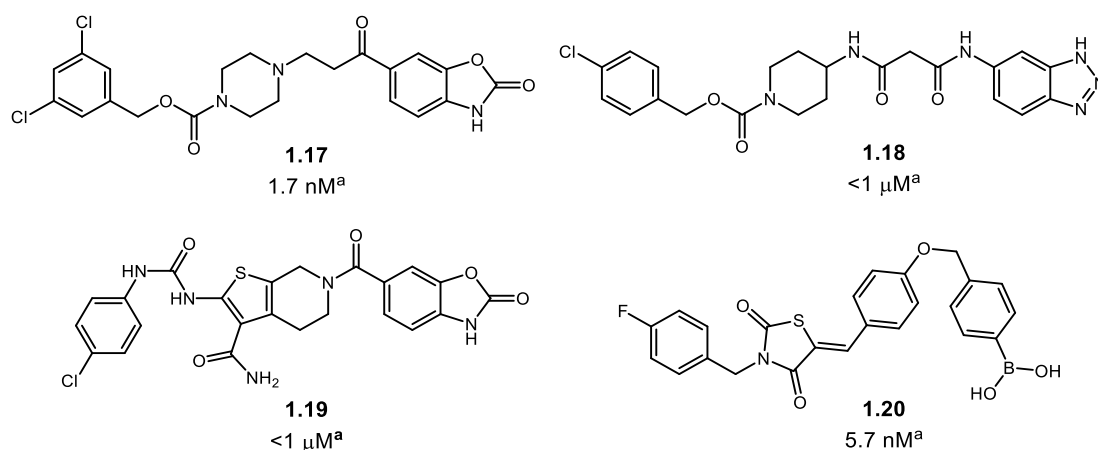
Figure 1.3. Piperidine and piperazine lipid-like derivatives as ATX inhibitors. [a]LPC choline release assay.

With respect to the endogenous ligand (**1**), it is perhaps unsurprising that many of the synthetic ligands developed for ATX have resembled the lipid chemotype: an acidic 'head' group linked through a variety of 'cores' to a lipophilic 'tail' (Figure 1.3:

1.17, **1.18**, **1.19**, and **1.20**).[43] However, a comparatively smaller number of inhibitors have been described that deviate from this common scaffold, for example PAT-347 (**1.21**), reported by PharmAkea Therapeutics[44, 45] (Figure 1.4). Crystal structures of the lipid-based inhibitors with ATX have been reported previously, showing that binding occurs within the catalytic site of ATX and thus these inhibitors compete for the same region that the natural ligand is known to bind.[21,46] In the recent report from PharmAkea,[45] the authors observed the small molecule inhibitor **1.21** to be a potent noncompetitive inhibitor of ATX, with a distinct mode of binding remote to the catalytic site. This compound was noted to have a scaffold similar to our compound of interest, the indole-derived inhibitor **1.22** originally reported by Amira Pharmaceuticals.[47-49] At the time of this report there was very little information available about the activity of **1.22** and its binding mode. The patent in which **1.21** and related analogues are claimed report the IC$_{50}$ values in ≤0.5 µM, >0.5 but ≤3 µM, or >3 µM categories;[44] similarly, the patents in which analogues of **1.22** are reported also categorise the activities (IC$_{50}$: <300 nM, 0.3-1 µM, or >1 µM).[47-49] From consideration of this data very little detailed SAR of these non-lipid-like ATX inhibitors can be extracted.
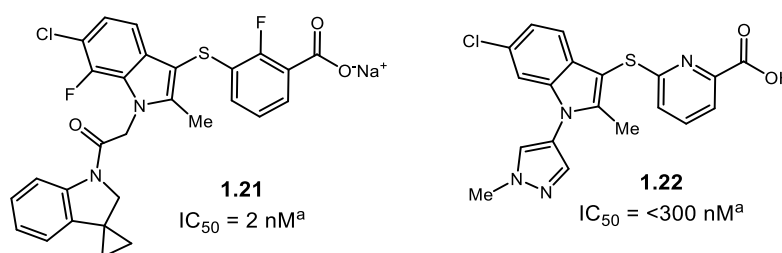
Figure 1.4. Indole derivative as ATX inhibitors. [a]LPC choline release assay.

More recently a series of non-zinc binding inhibitors of ATX have emerged in the literature. These compounds are designed to bind in the tunnel and hydrophobic

pocket of ATX, and therefore inhibit catalytic activity without occupying the catalytic site. One of these non-zinc binding inhibitors is currently in phase 2a clinical trials (FLORA; NCT02738801) for the treatment of idiopathic pulmonary fibrosis (IPF): GLPG1690 (**1.23**) reported by Galapagos (Figure 1.5). Compound **1.23** was shown to be a potent ATX inhibitor and displayed efficacy *in vivo* using an IPF model.[50, 51] Furthermore, the phase 1 study of this compound in healthy patients had shown good pharmacokinetics, an excellent safety profile, and a good LPA biomarker response.

1.23
131 nM[a]
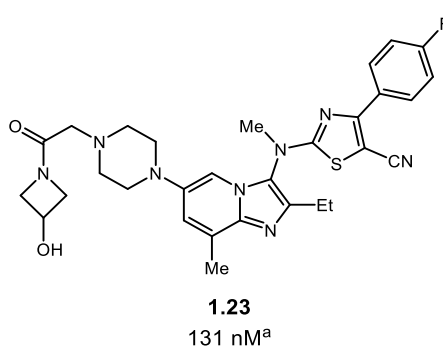
Figure 1.5. Non-zinc binding ATX inhibitor GLPG1690. [a]LPC choline release assay.

All of the ATX inhibitors developed thus far have displayed potency *in vitro* and some *in vivo*, however at the time of this report only one compound had entered clinical trials (**1.23**). As previously stated, the earlier lipid-like inhibitors are not druglike in terms of their physicochemical properties, and this has limited the testing *in vivo*. Thus it is important for the design of future ATX inhibitors to take into consideration physicochemical properties and aim to develop compounds with the necessary pharmacological properties for medicinal use.

1.1.6   Physicochemical Properties of Drug Compounds

1.1.6.1   Determining Druglikeness

The most widely known rule of thumb when designing drug molecules is Lipinski's "rule of five" reported in 2001.[52] The rule provides a set of parameters used to evaluate the druglikeness of a compound and determine how suitable it will be for oral dosage. It provides guidelines for four parameters that should be followed to aid the design of orally available drugs. The four parameters and guidelines are: hydrogen bond donors (HBD) <5; hydrogen bond acceptors (HBA) <10; molecular weight (MW) <500 Da, and the calculated distribution coefficient (clogP) <5.[52] The properties of the selected ATX inhibitors discussed previously are listed in Table 1.3, with the properties outside Lipinski's "rule of five" highlighted in red. These are the physicochemical properties related to the pharmacokinetics of drug compounds including its absorption, distribution, metabolism, elimination, and toxicity (ADMET). The average lipophilicity of marketed drugs has not changed significantly over several decades.[53] This demonstrates the fundamental importance of lipophilicity in drug discovery and highlights the need to consider this property when designing new compounds. As can been seen from the data in Table 1.3, the majority of these exemplar ATX inhibitors have high molecular weights as well as high clogP values, which are undesirable in potential drug molecules. These high values are characteristics associated with compounds that demonstrate poor absorption due to low aqueous solubility, which can lead to failure in the later stages of the drug discovery process.

Table 1.3. Physicochemical properties of exemplar ATX inhibitors evaluated using Lipinski's guidelines.

Inhibitor type	Compound	HBD	HBA	MW	clogP[a]
Lipid-like	1.14	1	4	461	6.46
	1.15	3	5	487	5.27
	1.16	3	4	397	5.15
Lipid-like (piperidine or piperazine based)	1.17	1	5	478	3.64
	1.18	3	5	471	2.05
	1.19	4	5	512	3.72
	1.20	2	5	463	4.80
Indole-based	1.21	0	3	561	6.33
	1.22[b]	1	4	399	3.87
Non-zinc binding	1.23	1	8	589	3.64

[a]Calculated using JChem for Office (Excel).[54] [b]Compound of interest to this study.

There have been a number of developments on the guidelines originally set out by Lipinski. In 2008 Gleeson defined that for the designing of druglike compounds MW should be <400 and clogP <4.[55] This was a conclusion drawn from the *in vitro* data of 30,000 GlaxoSmithKline (GSK) compounds including: solubility, permeability, bioavailability, plasma protein binding, volume of distribution, P-glycoprotein efflux, cytochrome P450 and human Ether-a-go-go Related Gene (hERG) inhibition.[55] All but one of the previously discussed exemplar ATX inhibitors fail when evaluated using Gleeson's guidelines for druglikeness (Table 1.4). The one exemplar that meets the criteria set by Gleeson is the indole-based inhibitor **1.22** from Amira Pharmaceuticals.

Table 1.4. Physicochemical properties of exemplar ATX inhibitors evaluated using Gleeson's guidelines.

Inhibitor type	Compound	HBD	HBA	MW	clogP[a]
Lipid-like	1.14	1	4	461	6.46
	1.15	3	5	487	5.27
	1.16	3	4	397	5.15
Lipid-like (piperidine or piperazine based)	1.17	1	5	478	3.64
	1.18	3	5	471	2.05
	1.19	4	5	512	3.72
	1.20	2	5	463	4.80
Indole-based	1.21	0	3	561	6.33
	1.22[b]	1	4	399	3.87
Non-zinc binding	1.23	1	8	589	3.64

[a]Calculated using JChem for Office (Excel).[54] [b]Compound of interest to this study.

Further analysis of *in vitro* data by Hughes *et al*. using a set of compounds from Pfizer found that toxicity issues were more prevalent in compounds with clogP >3 which again emphasised the need to design drugs with lower lipophilicity.[56] Hughes *et al*. demonstrated that the combination of high lipophilicity and lower topological polar surface area (PSA) increased the promiscuity of compounds leading to more off-target binding.[56] This predicts a higher risk of toxicity in all but one of the discussed ATX inhibitors as only compound **1.18** has the more favourable clogP <3. In 2009 Macdonald and Ritchie determined that there is a correlation between the number of aromatic rings in a compound and its physicochemical properties, including the clogP value.[57] Their analysis of 280 GSK compounds found that, as compounds progress though the drug discovery pipeline, the average number of

aromatic rings decreases from 3.3 in preclinical candidates to 2.3 at the proof of concept stage.[57] Thus to design more druglike compounds with a higher chance of becoming successful drugs, the number of aromatic rings should be limited. This idea of using the number of aromatic rings as an indicator of druglikeness was further developed within GSK and led to the "solubility forecast index" which later became the "property forecast index" (PFI).[58] Using a simple calculation (Equation 1) the risk factor of a compound could be predicted, with a value of >5 indicating high risk ADMET properties.[58]

$$PFI = clogD_{7.4} + \#Ar \qquad (Eq.1)$$

When the PFI of the discussed exemplar ATX inhibitors are calculated, the more current inhibitors are flagged as high risk compounds (Table 1.5).

Table 1.5. PFI of exemplar ATX inhibitors.

Inhibitor type	Compound	clogD$_{7.4}$[a]	#Ar	PFI
Lipid-like	1.14	3.83	0	3.8
	1.15	2.88	0	2.9
	1.16	2.78	1	3.8
Lipid-like (piperidine or piperazine based)	1.17	3.62	3	6.6
	1.18	2.01	3	5.0
	1.19	3.71	4	7.7
	1.20	4.78	3	7.8
Indole-based	1.21	2.88	4	6.9
	1.22[b]	1.47	4	5.5
Non-zinc binding	1.23	2.88	4	6.9

[a]Calculated using JChem for Office (Excel).[54] [b]Compound of interest to this study.

1.1.6.2 Ligand Efficiency

Over the past three decades the average molecular mass of approved pharmaceuticals has risen by only 50 Da whereas synthesised experimental compounds have risen by over 100 Da.[59] As a result, current molecules that are being published are larger and more lipophilic than approved oral drugs, characteristics which predict that these compounds have a higher probability of failure during clinical development.[60] This inflation in physicochemical properties can be linked back to larger and more lipophilic lead compounds, which during the lead optimisation process become larger and more lipophilic still. Larger lead compounds are often a product of the HTS detecting compounds with higher molecular weight and higher lipophilicity which can produce a higher binding affinity.[61] To try and combat this, lead compounds can be measured and ranked in order of their binding efficiency. There are a number of ligand efficiency (LE) metrics available that use *in vitro* activity data in relation to the physicochemical propertied to quantify how efficient the lead compound is in binding. The initial metrics for LE were derived using Gibbs free energy and the heavy atoms count (HAC) which provides a way to compare the average binding energy per atom in a molecule (Equations 2 and 3).[62] Alternatively, a simpler equation can be used (Equation 4), which is referred to as the ligand efficiency index (LEI).

$$LE = (-2.303(RT/HAC)) \text{ x } \log K_i \qquad\qquad (Eq.2)$$

$$LE = (1.37/HAC) \text{ x } pIC_{50} \qquad\qquad (Eq.3)$$

$$LEI = pIC_{50}/HAC \qquad\qquad (Eq.4)$$

Another metric often used is the lipophilic ligand efficiency (LLE) which combines *in vitro* potency with the lipophilicity of a compound (Equation 5). Lipophilicity is connected to a number of druglike properties including solubility and toxicity thus is it important that the LLE is considered in the drug discovery process.[63]

$$LLE = pIC_{50} - clogP \qquad\qquad (Eq.5)$$

As discussed previously, in the design of lead compounds lower MW and clogP are desirable properties to allow for the addition of mass and lipophilicity during the optimisation process.[63] Therefore, in the interest of producing drug candidates with a suitable ADMET profile, the target compounds in this project were designed with the aim of keeping MW <400 and clogP <4 to maintain leadlike qualities. Compounds were also compared based on LEI and LLE in order to prioritise active lead compounds and identify those which displayed both desirable physicochemical properties and good binding affinities. The generally accepted guideline of LEI for lead selection is >0.3, with the published average LEI of oral drugs at 0.45.[64] Retrospective analysis of exemplar drugs by Abbot showed that as a compound proceeds through the lead optimisation process each additional heavy atom added will contribute 0.3 kcal/mol of binding efficiency.[65] This validates the LEI value of 0.3 as a standard in medicinal chemistry and provides researchers with a benchmark to maintain during the optimisation of candidate drug compounds. Using the same calculations and reasoning, the ideal value for LLE is >5.[62] The LEI and LLE values of the exemplar ATX inhibitors discussed in Section 1.1.4 are shown in Table 1.6.

Table 1.6. LEI and LLE of exemplar ATX inhibitors.

Inhibitor type	Compound	IC_{50}	HAC	clogD$_{7.4}$[a]	LEI	LLE
Lipid-like	1.14	252 nM	28	3.827	0.32	2.8
	1.15	22 nM	28	2.881	0.37	4.8
	1.16	5.6 nM	27	2.781	0.42	5.5
Lipid-like (piperidine or piperazine based)	1.17	1.7 nM	32	3.624	0.37	5.1
	1.18	>1 µM	33	2.012	0.25[b]	4.0[b]
	1.19	>1 µM	35	3.713	0.23[b]	2.3[b]
	1.20	5.7 nM	33	4.783	0.34	3.5
Indole-based	1.21	2 nM	38	2.877	0.31	5.8
	1.22[c]	<300 nM	27	1.469	0.33[d]	5.1[d]
Non-zinc binding	1.23	131 nM	42	2.883	0.22	4.0

[a]Calculated using JChem for Office (Excel).[54] [b]IC_{50} 1 µM used in calculations. [c]Compound of interest to this study. [d]IC_{50} 300 nM used in calculations.

Although most of these compounds have the desired LEI values of >0.3, only four examples have good LLE values (>5). This is a result of the high lipophilicity associated with the lipid-like inhibitor chemotype. The two indole-based inhibitors **1.21** and **1.22**, which are smaller with lower clogD$_{7.4}$ than the more lipid-like inhibitors, have excellent LLE.

1.2 Project Aims

Compound **1.22**, originally reported by Amira Pharmaceuticals, was recognised to be an ATX inhibitor with a unique chemotype, but little detailed SAR was available from the patent literature. As the majority of ATX inhibitors are lipid-like with undesirable physicochemical properties, a further understanding of these indole-based inhibitors could provide valuable insight into the development of novel, more drug-like, ATX inhibitors. Using the limited data available, the key structural motifs of **1.22** were suggested to be (i) the 6-Cl of the indole, (ii) the substitution of the indole nitrogen, and (iii) the thiopyridine carboxylic acid (Figure 1.6). Our initial objective was to probe this emerging SAR further, to test the observations made from the patent data, and to more completely establish the contribution of each of these principal structural motifs towards potency through the synthesis and biological evaluation of a series of analogues.
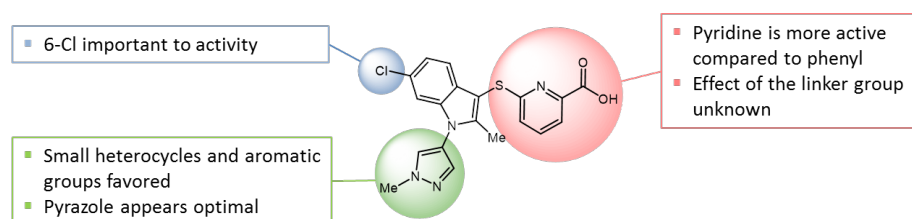
Figure 1.6. SAR of indole **1.22** extracted from data reported by Amira Pharmaceuticals.[47-49]

Furthermore, we aimed to identify the binding site for these analogues. During our SAR investigation into inhibitor **1.22**, a report from PharmAkea revealed the cocrystal of ATX with **1.21** bound in a distinct binding site, remote to the catalytic site.[45] Inhibitor **1.21** is structurally similar to our compound of interest, thus we set out to explore whether **1.22** and analogues also bound in the remote binding site.

1.3 Results and Discussion

1.3.1 Molecule Design

The first region of interest was the 6-Cl substitution of the indole ring. Analysis of the patent data had suggested this was an important region of the molecule, present in 98% of the active compounds, with changes to substituent or position on the ring having a direct effect on the activity observed. To explore this relationship in greater depth, a series of compounds were designed with alternative chloro regiochemistry, as well as removal or exchange of the chloro for alternative functional groups. Three alternatives were chosen to determine the optimal size and nature of the substituent: fluoro, methoxy, and methyl (Table 1.7).
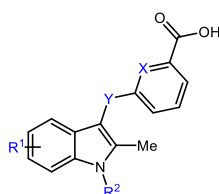
Table 1.7. Summary of analogues exploring 6-Cl.

Compound	R^1	R^2	X	Y
1.22	6-Cl	1-methylpyrazole	N	S
1.24	5-Cl	1-methylpyrazole	N	S
1.25	4-Cl	1-methylpyrazole	N	S
1.26	H	1-methylpyrazole	N	S
1.27	6-F	1-methylpyrazole	N	S
1.28	4-F	1-methylpyrazole	N	S
1.29	6-Me	1-methylpyrazole	N	S
1.30	4-Me	1-methylpyrazole	N	S

Table 1.7. *Continued.*

Compound	R^1	R^2	X	Y
1.31	6-MeO	1-methylpyrazole	N	S
1.32	4-MeO	1-methylpyrazole	N	S
1.33	7-Cl	H	N	S
1.34	6-Cl	H	N	S
1.35	5-Cl	H	N	S
1.36	4-Cl	H	N	S
1.37	H	H	N	S
1.38	6-F	H	N	S
1.39	4-F	H	N	S
1.40	6-Me	H	N	S
1.41	4-Me	H	N	S
1.42	6-MeO	H	N	S
1.43	4-MeO	H	N	S

The second region to be modified was at the *N*-1 position of the indole ring. The *N*-methyl pyrazole was replaced with a phenyl ring, cyclopentyl, and methyl to explore the tolerance of this region for a less polar aromatic ring as well as aliphatic groups. It was also important to determine whether a substituent on the indole *N* was required for activity. These analogues were made with and without the 6-Cl to further explore the importance of the chloro substituent. Furthermore, they were synthesised as the benzoic acids (X = CH) and as the pyridyl (X = N) analogues to provide further SAR (Table 1.8).
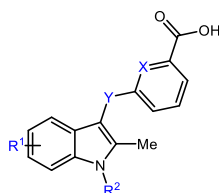
Table 1.8. Summary of analogues exploring indole *N*-substituent.

Compound	R^1	R^2	X	Y
1.44	6-Cl	Me	N	S
1.45	6-Cl	Cyclopentyl	N	S
1.46	6-Cl	Ph	N	S
1.47	H	Me	N	S
1.48	H	Cyclopentyl	N	S
1.49	H	Ph	N	S
1.50	4-Cl	H	CH	S
1.51	6-Cl	1-methylpyrazole	CH	S
1.52	6-Cl	H	CH	S
1.53	6-Cl	Me	CH	S
1.54	6-Cl	Cyclopentyl	CH	S
1.55	6-Cl	Ph	CH	S
1.56	H	1-methylpyrazole	CH	S
1.57	H	H	CH	S
1.58	H	Me	CH	S
1.59	H	Cyclopentyl	CH	S
1.60	H	Ph	CH	S

Finally, the thiopyridine carboxylic acid was modified, with changes made to the linker and the nature of the aromatic ring. The previously reported data in the patent literature contained little SAR around the linker area of the compound and therefore we were interested in converting the thioether to an ether (Y = O) or methylene (Y = CH$_2$) linker, as well as exploring the difference between pyridyl and phenyl analogues (Table 1.9). Unfortunately, efforts to synthesise the ether linked pyridyl compounds were unsuccessful (see Section 1.3.7. for further details).
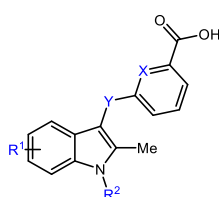
Table 1.9. Summary of analogues exploring the acidic region.

Compound	R^1	R^2	X	Y
1.61	6-Cl	1-methylpyrazole	N	CH$_2$
1.62	6-Cl	1-methylpyrazole	C	CH$_2$
1.63	6-Cl	1-methylpyrazole	C	O
1.64	6-Cl	H	C	O
1.65	H	1-methylpyrazole	N	CH$_2$
1.66	H	1-methylpyrazole	C	CH$_2$
1.67	H	1-methylpyrazole	C	O
1.68	H	H	C	O

There were also a number of additional deletion analogues synthesised in order to confirm the requirement of each motif. The indole was removed in the design of

compound **1.69**, the aromaticity of the acid was removed to form aliphatic acid analogue **1.70**, and finally the entire acid region was removed to give compound **1.72**. A summary of the targets successfully synthesised is shown in Figure 1.7.
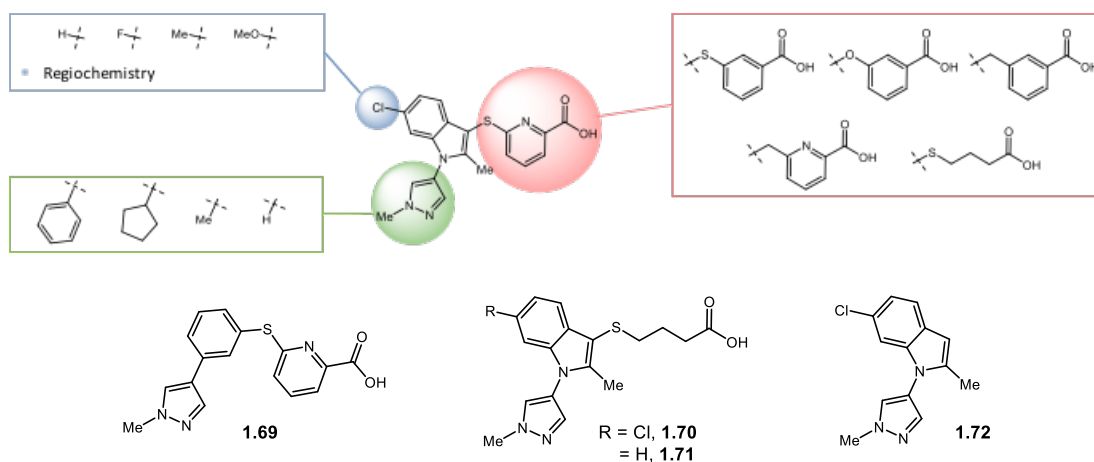
Figure 1.7. Summary of analogues designed to explore SAR of **1.22**.

1.3.2 Biological Evaluation

1.3.2.1 Bis-*p*NPP Assay Results

To evaluate our compound library, the first screen was performed using the bis-*p*NPP assay. This was selected based on its broad application throughout the ATX literature.[18] An initial screen was carried out using 30 µM of inhibitor allowing a rapid evaluation of the compounds. The criteria of >60% inhibition was set for a compound to be termed active and therefore progressed to further testing (Figure 1.8). Based on this initial survey of the activity of Amira compound **1.22** along with the 49 analogues in the bis-*p*NPP assay, we identified 10 inhibitors, including the patent compound **1.22.** These 10 compounds were tested again in the bis-*p*NPP assay using a concentration range of 30 nM − 30 µM inhibitor, to determine the IC_{50} for each of these compounds (Table 1.10).
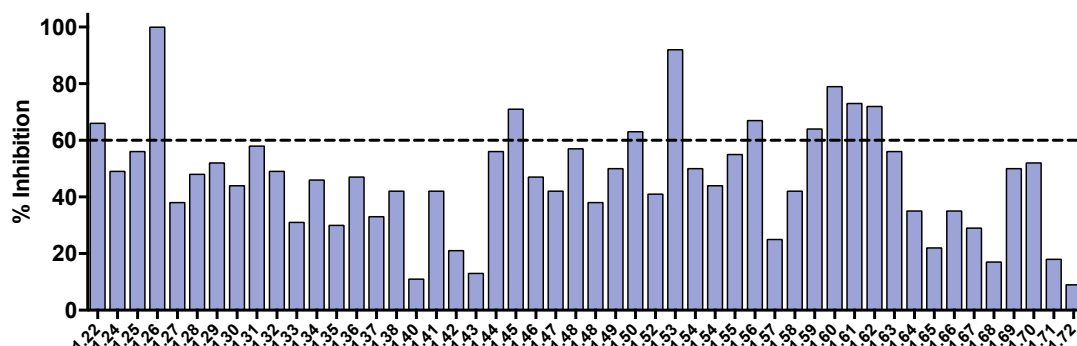
Figure 1.8. Bis-*p*NPP assay results, tested using 30 μM inhibitor with a >60% inhibition criterion. Average of n = 2.

Table 1.10. Results from bis-*p*NPP assays.

Compound	% inhibition at 30 μM[a]	IC$_{50}$[b]
1.22	66	22 nM
1.26	100	6 μM
1.45	71	2 μM
1.50	63	>30 μM
1.53	92	100 nM
1.56	67	3 μM
1.59	64	>30 μM
1.60	79	>30 μM
1.61	73	89 nM
1.62	72	33 nM

[a]Average of n= 2. [b]10 point curves, n = ≥2.

The Amira ATX inhibitor **1.22** was found to have an IC$_{50}$ of 22 nM, which was consistent with the value of <300 nM claimed in the patent (LPC choline release assay);[47-49] however, the IC$_{50}$ values observed in this set ranged from 22 nM to >30 μM. These results demonstrated that our first screen at an inhibitor concentration of

30 μM had not been a reliable indicator of activity. Importantly, on further inspection of the dose response curves (Figure 1.9), it was noted that when using the bis-*p*NPP assay, compound **1.22** showed only 60% maximal inhibition of ATX (40% hydrolysis of **1.12**), indicating that this analogue was not fully inhibiting the ATX hydrolysis of **1.12**, potentially implying a discrete binding mode compared to that of the artificial substrate.
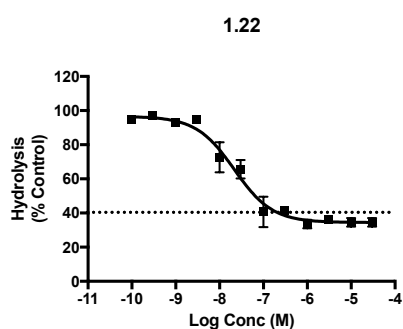
Figure 1.9. Testing of **1.22** in the bis-*p*NPP assay from 30 nM – 30 μM of inhibitor. Dashed line represents 60% criteria of initial screen.

A further 20 analogues were tested in the bis-*p*NPP assay confirming that partial inhibition was a consistent feature associated with this series (data not shown, see SI). Although the bis-*p*NPP assay has many advantages, there are risks associated with the use of unnatural substrates if the binding interactions with the target enzyme are dissimilar to those of the natural substrate. There are a number of reported examples where misleading results were observed when using ATX assays that employ the unnatural ligands FS-3, CPF4, and *p*NP-TMP.[35, 66, 67] The authors concluded that the discrepancies in assay datasets were the result of the inhibitor compounds and assay substrates binding to different regions of ATX. It has been well documented that the active site of ATX features three key regions with which small molecule inhibitors can interact: the catalytic site, the hydrophobic pocket, and

the tunnel.[20, 21, 68] Comparing the likely binding of the unnatural substrate **1.12** with that of ATX in complex with **1.2**, it is noted that while both bind at the catalytic site, the acyl chain of **1.2** shows additional extensive interactions with the hydrophobic pocket (Figure 1.10). This suggests that it is possible for small molecules to bind outside the catalytic site without inhibiting the hydrolysis of **1.12**, potentially resulting in false negative results in the bis-*p*NPP ATX assay.
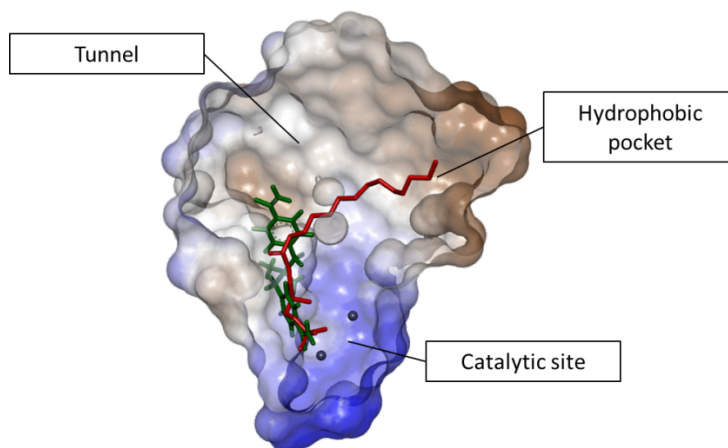
Figure 1.10. Three binding sites of ATX: Catalytic Site, Hydrophobic Pocket, and Tunnel. Complex of LPA 14:0 **1.2** (red) in mouse ATX (PDB 3NKN) with the docked position of bis-*p*NPP **1.12** (green) overlaid. Docked using GOLD[69] and viewed using Discovery Studio Visualizer.[25]

Indeed, the noncompetitive inhibitor **1.21** from PharmAkea, which shares a number of structural similarities to **1.22**, has been reported to bind an allosteric site within the tunnel.[44, 45] The authors observed that **1.21** inhibited the hydrolysis of the natural ligand **1.1** but not of the unnatural substrate **1.12**, showing that an inhibitor binding within the tunnel may not be detected using the bis-*p*NPP assay. Moreover, selected steroid analogues have recently been shown to bind the same site, with the activity of ATX in hydrolysing LPC allosterically inhibited but not its activity on *p*NP-TMP.[68] These reports led us to employ the natural substrate **1.1** in the LPC choline release

assay to further evaluate our inhibitors, gain a more complete understanding of the underlying SAR, and offer insight into potential binding modes.

1.3.2.2 LPC Choline Release Assay Results

Prior to testing the inhibition of ATX, a control reaction was run using three exemplar compounds to ensure that there was no incompatibility with the two coupling enzymes used in the assay: choline oxidase and HRP. Using choline chloride as the substrate, no inhibition was observed (see SI). Testing proceeded with an initial screen of all 50 compounds from 400 nM – 100 μM, 6 point curves, in triplicate, to identify active inhibitors. From this dataset, compounds that exhibited an IC_{50} <1 μM were tested further across a concentration gradient of 0.3 nM – 10 μM, 10 point curves, n ≥ 2, and the IC_{50} values were determined (compounds with IC_{50} >30 μM not shown, see SI). This assay provided us with robust inhibition data, with the more potent compounds showing full inhibition of ATX. Of the 50 analogues described in the current study, only four had been previously reported by Amira Pharmaceuticals (**1.22**, **1.51**, **1.53**, **1.55**).[47-49] The IC_{50} values determined in our LPC choline release assay were consistent with the values claimed in the patents (Table 1.11).

Table 1.11. LPC assay results.

Compound	IC_{50} (LPC, nM)
1.22	4[a]
1.24	258
1.26	1700
1.27	349

Table 1.11. *Continued.*

Compound	IC$_{50}$ (LPC, nM)
1.28	3500[b]
1.29	25
1.32	13000[b]
1.33	124
1.34	25
1.38	19000[b]
1.41	8200[b]
1.44	31
1.45	2800
1.46	-[c]
1.51	11[a]
1.52	747
1.53	1200[d]
1.54	27000[b]
1.55	81[a]
1.60	5800[b]
1.61	339
1.62	660
1.63	281
1.71	11000[b]

All tested from 0.3 nM – 10 μM, 10 point curves, n = 2. [a]Consistent with the value of < 300 nM claimed in the patent, LPC assay. [b]Incomplete curve observed, data extrapolated using GraphPad Prism to determine IC$_{50}$. [c]Unable to determine IC$_{50}$ due to solubility issues in the assay medium. [d]Consistent with the value of >1 uM claimed in the patent, LPC assay.

1.3.3   Enzyme Kinetic Studies

To explore the potential binding mode of this chemotype, enzyme kinetic studies were carried out in the presence of four representative inhibitors: compound **1.22**, **1.34**, **1.53**, and **1.55**. ATX activity for varying substrate concentrations (**1.1**) was measured in concentrations of each inhibitor. A mixed inhibition mathematical model was fitted to the original data to determine the value of alpha; values of alpha close to 1 indicate noncompetitive inhibition (Figure 1.11). [70]

$$
\begin{array}{ccccccccc}
E & + & S & \xrightleftharpoons{\alpha K_M} & ES & \xrightarrow{k_{cat}} & E & + & P \\
 & & + & & + & & & & \\
 & & I & & I & & & & \\
 & & \Big\Updownarrow K_i & & \Big\Updownarrow \alpha K_i & & & & \\
 & & EI & \xrightleftharpoons{\alpha K_M} & ESI & & & &
\end{array}
$$
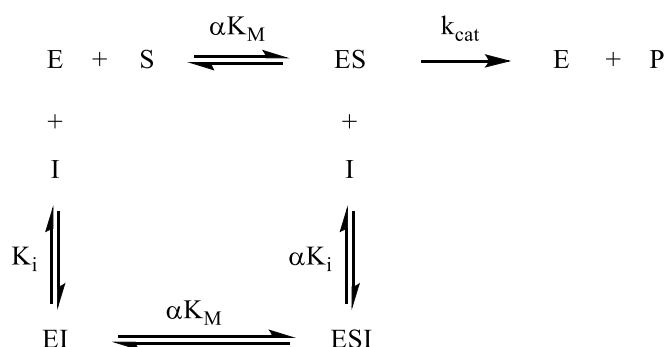
Figure 1.11. The constant "alpha". This defines the effect of an inhibitor binding has on the affinity of the enzyme for the substrate, a value close to 1 is indicative of noncompetitive inhibition. E, enzyme; S, substrate; P, product; I, inhibitor.

To graphically demonstrate the inhibition mode, we also present Lineweaver-Burk double reciprocal plots (Figure 1.12). These studies show that as the inhibitor concentration was increased, the V_{max} reduced but the K_M remained unchanged, which is indicative of noncompetitive inhibition. Consistently, the values of alpha for each of the compounds ranged between 0.6 and 2.6, characteristic of noncompetitive inhibition. Thus, all four exemplar compounds are strongly noncompetitive inhibitors. This data, along with the differences observed between the two ATX inhibition assays used, suggests that this chemotype has a distinct binding mode, remote to that of the catalytic site of ATX, similar to that reported for the three noncompetitive PharmAkea compounds.[44, 45]

1.22 IC$_{50}$ = 4 ±0.5 nM

1.34 IC$_{50}$ = 1700 ±400 nM

1.53 IC$_{50}$ = 1200 ±800 nM

1.55 IC$_{50}$ = 81 ±28 nM
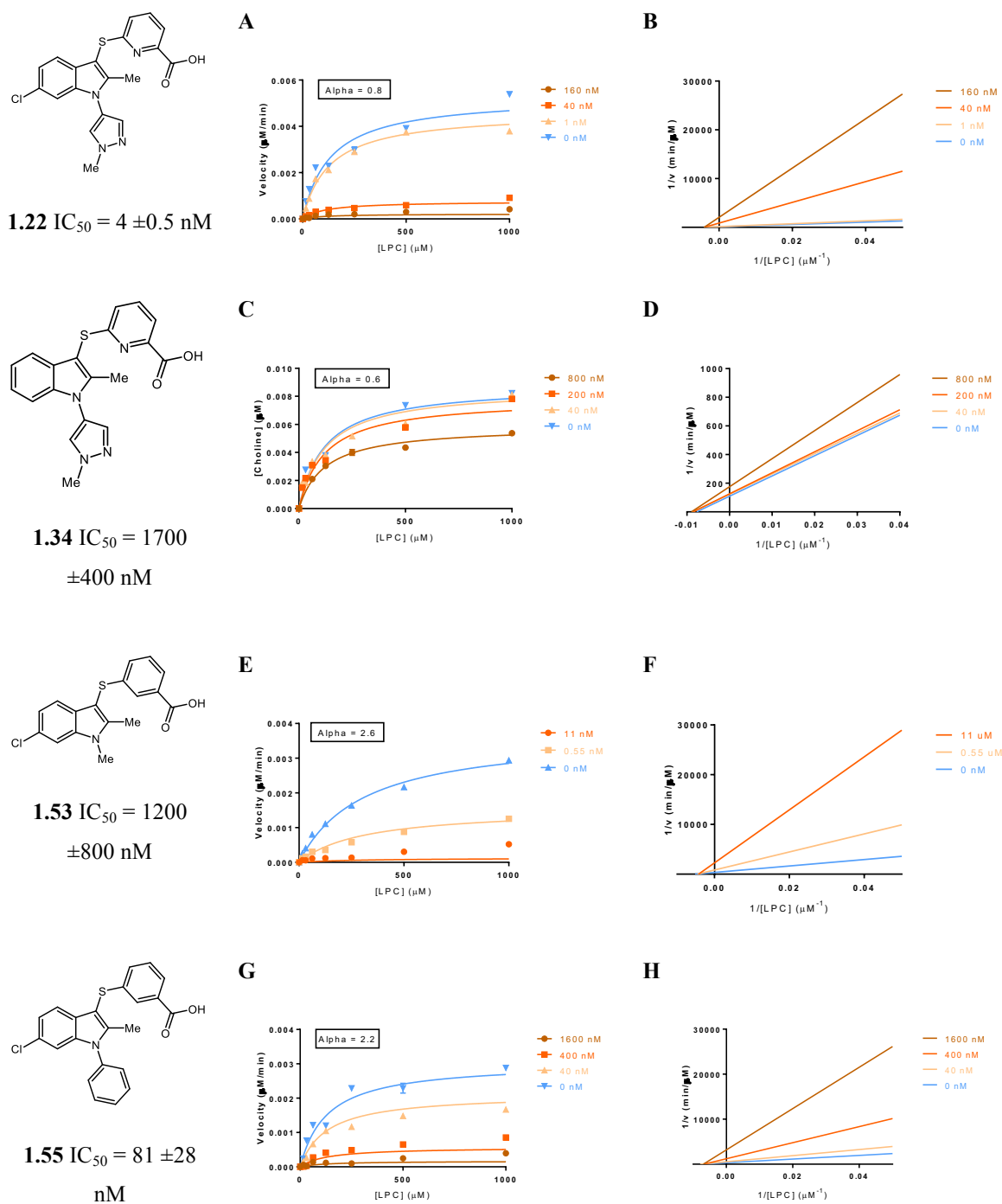
Figure 1.12. Enzyme kinetic studies using compounds **1.22**, **1.34**, **1.53**, and **1.55**. Compound **1.22**: α = 0.8. Compound **1.34**: α = 0.6. Compound **1.53**: α = 2.6. Compound **1.55**: α = 2.2. The data were plotted and the values generated using GraphPad Prism 6 from nonlinear regression analysis to an equation corresponding to the mixed inhibition model allowing the determination of alpha.

1.3.4 Structure-activity Relationships

Using the results from the LPC assay the SAR around this chemotype was defined. This has provided a better understanding of the features which contribute to its potency. During our examination of the patent data, it became apparent that the 6-Cl of compound **1.22** was of high importance to the potency. The deletion analogue **1.69**, in which the indole was removed with a phenyl ring used as the core, had resulted in a complete loss of activity (data not shown, see SI), thus confirming the importance of the indole core. To investigate the SAR of the 6-Cl substitution on the indole, a series of analogues were made varying the position of the chloro around the benzenoid ring, as well as removing the substituent (Table 1.12). We also aimed to explore the significance of the chloro by exchanging this for alternative functionalities: F, OMe, and Me.
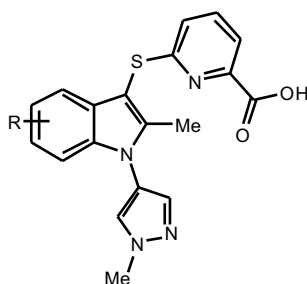
Table 1.12. SAR of indole ring.

Compound	R	IC$_{50}$ (LPC)
1.22	6-Cl	4 nM
1.24	5-Cl	258 nM
1.25	4-Cl	>30 μM

Table 1.12. *Continued.*

Compound	R	IC_{50} (LPC)
1.26	H	1700 nM
1.27	6-F	349 nM
1.28	4-F	3500 nM[a]
1.29	6-Me	25 nM
1.30	4-Me	13000 nM[a]
1.31	6-OMe	124 nM
1.32	4-OMe	>30 μM

[a]Incomplete curve observed, data extrapolated using GraphPad Prism to determine IC_{50}.

The effect of this chloro on potency was apparent throughout our results, with its presence increasing the potency in every example. It was also identified that the 6-position of the indole ring was optimal for the chloro, with the other regioisomers resulting in lowered or a complete loss of activity (Table 1.12). This can be noted in the comparison of compounds **1.22**, **1.24**, and **1.25**, with the movement of the chloro substituent around the indole ring.

In order to rationalise the effect of the 6-Cl, docking studies were performed using the apo form of the ATX enzyme (Figure 1.13). From this work it was proposed that the 6-Cl projects into a nearby hydrophobic cleft (Leu160, Ala164, Trp207, Trp161), making a series of hydrophobic interactions (Figure 1.13B). The 6-Cl substituent is a

vital motif for potency throughout this chemotype, therefore we hypothesise that the hydrophobic interactions of this substituent with the hydrophobic cleft are key contributors to the potency. It was possible to exchange the 6-Cl for alternative substituents (F, **1.27**; Me, **1.29**; OMe, **1.31**) and retain the activity, although the chloro was optimal. Based on our *in silico* model, a conclusion was drawn that the 6-Cl substituent provides the optimal size to fit within the hydrophobic pocket with a larger (Me, **1.29**) or smaller (F, **1.27**) substituent resulting in a small loss of potency.
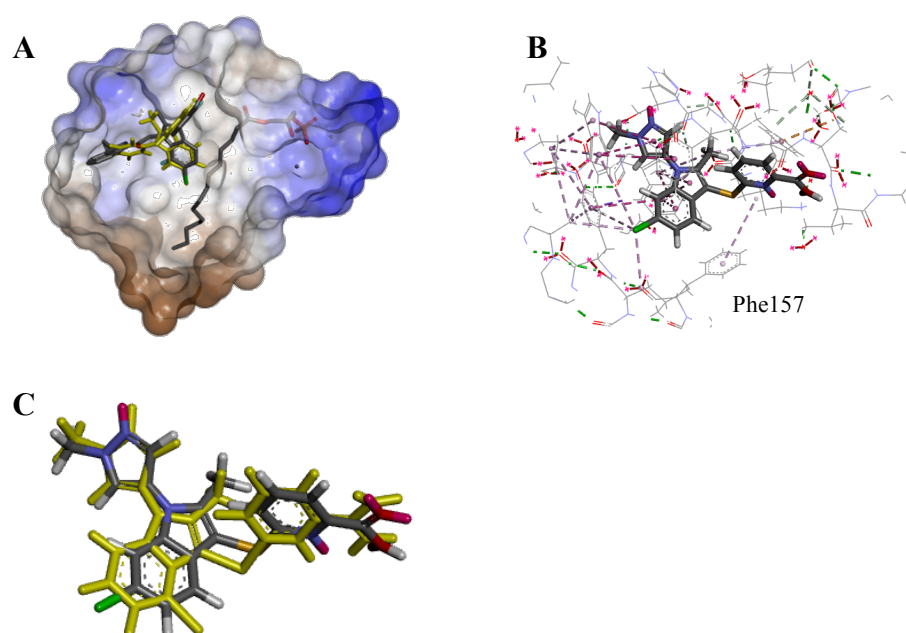
Figure 1.13. *In silico* studies created using co-crystal of ATX with **1.2** and **1.21** PDB 4ZG7. A: Model of **1.53** (yellow) overlayed with cocrystal of **1.21** (coloured by atom type) and ATX, with **1.2** residing in the catalytic site and hydrophobic pocket. B: Model of ATX with **1.22** highlighting possible interactions. C: Shift observed when 4-Cl substituted **1.25** is docked (yellow) vs. 6-Cl substituted **1.22** (coloured by atom type). Docked using GOLD[69] and viewed using Discovery Studio Visualizer.[25]

Moving these alternative substituents from the 6- to the 4-position of the indole resulted in loss of activity, providing further support to the importance of the 6-position. It was noted that with no substituent on the indole some activity was

retained with an IC_{50} of 1700 nM observed for compound **1.26**; however, introduction of a substituent to the 4-position resulted in loss of activity (**1.25**, **1.30**, **1.32**), with the exception of the 4-F which is tolerated (**1.28**), showing that substitution at this position prevents binding of these compounds. Using the *in silico* model, it can be suggested that a clash between the 4-position substituents and a nearby residue (Phe157) alters the binding of these analogues (Figure 1.13B). This shift in the binding position (Figure 1.13C) caused by the clash with the protein could explain the loss in potency observed when a substituent is introduced to the 4-position.

The next region to be explored was the substitution on the indole nitrogen. In order to establish whether the aromatic substituent was required for activity, and if the size of the substituent was important, three alternative substituents were used in place of the 1-methyl-pyrazole: methyl, cyclopentyl, and phenyl. Analogues with the unsubstituted indole were also synthesised to determine whether any substituent at this region was required for activity. Based on the patent data, the 1-methyl-pyrazole is important for activity and removal of this substituent did result in a reduction in potency; however, compound **1.34** with no decoration of the indole nitrogen, was a potent compound with an IC_{50} of 25 nM. Further analogues exploring the substitution of the indole nitrogen (methyl, cyclopentyl, phenyl) found that the 1-methyl-pyrazole remained the most active (Table 1.13). Unfortunately, we were unable to determine the IC_{50} of compound **1.46** due to poor solubility in the assay medium observed during the screening of this analogue. Our binding model had indicated possible π-π interactions for the 1-methyl-pyrazole of **1.22** with nearby residues (Trp207: pyrazole face to indole edge and Phe221: face to face). By changing the 1-methyl-

pyrazole to an aliphatic substituent these interactions are lost, thus resulting in a loss of activity. The methyl group of **1.44** was well tolerated, whereas the cyclopentyl substituent of **1.45** was found to cause a large drop in potency. These results suggest that the larger aliphatic substituent is detrimental, either through unfavourable interactions or by clashing with the protein; however, we did not observe either from consideration of our binding model.
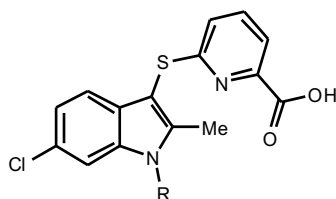
Table 1.13. SAR of indole nitrogen substituent, with 6-Cl.

Compound	R	IC$_{50}$ (LPC)
1.22	1-methyl-pyrazole	4 nM
1.34	H	25 nM
1.44	Me	31 nM
1.45	cyclopentyl	2800 nM
1.46	Ph	- [a]

[a]Unable to determine due to solubility issues in the assay medium.

The relationship between the 1-methyl-pyrazole and the 6-Cl was highlighted by altering the substitution of the indole nitrogen in a series of compounds that did not feature the 6-Cl substitution. In this series of analogues (Table 1.14), the only

compound to exhibit activity was that with the 1-methyl-pyrazole **1.26**, which shows that either the 6-Cl or the 1-methyl-pyrazole must be present for activity; however, the 6-Cl substituent has the most profound effect on activity.
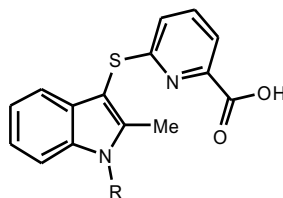
Table 1.14. SAR of indole nitrogen substituent, without 6-Cl.

Compound	R	IC$_{50}$ (LPC)
1.37	H	>30 μM
1.26	1-methyl-pyrazole	1700 nM
1.47	Me	>30 μM
1.48	cyclopentyl	>30 μM
1.49	Ph	>30 μM

This series of compounds was explored further via the synthesis of the analogous series with the nitrogen removed from the pyridine ring, thus allowing for the SAR of the pyridyl acid and the phenyl to be determined. The benzoic acid analogues demonstrated the same SAR as the pyridyl sub-series, with the 1-methyl-pyrazole (**1.51**) giving the best inhibition (Table 1.15). Fortunately, compound **1.55** showed good solubility in the assay medium, allowing for the IC$_{50}$ to be determined at 81 nM, unlike the pyridyl analogue **1.46** with which we had observed poor solubility

during screening in the LPC assay. This set of analogues additionally supports our observation from the data in Table 1.13; that it is beneficial to have a substituent of aromatic nature on the indole nitrogen, and although a cyclopentyl is unfavorable (**1.54**), smaller aliphatic groups can be tolerated (**1.53**).
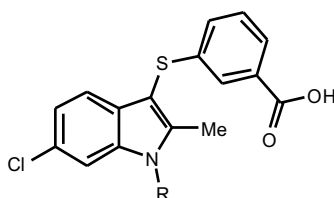
Table 1.15. SAR of indole nitrogen substituent in the benzoic acid analogues.

Compound	R	IC$_{50}$ (LPC)
1.51	1-methyl-pyrazole	11 nM
1.52	H	747 nM
1.53	Me	1200 nM
1.54	cyclopentyl	27000 nM[a]
1.55	Ph	81 nM

[a]Incomplete curve observed, data extrapolated using GraphPad Prism to determine IC$_{50}$.

The acidic group of this chemotype was also found to be vital for ATX activity, as shown by the two deletion analogues in which the thioether linked pyridine was removed (**1.72**) or exchanged for an aliphatic acid (**1.70**) which resulted in loss of activity (Table 1.16). During the docking studies of **1.22**, it was noted that both the indole ring and the 1-methyl-pyrazole substituent could potentially contribute to binding through π-π interactions; however, with the pyridyl acid orientated towards

the solvent it made no specific interactions with ATX, and only a potential H-bonding interaction with a crystallographic water molecule was identified. The loss of activity observed with **1.70** and **1.72** could indicate that the aromaticity is required for additional interactions not identified in our docking study, or that the increased number of rotatable bonds was unfavourable in the binding of this compound within ATX. By comparing the benzoic acid compound **1.51** with the corresponding pyridyl analogue **1.22** we observed no significant change in potency with removal of the pyridyl nitrogen; however, by comparing matched pair examples with *N*-substituents other than the 1-methyl-pyrazole, it can be noted that the pyridine in general improves potency (Table 1.13 vs. Table 1.15).
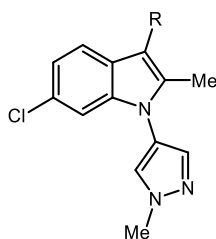
Table 1.16. SAR of the carboxylic acid region.

Compound	R	IC$_{50}$ (LPC)
1.22		4 nM
1.51		11 nM
1.70		>30 μM
1.72	H	>30 μM

The thioether linker was then explored through replacement with an ether or a methylene. Previous reports from the patent literature had disclosed no analogues with the methylene, and only five with an ether linker, thus we sought to fill the SAR gap with a set of analogues using an ether and methylene with both the pyridyl and benzoic acids. A large drop in potency was observed as a result of changing the thioether (**1.22**) to a methylene spacer (**1.61**). We also noted this trend in the benzoic acid analogues with the thioether (**1.51**) being superior to an ether (**1.63**) or methylene (**1.62**) linker, though both alternatives were tolerated (Table 1.17). Our docking model provided little insight into the effects of changing the linker (Figure 1.14); thus we hypothesise that the longer bond lengths of the thioether are beneficial to the binding of this chemotype. Furthermore, this subset again demonstrates the importance of the 6-Cl for activity and the superiority of the pyridyl analogues over the corresponding phenyl analogues.
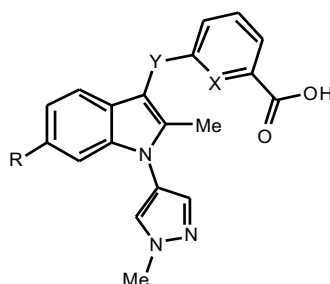
Table 1.17. SAR of the linker.

Compound	R	Y	X	IC$_{50}$ (LPC)
1.22	Cl	S	N	4 nM
1.61	Cl	CH$_2$	N	339 nM

Table 1.17. *Continued.*

Compound	R	Y	X	IC$_{50}$ (LPC)
1.26	H	S	N	1700 nM
1.65	H	CH$_2$	N	>30 µM
1.51	Cl	S	CH	11 nM
1.62	Cl	CH$_2$	CH	660 nM
1.63	Cl	O	CH	281 nM
1.56	H	S	CH	>30 µM
1.66	H	CH$_2$	CH	>30 µM
1.67	H	O	CH	>30 µM
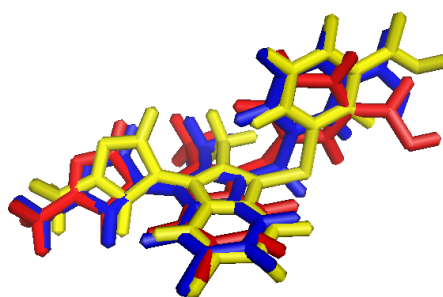
Figure 1.14. Overlay comparing docking poses of different linker groups: Thioether **1.51** (yellow); methylene **1.62** (blue); ether **1.63** (red).

1.3.5 Crystallographic Data

In order to confirm the binding mode of this chemotype, **1.55** (IC_{50} = 81 ±28 nM) was co-crystallised with ATX and the structure of this complex determined to 2.4 Å resolution, PDB 5LQQ. After molecular replacement and model adjustment difference, electron density in the tunnel close to the hydrophobic pocket could be observed, and compound **1.55** could be modelled in the difference density map. The docked position of **1.55** in our previously described *in silico* model with ATX (Figure 1.13) was found to be consistent with the binding mode observed in the cocrystal of **1.55** and ATX (Figure 1.15).
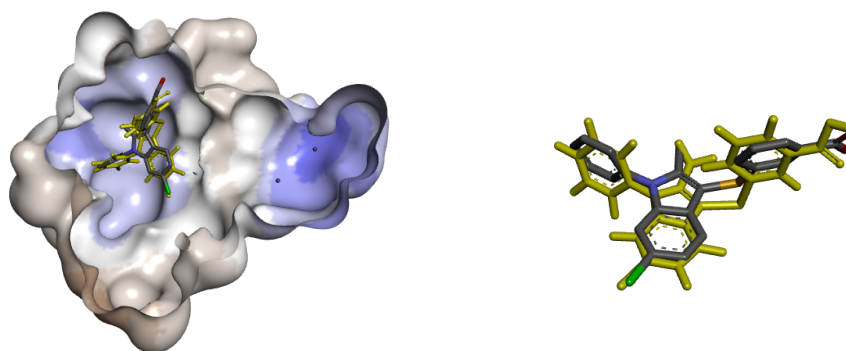
Figure 1.15. Crystal structure (PDB 5LQQ) vs docking model of **1.55** with ATX. Cocrystal structure of **1.55** (coloured by atom type) overlayed with docking model of **1.55** (yellow). Docked using GOLD[69] and viewed using Discovery Studio Visualizer[25] (see Section 1.5.6 for docking details).

The thioether, indole, and *N*-phenyl are very clear in the electron map; however, the benzoic acid is not well resolved, possibly due to disorder (Figure 1.16D). This structure allowed us to locate the binding mode of this chemotype and confirm a number of key binding interactions (Figure 1.16).
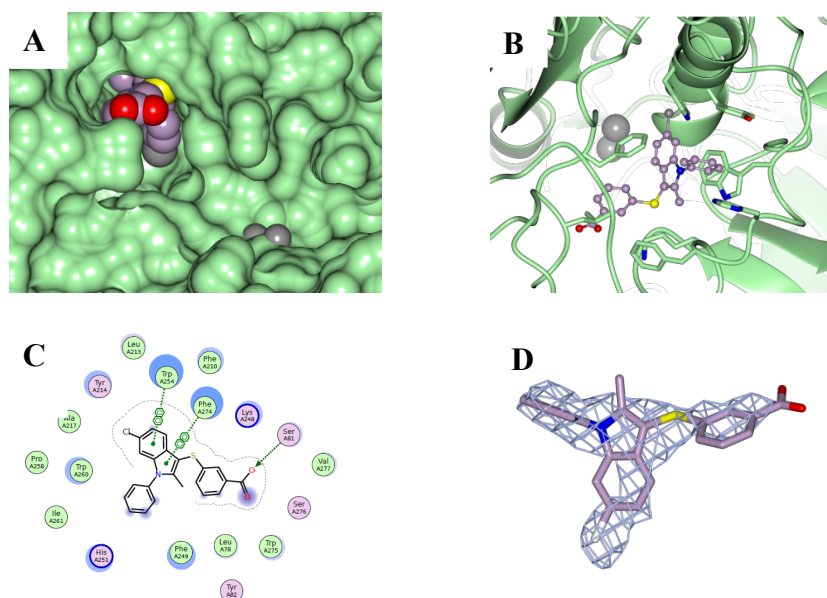
Figure 1.16. Crystallographic data of **1.55** with ATX. A: **1.55** bound within the tunnel, remote from the catalytic site. B: Stick and ball model of **1.55**. C: Ligand display for interaction and analysis (LIDIA) graph of **1.55**. D: Density map. Model and LIDIA graph built using COOT.[71] Images created using CCP4MG.[72]

Compound **1.55** binds in a very similar pose compared to the PharmAkea inhibitor **1.21** (PDB 4ZG7),[44, 45] which shares a number of structural similarities to analogue **1.55**. The placement of the thioether and indole moieties is nearly identical in the two structures, while the phenyl of **1.55** overlaps well with the cyclopropyl-dihydroindole in **1.21**. The 6-Cl substituent, shown to be vital for potency in our SAR studies, resides in a hydrophobic cleft, resulting in a series of interactions to nearby residues (Figure 1.13A). Both the indole ring and the *N*-phenyl substituent contribute to binding with a number of π-π interactions; however, the benzoic acid (**1.55**) appears to make few discernible interactions with ATX as it is orientated towards the solvent. In the case of compound **1.21**, however, the fluoro-benzoic acid makes interactions with the main chain amide of Val278, a well-ordered glycerol molecule, and a crystallographic water molecule (Figure 1.17A) and is thus very well defined in a

44

single conformation in the electron density map. This is in sharp contrast to the benzoic acid in **1.55** that is clearly disordered, which suggests that the fluoro substituent of the benzoic acid ring may help to order it in a defined position within the tunnel.
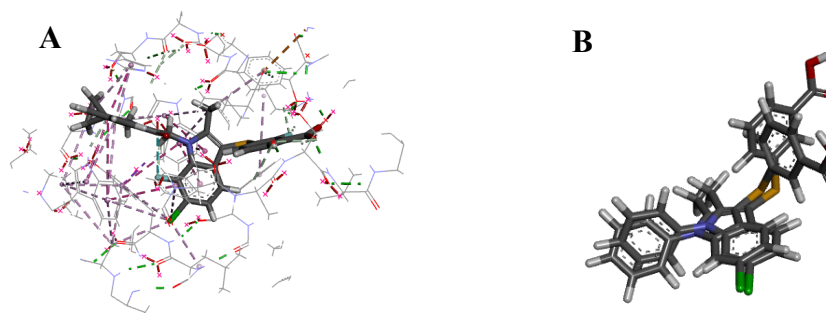
Figure 1.17. Further molecular modelling studies. A: Cocrystal of **1.21** with ATX (PDB 4ZG7) potential interactions. B: Rotation of the thioether. Docked using GOLD[69] and viewed using Discovery Studio Visualizer[25] (see Section 1.5.6 for docking details).

Alternatively, the presence of the phospholipid (**1.2**) in the structure of **1.21** bound to ATX, but not present in our structure with **1.55**, may help order this ring system. Docking studies result in an excellent overlay of **1.55** with **1.21** as expected, but the benzoic acid moiety was able to rotate around the thioether and project in a number of different vectors (Figure 1.17B). The disorder observed of the benzoic acid in the cocrystal structure of **1.55** with ATX supports the hypothesis that the thioether has rotational freedom.

1.3.6 Physicochemical Properties

ATX inhibitors that resemble the natural ligand have high molecular weight (MW) and high logD resulting in poor drug discovery potential. We were interested in the Amira compound **1.22**, not only due to its unique non-lipid chemotype, but also because its lower MW and improved lipophilicity it is potentially a more druglike

45

inhibitor. With this in mind, we evaluated some key physicochemical properties as well as potency for a selected number of the analogues synthesised. Table 1.18 details the physicochemical properties of the analogues in which the indole nitrogen substituent was varied (see SI for further properties measured). Compounds **1.22**, **1.34**, and **1.44** all showed good ligand efficiency in terms of both LEI and LLE; however, the introduction of the pyrazole in compound **1.22** improves both potency and LLE.
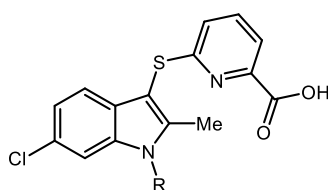
Table 1.18. Physicochemical properties of indole nitrogen substituent analogues.

Compound	R	MW	$logD_{7.4}$[a]	Sol.[b] (µM)	P_{app}[c] (nm s^{-1})	PSA[d]	IC_{50}[e]	LEI[f]	LLE[g]
1.22	1-methyl-pyrazole	399	2.70	377	23	76	4 nM	0.31	6
1.34	H	319	2.19	≥395	11	69	25 nM	0.36	5
1.44	Me	333	2.68	300	32	58	31 nM	0.34	5
1.45	cyclopentyl	386	4.05	336	290	58	2800 nM	0.21	1
1.46	Ph	395	4.30	485	155	58	-[h]	-	-

[a]logD, Chrom log D at pH 7.4; [b]Chemiluminescent nitrogen detection (CLND) kinetic aqueous solubility assay; [c]P_{app} permeability pH 7.4 assay; [d]Topological polar surface area (PSA) determined using JChem.[54] [e]IC_{50} in LPC choline release assay; [f] Ligand efficiency index, LEI = pIC_{50}/HA, where HA denotes the number of non-hydrogen atoms; [g]Lipophilic ligand efficiency, LLE = pIC_{50} − logD. [h]Unable to determine due to solubility issues in the assay medium.

As expected, the compounds with the more lipophilic *N*-substituents, cyclopentyl (**1.45**) and phenyl (**1.46**), had increased logD$_{7.4}$, lowered PSA, and increased permeability. All the analogues in this series had reasonable aqueous solubility when measured using a high throughput screening solubility assay, including compound **1.46** with which we had observed poor solubility in the assay medium. By comparing compounds **1.22** and **1.51** we were able to determine the effects that the pyridine ring has on the physicochemical properties of this chemotype (Table 1.19).
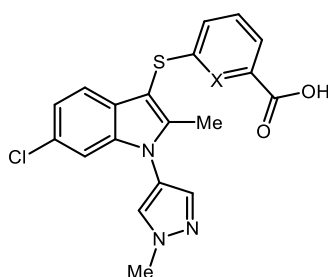
Table 1.19. Physicochemical properties of benzoic acid vs. pyridyl.

Compound	X	MW	logD$_{7.4}$[a]	Sol.[b] (µM)	P$_{app}$[c] (nm s^{-1})	PSA[d]	IC$_{50}$[e]	LEI[f]	LLE[g]
1.22	N	399	2.70	377	23	76	4 nM	0.31	6
1.51	CH	398	3.36	556	64	63	11 nM	0.30	5

[a]logD, Chrom log D at pH 7.4; [b]Chemiluminescent nitrogen detection (CLND) kinetic aqueous solubility assay; [c]P$_{app}$ permeability pH 7.4 assay; [d]Topological polar surface area (PSA) determined using JChem.[54] [e]IC$_{50}$ in LPC choline release assay; [f] Ligand efficiency index, LEI = pIC$_{50}$/HA, where HA denotes the number of non-hydrogen atoms; [g]Lipophilic ligand efficiency, LLE = pIC$_{50}$ − logD.

Although the activities and the LEI values of these two analogues are comparable, the lower logD$_{7.4}$ of **1.22** improves the LLE, giving it an excellent LLE value of 6. At first glance this can make **1.22** appear to be a more attractive molecule; however, the

introduction of the pyridine increases the PSA and lowers permeability of **1.22** and thus **1.51** is perhaps the more attractive analogue.

1.3.7 Synthesis

The known ATX inhibitor indole **1.22** along with analogues of Table 1.7, compounds **1.44**-**1.49**, and **1.69**-**1.71** were synthesised by two other members of our research group,[‡] full details of the preparation of these compounds can be found in our recent report.[73] An exemplar synthesis is shown in Scheme 1.4 with the preparation of **1.51**. Starting from the commercially available thiol, the required ketone was introduced via an alkylation reaction to access **1.74**. Initial syntheses followed the reported Fischer indole protocols from the Amira Pharmaceuticals patents, which involved refluxing in tBuOH for an extended period of time, and subsequent addition of two acid catalysts: HCl and AcOH. However, in the exploration of this key step it was discovered that a number of the Fischer indole reactions proceeded by refluxing the ketone with the respective hydrazine hydrochloride in EtOH without an additional acid catalyst. This provided a simpler method for the preparation of these indoles, and the reactions proceeded with fewer unwanted byproducts, thus, easing the purification process. The Fischer indole reaction to access the 6-Cl substituted product also produces the unwanted 4-Cl, these were successfully separated on silica to isolate the desired 6-Cl regioisomer **1.76** as the major product.

[‡] Analogues of Table 1.7, **1.45**-**1.49**, and **1.69**-**1.71** prepared by Dr Diana Castagna. Compound **1.44** was prepared by Dr Paloma Garcia.

Scheme 1.5. Synthesis of the Compound **1.51**.[a]
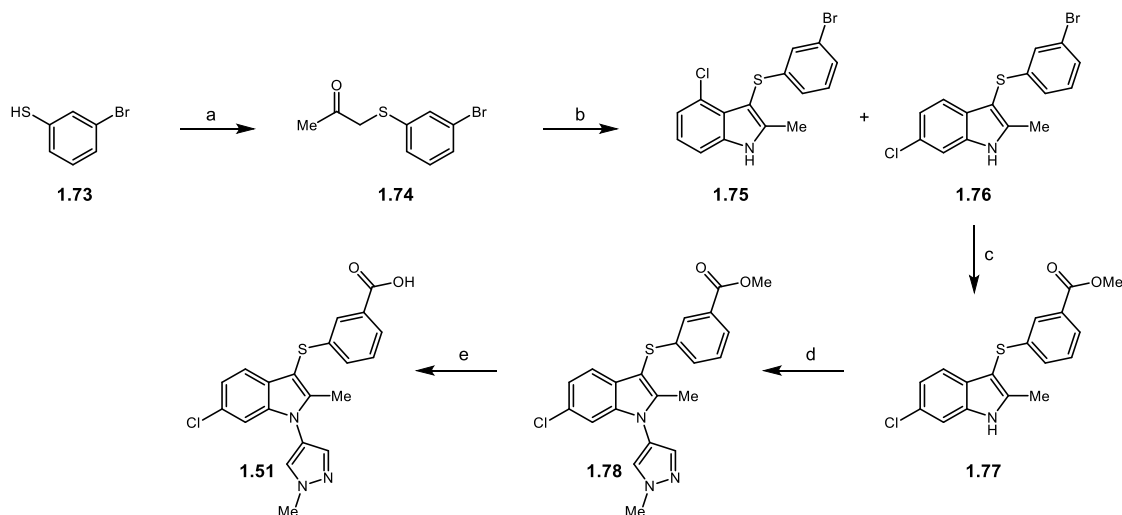
[a]Reagents and conditions: (a) chloroacetone, DIPEA, THF, reflux, 16 h, 83%; (b) EtOH, 3-chlorophenylhydrazine hydrochloride, reflux, 16 h, 22% **1.76**; (c) Herrmann's catalyst, $Mo(CO)_6$, [tBu$_3$PH]BF$_4$, DBU, MeOH/MeCN, 70 °C, 16 h, 77%; (d) 4-bromo-1-methylpyrazole, K_2CO_3, CuO, pyridine, 150 °C, 48 h, 59%; (e) 2 M aq. NaOH, THF, RT, 3 h, 24%.

The next step employed a methoxycarbonylation reaction to form the ester functionality and afford key intermediate **1.77**. Introduction of the 1-methyl-pyrazole substitution to the indole nitrogen in the penultimate step proved to be challenging, requiring harsh conditions and long reaction times during which partial hydrolysis of the ester occurred. As a result, the substitution reaction was often telescoped into the final step to fully hydrolyse the ester and produce the desired acid. From intermediate **1.76** a series of substitution reaction were carried out to investigate the SAR associated with the substituent on the indole nitrogen. In place of the 1-methyl-pyrazole three alternative substituents were used; methyl, cyclopentyl, and phenyl. The aliphatic substituents were introduced by an alkylation reaction using the corresponding alkyl halide and NaH. Following the alkylation step, hydrolysis of the corresponding ester revealed the desired carboxylic acid. The phenyl substituent was introduced using an alternative Ullmann coupling (see experimental section) to that

used previously with the 1-methyl-pyrazole. Using these approaches, the analogues

1.50-1.60 were successfully synthesised.

The oxygen-linked benzoic acid subset was synthesised using the Fischer indole

reaction that was employed with previous analogues described in Scheme 1.4.

Unfortunately, efforts to synthesise the corresponding ether linked pyridyl

compounds were unsuccessful (Scheme 1.6).

Scheme 1.6. Attempted synthesis of ether linked pyridyl analogues.[a]
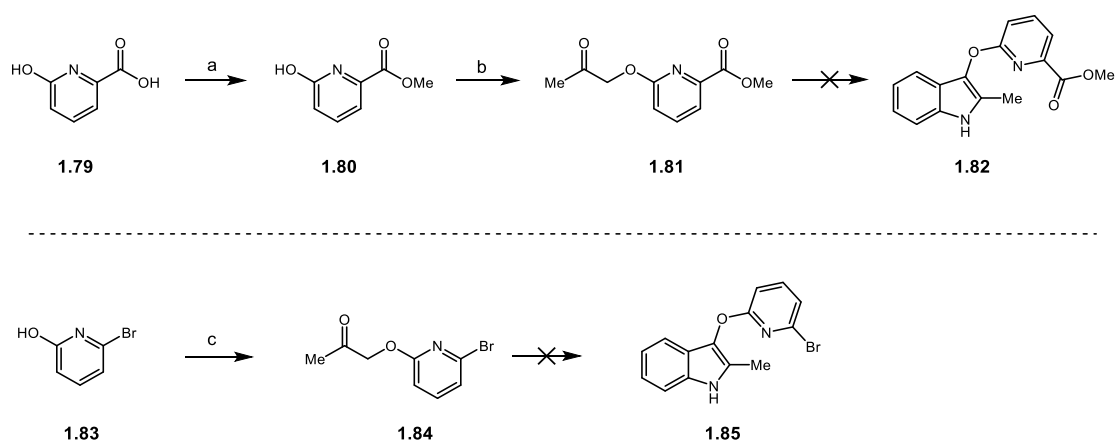
[a]Reagents and conditions: (a) thionyl chloride, MeOH, reflux, 16 h, 53%; (b) chloroacetone, K_2CO_3, acetone, reflux, 16 h, 87%; (c) chloroacetone, K_2CO_3, acetone, reflux, 16 h, 34%.

A series of Fischer indole reactions were attempted using intermediate **1.81**,

however, no desired product was observed. To determine whether the issue was with

the starting material **1.81**, an alternative ketone was then employed (**1.84**) but again

the desired indole was not observed with the dealkyation product **1.83** being the

major species isolated from the attempted Fischer indole reaction. It was at this point

that the Fischer indole synthesis was determined to be an unsuitable method for the

synthesis of the ether linked pyridyl analogues and an alternative route were

investigated (Scheme 1.7). A literature search of indoles ether linked to pyridines

revealed sparse precedent for compound such as **1.82**, **1.85** and **1.89**. One example

had been published by Ma and Ackermann,[74] who report to have synthesised their ether bond via a copper-catalysed arylation of phenols previously optimised by Maiti and Buchwald.[75]

Scheme 1.7. Alternative route towards the synthesis of ether linked pyridyl analogues.[a]
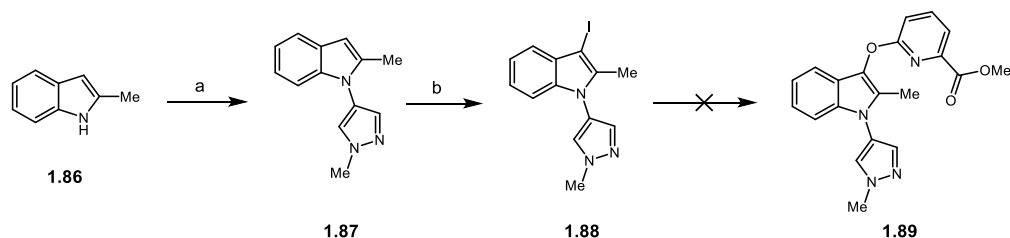
[a]Reagents and conditions: (a) 4-bromo-1-methylpyrazole, K_2CO_3, CuO, pyridine, 150 °C, 48 h, 42%; (b) I_2, KOH, DMF, RT, 16 h, 49%.

Through the synthesis of iodo intermediate **1.88** it was hoped that a cross-coupling would allow access to the desired ether linked pyridyl analogues. Unfortunately, this route was not successful and as a result the ether linked pyridyl analogues were not pursued any further (for attempted synthesis, see experimental section).

The Fischer indole synthesis was also attempted in the preparation of the methylene linked analogues (reaction not shown); however, this reaction was also unsuccessfully and an alternative synthetic strategy was employed. Using a two-step alkylation with the corresponding aldehyde, the required methylene linked aryl was introduced to the 3-position of the indole. Subsequent methoxycarbonylation, followed by substitution of the indole nitrogen, and a final hydrolysis, afforded the desired analogue **1.62** (Scheme 1.8).

Scheme 1.8. Synthesis of methylene linked analogue **1.62**.[a]
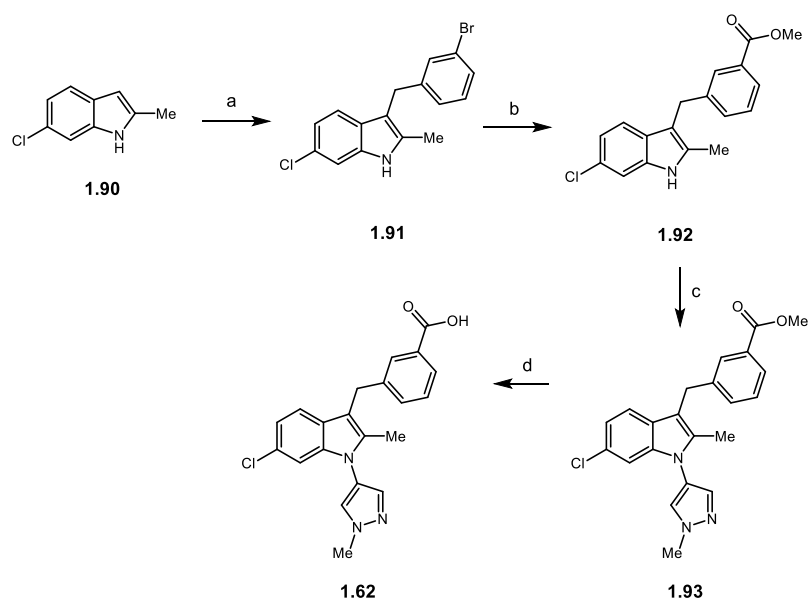
[a]Reagents and conditions: (a)(i) 3-bromobenzaldehyde, DCM, RT, 20 min (ii) Et$_3$SiH, TFA, DCM, RT, 1 h, 73%; (b) Herrmann's catalyst, Mo(CO)$_6$, [tBu$_3$PH]BF$_4$, DBU, MeOH/MeCN (1:4), 70 °C, 16 h, 67%; (c) 4-bromo-1-methylpyrazole, K$_2$CO$_3$, CuO, pyridine, 150 °C, 48 h; (d) 2 M aq. NaOH, THF, RT, 4 h, 2% over 2 steps.

It was discovered that by reordering the synthetic steps and installing the 1-methyl-pyrazole at an earlier stage, the *N*-substitution proceeded in a much improved yield than the late stage introduction used in previous synthesis. This alternative route, shown in Scheme 1.9, was then used to synthesise the remaining targets in this series of methylene linked analogues. By employing the two-step alkylation to intermediate **1.72** using 6-bromopicolinaldehyde the desired methylene linker was afforded in good yield.

Scheme 1.9. Synthesis of methylene linked analogue 1.81.[a]
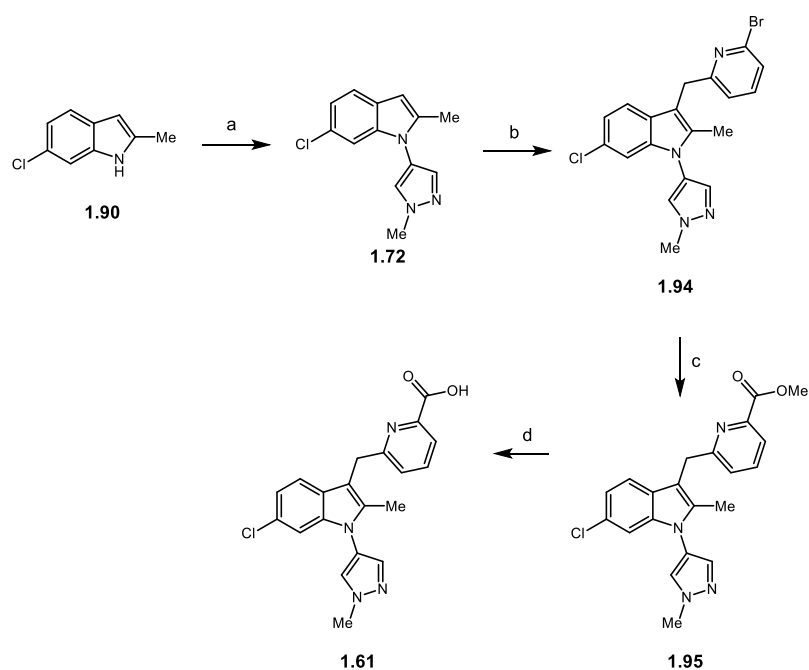
[a]Reagents and conditions: (a) 4-bromo-1-methylpyrazole, K_2CO_3, CuO, pyridine, 150 °C, 48 h, 79%; (b) (i) 6-bromopicolinaldehyde, DCM, RT, 20 min (ii) Et_3SiH, TFA, DCM, RT, 1 h, 56%; (c) Herrmann's catalyst, $Mo(CO)_6$, [tBu$_3$PH]BF$_4$, DBU, MeOH/MeCN (1:4), 70 °C, 16 h, 76%; (d) 2 M aq. NaOH, THF, RT, 16 h, 48%.

From the bromo intermediate **1.94** the ester functionality was introduced via a methoxycarbonylation reaction to give **1.95**, followed by hydrolysis to reveal the desired acid **1.61**. This route also provided the deletion analogue **1.72**, which did not feature the thiopyridine carboxylic acid motif of the patent compound **1.22**. This analogue was tested to further explore the SAR.

1.4 Conclusion

A series of analogues to explore the atypical ATX inhibitor **1.22**, previously reported by Amira Pharmaceuticals, were designed and synthesised. Through the biological assessment of our compound library using two different ATX assays, we established that some compounds inhibit hydrolysis of the natural substrate (LPC) but only partially inhibit activity with an artificial substrate. This suggested a binding mode outside of the orthosteric site which was further supported by kinetic studies and identified this chemotype as noncompetitive ATX inhibitors. A crystal structure of ATX bound to compound **1.21** confirmed that it binds within the tunnel, a recently described allosteric binding site.

This work has shown the importance of cross screening with an assay that uses the natural substrate to determine the true inhibitory activity of compounds for this enzyme. Using our biochemical and structural data, we were able to identify key SAR for this chemotype, in particular confirming the importance of the 6-Cl substituent. Studies carried out *in silico* were successful in identifying a hydrophobic cleft with which the 6-Cl can interact. These key interactions were later confirmed by the crystal structure.

Through the measurement of the physicochemical properties, this chemotype is shown to have consistently good aqueous solubility, with the more potent analogues possessing excellent LLE. This work has provided a more detailed insight into the SAR and binding mode of these small molecule ATX inhibitors, which could aid the design of new novel ATX inhibitors with non-lipid-like scaffolds.

1.5   Future Work

The SAR clearly identified the importance of the 6-Cl indole to the potency of this chemotype. It was shown that this substituent, which has a van der Waals (VDW) radius of 175 pm, was an ideal size for the binding, with the smaller fluoro (147 pm) or the larger methyl (200 pm) causing a loss of activity. One analogue that was not synthesised in this project was the 6-Br indole **1.96**, which with a VDW radius of 185 pm would provide further information about the ideal size of the 6-position substituent, Figure 1.18. Furthermore, it was found that the thioether linker was superior to the ether or methylene. Two further analogues that could provide more insight into the effect of the linker are the sulfoxide (**1.97**) or the sulfone (**1.98**). Based on the *in silico* studies, the thioether did not take part in any binding interactions; however, by oxidising the sulfur additional interactions could be targeted through the oxygen(s).
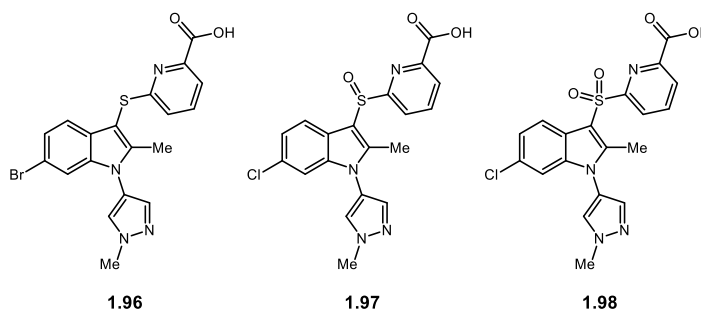
Figure 1.18. Further analogues to expand the SAR of **1.22**.

The assays used in this project tested the activity of the inhibitors against ATX *in vitro*. Further cell based assays should be carried out to determine whether these inhibitors show activity *in vivo*. Amira had reported that this chemotype showed activity in a number of *in vivo* assays, but no results were disclosed, thus further

screening using *in vivo* assays would provide valuable information for this chemotype.

In the introduction to this chapter the similarities between the compound of interest **1.22** and the analogue **1.21** recently reported by PharmAkea were noted. These two compounds share a number of structural similarities, thus it is perhaps unsurprising that they are both non-competitive inhibitors, which bind within the tunnel region of the ATX active site. PharmAkea also reported the compound **1.99**, but this analogue was found to bind within the hydrophobic pocket of ATX, Figure 1.19.[45] The hydrophobic pocket of ATX is not observed in the other members of the enzyme family, and thus inhibitors that bind to this region could provide better selectivity profiles than those that bind the catalytic site or tunnel.[76] Accordingly, an SAR exploration of **1.99** could provide insight into why this analogue binds differently to that of **1.22** and **1.21**. Furthermore, this SAR could provide the information required to design a potent and selective inhibitor of ATX with the good pharmacokinetic properties associated with these small molecule chemotypes.
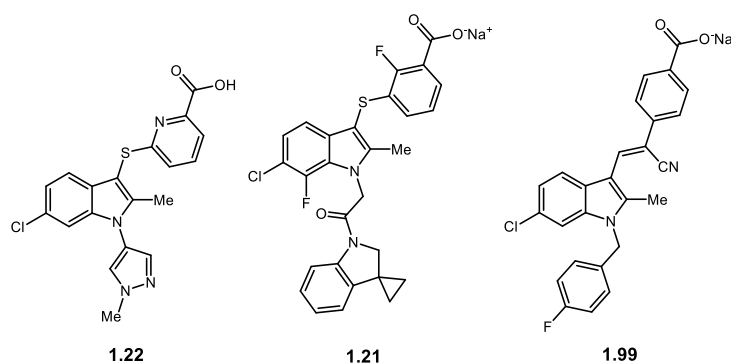
Figure 1.19. Comparison of tunnel binding compounds **1.21** and **1.22** vs. the hydrophobic pocket binding compound **1.99**.

1.6   Experimental

1.6.1   General Techniques

All reagents and solvents were obtained from commercial suppliers and were used without further purification unless otherwise stated. Purification was carried out according to standard laboratory methods.[77]

1.6.1.1   Purification of Solvents

i)   All solvents used for dry reactions were obtained from a PureSolv SPS-400-5 solvent purification system. These solvents were transferred to and stored in a septum-sealed oven-dried flask over previously activated 4 Å molecular sieves and purged with and stored under nitrogen.

ii)   Dichloromethane (DCM), ethyl acetate (EtOAc), methanol (MeOH), petroleum ether 40-60°, and cyclohexane for purification purposes were used as obtained from suppliers without further purification.

1.6.1.2   Purification of Starting Material

i)   Bromocyclopentane was distilled over anhydrous calcium carbonate under reduced pressure prior to use.

1.6.1.3   Experimental Details

i)   Air-sensitive reactions were carried out using conventional glassware. The glassware was oven-dried and purged with N_2 before use.

ii)   Purging refers to a vacuum/nitrogen-refilling procedure.

iii)   Reactions were carried out at 0 °C using ice/water baths.

iv)   Room temperature was generally ca. 18 °C.

v)   Reactions were carried out at elevated temperatures using a temperature-regulated hotplate/stirrer.

1.6.1.4   Purification of Products

i)   Thin layer chromatography was carried out using Merck silica plates coated with fluorescent indicator UV254. These were analysed under 254 nm UV light or developed using potassium permanganate solution.

ii)   Silica chromatography was carried out using ZEOprep 60 HYD 40-63 μm silica gel or IST Isolute Flash silica cartridges.

iii)   Reverse-phase HPLC purification was carried out using a Gilson 151 preparative HPLC using an Agilent Zorbax SB-C18 column at room temperature. Purification was performed using a gradient method, eluting with 5-80% MeCN/H_2O over 15 minutes at a flow rate of 10 mL/min. Fractions were collected automatically using a GX-271 liquid handler.

iv)   Reverse-phase ultra-performance liquid chromatography (UPLC) purification was carried out using an Acquity UPLC CSH C18 column at 40 °C. Purification was performed using a gradient method, eluting with 5-97% MeCN/10 mM $(NH_4)HCO_3$ in H_2O.

v)   Mass-directed automatic purification (MDAP) was carried out using a ZQ MS using alternate-scan positive and negative electrospray and a summed UV wavelength of 210-350 nm and an Xbridge C18 column (100 mm x 19 mm, 5 μm packing diameter, 20 mL/min flow rate) or Xbridge C18 column (150 mm x 30 mm, 5 μm packing diameter, 40 mL/min flow rate). Purification was performed using a gradient method at room temperature with the mobile phases as (A) 10 mM aqueous ammonium bicarbonate solution, adjusted to pH 10 with 0.88 M aqueous ammonia and (B) MeCN.

1.6.1.5 Analysis of Products

i)   Fourier Transformed Infra-Red (FTIR) spectra were obtained on one of three machines: (a) Shimadzu IRAffinity-1 machine; (b) A2 Technologies ATR spectrometer; (c) Agilent 5500a FTIR ATR.

ii) ^{1}H, ^{13}C, and ^{19}F NMR spectra were obtained on a one of four Bruker NMR spectrometers: (a) Advance III HD console, Ascend 500 MHz magnet, BBO smart probe; (b) Advance III console, 400 MHz Ultrashield magnet, Prodigy BBO probe, BB-H&F-D-05 Z; (c) Advance II console, 400 MHz 9.4 T Oxford unshielded magnet, BBFO-z-ATMA probe; (d) Advance III console, 600 MHz 14.1 T Bruker Ultrashield magnet, TBI-z probe. Chemical shifts are reported in ppm and coupling constants are reported in Hz with CDCl$_3$ referenced at 7.26 (^{1}H) and 77.16 ppm (^{13}C), CO(CD$_3$)$_2$ at 2.05 (^{1}H) and 29.84 ppm (^{13}C), and DMSO-d_6 at 2.50 (^{1}H) and 39.52 ppm (^{13}C), respectively.

iii) High-resolution mass spectra (HRMS) were obtained through analysis at the EPSRC National Mass Spectrometry Facility, University of Wales, Swansea or on a Micromass Q-Tof Ultima hybrid quadrupole time-of-flight mass spectrometer, with analytes separated on an Agilent 1100 Liquid Chromatograph equipped with a Phenomenex Luna C18(2) reversed phase column (100 mm x 2.1 mm, 3 μm packing diameter). LC conditions were 0.5 mL/min flow rate, 35 ºC, injection volume 2-5 μL. Gradient elution with (A) H$_2$O containing 0.1% (v/v) formic acid and (B) MeCN containing 0.1% (v/v) formic acid. Gradient conditions were initially 5% B, increasing linearly to 100% B over 6 min, remaining at

100% B for 2.5 min then decreasing linearly to 5% B over 1 min followed by an equilibration period of 2.5 min prior to the next injection.

1.6.2   General Experimental Procedures
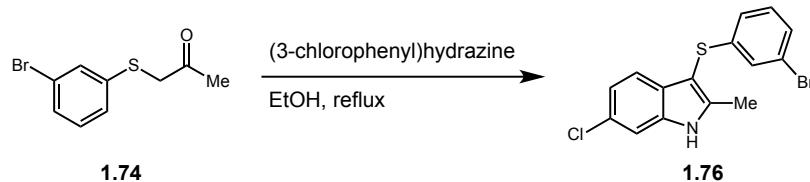
General Procedure A: Fischer Indole synthesis, for example the synthesis of 3-((3-bromophenyl)thio)-6-chloro-2-methyl-1*H*-indole (1.76). Prepared according to a modified version of the procedure described by Amira Pharmaceuticals.[47-49] A solution of (3-chlorophenyl)hydrazine hydrochloride (1.5 g, 8.18 mmol, 1 equiv.) and 1-((3-bromophenyl)thio)propan-2-one (**1.74**) (2 g, 8.18 mmol, 1 equiv.) in EtOH (40 mL, 0.2 M) was refluxed until the reaction was complete by TLC. The reaction mixture was then allowed to return to room temperature, concentrated under vacuum, and the residue purified using silica chromatography, eluting with 0-10% EtOAc/cyclohexane, to afford the title compound as a cream amorphous solid (639 mg, 22%).
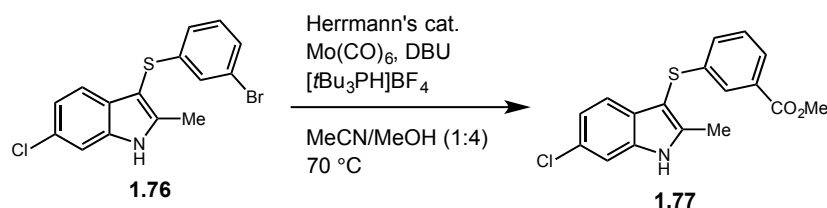
General Procedure B: Methoxycarbonylation. For example, **the synthesis of methyl 3-((6-chloro-2-methyl-1*H*-indol-3-yl)thio)benzoate (1.77).** *trans*-Bis(acetato)bis[*o*-(di-*o*-tolylphosphino)benzyl]dipalladium(II) (90 mg, 0.0959 mmol, 5 mol% was added to a solution of 3-((3-bromophenyl)thio)-6-chloro-2-methyl-1*H*-indole (**1.76**) (639 mg, 1.81 mmol, 1 equiv.), Mo(CO)$_6$ (478 mg, 1.81 mmol, 1

equiv.), [tBu$_3$PH]BF$_4$ (112 mg, 0.386 mmol, 20 mol%), and DBU (433 μL, 2.90 mmol, 1.6 equiv.) in MeCN/MeOH (20 mL, 1:4, 0.3 M). The reaction mixture was heated to 70 °C for 16 h then allowed to return to room temperature, concentrated under vacuum, and the residue purified using silica chromatography, eluting with 0-20% EtOAc/petroleum ether, to afford the title compound as a brown solid (463 mg, 77%).
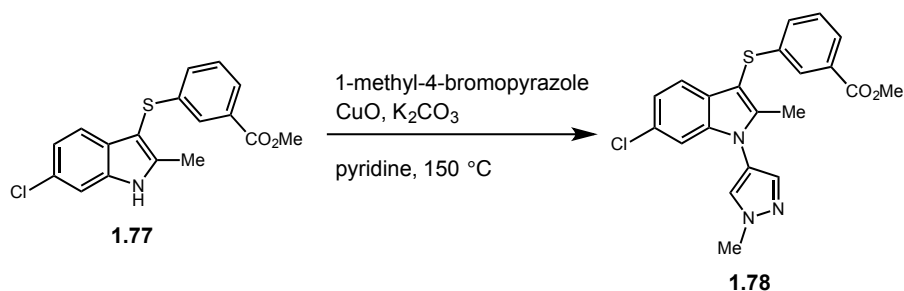
General Procedure C: *N*-Arylation, for example the synthesis of methyl 3-((6-chloro-2-methyl-1-(1-methyl-1*H*-pyrazol-4-yl)-1*H*-indol-3-yl)thio) benzoate (1.78). Prepared according to a modified version of the procedure described by Amira Pharmaceuticals.[47-49] To a microwave vial was added methyl 3-((6-chloro-2-methyl-1*H*-indol-3-yl)thio)benzoate (**1.77**) (100 mg, 0.302 mmol, 1 equiv.), CuO (48 mg, 0.604 mmol, 2 equiv.), K$_2$CO$_3$ (54 mg, 0.393 mmol, 1.3 equiv.), and 1-methyl-4-bromopyrazole (94 μL, 0.906 mmol, 3 equiv.). The vial was then sealed and purged with N$_2$ before the addition of pyridine (1 mL, 0.3 M). The reaction mixture was then heated to 150 °C for 48 h. The reaction mixture was then allowed to return to room temperature, diluted with EtOAc (15 mL), and washed with H$_2$O (3 x 10 mL). The organic layer was collected, dried (hydrophobic frit), concentrated under vacuum, and the residue purified using silica chromatography, eluting with 50% EtOAc/petroleum ether, to afford the title compound as a cream amorphous solid (74 mg, 59%).

1.78 → **1.51**
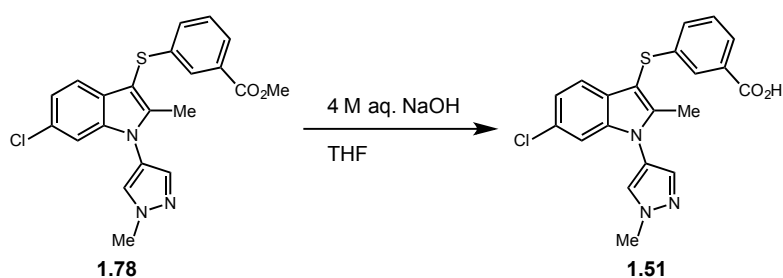
General Procedure D: Ester hydrolysis, for example the synthesis of 3-((6-chloro-2-methyl-1-(1-methyl-1*H*-pyrazol-4-yl)-1*H*-indol-3-yl)thio)benzoic acid (1.51). To a round bottomed flask was added a solution of methyl 3-((6-chloro-2-methyl-1-(1-methyl-1*H*-pyrazol-4-yl)-1*H*-indol-3-yl)thio)benzoate (**1.78**) (68 mg, 0.165 mmol, 1 equiv.) and 4 M aq. NaOH (1 mL) in THF (1 mL, 0.2 M) and the reaction stirred at room temperature until complete by TLC. The reaction mixture was then concentrated under vacuum to a residue that was purified using silica chromatography, eluting with 10% MeOH/DCM, to afford the title compound as a cream amorphous solid (16 mg, 24%).

1.100 → **1.101**
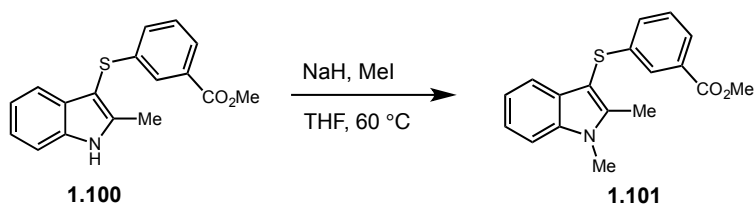
General Procedure E: *N*-Alkylation of the indole. For example, the synthesis of methyl 3-((1,2-dimethyl-1*H*-indol-3-yl)thio)benzoate (1.101). A solution of methyl 3-((2-methyl-1*H*-indol-3-yl)thio)benzoate (**1.100**) (200 mg, 0.673 mmol, 1 equiv.), and NaH 60% w/w (54 mg, 1.35 mmol, 2 equiv.) in THF (3 mL, 0.2 M) was heated to 60 °C for 1 h before adding MeI (84 μL, 1.35 mmol, 2 equiv.). The reaction mixture was heated to 60 °C for 16 h then allowed to return to room temperature, concentrated under vacuum, and the residue purified using silica chromatography,

eluting with 10% EtOAc/petroleum ether, to afford the title compound as a pale yellow amorphous solid (71 mg, 34%).
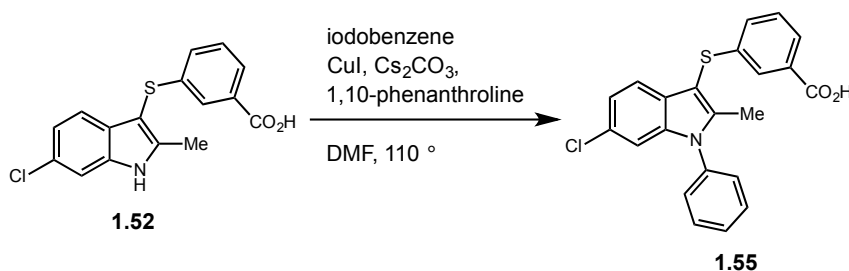
General Procedure F: Ullmann coupling, for example the synthesis of 3-((6-chloro-2-methyl-1-phenyl-1*H*-indol-3-yl)thio)benzoic acid (1.55). Prepared according to a modified version of a literature procedure for an Ullmann coupling.[78] To a microwave vial was added 3-((6-chloro-2-methyl-1*H*-indol-3-yl)thio)benzoic acid (**1.52**) (65 mg, 0.205 mmol, 1 equiv.), iodobenzene (46 µL, 0.409 mmol, 2 equiv.), CuI (19 mg, 0.102 mmol, 0.5 equiv.), Cs_2CO_3 (133 mg, 0.409 mmol, 2 equiv.), and 1,10-phenanthroline (37 mg, 0.205 mmol, 1 equiv.). The reaction vessel was then sealed and purged with N_2 before addition of DMF (1 mL, 0.2 M). The reaction was then heated to 110 °C for 48 h. The reaction mixture was then diluted with H_2O (15 mL) and extracted with EtOAc (3 x 10 mL). The combined organics were dried (hydrophobic frit), and concentrated under vacuum to a residue that was purified by reverse-phase HPLC to afford the title compound as a white amorphous solid (11 mg, 14%).
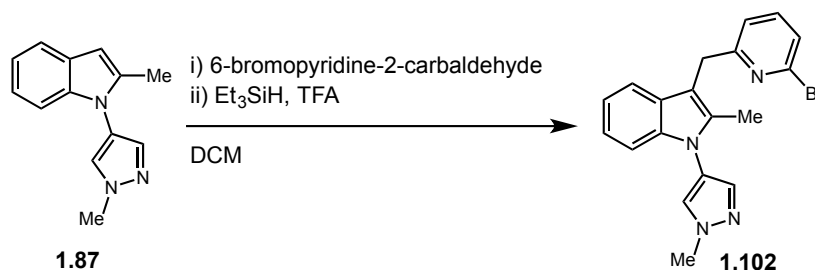
General Procedure G: Two-step alkylation. For example, the synthesis of 3-((6-bromopyridin-2-yl)methyl)-2-methyl-1-(1-methyl-1*H*-pyrazol-4-yl)-1*H*-indole (1.102). 6-Bromopyridine-2-carbaldehyde (91 mg, 0.488 mmol, 1.03 equiv.) was added to a solution of 2-methyl-1-(1-methyl-1*H*-pyrazol-4-yl)-1*H*-indole (**1.87**) (100 mg, 0.474 mmol, 1 equiv.) in DCM (2 mL, 0.2 M) at 0 °C and stirred for 20 min. Et₃SiH (84 µL, 0.529 mmol, 1.1 equiv.) and TFA (47 µL, 0.610 mmol, 1.3 equiv.) were then added to the reaction mixture and stirred for a further 1 h, during which the reaction mixture was allowed to return to room temperature. The resulting solution was then quenched with sat. aq. NaHCO₃ and extracted using DCM (20 mL). The organic layer was collected, dried (hydrophobic frit), concentrated under vacuum, and the residue purified using silica chromatography, eluting with 20-60% EtOAc/petroleum ether, to afford the title compound as a yellow gum (158 mg, 87%).

1.6.3   Preparation of Compound 1.50-1.68, 1.72-1.95, and 1.100-1.109.

For preparation of compounds **1.22**, **1.24-1.49**, and **1.69-1.71** see Miller *et al.*[73]

Synthesis of 3-((4-chloro-2-methyl-1*H*-indol-3-yl)thio)benzoic acid (1.50) and 3-((6-chloro-2-methyl-1*H*-indol-3-yl)thio)benzoic acid (1.52). Prepared according to General Procedure A using (3-chlorophenyl)hydrazine hydrochloride (3.3 g, 18.6 mmol, 1 equiv.) and 1-((3-bromophenyl)thio)propan-2-one (**1.74**) (4.6 g, 18.6 mmol, 1 equiv.) in EtOH (90 mL, 0.2 M). Following aqueous work-up, the reaction mixture was then used in the next step without further purification. The crude material was used according to General Procedure B using *trans*-bis(acetato)bis[*o*-(di-*o*-tolylphosphino)benzyl]dipalladium(II) (200 mg, 0.213 mmol, 1 mol%), Mo(CO)₆ (4.9 g, 18.6 mmol, 1 equiv.), [*t*Bu₃PH]BF₄ (1.08 g, 3.72 mmol, 20 mol%), and DBU

(4.2 mL, 27.9 mmol, 1.5 equiv.) in MeCN/4 M aq. NaOH (60 mL, 1:4, 0.3 M). 1 g of crude material was purified by MDAP to afford 3-((4-chloro-2-methyl-1H-indol-3-yl)thio)benzoic acid (**1.50**) as a cream amorphous solid (100 mg, 2% over 2 steps) and 3-((6-chloro-2-methyl-1H-indol-3-yl)thio)benzoic acid (**1.52**) as a cream amorphous solid (70 mg, 1% over 2 steps). 3-((4-Chloro-2-methyl-1H-indol-3-yl)thio)benzoic acid (**1.50**): ^{1}H NMR (400 MHz, CO(CD$_3$)$_2$) δ: 11.04 (br s, 1H), 7.80-7.69 (m, 2H), 7.40 (dd, J = 7.8, 1.0 Hz, 1H), 7.35-7.27 (m, 1H), 7.23 (d, J = 8.2 Hz, 1H), 7.13-6.98 (m, 2H), 2.53 (s, 3H). CO$_2$H proton not observed. ^{13}C NMR (101 MHz, CO(CD$_3$)$_2$) δ: 167.9, 145.3, 143.0, 138.5, 132.3, 130.2, 129.6, 126.9, 126.7, 126.5, 125.8, 123.1, 122.3, 111.2, 97.7, 12.0. υ$_{max}$ (neat): 3410, 2869, 2658, 2543, 1681, 1569, 1537 cm^{-1}. HRMS: exact mass calculated for [M+H]$^+$ (C$_{16}$H$_{13}$ClNO$_2$S) m/z requires 318.0174, m/z found 318.0167. 3-((6-Chloro-2-methyl-1H-indol-3-yl)thio)benzoic acid (**1.52**): ^{1}H NMR (400 MHz, CO(CD$_3$)$_2$) δ: 10.84 (br s, 1H), 7.76-7.72 (m, 2H), 7.47 (d, J = 1.8 Hz, 1H), 7.40 (d, J = 8.4 Hz, 1H), 7.32 (app t, J = 7.5 Hz, 1H), 7.26-7.23 (m, 1H), 7.07 (dd, J = 8.4, 1.9 Hz, 1H), 2.53 (s, 3H). CO$_2$H proton not observed. ^{13}C NMR (101 MHz, CO(CD$_3$)$_2$) δ: 167.3, 144.3, 141.0, 137.4, 132.1, 130.5, 129.8, 129.7, 128.0, 127.2, 126.9, 121.5, 120.0, 112.1, 98.5, 12.0. υ$_{max}$ (neat): 3385, 2850, 2665, 2549, 1667, 1591, 1570, 1539 cm^{-1}. HRMS: exact mass calculated for [M+H]$^+$ (C$_{16}$H$_{13}$ClNO$_2$S) m/z requires 318.0174, m/z found 318.0163.

Synthesis of 3-((6-chloro-2-methyl-1-(1-methyl-1H-pyrazol-4-yl)-1H-indol-3-yl)thio)benzoic acid (1.51). Prepared according to General Procedure D using methyl 3-((6-chloro-2-methyl-1-(1-methyl-1H-pyrazol-4-yl)-1H-indol-3-yl)thio) benzoate (**1.78**) (68 mg, 0.165 mmol, 1 equiv.) and 4 M aq. NaOH (1 mL) in THF (1 mL, 0.2 M). Purified using silica chromatography, eluting with 10% MeOH/DCM, to

afford the title compound as a cream amorphous solid (16 mg, 24%). ^{1}H NMR (500 MHz, CO(CD$_3$)$_2$): δ 11.29 (br s, 1H), 8.09 (s, 1H), 7.80 (s, 1H), 7.76 (d, J = 7.6 Hz, 1H), 7.72 (s, 1H), 7.46 (d, J = 8.4 Hz, 1H), 7.35 (app t, J = 7.7 Hz, 1H), 7.29 (d, J = 7.9 Hz, 1H), 7.22 (s, 1H), 7.14 (dd, J = 8.4, 1.7 Hz, 1H), 4.04 (s, 3H), 2.42 (s, 3H). ^{13}C NMR (126 MHz, CO(CD$_3$)$_2$): δ 146.4, 140.4, 140.0, 137.2, 132.3, 130.8, 130.0, 129.2, 129.0, 128.8, 127.5, 127.2, 122.4, 120.3, 119.3, 111.4, 100.0, 39.9, 11.7. One carbon not observed/coincident. υ$_{max}$ (neat): 2920, 2848, 1718, 1571, 1537 cm^{-1}. HRMS: exact mass calculated for [M-H]$^-$ (C$_{20}$H$_{15}$ClN$_3$O$_2$S) m/z requires 398.0548, m/z found 398.0539.

Synthesis of 3-((6-chloro-1,2-dimethyl-1H-indol-3-yl)thio)benzoic acid (1.53). Prepared according to General Procedure F using methyl 3-((6-chloro-2-methyl-1H-indol-3-yl)thio)benzoate (**1.77**) (200 mg, 0.604 mmol, 1 equiv.), NaH 60% w/w (193 mg, 4.82 mmol, 8 equiv.) and MeI (150 μL, 2.41 mmol, 4 equiv.) in DMF (3 mL, 0.2 M). Following aqueous work-up, the reaction mixture was then used in the next step without further purification. The crude material was used according to General Procedure C using 4 M aq. NaOH (5 mL) in THF (3 mL, 0.2 M). Purified by reverse-phase HPLC to afford the title compound as a cream amorphous solid (2 mg, 1% over 2 steps). ^{1}H NMR (400 MHz, CDCl$_3$) δ: 7.82-7.73 (m, 2H), 7.43 (d, J = 8.4 Hz, 1H), 7.35 (d, J = 1.7 Hz, 1H), 7.23 (app t, J = 7.7 Hz, 1H), 7.19-7.13 (m, 1H), 7.09 (dd, J = 8.4, 1.8 Hz, 1H), 3.75 (s, 3H), 2.51 (s, 3H). CO$_2$H proton not observed. ^{13}C NMR (151 MHz, CDCl$_3$) δ: 170.1, 144.0, 140.6, 137.7, 130.6, 129.8, 129.0, 128.2, 128.1, 127.2, 126.6, 121.4, 119.8, 109.5, 98.0, 30.7, 11.1. υ$_{max}$ (neat): 3436, 2900, 2651, 2543, 1679, 1574 cm^{-1}. HRMS: exact mass calculated for [M-H]$^-$ (C$_{17}$H$_{13}$ClNO$_2$S) m/z requires 332.0330, m/z found 332.0324.

Synthesis of 3-((6-chloro-1-cyclopentyl-2-methyl-1*H*-indol-3-yl)thio)benzoic acid

(1.54). Prepared according to General Procedure F using methyl 3-((6-chloro-2-methyl-1*H*-indol-3-yl)thio)benzoate (**1.77**) (25 mg, 0.0755 mmol, 1 equiv.), NaH 60% w/w (24 mg, 0.602 mmol, 8 equiv.) and bromocyclopentane (32 μL, 0.301 mmol, 4 equiv.) in DMF (1 mL, 0.1 M). Following aqueous work-up, the reaction mixture was then used in the next step without further purification. The crude material was used according to General Procedure C using 4 M aq. NaOH (1 mL) in THF (1 mL, 0.1 M). Purified using silica chromatography, eluting with 0-20% EtOAc/petroleum ether, to afford the title compound as a pale yellow gum (2 mg, 7% over 2 steps). ^{1}H NMR (400 MHz, CO(CD$_3$)$_2$) δ: 7.78-7.69 (m, 2H), 7.59 (d, *J* = 1.7 Hz, 1H), 7.46 (d, *J* = 8.4 Hz, 1H), 7.32 (app t, *J* = 7.8 Hz, 1H), 7.21-7.18 (m, 1H), 7.09 (dd, *J* = 8.4, 1.8 Hz, 1H), 5.20-5.04 (m, 1H), 2.62 (s, 3H), 2.28-2.19 (m, 4H), 2.16-2.06 (m, 2H), 1.91-1.78 (m, 2H). CO$_2$H proton not observed. ^{13}C NMR (151 MHz, CO(CD$_3$)$_2$) δ: 145.9, 141.1, 136.4, 130.6, 130.2, 130.0, 127.9, 127.4, 127.1, 121.6, 120.7, 112.4, 98.8, 58.4, 30.8, 25.8, 12.1. Two carbons not observed/coincident. υ_{max} (neat): 3406, 2924, 2872, 1716, 1608, 1593, 1577, 1534 cm^{-1}. HRMS: exact mass calculated for [M+H]$^+$ (C$_{21}$H$_{21}$ClNO$_2$S) *m/z* requires 388.0945, *m/z* found 388.0948.

Synthesis of 3-((6-chloro-2-methyl-1-phenyl-1*H*-indol-3-yl)thio)benzoic acid 1.55). Prepared according to General Procedure F using 3-((6-chloro-2-methyl-1*H*-indol-3-yl)thio)benzoic acid (**1.52**) (65 mg, 0.205 mmol, 1 equiv.), iodobenzene (46 μL, 0.409 mmol, 2 equiv.), CuI (19 mg, 0.102 mmol, 0.5 equiv.), Cs$_2$CO$_3$ (133 mg, 0.409 mmol, 2 equiv.), and 1,10-phenanthroline (37 mg, 0.205 mmol, 1 equiv.) in DMF (1 mL, 0.2 M). Purified by reverse-phase HPLC to afford the title compound as

a white amorphous solid (11 mg, 14%). ^{1}H NMR (400 MHz, CO(CD$_3$)$_2$) δ: 7.81 (dd, J = 2.4, 1.1 Hz, 1H), 7.77 (dt, J = 7.3, 1.5 Hz, 1H), 7.73-7.66 (m, 2H), 7.66-7.59 (m, 1H), 7.59-7.54 (m, 2H), 7.51(d, J = 8.4 Hz, 1H), 7.40-7.27 (m, 2H), 7.16 (dd, J = 8.4, 1.8 Hz, 1H), 7.13-7.08 (m, 1H), 2.41 (s, 3H). CO$_2$H proton not observed. ^{13}C NMR (101 MHz, CO(CD$_3$)$_2$) δ: 165.7, 144.1, 139.0, 138.0, 136.3, 130.9, 129.5, 129.3, 128.6, 128.5, 127.4, 126.0, 125.7, 121.0, 119.0, 109.8, 99.0, 10.4. Two carbons not observed/coincident. $υ_{max}$ (neat): 3058, 2978, 2924, 2658, 1690, 1593, 1577, 1536, 1502 cm^{-1}. HRMS: exact mass calculated for [M-H]$^-$ (C$_{22}$H$_{15}$ClNO$_2$S) m/z requires 394.0487, m/z found 394.0480.

Synthesis of 3-((2-methyl-1-(1-methyl-1H-pyrazol-4-yl)-1H-indol-3-yl)thio) benzoic acid (1.56). Prepared according to General Procedure D using methyl 3-((2-methyl-1H-indol-3-yl)thio)benzoate (**1.100**) (202 mg, 0.680 mmol, 1 equiv.), 4-bromo-1-methyl-1H-pyrazole (209 μL, 2.02 mmol, 3 equiv.), CuO (108 mg, 1.35 mmol, 2 equiv.), and K$_2$CO$_3$ (122 mg, 0.884 mmol, 1.3 equiv.) in pyridine (2 mL, 0.3 M). Purified using reverse-phase HPLC to afford the title compound as a dark red amorphous solid (22 mg, 9%). ^{1}H NMR (400 MHz, CDCl$_3$): δ 8.33 (s, 1H), 7.81 (app t, J = 1.7 Hz, 1H), 7.72-7.69 (m, 1H), 7.52 (d, J = 7.8 Hz, 1H), 7.33 (dd, J = 4.8, 3.9 Hz, 1H), 7.21-7.19 (m, 2H), 7.16-7.12 (m, 2H), 3.86 (s, 3H), 2.51 (s, 3H). ^{13}C NMR (126 MHz, CDCl$_3$): δ 166.9, 141.3, 140.3, 135.5, 130.6, 130.1, 129.8, 128.7, 126.6, 125.8, 122.3, 120.8, 118.8, 110.8, 98.7, 52.2, 12.1. Three carbons not observed/coincident. $υ_{max}$ (neat): 3381, 3375, 1695, 1572, 1539 cm^{-1}. HRMS: exact mass calculated for [M-H]$^-$ (C$_{20}$H$_{16}$N$_3$O$_2$S) m/z requires 362.0969, m/z found 362.0967.

Synthesis of 3-((2-methyl-1*H*-indol-3-yl)thio)benzoic acid (1.57). Prepared according to General Procedure C using methyl 3-((2-methyl-1*H*-indol-3-yl)thio)benzoate (**1.100**) (100 mg, 0.337 mmol, 1 equiv.) and 2 M aq. NaOH (1 mL) in THF (1 mL, 0.3 M). Purified by reverse-phase HPLC to afford the title compound as a cream amorphous solid (71 mg, 74%). ^{1}H NMR (400 MHz, CO(CD$_3$)$_2$): δ 10.71 (br s, 1H), 7.76 (app t, *J* = 1.5 Hz, 1H), 7.74-7.72 (m, 1H), 7.48-7.39 (m, 2H), 7.30 (app t, *J* = 7.7 Hz, 1H), 7.25-7.22 (m, 1H), 7.15-7.11 (m, 1H), 7.07-7.04 (m, 1H), 2.53 (s, 3H). One exchangeable proton not observed. ^{13}C NMR (101 MHz, CO(CD$_3$)$_2$): δ 167.4, 143.1, 141.6, 137.0, 132.1, 131.0, 130.4, 129.7, 127.1, 126.7, 122.7, 121.1, 118.8, 112.1, 97.9, 12.0. υ$_{max}$ (neat): 3390, 3057, 2885, 2654, 2546, 1686, 1570, 1543 cm^{-1}. HRMS: exact mass calculated for [M+H]$^+$ (C$_{16}$H$_{14}$NO$_2$S) *m/z* requires 284.0740, *m/z* found 284.0740.

Synthesis of 3-((1,2-dimethyl-1*H*-indol-3-yl)thio)benzoic acid (1.58). Prepared according to General Procedure C using methyl 3-((1,2-dimethyl-1*H*-indol-3-yl)thio)benzoate (**1.101**) (54 mg, 0.174 mmol, 1 equiv.) and 2 M aq. NaOH (1 mL) in THF (1 mL, 0.2 M). Purified by reverse-phase HPLC to afford the title compound as a cream amorphous solid (31 mg, 60%). ^{1}H NMR (400 MHz, CDCl$_3$): δ 7.84 (app t, *J* = 1.5Hz, 1H), 7.76-7.74 (m, 1H), 7.55 (d, *J* = 7.8 Hz, 1H), 7.36 (d, *J* = 8.2 Hz, 1H), 7.25-7.11 (m, 4H), 3.79 (s, 3H), 2.53 (s, 3H). CO$_2$H proton not observed. ^{13}C NMR (101 MHz, CDCl$_3$): δ 171.1, 143.2, 141.1, 137.3, 130.7, 129.8, 129.7, 128.9, 127.2, 126.4, 122.1, 120.8, 118.9, 109.3, 97.4, 30.6, 11.0. υ$_{max}$ (neat): 2922, 2546, 1680, 1572, 1521 cm^{-1}. HRMS: exact mass calculated for [M+H]$^+$ (C$_{17}$H$_{16}$NO$_2$S) *m/z* requires 298.0896, *m/z* found 298.0893.

Synthesis of 3-((1-cyclopentyl-2-methyl-1*H*-indol-3-yl)thio)benzoic acid (1.59).

Prepared according to General Procedure F using methyl 3-((2-methyl-1*H*-indol-3-yl)thio)benzoate (**1.100**) (200 mg, 0.673 mmol, 1 equiv.), NaH 60% w/w (216 mg, 5.39 mmol, 8 equiv.), and bromocyclopentane (288 μL, 2.69 mmol, 4 equiv.) in DMF (3 mL, 0.2 M). Following aqueous work-up, the reaction mixture was then used in the next step without further purification. The crude material was used according to General Procedure C using 4 M aq. NaOH (5 mL) in THF (3 mL, 0.2 M). Purified by reverse-phase HPLC to afford the title compound as a white amorphous solid (15 mg, 6% over 2 steps). ^{1}H NMR (400 MHz, CO(CD$_3$)$_2$): δ 7.78-7.70 (m, 2H), 7.57 (d, *J* = 8.3 Hz, 1H), 7.49 (d, *J* = 7.5 Hz, 1H), 7.30 (app t, *J* = 7.7 Hz, 1H), 7.22-7.17 (m, 1H), 7.17-7.12 (m, 1H), 7.09-7.07 (m, 1H), 5.14-5.05 (m, 1H), 2.61 (s, 3H), 2.37-2.23 (m, 2H), 2.23-2.07 (m, 4H), 1.92-1.73 (m, 2H). CO$_2$H proton not observed. ^{13}C NMR (101 MHz, CO(CD$_3$)$_2$): δ 167.2, 144.5, 141.6, 135.9, 132.1, 131.4, 130.4, 129.8, 127.2, 126.8, 122.3, 121.0, 119.5, 112.5, 97.9, 58.2, 30.6, 25.8, 11.7. υ_{max} (neat): 3388, 2976, 2954, 2870, 2660, 2539, 1668, 1591, 1571, 1530 cm^{-1}. HRMS: exact mass calculated for [M-H]$^-$ (C$_{21}$H$_{20}$NO$_2$S) *m/z* requires 350.1220, *m/z* found 350.1216.

Synthesis of 3-((2-methyl-1-phenyl-1*H*-indol-3-yl)thio)benzoic acid (1.60).

Prepared according to General Procedure B using methyl 3-((2-methyl-1*H*-indol-3-yl)thio)benzoate (**1.100**) (127 mg, 0.428 mmol, 1 equiv.), iodobenzene (95 μL, 0.856 mmol, 2 equiv.), CuI (41 mg, 0.214 mmol, 0.5 equiv.), Cs$_2$CO$_3$ (279 mg, 0.856 mmol, 2 equiv.), and 1,10-phenanthroline (77 mg, 0.428 mmol, 1 equiv.) in DMF (1 mL, 0.4 M). Following aqueous work-up, the reaction mixture was then used in the next step without further purification. The crude material was used according to

General Procedure C using 4 M aq. NaOH (1 mL) in THF (2 mL, 0.2 M). Purified by reverse-phase HPLC to afford the title compound as a cream amorphous solid (14 mg, 9% over 2 steps). ^{1}H NMR (400 MHz, CDCl$_3$): δ 7.95-7.89 (m, 1H), 7.82-7.76 (m, 1H), 7.63-7.55 (m, 3H), 7.54-7.48 (m, 1H), 7.41 (dd, J = 8.3, 1.3 Hz, 2H), 7.29-7.26 (m, 2H), 7.20-7.12 (m, 3H), 2.40 (s, 3H). CO$_2$H proton not observed. ^{13}C NMR (101 MHz, CDCl$_3$): δ 143.4, 140.6, 138.2, 137.6, 130.8, 129.8, 129.6, 129.0, 128.6, 128.1, 127.4, 126.6, 122.6, 121.4, 118.8, 110.6, 99.5, 11.9. Two carbons not observed/coincident. υ$_{max}$ (neat): 2917, 2852, 2651, 2536, 1679, 1597, 1571, 1530, 1501 cm^{-1}. HRMS: exact mass calculated for [M-H]$^-$ (C$_{22}$H$_{16}$NO$_2$S) m/z requires 358.0907, m/z found 358.0900.

Synthesis of 6-((6-chloro-2-methyl-1-(1-methyl-1H-pyrazol-4-yl)-1H-indol-3-yl)methyl) picolinic acid (1.61). Prepared according to General Procedure C using methyl 6-((6-chloro-2-methyl-1-(1-methyl-1H-pyrazol-4-yl)-1H-indol-3-yl)methyl) picolinate (**1.95**) (50 mg, 0.126 mmol, 1 equiv.) and 2 M aq. NaOH (2 mL) in THF (2 mL, 0.1 M). Purified by reverse-phase HPLC to afford the title compound as a yellow oil (23 mg, 48%). ^{1}H NMR (400 MHz, CO(CD$_3$)$_2$): δ 8.10-7.82 (m, 3H), 7.61 (s, 1H), 7.56 (d, J = 8.4 Hz, 1H), 7.52 (dd, J = 7.6, 1.0 Hz, 1H), 7.08 (d, J = 1.8 Hz, 1H), 7.01 (dd, J= 8.4, 1.9 Hz, 1H), 4.37 (s, 2H), 4.01 (s, 3H), 2.36 (s, 3H). CO$_2$H proton not observed. ^{13}C NMR (101 MHz, CO(CD$_3$)$_2$): δ 165.3, 161.9, 147.1, 139.7, 139.6, 137.3, 137.1, 128.9, 127.7, 127.7, 127.5, 122.2, 120.9, 120.2, 119.9, 110.5, 110.4, 39.8, 33.4, 11.1. υ$_{max}$ (neat): 3097, 2922, 1716, 1684, 1670, 1610, 1588 cm^{-1}. HRMS: exact mass calculated for [M+H]$^+$ (C$_{20}$H$_{18}$ClN$_4$O$_2$) m/z requires 383.1084, m/z found 383.1084.

Synthesis of 3-((6-chloro-2-methyl-1-(1-methyl-1*H*-pyrazol-4-yl)-1*H*-indol-3-yl)methyl) benzoic acid (1.62). Prepared according to General Procedure D using methyl 3-((6-chloro-2-methyl-1*H*-indol-3-yl)methyl)benzoate (**1.92**) (345 mg, 1.10 mmol, 1 equiv.), 4-bromo-1-methyl-1*H*-pyrazole (227 µL, 2.20 mmol, 2 equiv.), CuO (176 mg, 2.20 mmol, 2 equiv.), and K_2CO_3 (197 mg, 1.43 mmol, 1.3 equiv.) in pyridine (3 mL, 0.4 M). Following aqueous work-up, the reaction mixture was then used in the next step without further purification. The crude material was used according to General Procedure C using 2 M aq. NaOH (2 mL) in THF (2 mL, 0.5 M). Purified by reverse-phase HPLC to afford the title compound as a white amorphous solid (5 mg, 1% over 2 steps). ^{1}H NMR (400 MHz, $CO(CD_3)_2$): δ 8.00-7.94 (m, 2H), 7.85 (d, *J*= 7.6 Hz, 1H), 7.62 (s, 1H), 7.52 (dd, *J* = 7.7, 0.6 Hz, 1H), 7.45-7.36 (m, 2H), 7.08 (d, *J* = 1.7 Hz, 1H), 7.00 (dd, *J* = 8.4, 1.9 Hz, 1H), 4.21 (s, 2H), 4.01 (s, 3H), 2.32 (s, 3H). CO_2H proton not observed. ^{13}C NMR (151 MHz, $CO(CD_3)_2$): δ 167.7, 143.0, 139.6, 137.3, 136.6, 133.7, 131.6, 130.3, 129.4, 128.9, 128.1, 127.7, 127.6, 120.8, 120.1, 119.9, 111.7, 110.5, 39.8, 30.6, 11.1. υ_{max} (neat): 2922, 2554, 2361, 2153, 1693, 1606, 1585 cm^{-1}. HRMS: exact mass calculated for $[M+H]^+$ ($C_{21}H_{19}ClN_3O_2$) *m/z* requires 382.1131, *m/z* found 382.1134.

Synthesis of 3-((6-chloro-2-methyl-1-(1-methyl-1*H*-pyrazol-4-yl)-1*H*-indol-3-yl)oxy) benzoic acid (1.63). Prepared according to General Procedure E using (3-chlorophenyl)hydrazine hydrochloride (1.9 g, 10.8 mmol, 1 equiv.) and ethyl 3-(2-oxopropoxy)benzoate (**1.103**) (2.4 g, 10.8 mmol, 1 equiv.) in EtOH (50 mL, 0.2 M). 1 g of the crude material was then used according to General Procedure D using 4-bromo-1-methyl-1*H*-pyrazole (940 µL, 9.10 mmol, 3 equiv.), CuO (1.4 g, 18.2 mmol, 6 equiv.), and K_2CO_3 (1.6 g, 11.8 mmol, 4 equiv.) in pyridine (15 mL, 0.7 M).

Following aqueous work-up, the reaction mixture was then used in the next step without further purification. The crude material was used according to General Procedure C using 2 M aq. NaOH (30 mL) in THF (15 mL, 0.7 M). Purified by reverse-phase HPLC to afford the title compound as a cream amorphous solid (36 mg, 1% over 3 steps). ^{1}H NMR (400 MHz, CO(CD$_3$)$_2$): δ 8.05 (s, 1H), 7.77-7.67 (m, 2H), 7.62 (dd, J = 2.6, 1.5 Hz, 1H), 7.45 (app t, J = 7.9 Hz, 1H), 7.26 (dd, J = 8.3, 2.7 Hz, 1H), 7.24-7.16 (m, 2H), 7.03 (dd, J= 8.4, 1.9 Hz, 1H), 4.03 (s, 3H), 2.21 (s, 3H). CO$_2$H proton not observed. ^{13}C NMR (101 MHz, CO(CD$_3$)$_2$): δ 167.3, 160.0, 137.2, 137.0, 133.1, 131.1, 130.7, 129.4, 129.1, 128.3, 124.1, 121.3, 120.8, 120.4, 119.2, 118.6, 116.8, 111.0, 39.8, 9.5. υ_{max} (neat): 3122, 2949, 2921, 1696, 1606, 1584 cm^{-1}. HRMS: exact mass calculated for [M+H]$^+$ (C$_{20}$H$_{17}$ClN$_3$O$_3$) m/z requires 384.0924, m/z found 384.0926.

Synthesis of 3-((6-chloro-2-methyl-1H-indol-3-yl)oxy)benzoic acid (1.64). Prepared according to General Procedure C using ethyl 3-((6-chloro-2-methyl-1H-indol-3-yl)oxy)benzoate (**1.104**) (150 mg, 0.454 mmol, 1 equiv.) and 2 M aq. NaOH (1 mL) in THF (1 mL, 0.4 M). Purified by reverse-phase HPLC to afford the title compound as an orange amorphous solid (30 mg, 22%). ^{1}H NMR (400 MHz, CO(CD$_3$)$_2$): δ 9.95 (br s, 1H), 7.44-7.41 (m, 1H), 7.28 (dd, J = 2.5, 1.5 Hz, 1H), 7.16 (app t, J = 7.9 Hz, 1H), 7.13 (d, J = 1.7 Hz, 1H), 6.94 (dd, J = 8.2, 2.6 Hz, 1H), 6.87 (d, J = 8.4 Hz, 1H), 6.69 (dd, J = 8.4, 1.8 Hz, 1H), 2.05 (s, 3H). One exchangeable proton not observed. ^{13}C NMR (101 MHz, CO(CD$_3$)$_2$): δ 167.3, 160.4, 134.7, 133.2, 130.6, 130.4, 127.5, 126.9, 123.9, 120.7, 120.5, 118.4, 116.7, 112.0, 111.9, 10.1. υ_{max} (neat): 3327, 3071, 1690, 1601, 1585, 1520 cm^{-1}. HRMS: exact mass calculated for [M+H]$^+$ (C$_{16}$H$_{13}$ClNO$_3$) m/z requires 304.0549, m/z found 304.0544.

Synthesis of 6-((2-methyl-1-(1-methyl-1*H*-pyrazol-4-yl)-1*H*-indol-3-yl)methyl) picolinic acid (1.65). Prepared according to General Procedure C using methyl 6-((2-methyl-1-(1-methyl-1*H*-pyrazol-4-yl)-1*H*-indol-3-yl)methyl)picolinate (**1.105**) (50 mg, 0.139 mmol, 1 equiv.) and 2 M aq. NaOH (1 mL) in THF (1 mL, 0.1 M). Purified by reverse-phase HPLC to afford the title compound as a green gum (21 mg, 44%). ^{1}H NMR (400 MHz, CDCl$_3$): δ 10.50 (br s, 1H), 8.15 (d, J = 7.6 Hz, 1H), 7.97 (app t, J = 7.8 Hz, 1H), 7.66 (s, 1H), 7.59 (s, 1H), 7.50 (d, J = 7.9 Hz, 1H), 7.39 (d, J = 7.5 Hz, 1H), 7.15 (d, J = 3.6 Hz, 2H), 7.11 (dd, J = 7.7, 4.1 Hz, 1H), 4.53 (s, 2H), 4.06 (s, 3H), 2.28 (s, 3H). ^{13}C NMR (101 MHz, CDCl$_3$): δ 163.4, 159.8, 144.8, 142.1, 138.4, 137.0, 135.6, 128.3, 127.8, 127.7, 122.9, 122.3, 120.8, 120.2, 117.8, 110.2, 107.4, 39.7, 31.1, 11.0. υ_{max} (neat): 3103, 2950, 1725, 1716, 1696, 1670, 1616, 1588 cm^{-1}. HRMS: exact mass calculated for [M-H]$^-$ (C$_{20}$H$_{17}$N$_4$O$_2$) m/z requires 345.1357, m/z found 345.1355.

Synthesis of 3-((2-methyl-1-(1-methyl-1*H*-pyrazol-4-yl)-1*H*-indol-3-yl)methyl) benzoic acid (1.66). Prepared according to General Procedure C using methyl 3-((2-methyl-1-(1-methyl-1*H*-pyrazol-4-yl)-1*H*-indol-3-yl)methyl)benzoate (**1.109**) (100 mg, 0.278 mmol, 1 equiv.) and 2 M aq. NaOH (2 mL) in THF (2 mL, 0.1 M). Purified by reverse-phase HPLC to afford the title compound as cream amorphous solid (10 mg, 10%). ^{1}H NMR (400 MHz, CO(CD$_3$)$_2$): δ 7.99 (s, 1H), 7.92 (s, 1H), 7.84 (d, J = 7.7 Hz, 1H), 7.59 (d, J = 0.6 Hz, 1H), 7.53 (d, J = 7.6 Hz, 1H), 7.44 (d, J = 7.2 Hz, 1H), 7.38 (app t, J = 7.7 Hz, 1H), 7.14-6.95 (m, 3H), 4.21 (s, 2H), 4.01 (s, 3H), 2.33 (s, 3H). CO$_2$H proton not observed. ^{13}C NMR (151 MHz, CO(CD$_3$)$_2$): δ 143.4, 139.1, 137.3, 135.2, 133.8, 131.5, 130.3, 129.3, 129.0, 128.6, 128.0, 122.0, 120.7, 120.5, 118.8, 111.5, 110.6, 39.7, 30.8, 11.0. One carbon not

observed/coincident. υ_{max} (neat): 3113, 3051, 2918, 2467, 1699, 1605, 1584 cm^{-1}.

HRMS: exact mass calculated for [M-H]$^-$ (C$_{21}$H$_{18}$N$_3$O$_2$) m/z requires 344.1405, m/z found 344.1403.

Synthesis of 3-((2-methyl-1-(1-methyl-1H-pyrazol-4-yl)-1H-indol-3-yl)oxy) benzoic acid (1.67). Prepared according to General Procedure D using ethyl 3-((2-methyl-1H-indol-3-yl)oxy)benzoate (**1.106**) (94 mg, 0.319 mmol, 1 equiv.), 4-bromo-1-methyl-1H-pyrazole (99 µL, 0.956 mmol, 3 equiv.), CuO (51 mg, 0.638 mmol, 2 equiv.), and K$_2$CO$_3$ (57 mg, 0.415 mmol, 1.3 equiv.) in pyridine (1 mL, 0.3 M). Following aqueous work-up, the reaction mixture was then used in the next step without further purification. The crude material was used according to General Procedure C using 2 M aq. NaOH (1 mL) in THF (1 mL, 0.3 M). Purified by reverse-phase HPLC to afford the title compound as a brown oil (4 mg, 4% over 2 steps). ^{1}H NMR (400 MHz, CDCl$_3$): δ 7.75-7.71 (m, 1H), 7.72-7.69 (m, 1H), 7.64 (s, 1H), 7.59 (s, 1H), 7.37 (app t, J = 7.9 Hz, 1H), 7.30-7.23 (m, 2H), 7.22-7.17 (m, 1H), 7.15-7.11 (m, 1H), 7.08-7.02 (m, 1H), 4.04 (s, 3H), 2.12 (s, 3H). CO$_2$H proton not observed. ^{13}C NMR (101 MHz, CDCl$_3$): δ 170.8, 159.4, 137.4, 136.0, 130.9, 130.8, 129.8, 127.7, 127.2, 123.7, 122.1, 121.0, 120.9, 120.3, 119.8, 117.2, 117.0, 110.3, 39.9, 9.6. υ_{max} (neat): 3121, 3053, 2947, 1697, 1583 cm^{-1}. HRMS: exact mass calculated for [M+H]$^+$ (C$_{20}$H$_{18}$N$_3$O$_3$) m/z requires 348.1343, m/z found 348.1344.

Synthesis of 3-((2-methyl-1H-indol-3-yl)oxy)benzoic acid (1.68). Prepared according to General Procedure C using ethyl 3-((2-methyl-1H-indol-3-yl)oxy)benzoate (**1.106**) (50 mg, 0.169 mmol, 1 equiv.) and 1 M aq. NaOH (1 mL) in THF (2 mL, 0.1 M). Purified by reverse-phase HPLC to afford the title compound as a brown oil (8 mg, 18%). ^{1}H NMR (400 MHz, CDCl$_3$): δ 7.74-7.71 (m, 1H), 7.70-

7.64 (m, 2H), 7.35 (app t, J = 7.9 Hz, 1H), 7.32-7.28 (m, 1H), 7.24-7.18 (m, 1H), 7.16-7.12 (m, 1H), 7.07-6.99 (m, 1H), 2.34 (s, 3H). NH and CO_2H protons not observed. ^{13}C NMR (101 MHz, $CDCl_3$): δ 170.9, 159.5, 133.3, 130.7, 130.1, 129.7, 124.3, 123.6, 122.0, 121.5, 120.9, 119.9, 117.2, 116.9, 111.0, 10.4. ν_{max} (neat): 3404, 2920, 2558, 1690, 1584, 1572 cm^{-1}. HRMS: exact mass calculated for [M+H]$^+$ ($C_{16}H_{14}NO_3$) m/z requires 268.0968, m/z found 268.0971.

Synthesis of 6-chloro-2-methyl-1-(1-methyl-1*H*-pyrazol-4-yl)-1*H*-indole (1.72).
Prepared according to General Procedure D using 6-chloro-2-methyl-1*H*-indole (**1.90**) (300 mg, 1.81 mmol, 1 equiv.), 4-bromo-1-methyl-1*H*-pyrazole (224 μL, 2.17 mmol, 1.2 equiv.), CuO (290 mg, 3.62 mmol, 2 equiv.), and K_2CO_3 (325 mg, 2.36 mmol, 1.3 equiv.) in pyridine (3.5 mL, 0.5 M). Purified using silica chromatography, eluting with 0-30% EtOAc/petroleum ether, to afford the title compound as a brown amorphous solid (351 mg, 79%). ^1H NMR (400 MHz, $CDCl_3$): δ 7.56 (s, 1H), 7.50 (s, 1H), 7.42 (d, J = 8.3 Hz, 1H), 7.13-7.08 (m, 1H), 7.06 (dd, J = 8.3, 1.9 Hz, 1H), 6.33 (s, 1H), 4.01 (s, 3H), 2.27 (s, 3H). ^{13}C NMR (101 MHz, $CDCl_3$): δ 139.4, 138.6, 137.3, 127.5, 127.2, 126.8, 120.8, 120.5, 119.7, 110.1, 101.2, 39.8, 13.2. ν_{max} (neat): 3119, 2943, 1715, 1676, 1607, 1580 cm^{-1}. HRMS: exact mass calculated for [M+H]$^+$ ($C_{13}H_{13}ClN_3$) m/z requires 248.0763, m/z found 248.0766.

Synthesis of 1-((3-bromophenyl)thio)propan-2-one (1.74). A flask containing 3-bromothiophenol (**1.73**) (273 μL, 2.65 mmol, 1 equiv.) in THF (15 mL, 0.2 M) was cooled to 0 °C. DIPEA (2.3 mL, 13.2 mmol, 5 equiv.) was added portion wise and allowed to stir for 30 min before the addition of chloroacetone (2.3 mL, 29.0 mmol, 11 equiv.). The reaction mixture was then allowed to warm to room temperature and stirred for 16 h. The reaction mixture was concentrated under vacuum, diluted with

EtOAc (30 mL) and washed with H_2O (30 mL). The organic layer was collected, dried (hydrophobic frit), and concentrated under vacuum. Purified using silica chromatography, eluting with 0-40% EtOAc/petroleum ether, to afford the title compound as a colourless oil (540 mg, 83%). ^{1}H NMR (400 MHz, CDCl$_3$): δ 7.45 (app t, J = 1.8 Hz, 1H), 7.33-7.29 (m, 1H), 7.24-7.20 (m, 1H), 7.13 (t, J = 7.9 Hz, 1H), 3.68 (s, 2H), 2.26 (s, 3H). ^{13}C NMR (101 MHz, CDCl$_3$): δ 202.8, 137.2, 131.6, 130.4, 129.8, 127.6, 122.9, 44.3, 28.1. υ_{max} (neat): 3050, 1571, 1559 cm^{-1}. HRMS: exact mass calculated for [M+H]$^+$ (C$_9$H$_{10}$BrOS) requires m/z 246.9609, found m/z 246.9601.

Synthesis of 3-((3-bromophenyl)thio)-6-chloro-2-methyl-1*H*-indole (1.76). Prepared according to General Procedure A using (3-chlorophenyl)hydrazine hydrochloride (1.5 g, 8.18 mmol, 1 equiv.) and 1-((3-bromophenyl)thio)propan-2-one (**1.74**) (2 g, 8.18 mmol, 1 equiv.) in EtOH (40 mL, 0.2 M). Purified by silica chromatography, eluting with 0-10% EtOAc/petroleum ether, to afford the title compound as a cream amorphous solid (639 mg, 22%). ^{1}H NMR (400 MHz, CO(CD$_3$)$_2$) δ: 10.97 (br s, 1H), 7.48 (d, J = 1.9 Hz, 1H), 7.38 (d, J = 8.4 Hz, 1H), 7.26-7.23 (m, 1H), 7.15 (app t, J = 7.9 Hz, 1H), 7.11 (app t, J = 1.8 Hz, 1H), 7.08 (dd, J = 8.4 Hz, 1H), 7.03-7.01 (m, 1H), 2.52 (s, 3H). ^{13}C NMR (101 MHz, CDCl$_3$): δ 143.0, 142.8, 136.3, 132.2, 129.5, 127.3, 127.0, 125.4, 123.4, 122.4, 122.2, 121.8, 109.1, 97.8, 11.7. υ_{max} (neat): 3409, 1573, 1557, 1536 cm^{-1}. HRMS: exact mass calculated for [M+H]$^+$ (C$_{15}$H$_{12}$BrClNS) m/z requires 353.9534, m/z found 353.9529.

Synthesis of methyl 3-((6-chloro-2-methyl-1*H*-indol-3-yl)thio)benzoate (1.77). Prepared according to General Procedure B using *trans*-bis(acetato)bis[*o*-(di-*o*-tolylphosphino)benzyl]dipalladium(II) (90 mg, 0.0959 mmol, 5 mol%), 3-((3-

bromophenyl)thio)-6-chloro-2-methyl-1*H*-indole (**1.76**) (639 mg, 1.81 mmol, 1 equiv.), Mo(CO)$_6$ (478 mg, 1.81 mmol, 1 equiv.), [*t*Bu$_3$PH]BF$_4$ (112 mg, 0.386 mmol, 20 mol%), and DBU (433 µL, 2.90 mmol, 1.6 equiv.) in MeCN/MeOH (20 mL, 1:4, 0.3 M). Purified by column chromatography, eluting with 0-20% EtOAc/petroleum ether, to afford the title compound as a cream amorphous solid (463 mg, 77%). ^{1}H NMR (400 MHz, CO(CD$_3$)$_2$) δ: 10.92 (br s, 1H), 7.73-7.66 (m, 2H), 7.47 (d, J = 1.8 Hz, 1H), 7.38 (d, J = 8.4 Hz, 1H), 7.34-7.30 (m, 1H), 7.25-7.18 (m, 1H), 7.07 (dd, J = 8.4, 1.9 Hz, 1H), 3.81 (s, 3H), 2.53 (s, 3H). ^{13}C NMR (101 MHz, CO(CD$_3$)$_2$) δ: 166.8, 144.4, 141.2, 137.4, 131.9, 130.6, 130.0, 129.7, 128.1, 126.9, 126.6, 121.6, 120.0, 112.1, 98.4, 52.4, 12.0. υ$_{max}$ (neat): 3405, 3321, 2950, 1699, 1621, 1591, 1575, 1539 cm^{-1}. HRMS: exact mass calculated for [M+H]$^+$ (C$_{17}$H$_{15}$ClNO$_2$S) *m/z* requires 334.0476, *m/z* found 334.0474.

Synthesis of methyl 3-((6-chloro-2-methyl-1-(1-methyl-1*H*-pyrazol-4-yl)-1*H*-indol-3-yl)thio)benzoate (1.78). Prepared according to General Procedure C using methyl 3-((6-chloro-2-methyl-1*H*-indol-3-yl)thio)benzoate (**1.77**) (100 mg, 0.302 mmol, 1 equiv.), CuO (48 mg, 0.604 mmol, 2 equiv.), K$_2$CO$_3$ (54 mg, 0.393 mmol, 1.3 equiv.), and 1-methyl-4-bromopyrazole (94 µL, 0.906 mmol, 3 equiv.) in pyridine (1 mL, 0.3 M). Purified using silica chromatography, eluting with 50% EtOAc/petroleum ether, to afford the title compound as a cream amorphous solid (74 mg, 59%). ^{1}H NMR (400 MHz, CDCl$_3$): δ 7.83-7.82 (m, 1H), 7.74-7.72 (m, 1H), 7.63 (s, 1H), 7.61 (s, 1H), 7.44 (d, J = 8.3 Hz, 1H), 7.23 (app t, J = 7.7 Hz, 1H), 7.19-7.15 (m, 2H), 7.11 (dd, J = 8.4, 1.8 Hz, 1H), 4.05 (s, 3H), 3.87 (s, 3H), 2.38 (s, 3H). ^{13}C NMR (101 MHz, CDCl$_3$): δ 166.9, 144.7, 139.7, 139.2, 137.2, 130.9, 130.1, 129.0, 128.7, 128.1, 127.7, 127.0, 126.2, 122.1, 119.8, 119.3, 110.6, 100.1, 52.4,

40.0, 11.8. υ_{max} (neat): 3057, 2985, 2945, 2920, 2883, 2848, 1710, 1606, 1570, 1539 cm^{-1}. HRMS: exact mass calculated for [M+H]$^+$ (C$_{21}$H$_{19}$ClN$_3$O$_2$S) *m/z* requires 414.0850, *m/z* found 414.0851.

Synthesis of methyl 6-hydroxypicolinate (1.80). Thionyl chloride (1.2 mL, 15.8 mmol, 1.1 equiv.) was added to a solution of 6-hydroxypicolinic acid (**1.79**) (2 g, 14.4 mmol, 1 equiv.) in 70 mL MeOH (0.2 M) at 0 °C. The resulting solution was then heated to reflux for 16 h, allowed to cool to room temperature, and then concentrated under vacuum. The residue was dissolved in 50 mL DCM and washed with 50 mL sat. aq. NaHCO$_3$. The organic layer was collected, dried (hydrophobic frit), then concentrated under vacuum to afford the title compound as a white solid (1.16 g, 53%). ^{1}H NMR (400 MHz, CDCl$_3$): δ 11.22 (br s, 1H), 7.42 (dd, *J* = 9.2, 6.8 Hz, 1H), 6.94 (dd, *J* = 6.8, 1.0 Hz, 1H), 6.80 (dd, *J* = 9.2, 1.0 Hz, 1H), 3.92 (s, 3H). ^{13}C NMR (101 MHz, CDCl$_3$): δ 163.2, 161.5, 139.7, 134.0, 127.0, 109.6, 53.3. υ_{max} (neat): 3028, 2947, 2360, 2158, 1734, 1649, 1604 cm^{-1}. HRMS: exact mass calculated for [M+H+] (C$_7$H$_8$NO$_3$) *m/z* requires 154.0499 *m/z* found 154.0495.

Synthesis of methyl 6-(2-oxopropoxy)picolinate (1.81). Chloroacetone (936 μL, 11.8 mmol, 1 equiv.) was added dropwise to a solution of methyl 6-hydroxypicolinate (**1.80**) (1.8 g, 11.8 mmol, 1 equiv.) and K$_2$CO$_3$ (3.2 g, 23.5 mmol, 2 equiv.) in 60 mL acetone (0.2 M) at 0°C. The resulting reaction mixture was then heated at reflux for 16 h. Purified using silica chromatography, eluting with 100% EtOAc, to afford the title compound as a cream amorphous solid (2.15 g, 87%). ^{1}H NMR (400 MHz, CDCl$_3$): δ 7.76 – 7.71 (m, 2H), 7.07 (dd, *J* = 5.1, 4.0 Hz, 1H), 4.98 (s, 2H), 3.93 (s, 3H), 2.27 (s, 3H). ^{13}C NMR (126 MHz, CDCl$_3$): δ 204.0, 165.4, 162.2, 145.2, 139.8, 119.5, 115.4, 70.1, 52.7, 26.8. υ_{max} (neat): 2953, 1728, 1595,

1575 cm^{-1}. HRMS: exact mass calculated for [M+H+] (C$_{10}$H$_{12}$NO$_4$) *m/z* requires 210.0761 *m/z* found 210.0760.

Attempted syntheses of methyl 6-((2-methyl-1*H*-indol-3-yl)oxy)picolinate (1.82).

Reaction 1:

Synthesis was first attempted according to General Procedure A using methyl 6-(2-oxopropoxy)picolinate (**1.81**) (500 mg, 2.39 mmol, 1 equiv.) and phenylhydrazine hydrogenchloride (349 mg, 2.39 mmol, 1 equiv.) in 10 mL EtOH (0.2 M) for 2 h, however, no desired product was observed.

Reaction 2:

The reaction was then repeated following General Procedure A using methyl 6-(2-oxopropoxy)picolinate (**1.81**) (200 mg, 0.957 mmol, 1 equiv.) and phenylhydrazine hydrogenchloride (138 mg, 0.957 mmol, 1 equiv.) in 10 mL EtOH (0.1 M) for 16 h. No desired product was observed, with methyl 6-hydroxypicolinate (**1.80**) isolated as the major product (58 mg, 40%).

Reaction 3:

The reaction was then repeated following General Procedure A using methyl 6-(2-oxopropoxy)picolinate (**1.81**) (200 mg, 0.957 mmol, 1 equiv.) and phenylhydrazine hydrogenchloride (138 mg, 0.957 mmol, 1 equiv.) in 10 mL EtOH (0.1 M) for 2 h, with additional 1 M HCl in ether (0.2 mL) and AcOH (0.2 mL), however, no desired product was observed.

Reaction 4:

The reaction was then repeated following General Procedure A using methyl 6-(2-oxopropoxy)picolinate (**1.81**) (200 mg, 0.957 mmol, 1 equiv.) and phenylhydrazine hydrogenchloride (138 mg, 0.957 mmol, 1 equiv.) in 10 mL EtOH (0.1 M) for 2 h,

with additional citric acid (18 mg, 0.096 mmol, 10 mol%) however, no desired product was observed.

Synthesis of 1-((6-bromopyridin-2-yl)oxy)propan-2-one (1.84). NaH 60% w/w (172 mg, 4.30 mmol, 1.5 equiv.) was added to a solution of 6-bromopyridin-2-ol (**1.83**) (500 mg, 2.87 mmol, 1 equiv.) in 15 mL PhMe (0.2 M) at 0 °C then refluxed for 1 h. Chloroacetone (228 μL, 2.87 mmol, 1 equiv.) was then added and the reaction mixture was refluxed for a further 16 h. The reaction mixture was then allowed to cool to room temperature, diluted with 20 mL EtOAc and washed with 2 x 20 mL H_2O. The organic layer was collected, dried (hydrophobic frit), and concentrated under vacuum. Purified using silica chromatography, eluting with 50-100% EtOAc/petroleum ether, to afford the title compound as a pale brown amorphous solid (227 mg, 34%). ^{1}H NMR (400 MHz, CDCl$_3$): δ 7.36 (dd, J = 9.7, 2.7 Hz, 1H), 7.27 (dd, J = 2.7, 0.4 Hz, 1H), 6.46 (d, J = 9.8 Hz, 1H), 4.65 (s, 2H), 2.24 (s, 3H). ^{13}C NMR (101 MHz, CDCl$_3$): δ 200.2, 160.7, 143.3, 138.0, 121.9, 98.0, 57.8, 27.6. υ_{max} (neat): 3039, 2937, 2158, 1967, 1728, 1666, 1587, 1527 cm^{-1}. HRMS: exact mass calculated for [M+H+] ($C_8H_9BrNO_2$) m/z requires 229.9811, 231.9791 m/z found 229.9814, 231.9789.

Attempted syntheses of 3-((6-bromopyridin-2-yl)oxy)-2-methyl-1H-indole (1.85).

Reaction 1:

Synthesis was first attempted according to General Procedure A using 1-((6-bromopyridin-2-yl)oxy)propan-2-one (**1.84**) (217 mg, 0.943 mmol, 1 equiv.) and phenylhydrazine hydrochloride (169 mg, 0.943 mmol, 1 equiv.) in 5 mL EtOH (0.2 M) for 2 h. No desired product was observed and further analysis by LCMS identified 6-bromopyridin-2-ol (**1.83**) as the major product.

Reaction 2:

A second reaction was trialled according to General Procedure A using 1-((6-bromopyridin-2-yl)oxy)propan-2-one (**1.84**) (217 mg, 0.943 mmol, 1 equiv.) and phenylhydrazine hydrochloride (169 mg, 0.943 mmol, 1 equiv.) in 5 mL EtOH (0.2 M) with additional 1 M HCl in ether (0.2 mL) and AcOH (0.2 mL), however, no desired product was observed.

Synthesis of 2-methyl-1-(1-methyl-1*H*-pyrazol-4-yl)-1*H*-indole (1.87). Prepared according to General Procedure D using 2-methyl-1*H*-indole **1.86** (1 g, 7.63 mmol, 1 equiv.), 4-bromo-1-methyl-1*H*-pyrazole (1.2 mL, 11.4 mmol, 1.5 equiv.), CuO (1.2 g, 15.3 mmol, 2 equiv.), and K_2CO_3 (1.4 g, 9.92 mmol, 1.3 equiv.) in pyridine (10 mL, 0.8 M). Purified using silica chromatography, eluting with 0-30% EtOAc/petroleum ether, to afford the title compound as a brown amorphous solid (679 mg, 42%). ^{1}H NMR (400 MHz, CDCl$_3$): δ 7.58 (s, 1H), 7.57-7.52 (m, 1H), 7.50 (s, 1H), 7.17-7.07 (m, 3H), 6.37 (s, 1H), 4.01 (s, 3H), 2.31 (s, 3H). ^{13}C NMR (101 MHz, CDCl$_3$): δ 138.9, 137.7, 137.4, 128.3, 127.4, 121.2, 120.3, 120.2, 119.7, 110.0, 101.2, 39.8, 13.3. υ_{max} (neat): 3114, 3051, 2984, 2941, 2919, 1612, 1586, 1560 cm^{-1}. HRMS: exact mass calculated for [M+H]$^+$ (C$_{13}$H$_{14}$N$_3$) *m/z* requires 212.1182, *m/z* found 212.1182.

Synthesis of 3-iodo-2-methyl-1-(1-methyl-1*H*-pyrazol-4-yl)-1*H*-indole (1.88). Iodine (341 mg, 1.34 mmol, 1.1 equiv.) was added to a solution of 2-methyl-1-(1-methyl-1*H*-pyrazol-4-yl)-1*H*-indole (**1.87**) (300 mg, 1.22 mmol, 1 equiv) and KOH (171 mg, 3.05 mmol, 2.5 equiv.) in 2 mL DMF (0.6 M) then stirred at room temperature for 16 h. The resulting solution was diluted with 10 mL EtOAc and washed with 10 mL conc. aq. $Na_2S_2O_5$ followed by 10 mL H_2O. The organic layer

was dried (hydrophobic frit) and concentrated under vacuum. The residue was then triturated using hexane to afford a cream amorphous solid (225 mg, 49%), which was used in the next step without further purification.

Attempted syntheses of methyl 6-((2-methyl-1-(1-methyl-1*H*-pyrazol-4-yl)-1*H*-indol-3-yl)oxy)picolinate (1.89).

Reaction 1:

A flask containing 3-iodo-2-methyl-1-(1-methyl-1*H*-pyrazol-4-yl)-1*H*-indole (**1.88**) (100 mg, 0.297 mmol, 1 equiv.), methyl 6-hydroxypicolinate (54 mg, 0.356 mmol, 1.2 equiv.), pyridine-2,6-dicarboxylic acid (4 mg, 0.030 mmol, 10 mol%), CuI (3 mg, 0.015 mmol, 5 mol%) and K_3PO_4 (126 mg, 0.594 mmol, 2 equiv.) in 1 mL DMSO (0.3 M) was heated to 110 °C under nitrogen for 24 h, however, no reaction occurred and only the starting materials remained.

Reaction 2:

A flask containing 3-iodo-2-methyl-1-(1-methyl-1*H*-pyrazol-4-yl)-1*H*-indole (**1.88**) (100 mg, 0.297 mmol, 1 equiv.), methyl 6-hydroxypicolinate (54 mg, 0.356 mmol, 1.2 equiv.), pyridine-2,6-dicarboxylic acid (4 mg, 0.030 mmol, 10 mol%), CuI (56 mg, 0.297 mmol, 1 equiv.) and K_3PO_4 (126 mg, 0.594 mmol, 2 equiv.) in 1 mL distilled DMF (0.3 M) was heated to 110 °C under nitrogen for 24 h, however, no reaction occurred and only the starting materials remained.

Synthesis of 3-(3-bromobenzyl)-6-chloro-2-methyl-1*H*-indole (1.91). Prepared according to General Procedure H using 3-bromobenzaldehyde (442 mg, 2.39 mmol, 1.1 equiv.), 6-chloro-2-methyl-1*H*-indole (**1.90**) (360 mg, 2.17 mmol, 1 equiv.), Et₃SiH (451 µL, 2.83 mmol, 1.3 equiv.), and TFA (249 µL, 3.26 mmol, 1.5 equiv.) in DCM (10 mL, 0.2 M). Purified using silica chromatography, eluting with 0-5%

EtOAc/petroleum ether, to afford the title compound as a white amorphous solid (587 mg, 73%). ^{1}H NMR (600 MHz, CO(CD$_3$)$_2$): δ 10.10 (br s, 1H), 7.38 (s, 1H), 7.34-7.28 (m, 3H), 7.23 (d, J = 7.7 Hz, 1H), 7.18 (app t, J = 7.8 Hz, 1H), 6.93 (dd, J = 8.5, 1.8 Hz, 1H), 4.06 (s, 2H), 2.42 (s, 3H). ^{13}C NMR (151 MHz, CO(CD$_3$)$_2$): δ 145.7, 134.5, 131.9, 131.0, 129.5, 128.3, 128.1, 126.8, 122.8, 119.9, 119.7, 111.1, 110.2, 30.0, 11.6. One carbon not observed/coincident. υ$_{max}$ (neat): 3409, 3053, 2911, 2850, 1692, 1613, 1593, 1567 cm^{-1}. HRMS: exact mass calculated for [M+H]$^+$ (C$_{16}$H$_{14}$BrClN) m/z requires 337.9948, m/z found 337.9947.

Synthesis of methyl 3-((6-chloro-2-methyl-1H-indol-3-yl)methyl)benzoate (1.92).
Prepared according to General Procedure G using *trans*-bis(acetato)bis[o-(di-o-tolylphosphino)benzyl] dipalladium(II) (77 mg, 0.0821 mmol, 5 mol%), 3-(3-bromobenzyl)-6-chloro-2-methyl-1H-indole (**1.91**) (551 mg, 1.65 mmol, 1 equiv.), Mo(CO)$_6$ (436 mg, 1.65 mmol, 1 equiv.), [tBu$_3$PH]BF$_4$ (96 mg, 0.330 mmol, 20 mol%), and DBU (370 μL, 2.48 mmol, 1.5 equiv.) in MeCN/MeOH (10 mL, 1:4, 0.2 M). Purified using silica chromatography, eluting with 0-15% EtOAc/petroleum ether, to afford the title compound as a pale yellow amorphous solid (348 mg, 67%). ^{1}H NMR (400 MHz, CO(CD$_3$)$_2$): δ 10.11 (br s, 1H), 7.89 (s, 1H), 7.81-7.78 (m, 1H), 7.53-7.44 (m, 1H), 7.37 (app t, J = 7.7 Hz, 1H), 7.33-7.28 (m, 2H), 6.91 (dd, J = 8.4, 1.9 Hz, 1H), 4.13 (s, 2H), 3.83 (s, 3H), 2.43 (s, 3H). ^{13}C NMR (101 MHz, CO(CD$_3$)$_2$): δ 167.3, 143.5, 137.2, 134.4, 133.8, 131.2, 129.9, 129.3, 128.4, 127.7, 126.8, 119.9, 119.8, 111.2, 110.6, 52.2, 30.3, 11.7. υ$_{max}$ (neat): 3328, 2945, 2896, 1705, 1621, 1608 cm^{-1}. HRMS: exact mass calculated for [M+H]$^+$ (C$_{18}$H$_{17}$ClNO$_2$) m/z requires 316.0913, m/z found 316.0914.

Synthesis of 3-((6-bromopyridin-2-yl)methyl)-6-chloro-2-methyl-1-(1-methyl-1*H*-pyrazol-4-yl)-1*H*-indole (1.94). Prepared according to General Procedure H using 6-bromopyridine-2-carbaldehyde (91 mg, 0.489 mmol, 1.2 equiv.), 6-chloro-2-methyl-1-(1-methyl-1*H*-pyrazol-4-yl)-1*H*-indole (**1.72**) (100 mg, 0.406 mmol, 1 equiv.), Et$_3$SiH (84 μL, 0.529 mmol, 1.3 equiv.), and TFA (47 μL, 0.610 mmol, 1.5 equiv.) in DCM (2 mL, 0.2 M). Purified using silica chromatography, eluting with 0-50% EtOAc/petroleum ether, to afford the title compound as a yellow oil (94 mg, 56%). ^{1}H NMR (400 MHz, CO(CD$_3$)$_2$): δ 7.96 (s, 1H), 7.60 (s, 1H), 7.57 (app t, *J* = 7.7 Hz, 1H), 7.51 (d, *J* = 8.4 Hz, 1H), 7.39 (d, *J* = 7.8 Hz, 1H), 7.22 (d, *J* = 7.2 Hz, 1H), 7.08 (d, *J* = 1.6 Hz, 1H), 7.02 (dd, *J* = 8.4, 1.9 Hz, 1H), 4.23 (s, 2H), 4.01 (s, 3H), 2.33 (s, 3H). ^{13}C NMR (101 MHz, CDCl$_3$): δ 163.8, 141.9, 140.4, 139.5, 137.3, 137.1, 128.9, 127.6, 126.2, 122.4, 120.8, 120.2, 119.9, 110.5, 110.3, 39.8, 33.5, 11.1. One carbon not observed/coincident. υ$_{max}$ (neat): 3114, 2921, 1612, 1582, 1554 cm^{-1}. HRMS: exact mass calculated for [M+H]$^+$ (C$_{19}$H$_{17}$BrClN$_4$) *m/z* requires 417.0297, *m/z* found 417.0294.

Synthesis of methyl 6-((6-chloro-2-methyl-1-(1-methyl-1*H*-pyrazol-4-yl)-1*H*-indol-3-yl)methyl)picolinate (1.95). Prepared according to General Procedure G using *trans*-bis(acetato)bis[*o*-(di-*o*-tolylphosphino)benzyl]dipalladium(II) (9 mg, 0.00959 mmol, 5 mol%), 3-((6-bromopyridin-2-yl)methyl)-6-chloro-2-methyl-1-(1-methyl-1*H*-pyrazol-4-yl)-1*H*-indole (**1.94**) (84 mg, 0.202 mmol, 1 equiv.), Mo(CO)$_6$ (53 mg, 0.202 mmol, 1 equiv.), [*t*Bu$_3$PH]BF$_4$ (12 mg, 0.0414 mmol, 20 mol%), and DBU (45 μL, 0.303 mmol, 1.5 equiv.) in MeCN/MeOH (2.5 mL, 1:4, 0.1 M). Purified using silica chromatography, eluting with 50-70% EtOAc/petroleum ether, to afford the title compound as a cream amorphous solid (61 mg, 76%). ^{1}H NMR

(400 MHz, CO(CD$_3$)$_2$): δ 7.96 (s, 1H), 7.88 (dd, J = 7.7, 1.0 Hz, 1H), 7.80 (app t, J = 7.7 Hz, 1H), 7.60 (s, 1H), 7.56 (d, J = 8.4 Hz, 1H), 7.40 (dd, J = 7.8, 1.0 Hz, 1H), 7.07 (d, J = 1.7 Hz, 1H), 7.00 (dd, J = 8.4, 1.9 Hz, 1H), 4.32 (s, 2H), 4.01 (s, 3H), 3.93 (s, 3H), 2.36 (s, 3H). ^{13}C NMR (151 MHz, CO(CD$_3$)$_2$): δ 166.5, 162.6, 148.6, 139.5, 138.4, 137.3, 137.0, 128.9, 127.7, 127.6, 126.5, 123.2, 120.8, 120.4, 119.9, 110.7, 110.4, 52.6, 39.8, 34.0, 11.1. υ$_{max}$ (neat): 3086, 3057, 2950, 2917, 2855, 1712, 1610, 1593, 1584 cm^{-1}. HRMS: exact mass calculated for [M+H]$^+$ (C$_{21}$H$_{20}$ClN$_4$O$_2$) m/z requires 397.1240, m/z found 397.1236.

Synthesis of methyl 3-((2-methyl-1H-indol-3-yl)thio)benzoate (1.100). Prepared according to General Procedure G using *trans*-bis(acetato)bis[o-(di-o-tolylphosphino)benzyl]dipalladium(II) (183 mg, 0.195 mmol, 5 mol%), 3-((3-bromophenyl)thio)-2-methyl-1H-indole (**1.107**) (1.2 g, 3.77 mmol, 1 equiv.), Mo(CO)$_6$ (995 mg, 3.77 mmol, 1 equiv.), [tBu$_3$PH]BF$_4$ (219 mg, 0.754 mmol, 20 mol%), and DBU (844 μL, 5.66 mmol, 1.5 equiv.) in MeCN/MeOH (20 mL, 1:4, 0.2 M) to afford the title compound as a brown amorphous solid (1.03 g, 92%). ^{1}H NMR (500 MHz, CDCl$_3$): δ 8.49 (br s, 1H), 7.81 (s, 1H), 7.70 (d, J = 7.6 Hz, 1H), 7.51 (d, J = 7.8 Hz, 1H), 7.34 (d, J = 8.0 Hz, 1H), 7.22-7.09 (m, 4H), 3.86 (s, 3H), 2.50 (s, 3H). ^{13}C NMR (126 MHz, CDCl$_3$): δ 166.9, 141.4, 140.4, 135.6, 130.6, 130.1, 129.8, 128.7, 126.6, 125.8, 122.2, 120.8, 118.8, 110.8, 52.1, 29.1, 12.1. υ$_{max}$ (neat): 3327, 2850, 1710 cm^{-1}. HRMS: exact mass calculated for [M-H]$^-$ (C$_{17}$H$_{14}$NO$_2$S) m/z requires 296.0751, m/z found 296.0753.

Synthesis of methyl 3-((1,2-dimethyl-1H-indol-3-yl)thio)benzoate (1.101). Prepared according to General Procedure F using methyl 3-((2-methyl-1H-indol-3-yl)thio)benzoate (**1.100**) (200 mg, 0.673 mmol, 1 equiv.), NaH 60% w/w (54 mg,

1.35 mmol, 2 equiv.), and MeI (84 μL, 1.35 mmol, 2 equiv.) in THF (3 mL, 0.2 M). Purified using silica chromatography, eluting with 10% EtOAc/petroleum ether, to afford the title compound as a pale yellow amorphous solid (71 mg, 34%). ^{1}H NMR (500 MHz, CDCl$_3$): δ 7.87 (s, 1H), 7.74 (dd, J = 7.6, 1.2 Hz, 1H), 7.59 (d, J = 7.8 Hz, 1H), 7.38 (d, J = 8.2 Hz, 1H), 7.28 (app t, J = 7.1 Hz, 1H), 7.24-7.11 (m, 3H), 3.90 (s, 3H), 3.79 (s, 3H), 2.56 (s, 3H). ^{13}C NMR (126 MHz, CDCl$_3$): δ 166.9, 143.1, 140.8, 137.3, 130.7, 129.9, 129.6, 128.8, 126.7, 125.8, 122.0, 120.7, 118.9, 109.3, 97.5, 52.2, 30.5, 11.0. υ_{max} (neat): 2949, 1722, 1572, 1527 cm^{-1}. HRMS: exact mass calculated for [M+H]$^+$ (C$_{18}$H$_{18}$NO$_2$S) m/z requires 312.1053, m/z found 312.1055.

Synthesis of 3-((6-bromopyridin-2-yl)methyl)-2-methyl-1-(1-methyl-1*H*-pyrazol-4-yl)-1*H*-indole (1.102). Prepared according to General Procedure H using 6-bromopyridine-2-carbaldehyde (91 mg, 0.489 mmol, 1.03 equiv.), 2-methyl-1-(1-methyl-1*H*-pyrazol-4-yl)-1*H*-indole (**1.87**) (100 mg, 0.474 mmol, 1 equiv.), Et$_3$SiH (84 μL, 0.529 mmol, 1.1 equiv.), and TFA (47 μL, 0.610 mmol, 1.3 equiv.) in DCM (2 mL, 0.2 M). Purified using silica chromatography, eluting with 20-60% EtOAc/petroleum ether, to afford the title compound as a yellow gum (158 mg, 85%). ^{1}H NMR (400 MHz, CDCl$_3$): δ 7.58 (s, 1H), 7.52 (s, 1H), 7.44 (dd, J = 6.6, 1.5 Hz, 1H), 7.34 (app t, J= 7.7 Hz, 1H), 7.27 (d, J = 8.7 Hz, 1H), 7.19-7.05 (m, 3H), 6.98 (dd, J = 7.5, 0.7 Hz, 1H), 4.29 (s, 2H), 4.01 (s, 3H), 2.27 (s, 3H). ^{13}C NMR (101 MHz, CDCl$_3$): δ 163.2, 141.3, 138.9, 138.3, 137.5, 135.2, 128.0, 127.5, 125.4, 121.7, 121.2, 120.3, 120.2, 118.2, 110.0, 109.1, 39.8, 33.2, 11.1. υ_{max} (neat): 3114, 3051, 2921, 1616, 1582, 1554 cm^{-1}. HRMS: exact mass calculated for [M+H]$^+$ (C$_{19}$H$_{18}$BrN$_4$) m/z requires 383.0689, m/z found 383.0686.

Synthesis of ethyl 3-(2-oxopropoxy)benzoate (1.103). Chloroacetone (2.4 mL, 30.1 mmol, 1 equiv.) was added to a stirred suspension of ethyl 3-hydroxybenzoate (5 g, 30.1 mmol, 1 equiv.) and K_2CO_3 (8.3 g, 60.2 mmol, 2 equiv.) in acetone (150 mL, 0.2 M). The reaction mixture was heated to 60 °C for 16 h then allowed to return to room temperature and concentrated under vacuum. The residue was then dissolved in EtOAc (100 mL) and washed with H_2O (100 mL), followed by 4 M aq. NaOH (100 mL). The organic layer was collected, dried (hydrophobic frit), and concentrated under vacuum. Purified using silica chromatography, eluting with 10% EtOAc/petroleum ether, to afford the title compound as a yellow liquid (3.7 g, 55%). ^{1}H NMR (500 MHz, CDCl$_3$): δ 7.70-7.68 (m, 1H), 7.53 (dd, J = 2.6, 1.4 Hz, 1H), 7.37 (app t, J = 8.0 Hz, 1H), 7.10 (dd, J = 8.2, 2.7, 1H), 4.60 (s, 2H), 4.37 (q, J = 7.1 Hz, 2H), 2.29 (s, 3H), 1.39 (t, J = 7.1 Hz, 3H). ^{13}C NMR (126 MHz, CDCl$_3$): δ 205.0, 166.3, 157.8, 132.3, 129.8, 123.1, 119.8, 115.0, 73.2, 61.3, 26.8, 14.4. υ_{max} (neat): 2980, 2906, 1714, 1585 cm^{-1}. HRMS: exact mass calculated for [M+H]$^+$ ($C_{12}H_{15}O_4$) m/z requires 223.0965, m/z found 223.0966.

Synthesis of ethyl 3-((6-chloro-2-methyl-1*H*-indol-3-yl)oxy)benzoate (1.104). Prepared according to General Procedure A using (3-chlorophenyl)hydrazine hydrochloride (1.6 g, 9.01 mmol, 1 equiv.) and ethyl 3-(2-oxopropoxy)benzoate (**1.103**) (2 g, 9.01 mmol, 1 equiv.) in *t*BuOH (90 mL, 0.1 M) with additional 1 M HCl in Et$_2$O (27 mL) and AcOH (10 mL). Purified by silica chromatography, eluting with 10% EtOAc/petroleum ether, to afford the title compound as a pale brown amorphous solid (845 mg, 28%). ^{1}H NMR (600 MHz, CDCl$_3$): δ 7.72-7.65 (m, 2H), 7.62 (dd, J = 2.5, 1.6 Hz, 1H), 7.31 (app t, J = 8.0 Hz, 1H), 7.29 (d, J = 1.6 Hz, 1H), 7.13 (d, J = 8.4 Hz, 1H), 7.10 (dd, J = 8.3, 2.6 Hz, 1H), 6.98 (dd, J = 8.4, 1.8 Hz,

1H), 4.34 (q, J = 7.1 Hz, 2H), 2.32 (s, 3H), 1.36 (t, J = 7.1 Hz, 3H). NH proton not observed. ^{13}C NMR (151 MHz, CDCl$_3$): δ 166.4, 159.2, 133.6, 132.2, 129.6, 129.4, 127.9, 125.1, 123.1, 120.7, 120.3, 119.8, 118.2, 116.6, 111.0, 61.2, 14.4, 10.4. υ$_{max}$ (neat): 3350, 2982, 1713, 1701, 1585 cm^{-1}. HRMS: exact mass calculated for [M+H]$^+$ (C$_{18}$H$_{17}$ClNO$_3$) m/z requires 332.0862, m/z found 332.0867.

Synthesis of methyl 6-((2-methyl-1-(1-methyl-1H-pyrazol-4-yl)-1H-indol-3-yl)methyl)picolinate (1.105). Prepared according to General Procedure G using $trans$-bis(acetato)bis[o-(di-o-tolylphosphino)benzyl] dipalladium(II) (17 mg, 0.0181 mmol, 5 mol%), 3-((6-bromopyridin-2-yl)methyl)-2-methyl-1-(1-methyl-1H-pyrazol-4-yl)-1H-indole (**1.102**) (140 mg, 0.367 mmol, 1 equiv.), Mo(CO)$_6$ (97 mg, 0.367 mmol, 1 equiv.), [tBu$_3$PH]BF$_4$ (21 mg, 0.0724 mmol, 20 mol%), and DBU (82 μL, 0.550 mmol, 1.5 equiv.) in MeCN/MeOH (2.5 mL, 1:4, 0.1 M). Purified using silica chromatography, eluting with 50-100% EtOAc/petroleum ether, to afford the title compound as a yellow oil (55 mg, 42%). ^{1}H NMR (400 MHz, CDCl$_3$): δ 7.94 (d, J = 7.6 Hz, 1H), 7.62 (app t, J = 7.8 Hz, 1H), 7.59 (s, 1H), 7.53 (s, 1H), 7.42 (d, J = 7.4 Hz, 1H), 7.22-7.04 (m, 4H), 4.44 (s, 2H), 4.04 (s, 3H), 4.02 (s, 3H), 2.27 (s, 3H). ^{13}C NMR (101 MHz, CDCl$_3$): δ 166.2, 162.2, 147.4, 138.4, 137.5, 135.2, 128.1, 127.5, 125.9, 122.8, 121.7, 120.4, 120.2, 118.3, 110.0, 109.3, 53.1, 39.9, 33.6, 11.1. One carbon not observed/coincident. υ$_{max}$ (neat): 3118, 3090, 3001, 2943, 2919, 2855, 1716, 1617, 1591 cm^{-1}. HRMS: exact mass calculated for [M+H]$^+$ (C$_{21}$H$_{21}$N$_4$O$_2$) m/z requires 361.1659, m/z found 361.1660.

Synthesis of ethyl 3-((2-methyl-1H-indol-3-yl)oxy)benzoate (1.106). Prepared according to General Procedure A using phenylhydrazine hydrochloride (653 mg, 4.50 mmol, 1 equiv.) and ethyl 3-(2-oxopropoxy)benzoate (**1.103**) (1 g, 4.50 mmo, 1

equiv.) in tBuOH (45 mL, 0.1 M) with additional 1 M HCl in Et$_2$O (14 mL) and AcOH (14 mL). Purified by reverse-phase HPLC to afford the title compound as a pale brown amorphous solid (167 mg, 12%). ^{1}H NMR (500 MHz, CDCl$_3$): δ 7.91 (s, 1H), 7.79-7.71 (m, 2H), 7.34 (app t, J = 8.2 Hz, 1H), 7.28 (app t, J = 7.6 Hz, 2H), 7.20-7.12 (m, 2H), 7.06 (app t, J = 7.5 Hz, 1H), 4.39 (q, J = 7.1 Hz, 2H), 2.29 (s, 3H), 1.40 (t, J = 7.1 Hz, 3H). ^{13}C NMR (126 MHz, CDCl$_3$): δ 166.6, 159.4, 133.2, 132.0, 130.0, 129.5, 124.4, 122.9, 121.7, 121.5, 119.8, 119.7, 117.1, 116.6, 111.0, 61.2, 14.4, 10.1. υ$_{max}$ (neat): 3370, 2980, 1715, 1697, 1620, 1584 cm^{-1}. HRMS: exact mass calculated for [M+H]$^+$ (C$_{18}$H$_{18}$NO$_3$) m/z requires 296.1281, m/z found 296.1284.

Synthesis of 3-((3-bromophenyl)thio)-2-methyl-1H-indole (1.107). Prepared according to General Procedure E using phenylhydrazine hydrochloride (592 mg, 4.08 mmol, 1 equiv.) and 1-((3-bromophenyl)thio)propan-2-one (**1.74**) (1 g, 4.08 mmol, 1 equiv.) in EtOH (20 mL, 0.2 M). Purified using silica chromatography, eluting with 0-10% EtOAc/petroleum ether, to afford the title compound as a brown oil (1.2 g, 92%). ^{1}H NMR (400 MHz, CDCl$_3$): δ 8.30 (br s, 1H), 7.52 (d, J = 7.8 Hz, 1H), 7.36 (d, J = 8.0 Hz, 1H), 7.23-7.19 (m, 1H), 7.18-7.11 (m, 3H), 7.00 (app t, J = 8.1 Hz, 1H), 6.98-6.92 (m, 1H), 2.52 (s, 3H). ^{13}C NMR (101 MHz, CDCl$_3$): δ 142.1, 141.5, 135.6, 130.1, 127.9, 127.7, 124.1, 123.0, 122.5, 121.0, 118.9, 110.9, 98.5, 12.3. One carbon not observed/coincident. υ$_{max}$ (neat): 3392, 3055, 2980, 1573, 1556 cm^{-1}. HRMS: exact mass calculated for [M+H]$^+$ (C$_{15}$H$_{13}$BrNS) m/z requires 319.9925, m/z found 319.9931.

Synthesis of 3-(3-bromobenzyl)-2-methyl-1-(1-methyl-1H-pyrazol-4-yl)-1H-indole (1.108). Prepared according to General Procedure H using 2-

bromobenzaldehyde (90 mg, 0.486 mmol, 1.02 equiv.), 2-methyl-1-(1-methyl-1*H*-pyrazol-4-yl)-1*H*-indole (**1.87**) (100 mg, 0.474 mmol, 1 equiv.), Et$_3$SiH (84 μL, 0.529 mmol, 1.1 equiv.), and TFA (47 μL, 0.610 mmol, 1.3 equiv.) in DCM (2 mL, 0.2 M). Purified using silica chromatography, eluting with 20-50% EtOAc/petroleum ether, to afford the title compound as a yellow gum (165 mg, 89%). ^{1}H NMR (400 MHz, CDCl$_3$): δ 7.60 (s, 1H), 7.53 (s, 1H), 7.46-7.38 (m, 2H), 7.30 (d, *J* = 7.8 Hz, 1H), 7.21-7.04 (m, 5H), 4.09 (s, 2H), 4.02 (s, 3H), 2.26 (s, 3H). ^{13}C NMR (101 MHz, CDCl$_3$): δ 144.1, 138.3, 137.5, 134.6, 131.4, 130.0, 129.1, 128.1, 127.6, 127.1, 122.6, 121.5, 120.4, 120.0, 118.2, 110.5, 109.9, 39.8, 30.3, 11.1. υ$_{max}$ (neat): 3116, 3053, 2986, 2941, 2919, 1614, 1582, 1569 cm^{-1}. HRMS: exact mass calculated for [M+H]$^+$ (C$_{20}$H$_{19}$BrN$_3$) *m/z* requires 382.0736, *m/z* found 382.0737.

Synthesis of methyl 3-((2-methyl-1-(1-methyl-1*H*-pyrazol-4-yl)-1*H*-indol-3-yl)methyl)benzoate (1.109). Prepared according to General Procedure G using *trans*-bis(acetato)bis[*o*-(di-*o*-tolylphosphino)benzyl]dipalladium(II) (19 mg, 0.0202 mmol, 5 mol%), 3-(3-bromobenzyl)-2-methyl-1-(1-methyl-1*H*-pyrazol-4-yl)-1*H*-indole (**1.108**) (150 mg, 0.395 mmol, 1 equiv.), Mo(CO)$_6$ (104 mg, 0.395 mmol, 1equiv.), [*t*Bu$_3$PH]BF$_4$ (23 mg, 0.0793 mmol, 20 mol%), and DBU (88 μL, 0.593 mmol, 1.5 equiv.) in MeCN/MeOH (2.5 mL, 1:4, 0.2 M). Purified using silica chromatography, eluting with 50-70% EtOAc/petroleum ether, to afford the title compound as a yellow oil (111 mg, 78%). ^{1}H NMR (400 MHz, CDCl$_3$): δ 7.99 (s, 1H), 7.85 (d, *J* = 7.8 Hz, 1H), 7.59 (s, 1H), 7.53 (s, 1H), 7.41 (app t, *J* = 8.0 Hz, 2H), 7.31 (app t, *J* = 7.7 Hz, 1H), 7.18-7.01 (m, 3H), 4.16 (s, 2H), 4.01 (s, 3H), 3.90 (s, 3H), 2.27 (s, 3H). ^{13}C NMR (101 MHz, CDCl$_3$): δ 167.4, 142.1, 138.3, 137.5, 134.5, 133.1, 130.3, 129.6, 128.6, 128.1, 127.6, 127.3, 121.5, 120.4, 120.0, 118.2, 110.8,

109.9, 52.2, 39.8, 30.6, 11.1. υ_{max} (neat): 3116, 3051, 2949, 2919, 1718, 1608, 1584 cm^{-1}. HRMS: exact mass calculated for $[M+H]^{+}$ ($C_{22}H_{22}N_3O_2$) *m/z* requires 360.1707, *m/z* found 360.1705.

1.6.4 Bis-*p*NPP Inhibition Assay.

Molecules were tested for their ability to inhibit autotaxin activity using the Autotaxin Inhibitor Screening Kit (Cayman Chemical) with modifications to the manufacturer's protocol. Briefly, in a 96 well plate 20 ng/mL autotaxin was incubated with 1 mM bis-*p*NPP at 30 °C for 30 min in 50 mM Tris-HCl buffer (pH 8.5) containing 10 mM $CaCl_2$ and 0.02% triton X. Liberated bis-*p*-nitrophenol was measured using a Wallac Victor2 1420 multilabel counter (Perkin Elmer, Beaconsfield, UK) in absorbance mode at 405 nm. The background was determined by incubating bis-*p*NPP in the absence of enzyme. Activity of the compounds was determined by subtracting the average background optical density from all results and expressing the compound activity as a percentage of the enzyme-substrate reaction in the absence of compound. Compounds were screened against autotaxin at a single concentration or using a dose response curve. Single concentration screens were carried out at an inhibitor concentration of 30 μM; samples which showed inhibition of 60% or greater were considered to be active and progressed to further testing. Dose response curves were performed in the concentration range of 30 nM to 30 μM, or 2 nM to 50 μM, ten point curves. Compounds which showed inhibition of less than 60% at 30 μM or a IC_{50} value greater than 30 μM were considered inactive. Data was expressed as mean ± SEM, plotted, and the IC_{50} values were calculated using Graph Pad Prism version 6.00 for Windows, GraphPad Software, La Jolla California USA, www.graphpad.com.

1.6.5   LPC Choline Release Assay.

All biochemical studies were performed with human ATX (hATX). ATX lysoPLD

activity was measured by choline release from LPC. 20 nM ATX (prepared from

HEK 293 Flp-In cells, see SI) was incubated with 150 μM LPC(18:1) in a final

volume of 100 μL buffer containing 50 mM Tris pH 7.4, 0.01% Triton X-100, 50

mM $CaCl_2$, 1 Unit mL^{-1} choline oxidase, 2 Unit mL^{-1} HRP, 2 mM homovanilic acid

(HVA). The relative amount of released choline was measured by HVA fluorescence

in a 96-well plate (Corning). Fluorescent intensity was determined at λex/λem =

320/450 nm every 30 seconds for 90 minutes with a Fluorostar plate reader (BMG

Labtech). All compounds were screened initially from 400 nM to 100 μM, n = 3, and

categorised into one of four IC_{50} categories: (i) <1 μM; (ii) 1-10 μM; (iii) 10-20 μM;

(iv) >30 μM. Further screening of active compounds was then carried out from 0.5

nM to 10 μM, n ≥ 2. Data analysis was performed using GraphPad Prism version

6.00   for   Windows,   GraphPad   Software,   La   Jolla   California   USA,

www.graphpad.com

1.6.6   Molecular Modeling.

GOLD[69] software version 5.4.1 was used for the docking studies of analogues with

double mutant hATX (PDB 4ZG7, cocrystal of **1.21** with ATX). Starting with the

energy minimised structure of the inhibitor (minimised using the MM2 calculation,

Chem3D Pro software version 13.0.2.3021) the GOLD wizard was used to carry out

the molecular modelling. The binding site was defined to within 7 Å of the

PharmAkea analogue **1.21** and the docking was carried out using the slow method

and the top poses were examined further visually. The docking solutions were

viewed using Discovery Studio Visualizer[25] with the protein surface coloured by

hydrophobicity. By comparing the docking solutions to the binding mode of **1.21**, the pose of the inhibitor which gave the best overlay was selected for the basis of our docking model.

Chapter 2

Lead Optimisation of Small Molecule Non-RGD-mimetic Inhibitors for Integrin
Targets

2 Chapter 2: Lead Optimisation of Small Molecule Non-RGD-mimetic Inhibitors for Integrin Targets

2.1 Introduction

2.1.1 Integrins

Integrins are heterodimeric cell adhesion receptors that mediate the attachment of cells to the extracellular matrix (ECM) and are vital in cell to cell interactions.[79] These receptors were named "integrins" to represent the important role that they play in maintaining the integrity of the cytoskeletal-ECM linkage.[80] By recognising binding motifs in ECM proteins, integrins enable adhesion, migration, and proliferation of cells in their biological environment. At the time of this report, there are 24 known integrins in humans, each of which is composed of two non-covalently associated subunits: an α domain and a β domain (Figure 2.1).[79] These domains exist solely as dimeric species at the cell surface; there is an excess of the β subunit found within the cell, and the availability of α subunit counterparts determines the number of receptors that move to the cell surface.[81]
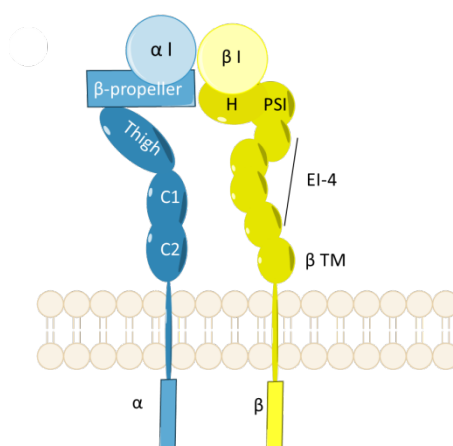
Figure 2.1. Illustrative representation of an RGD integrin: α domain (blue), β domain (yellow).

The α domain has an αI head positioned on a seven-bladed β-propeller which is supported by the leg structure; this is composed of a thigh, a calf-1 (C1), and a calf-2 domain (C2). Similarly, the β domain features a βI domain at its head, as well as a hybrid domain (H) and a plexin-sempahorin-integrin (PSI) domain, which are supported by a leg consisting of four cysteine-rich epidermal growth factor (EGF) repeats.[79] The αI and βI domains contain the cations found within the aptly named metal-ion-dependent adhesion site (MIDAS): it is at the interface of these two domains that ligand binding takes place.[82] The integrin receptors have flexible structures with a number of different conformations; the three main conformations are inactive, extended, and ligand occupied (Figure 2.2), which can be recognised by the conformation of the receptor.[83]
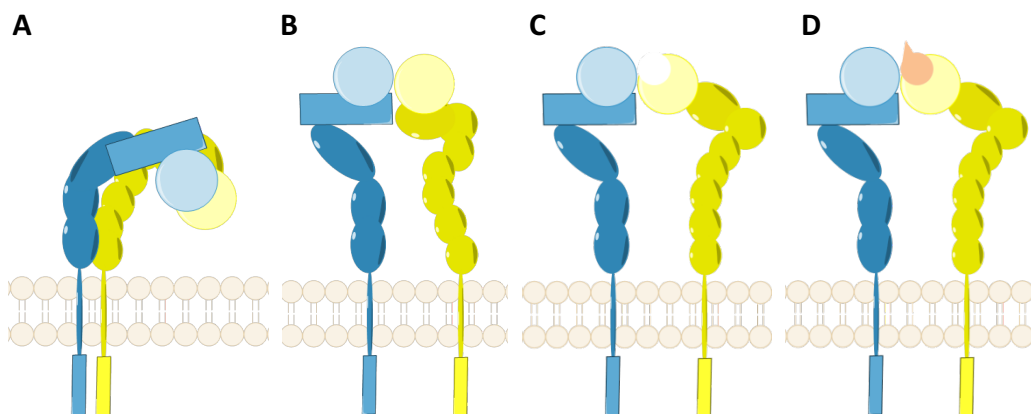
Figure 2.2. RGD integrin conformations: α domain (blue), β domain (yellow), and ligand (orange). A: Bent, inactive; B: Extended, closed headpiece conformation; C: Extended, open headpiece conformation; D: Ligand bound, open headpiece conformation. Based on previously reported structural information.[83]

The conformational changes can be caused by "inside-out" signalling, during which proteins within the cell bind to the transmembrane base of the β domain and induce the change in conformation outside the cell.[84] Alternatively, "outside-in" signalling

occurs when the integrin ectodomain interacts with a ligand, allowing the cell to sense and react to the extracellular environment.[84] In the inactive state the integrin is bent over towards the membrane and has a low affinity for ligands (Figure 2.2A); however, when the receptor extends out from the cell surface (Figure 2.2B), and the β H domain undergoes concomitant conformational change (Figure 2.2C), the receptor is primed and thus the integrin is activated. It is during this activated state that the ligands can bind to the open headpiece; however, there is evidence that integrins can bind ligands while in the bent, or partially bent, conformations.[85,86] A recent report, using biostructural studies of $\alpha_v\beta_3$ in complex with a physiologic ligand, has shown that key π-π interactions with Tyr122 of the β3 subdomain may be central to interacting with the inactive integrin without inducing any conformational changes in the receptor.[87] The inhibition of integrins can be achieved by preventing the activation of the receptor or by blocking the binding site, with the latter being the more common approach.[88] Each integrin recognises a specific type of ECM protein, thus the integrin family can be categorised into subsets based on the endogenous ligand; (i) leukocyte, (ii) collagen, (iii) tripeptide arginine-glycine-aspartic acid (RGD), or (iv) laminin (Figure 2.3).
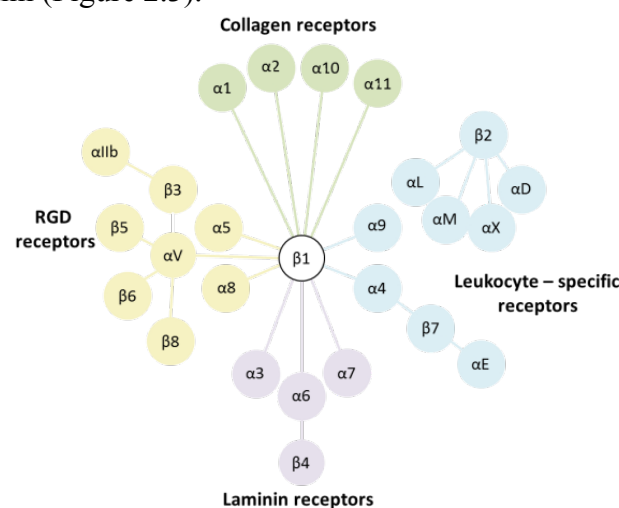
Figure 2.3. Integrin family, categorised by ligand type.

The RGD receptors are of particular therapeutic interest, with implications in thrombosis, fibrosis, and cancer, among other disease classes.[88] Accordingly, this class of receptor is, and has been, an active area for the development of novel medicines.

2.1.2 Inhibition of the RGD-binding Integrins

As discussed previously, integrins are known to enable adhesion, migration, and proliferation of cells in their biological environment and as a result they have been recognised as targets for a number of disease states. The therapeutic targets associated with the RGD integrins are summarised in Table 2.1.

Table 2.1. RGD integrin therapeutic targets

Integrin	Therapeutic Target
$\alpha_{IIb}\beta_3$	Thrombolytic disorders
$\alpha_v\beta_1$	Fibrosis
$\alpha_v\beta_3$	Cancer, brittle bones
$\alpha_v\beta_5$	Cancer, brittle bones
$\alpha_v\beta_6$	Fibrosis
$\alpha_v\beta_8$	Fibrosis
$\alpha_5\beta_1$	Angiogenesis, infectious disorders
$\alpha_8\beta_1$	Kidney disease

In the 1990s the first successful RGD integrin inhibitors were approved to reduce the risk of ischaemic events in patients undergoing percutaneous coronary intervention and those with acute coronary syndromes.[89] These pioneering inhibitors targeted the platelet $\alpha_{IIb}\beta_3$ integrin, also known as glycoprotein receptor (GP)-IIb/IIIa, an important target for the prevention of clot formation. This receptor is expressed uniquely on the surface of platelets and megakaryocytes, a type of platelet-producing cell in the bone marrow.[90] The three approved inhibitors are the antibody fragment abciximab,[91,92] and two small-molecule inhibitors eptifibatide,[93,94] and tirofiban[95,96]

(for a recent review see King *et al.*[97]). Although successful, these intravenously administered inhibitors are restricted to high-risk patients. Attempts to develop inhibitors for oral dosing were able to overcome the physicochemical challenges allied to zwitterionic compounds but there were issues related to pharmacology, with some orally-active antagonists of $\alpha_{IIb}\beta_3$ associated with a 30-35% increase in the risk of death due to partial agonism causing the opposite pharmacological effect.[98,99] Over eight million people have been treated using $\alpha_{IIb}\beta_3$ antagonists,[100] and to date $\alpha_{IIb}\beta_3$ remains to be the only RGD integrin for which pharmaceutical agents have been approved. The current clinical progress of selected RGD drugs is summarised in Table 2.2 (for a recent review of integrin-based therapeutics see Ley *et al.[101]*).

Table 2.2: Summary of RGD integrin inhibitors
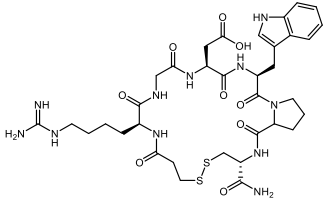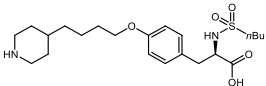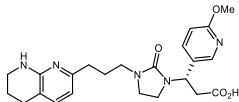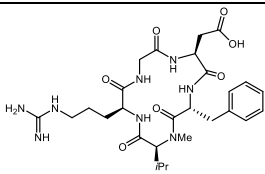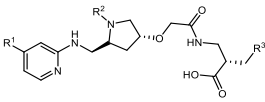
Name	Structure	Target Integrin(s)	Therapeutic Target (Stage)	MW[a]	clogP[b]	PSA[c]
Abciximab[91,92] (ReoPro)	Antibody fragment	$\alpha_{IIb}\beta_3$	Thrombosis (Approved)	-	-	-
Eptifibatide[93,94] (Integrilin)		$\alpha_{IIb}\beta_3$	Thrombosis (Approved)	832	-5.06	328
Tirofiban[95,96] (Aggrastat)		$\alpha_{IIb}\beta_3$	Thrombosis (Approved)	441	0.598	112
Etaracizumab[102,103]	Monoclonal antibody	$\alpha_v\beta_3$	Melanoma (Phase II), solid tumors (Phase I)	-	-	-
MK0429[104-106] (L-000845704)		$\alpha_v\beta_3$ $\alpha_v\beta_5$	Prostate cancer (Phase I), osteoporosis (Phase II)	440	-0.307	111

Table 2.2. *Continued.*

Name	Structure	Target Integrin(s)	Therapeutic Target (Stage)	MW[a]	clogP[b]	PSA[c]
Cilengitide[107-109]		$\alpha_v\beta_3$ $\alpha_v\beta_5$ $\alpha_5\beta_1$	Glioblastoma (Phase III)	589	-3.68	240
JSM6427‡[110]		$\alpha_v\beta_5$	Age-related macular degeneration (Phase I)	-	-	-
Volociximab[111, 112]	Monoclonal antibody	$\alpha_5\beta_1$	Solid tumors (Phase I)	-	-	-

[a]Molecular weight (MW); [b]Calculated logP (clogP); [c]Topological polar surface area (PSA). Properties determined using JChem for Office (Excel).[54] ‡ R groups not disclosed.

From consideration of the structures in Table 2.2, it can be noted that the non-peptide small-molecule inhibitors still retain RGD mimetics (or KGD) and thus resemble the native ligands of these integrins (Figure 2.4).
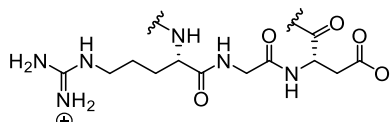
Figure 2.4. RGD peptide sequence.

It is understood that in the binding of the RGD sequence the acid coordinates with the Mg^{2+} and the arginine group resides in a narrow cleft on the β domain forming salt bridges with Asp150 and Asp218;[113] RGD-mimetic inhibitors are designed to make the same interactions as the native ligand. Although these zwitterionic peptidomimetics provide potency, they often suffer from sub-optimal *in vivo*

101

pharmacokinetic profiles due to their high MW, high PSA, low clogP, and, in some cases, high conformational flexibility. Furthermore, the use of oral RGD-mimetic $\alpha_{IIb}\beta_3$ inhibitors has led to a major issue in relation to pharmacology, as the compounds also have the potential to activate the receptor.[114] The approved $\alpha_{IIb}\beta_3$ inhibitors discussed previously have been reported to also cause partial agonism, and as a result cause the opposite pharmacological effect.[115,116] This reported partial agonism is a result of allosteric changes upon binding, which prime the receptor. A preclinical study by Reynold *et al*. found that the $\alpha_v\beta_3$ antagonist cilengitide may promote tumor growth *in vitro*;[117] however, these results are highly debated, with many clinical trials of cilengitide indicating no safety signal.[118]

One RGD-mimetic small molecule antagonist of $\alpha_{IIb}\beta_3$ that does not induce receptor priming upon binding is UR-2922 (**2.1**), which is the active form of the prodrug UR-3216 (**2.2**) (Figure 2.5). This antagonist, developed by Ube, has been shown to bind tightly to resting platelets, with a Ki of <1 nM. The excellent potency, along with slow dissociation and rapid clearance of the unbound drug, is advantageous for oral dosing of this antagonist.[119,120] Although **2.1** has the RGD-mimetic of the typical RGD integrin antagonist, no partial agonism of the $\alpha_{IIb}\beta_3$ receptor has been reported as a result of it binding. Modelling studies carried out by Cox *et al*. suggested that this analogue does not interact with the MIDAS, and thus does not activate the receptor.[88] Instead of interacting with the cation, the authors propose that the carboxyl group of **2.1** forms an H-bond with Tyr166 and a salt bridge with Arg165. This proposed alternative binding of the acidic motif, along with additional π-π interactions with Phe160, would distinguish this RGD-mimetic inhibitor from the compounds described in Table 2.2; however, it is surprising that an RGD-mimetic

inhibitor would bind via an alternative binding mode, and no biostructural evidence was reported to support the author's hypothesis.
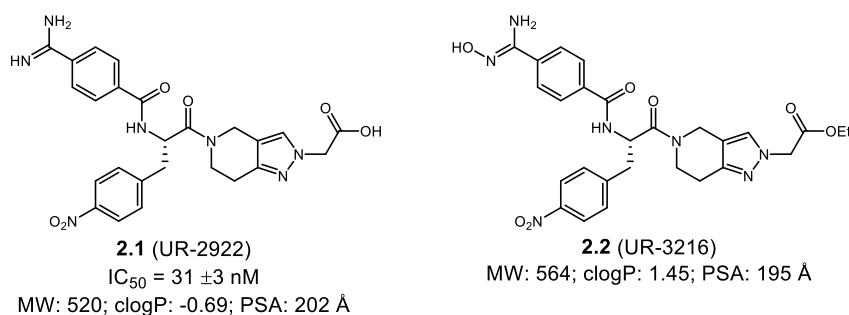
Figure 2.5. $\alpha_{IIb}\beta_3$ antagonist **2.1** and the prodrug form **2.2**. IC$_{50}$ for inhibition of ADP-induced aggregation of platelets (human).[119,120]

A potential approach to avoid this unwanted activation of $\alpha_{IIb}\beta_3$ is to design inhibitors that block the binding site without forming the interactions made by the native RGD sequence. Thus the design of non-RGD-mimetic inhibitors could identify effective small-molecule antagonists that do not activate the integrin. This is a particularly promising strategy for integrin therapeutics targeting the RGD subfamily as the increase in mortality associated with the failed attempts at oral $\alpha_{IIb}\beta_3$ antagonists has been attributed to the ability of RGD-mimetic inhibitors to prime the receptor.[98,99] Furthermore, the development of non-RGD-mimetic inhibitors could lead to a more synthetically tractable series, that could provide easier explorations of SAR. By avoiding the RGD-mimetic, compounds may also have the potential to possess more favorable physicochemical properties, and therefore improved pharmacokinetic profiles.

2.1.3 Emergence of Non-RGD-mimetic Inhibitors

2.1.3.1 $\alpha_{IIb}\beta_3$ Non-RGD-mimetic Inhibitors

The first non-RGD-mimetic inhibitor of $\alpha_{IIb}\beta_3$ was identified in 2008 by Blue *et al*.

using a medium throughput screen (MTS) of 33,264 small molecules.[121] This

inhibitor, termed RUC-1 (**2.3**, IC_{50} = 9.7 ±1 μM), was reported to be effective and

selective at $\alpha_{IIb}\beta_3$, with no activity observed at the related integrin $\alpha_v\beta_3$, Figure 2.6.

Through docking studies, **2.3** was determined to interact only with the α_{IIb} domain

and not with the β_3 subunit, thus explaining the specificity over $\alpha_v\beta_3$ displayed by this

inhibitor. The authors also reported that this compound did not show any agonism of

the integrin and hypothesised that the lack of interactions with the MIDAS metal ion

may be the reason for this. Mutagenesis studies were carried out which supported the

proposed binding mode.[122] Subsequently, the cocrystal structure of **2.3** with $\alpha_{IIb}\beta_3$

confirmed that the binding site was localised to the α_{IIb} domain and provided further

insight into this small molecule inhibitor.[123] This crystal structure revealed that **2.3**

binds to the closed conformation of the integrin headpiece and does not result in any

priming of the receptor (PDB 3NIF). This is in contrast to RGD-mimetic antagonists,

which have been shown to activate $\alpha_{IIb}\beta_3$ resulting in partial agonism.[114,115] The

Coller group were able to develop **2.3** further, through structure-based design, and

produce an analogue with approximately 100-fold higher affinity, termed RUC-2

(**2.4**, IC_{50} = 95 ±5 nM), Figure 2.6.[124] This more potent analogue was cocrystallised

with $\alpha_{IIb}\beta_3$, but no density for the metal ion at the MIDAS was observed (PDB

3T3M). It was noted that **2.4** had the same binding interactions as **2.3** but with

additional interactions in the β_3 βI domain. The primary amine of **2.4** was discovered

to compete with the Mg^{2+} for interactions with the carboxyl oxygen of Glu220; thus,

in high enough concentration, **2.4** displaced the metal ion of the MIDAS, explaining its absence from the cocrystal. Furthermore, the authors report that **2.4** does not activate the integrin upon binding, thus preventing any unwanted signaling. This compound is the first in a novel class of integrin antagonists termed "ion displacement ligands" by the developers of **2.4**.[125] In 2014 the Coller group reported the SAR surrounding the optimisation of **2.4**.[125] Two analogues were disclosed: RUC-3 (**2.5**) and RUC-4 (**2.6**), and the results of their docking studies compared with the binding of **2.4** suggested that additional water-mediated interactions of the nitrogen atoms with the receptor were responsible for the differences in the potencies observed, Figure 2.6. Unfortunately, **2.5** was found to be unstable in solution (DMSO or aqueous), and as a result was deprioritised. Through the ADMET profiling of **2.4** and **2.6**, it was found that **2.6** had a modest microsomal stability profile (23.2 μL/min/mg, human) whereas **2.4** was highly resistant (-1.16 μL/min/mg, human). Incorporation of a nitrogen into the aromatic ring at the core to give **2.6** increased the aqueous solubility (thermodynamic solubility at pH 7.4: **2.4** 28.0 μg/mL; **2.6** 239.5 μg/mL) and maintained the potency. This chemotype was recently patented,[126] and further research is underway for the development of the more water soluble **2.6** towards a pre-hospital treatment of myocardial infraction.[127]

2.3 (RUC-1)[44]
$IC_{50} = 9.7 \pm 1$ µM
MW: 265; clogP: 1.25; PSA: 65 Å

2.4 (RUC-2)[47]
$IC_{50} = 95 \pm 5$ nM
MW: 385; clogP: 0.72; PSA: 122 Å

2.5 (RUC-3)
$IC_{50} = 33$ nM
MW: 386; clogP: 0.10; PSA: 135 Å

2.6 (RUC-4)
$IC_{50} = 45$ nM
MW: 386; clogP: -0.50; PSA: 135 Å
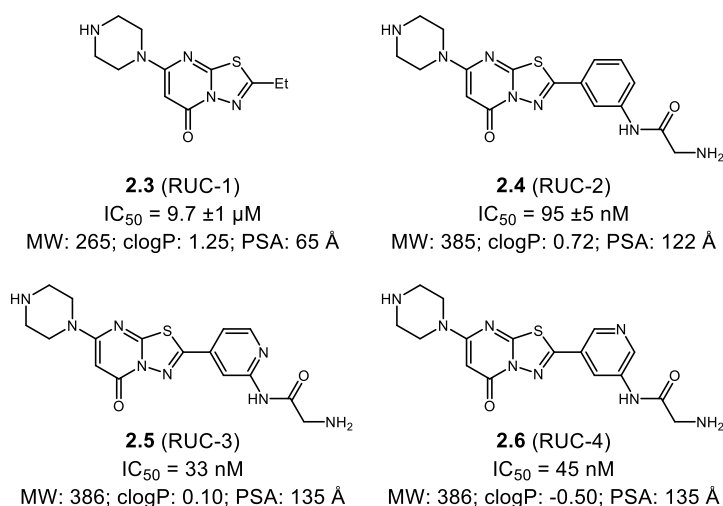
Figure 2.6. RUC-1 (**2.3**),[44] RUC-2 (**2.4**),[47] RUC-3 (**2.5**), and RUC-4 (**2.6**)[48] from the Coller group. IC_{50} for inhibition of ADP-induced aggregation of platelets (human).

Based on the unique binding mode of **2.3** and **2.4**, Negri *et al*. carried out a structure-based virtual screen with the aim of identifying new small molecule antagonists of $\alpha_{IIb}\beta_3$.[128] Over 2.5 million "lead-like" compounds of the ZINC database[129] were screened, and then five potential antagonists were selected from the top 500 scoring compounds. The ligands were selected based on the interactions observed during modelling, diversity of chemotype, and their commercial availability. Of the five compounds purchased (termed MSSM-1-5), four were successfully tested for biological activity against $\alpha_{IIb}\beta_3$, and two were found to show micromolar inhibition of $\alpha_{IIb}\beta_3$, including MSSM-1 (**2.7**), Figure 2.7. These novel inhibitors were also found to show specificity for their desired integrin over $\alpha_v\beta_3$, and no undesired priming of the receptor was observed. In 2015 a second virtual screen of antagonists for $\alpha_{IIb}\beta_3$ was reported by Wang *et al*.[130] This work combined the structure-based *in silico* screen with a ligand-based pharmacophore screen of over 7.3 million "drug-like" compounds from the ZINC database. Their campaign identified 11 commercially available compounds, which were obtained and tested for their inhibitory effect

against platelet aggregation. Three compounds were found to exhibit micromolar activity, with compound **2.8** displaying the highest potency, Figure 2.7. Wang *et al.* also comment that this potential antagonist is predicted to have good solubility, permeability, ADMET properties, and low toxicity *in vivo*. This is perhaps surprising as the basic 4-aminopyridine motif will increase the polarity of **2.8**, thus lowering the permeability of this inhibitor; however, no measured permeability or pharmacokinetics were reported. With few non-RGD-mimetic inhibitors known in the literature, broad *in silico* screening appears to be a valuable tool for identifying novel scaffolds, but it is limited by the database(s) used.

2.7
IC$_{50}$ = 12 ±1 μM
MW: 347; clogP: 2.52; PSA: 142 Å

2.8
IC$_{50}$ = 20 ±4 μM
MW: 343; clogP: 0.03; PSA: 103 Å
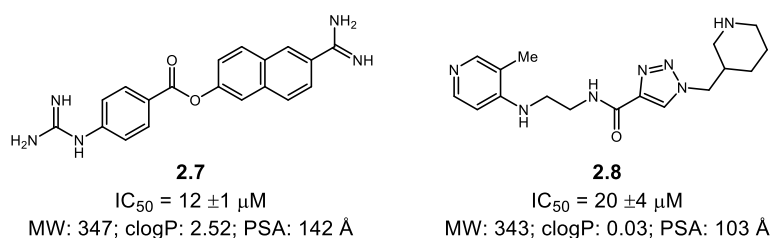
Figure 2.7. α$_{IIb}$β$_3$ inhibitors identified by virtual screening. IC$_{50}$ for inhibition of ADP-induced aggregation of platelets (human).[128, 130]

A more recent report from Polishchuk *et al.* used quantitative structure–activity relationship (QSAR) and pharmacophore models to screen a number of databases for novel α$_{IIb}$β$_3$ antagonists, but no hit compounds were identified.[131] The authors concluded that this was the result of the low number of zwitterionic compounds available in the commercial libraries used for their screen. Thus, the group used their models to design focused libraries of novel compounds, which were screened to identify ligands that could bind either the open or the closed form of the αIIbβ3 receptor. In order to model ligands for the open form, the RGD-mimetic inhibitor Tirofiban was used, whereas the closed form analogues were based on **2.4**. The

virtual hit compounds were synthesised and through biological screening, one low nanomolar inhibitor for the closed receptor was successfully identified (compound **2.9**). Docking studies carried out using compound **2.9** showed a similar binding mode to that of **2.4**, but this analogue showed superior levels of potency with an IC_{50} of 11 nM, Figure 2.8. A key feature of their model for a closed form binder was a distance of 15.8 Å between two positively charged centers. The authors later confirmed this hypothesis using a series of analogues in which this distance was varied.[132] This study showed that shortening the compound by one carbon (compound **2.10**) caused a greater than 100-fold decrease in potency, and lengthening by one carbon (compound **2.11**) was also unfavorable, resulting in micromolar inhibition, Figure 2.8.
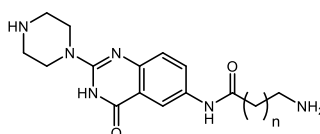
2.9, n = 2, IC_{50} = 11 ±1 nM; MW: 316; clogP: -0.95; PSA: 118 Å
2.10, n = 1, IC_{50} = 150 ±25 nM; MW: 302; clogP: -1.19; PSA: 118 Å
2.11, n = 3, IC_{50} = 1.4 ±0.17 μM; MW: 330; clogP: -0.91; PSA: 118 Å

Figure 2.8. $\alpha_{IIb}\beta_3$ non-RGD-mimetic inhibitors designed from **2.4**. IC_{50} for inhibition of ADP-induced aggregation of platelets (human).[131,132]

2.1.3.2 $\alpha_v\beta_3$ Non-RGD-mimetic Inhibitors

To the best of the author's knowledge, the first example of a non-RGD-mimetic inhibitor of an RGD integrin was reported by Dayma *et al.* in 2006.[133] This work utilised common feature pharmacophore models, which were derived from known $\alpha_v\beta_3$ inhibitors. Two databases were screened (NCI2000 and Chemical Diversity) using the pharmacophore model, to give over 400 compounds. Hit compounds were then filtered by physicochemical properties, structural diversity, and commercially availability, to give 29 potential antagonists, which were obtained for further

investigation. Through in vitro evaluation, four compounds were found to inhibit $\alpha_v\beta_3$, including the non-RGD-mimetic compound **2.12**, Figure 2.9. The authors recognised the novelty of this inhibitor and carried out a small SAR study, which identified inhibitor **2.13** with a 800-fold higher affinity than the initial hit **2.12**. This subnanomolar non-RGD-mimetic $\alpha_v\beta_3$ inhibitor was shown to have low cytotoxicity, and therefore the authors suggest this inhibitor has potential for the development of a noncytotoxic anticancer therapy. The 2-imino-rhodanine motifs at the core of **17** and **18** are often identified as screening hits, and thus are recognised pan-assay interference compounds (PAINS); therefore, these inhibitors may be unsuitable for further development.[134]

2.12
IC_{50} = 240 nM
MW: 398; clogP: 3.54; PSA: 102 Å

2.13
IC_{50} = 0.03 nM
MW: 433; clogP: 3.56; PSA: 91 Å
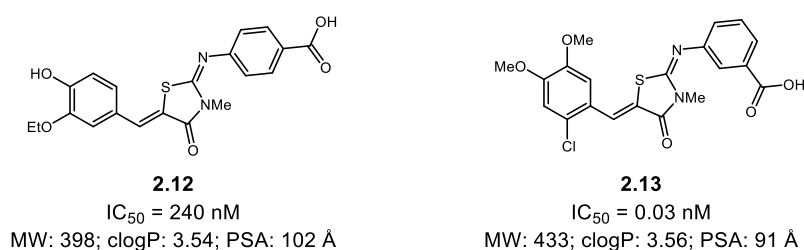
Figure 2.9. $\alpha_v\beta_3$ inhibitors identified by Dayam *et al*. IC_{50} for inhibition of $\alpha_v\beta_3$ receptor binding assay.[133]

This work was closely followed by a report from Zhou *et al*. in which a number of small molecule inhibitors of $\alpha_v\beta_3$ that lacked the aspartic acid mimetic were discovered.[135] By using a crystal structure of $\alpha_v\beta_3$ in complex with an RGD ligand (PDB 1L5G, Xiong *et al.*[113]), this group carried out a virtual screen of 88,695 commercially available organic compounds. A rigorous triage of docking results was used to successfully identify 50 potential inhibitors for biological testing. From the compounds that were selected for testing, seven were found to have inhibitory activity with an IC_{50} of <200 μM. The most potent of the hit compounds was

inhibitor **2.14** with an IC$_{50}$ = 38.5 ±1.7 μM, which was progressed onto further testing *in vitro* and found to effectively inhibit cell migration and angiogenesis, Figure 2.10. Zhou *et al.* went on to explore this non-RGD-mimetic small molecule further through the synthesis of a series of analogues, which led to the identification of another inhibitor of similar potency, compound **2.15** (IC$_{50}$ = 33.5 ±3.1 μM), Figure 2.10. Docking studies of this compound identified that, in the most energetically favorable binding pose, the biguanide group can interact with a number of residues in the MIDAS through a series of H-bonds. This predicts that inhibitors of this chemotype will interact with the receptor through a significantly different binding mode than that of the more classic RGD-mimetic inhibitors, which is surprising as the biguanide might be expected to mimic the arginine. Unfortunately, no further structural information was obtained, and thus the alternative binding mode of these compounds remains unconfirmed. The authors do not report whether these non-RGD-mimetic compounds are both antagonists and/or partial agonists of the receptor; nevertheless, both inhibitor **2.14** and **2.15** having the low molecular weight of 246 Da makes the ligand efficiency of these compounds high.

2.14
IC$_{50}$ = 38.5 ±1.7 μM
MW: 246; clogP: 1.93; PSA: 101 Å

2.15
IC$_{50}$ = 33.5 ±3.1 μM
MW: 246; clogP: 1.93; PSA: 101 Å
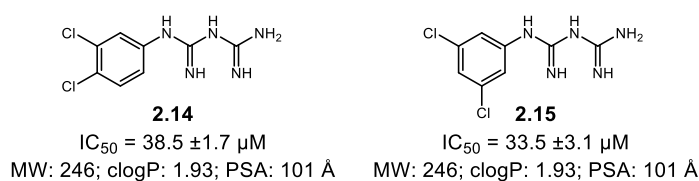
Figure 2.10. α$_v$β$_3$ inhibitors identified by Zhou *et al.* IC$_{50}$ for inhibition of α$_v$β$_3$-mediated cell adhesion.[135]

Another series of small molecule non-RGD-mimetic α$_v$β$_3$ inhibitors was reported by Elliot *et al.* in 2009.[136] This group had taken an alternative strategy and designed a series of novel inhibitors without the arginine motif. Their approach began with the

screening of low molecular weight carboxylic acids and acid isosteres, from which they identified the hit compound **2.16**, Figure 2.11. This initial hit had a promising IC_{50} of 800 nM, thus demonstrating that it is possible to achieve good affinity with $\alpha_v\beta_3$ using a non-RGD-mimetic chemotype, but the authors do not report any details of the assay used. Through exploration of the SAR, Elliot *et al.* were able to improve this potency with the development of lead compound **2.17** with an IC_{50} of 11 nM; however, the compound had limited permeability (0.021×10^6 cm s^{-1}) and the authors comment that there was only modest selectivity for $\alpha_v\beta_3$ over $\alpha_{IIb}\beta_3$. Based on analysis of previously reported crystal structures of these two integrins (PDB 1L5G vs. 1TY7) and modelling studies, the authors hypothesised that altering the *ortho* position of the sulfonamide could improve the selectivity. Through the synthesis of further *ortho* substituted analogues compound **2.18** was discovered, with an IC_{50} of 700 nM and a >130-fold selectivity for their desired target $\alpha_v\beta_3$ over $\alpha_{IIb}\beta_3$. This work shows that it is possible to design nanomolar inhibitors of $\alpha_v\beta_3$ without the use of an RGD-mimetic, although the PSA values of these inhibitors are high.

2.16
IC_{50} = 800 nM
MW: 328; clogP: 1.06; PSA: 115 Å

2.17
IC_{50} of 11 nM
MW: 394; clogP: 1.16; PSA: 133 Å

2.18
IC_{50} of 700 nM
MW: 368; clogP: 0.35; PSA: 138 Å
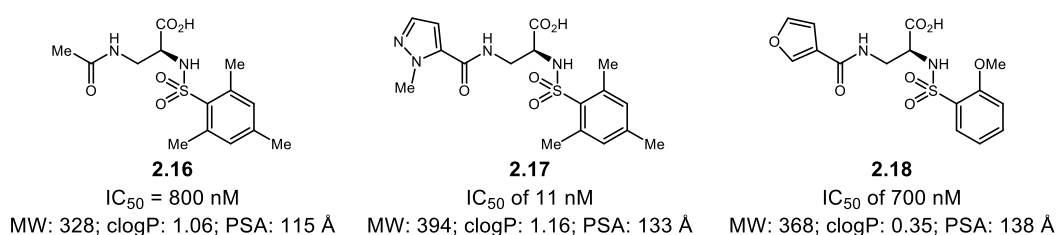
Figure 2.11. $\alpha_v\beta_3$ inhibitors identified by Elliot *et al.*[136] Assay protocol not reported.

2.1.3.3 $\alpha_5\beta_1$ Non-RGD-mimetic Inhibitors

In 2007 a patent by AstraZeneca was reported claiming a series of small molecule inhibitors of the RGD integrin $\alpha_5\beta_1$.[137] The majority of compounds covered by the patent had the RGD-mimetics, but there were a small number of inhibitors claimed

which did not fit this chemotype; for example, compound **2.19** which lacks the arginine mimetic, Figure 2.12. This inhibitor was reported to have an IC_{50} of 4 μM in a cell adhesion assay and an IC_{50} of 466 nM using a second electrochemiluminescence ligand binding assay. Thus showing that this compound was able to inhibit $α_5β_1$ *in vitro*, however, no *in vivo* data was reported. Although **2.19** is a non-RGD-mimetic inhibitor, this compound is quite large and lipophilic, with the high MW of 545 Da and high clogP of 5.44. Based on these physicochemical properties **2.19** might be predicted to suffer from poor ADMET; however, no measured pharmacokinetics were disclosed.
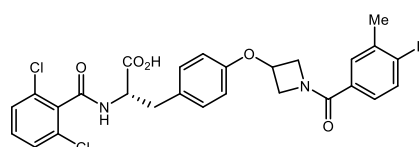
2.19
IC_{50} = 466 nM[a]; IC_{50} = 4 μM[b]
MW: 545; clogP: 5.44; PSA: 99 Å

Figure 2.12. $α_5β_1$ inhibitor **2.19** reported by AstraZeneca.[137] [a]Electrochemiluminescence ligand binding assay. [b]Cell adhesion assay.

More recently, another non-RGD-mimetic inhibitor of $α_5β_1$ was reported by Kang and Kim.[138] Termed IPS-05002, compound **2.20** was identified by a screen of a phytochemical compound library using a ProteoChip-based protein-protein interaction assay for $α_5β_1$ antagonists. This compound showed micromolar inhibition of $α_5β_1$ in a cell proliferation assay and a cell migration assay, Figure 2.13. Furthermore, the authors report that this antagonist inhibits cell adhesion and tubular network formation, and thus **2.20** may inhibit angiogenesis. This experimental evidence shows the potential for this novel small molecule to be developed into a potent antagonist; however, the complex structure may limit an SAR exploration of this scaffold if the synthetic route is not amenable to diversification.
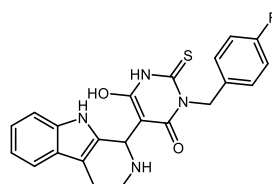
2.20 (IPS-05002)
IC_{50} = 20.5 ±0.56 μM^a; IC_{50} = 15.52 μM^b
MW: 422; clogP: 2.58; PSA: 88 Å

Figure 2.13. $\alpha_5\beta_1$ inhibitor **2.20**.[138] [a]Cell proliferation assay. [b]Cell migration assay.

In summary, the RGD integrins are recognised therapeutic targets. Numerous RGD inhibitors have been evaluated clinically for a range of therapeutic indications. For example $\alpha_v\beta_3/\alpha_v\beta_5$ inhibitor cilengitide alone has been studied in at least 35 clinical trials with issues appearing to be efficacy rather than safety. To date however, inhibitors have been approved for only one integrin from this class namely intravenous $\alpha_{IIb}\beta_3$. Safety issues were seen with oral $\alpha_{IIb}\beta_3$ inhibitors and ascribed to conformational changes in the receptor upon binding. The emergence of small molecule non-RGD-mimetic inhibitors has led to the discovery of new chemotypes with the promise of much increased synthetic tractability, which inhibit the RGD integrins, without – in the case of $\alpha_{IIb}\beta_3$ - the activation of the receptor, but the development of an efficacious, safe drug from this new generation of inhibitors is yet to be achieved. Initial compounds were identified using MTS and virtual screening, however, biostructural information on the non-RGD-mimetic inhibitors bound to the receptor, along with advancements in the understanding of the unwanted integrin priming, has provided clues to the rational design of novel non-RGD-mimetic compounds. This new generation of RGD-integrin antagonists could lead to the development of a safe and efficacious oral dosing $\alpha_{IIb}\beta_3$ inhibitor, and help realise the potential of the RGD integrins as therapeutic targets.

2.2   Project Aims

As discussed previously, the design of non-RGD-mimetic inhibitors for RGD integrins has led to the development of potent inhibitors without the unwanted priming of the integrin receptor. This strategy has been successfully applied to the integrin $\alpha_{IIb}\beta_3$ to produce low nM inhibitors with favourable physicochemical properties. We aimed to use the information available from the current literature to aid the design of non-RGD-mimetic inhibitors for the $\alpha_v\beta_3$ integrin. RUC-2 (**2.4**) has been shown to have a specificity for $\alpha_{IIb}\beta_3$ over $\alpha_v\beta_3$, which can be explained by the piperazine motif being too large to bind within the active site of the latter, Figure 2.14A. By overlaying the crystal structures of $\alpha_{IIb}\beta_3$ and $\alpha_v\beta_3$ a key difference in the position of the acidic residues was noted, Figure 2.14B. By targeting this alternative acidic residue it was hoped that specificity for $\alpha_{IIb}\beta_3$ over $\alpha_v\beta_3$ could be realised.
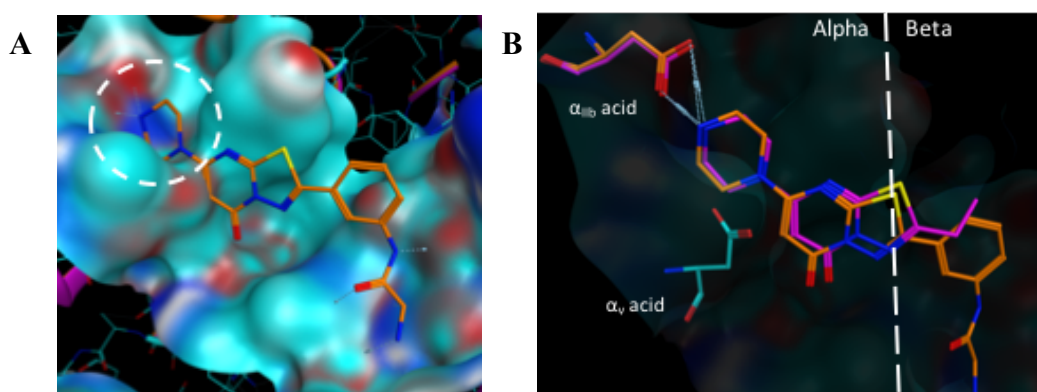
Figure 2.14. A: **2.4** docked within $\alpha_v\beta_3$ with the protein clash highlighted. B: Crystal structures overlays of $\alpha_{IIb}\beta_3$ and $\alpha_v\beta_3$ with the different acidic residues highlighted.[‡]

This structural information provided a starting point for the design of novel $\alpha_v\beta_3$ non-RGD-mimetic inhibitors. The reported cocrystal of **2.4** with $\alpha_{IIb}\beta_3$ revealed that the

---

[‡] Docking carried out by Dr Sandeep Pal, GSK

primary amine of this inhibitor, and analogues thereof, displaces the metal ion found within the β_3 domain during binding. Thus, we sought out to design new small molecule non-RGD-mimetic inhibitors of $\alpha_v\beta_3$ by maintaining the 2-amino-*N*-phenylacetamide of **2.4** to bind within the β_3 domain, but altering the remaining structure to interact with the α_v domain over α_{IIb}, Figure 2.15.
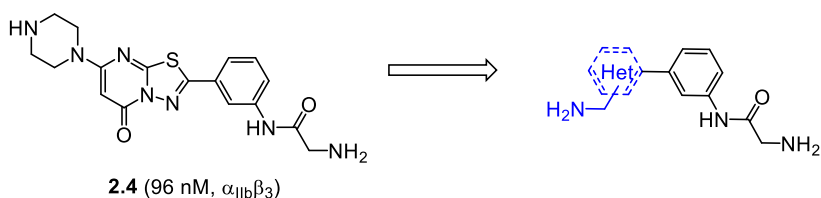
Figure 2.15. Design of novel non-RGD-mimetic $\alpha_v\beta_3$ inhibitors from **2.4**.

Compounds were designed to include a second basic centre on the molecule, which was intending to interact with the acidic residues within the binding site. The design template, Figure 2.16, also aimed to explore different heterocycles, which would project the basic nitrogen in different vectors.
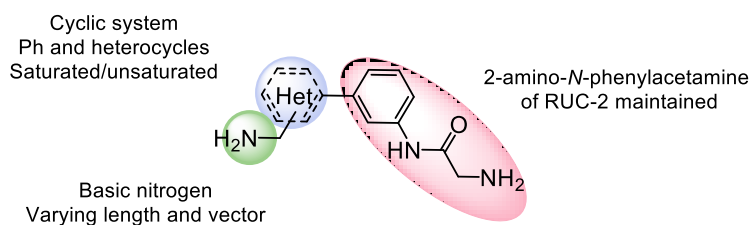
Figure 2.16. Molecule design of novel $\alpha_v\beta_3$ inhibitors.

It was hoped that using this design template a lead molecule would be identified, which could then be optimised further. Compounds were also designed with the physicochemical properties in mind. By maintaining a low MW and avoiding any zwitterionic compounds, it was hoped that any lead compounds identified would possess good druglike properties.

2.3   Results and Discussion

2.3.1   Biological Evaluation

2.3.1.1   Cell Assay

The cell adhesion assay was carried out in house at GSK using the previously reported protocol.[139] An assay plate is coated with a known ligand for the integrin being tested against. Once coated, labelled cells are added to the plate and incubated for a set time to allow the cells to adhere to the receptors. The cells are pre-labelled with a fluorescent marker for the adhesion to be measured. The plate is then washed to remove any un-adhered cells and the adhered cells quantified by measuring the fluorescence. For the screening of compounds in a dose-response mode, a set concentration of potential inhibitor is added to the plate concurrently with the labelled cells. Inhibition can then be determined by measuring the fluorescence of any adhered cells after the plate is washed. The concentration range of the cell assay used in this project allowed for the measurement of pIC_{50} values >5.0.
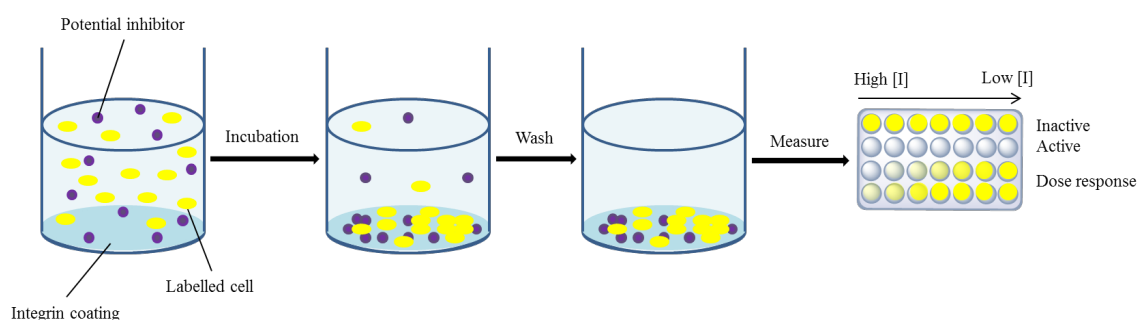
Figure 2.17. Schematic representation of cell adhesion assay. [I] = inhibitor concentration.

2.3.1.2   Fluorophore Probe Assay

At the time of this report, the fluorophore probe (FP) assay employed at GSK had not yet been published and thus the details are not disclosed herein; however, a brief overview is provided for the readers understanding. The integrin required for the

116

assay is added to a plate containing the compounds being assayed. After a set time of incubation to allow binding, the FP is added and the assay mixture is incubated again during which time the probe will compete with the inhibitor for the receptors. The quantity of bound FP is then measured, and thus the inhibition can be determined. The concentration range of the FP assay used in this project allowed for the measurement of pIC_{50} values >4.0.

2.3.2 Structure-activity Relationships

The first series of compounds were simple six membered heterocycles, and one phenyl, that featured the aniline motif. Initial compounds were designed with an aniline in the *meta* position as *in silico* work had predicted this to be the best vector for the basic group to target the acidic residue. Although one *para* amine was also included as the model predicted this position to be able to form similar interactions to that of the *meta*, Figure 2.18.
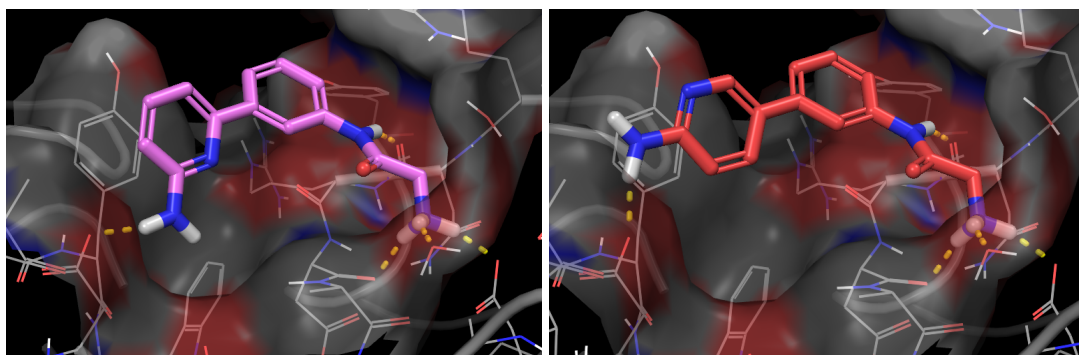
Figure 2.18 *In silico* study of **2.21** (left) and **2.25** (right). Docked and visualised using LiveDesign.[140]

A set of a seven analogues were synthesised to explore this hypothesis. Unfortunately, this template was unsuccessful with these first analogues showing no activity at our target integrin, Table 2.3.
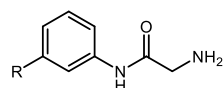
Table 2.3. Initial aniline analogues. NT = not tested.

Compound	R	Cell Assay			FP Assay				
		$\alpha_v\beta_1$	$\alpha_v\beta_3$	$\alpha_v\beta_6$	$\alpha_v\beta_1$	$\alpha_v\beta_3$	$\alpha_v\beta_5$	$\alpha_v\beta_6$	$\alpha v\beta_8$
2.21		<4.9	<4.9	<4.9	4.5	<4.0	<4.0	4.1	4.2
2.22		<4.8	<4.8	<4.8	<3.9	<3.9	<3.9	<3.9	<3.9
2.23		<5.0	<5.0	<5.0	4.9	<4.1	<4.1	<4.1	<4.1
2.24		<5.0	<5.0	<5.0	<4.1	<4.1	<4.1	<4.1	<4.1
2.25		<4.9	<4.9	<4.9	<3.9	<3.9	<3.9	<3.9	<3.9
2.26		<5.0	NT	<5.0	<4.1	<4.1	<4.1	<4.1	<4.1
2.27		<4.9	NT	<4.9	<4.0	<4.0	<4.0	<4.0	<4.0

To explore a wide area of chemical space, some more elaborate heterocycles were evaluated using the *in silico* studies. The imidazopyridine amine **2.28** was predicted to form a bidentate interaction with a nearby acidic residue in the docking model, Figure 2.19. Unfortunately, no activity was observed when this analogue was tested in either the cell assay or the FP assay, Table 2.4. Two different tetrahydronaphthyridine compounds (**2.35** and **2.36**) were found to show off-target micromolar activity, but no inhibition of the integrin of interest, $\alpha_v\beta_3$, was observed.
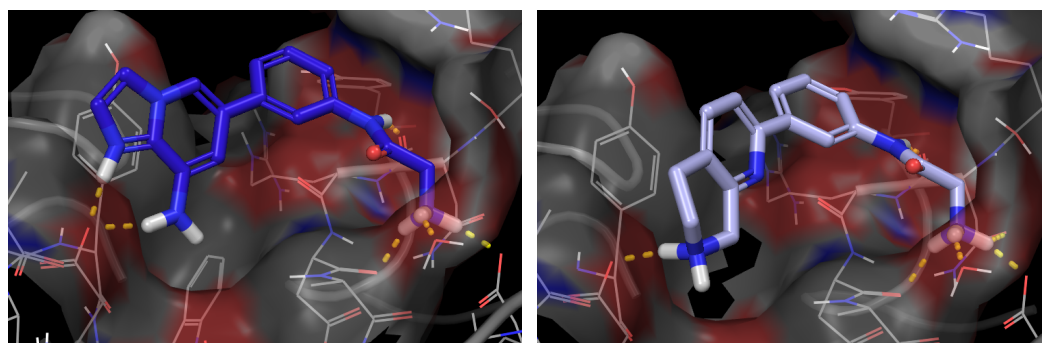
Figure 2.19 *In silico* study of **2.28** (left) and **2.32** (right). Docked and visualised using LiveDesign.[140]
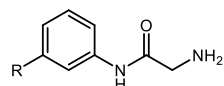
Table 2.4. Further heterocycles. NT = not tested.

Compound	R	Cell Assay			FP Assay				
		$\alpha_v\beta_1$	$\alpha_v\beta_3$	$\alpha_v\beta_6$	$\alpha_v\beta_1$	$\alpha_v\beta_3$	$\alpha_v\beta_5$	$\alpha_v\beta_6$	$\alpha v\beta_8$
2.28		<5.0	<5.0	<5.0	<4.1	<4.1	<4.1	<4.1	<4.1
2.29		<5.0	<5.0	<5.0	4.3	<4.1	<4.1	<4.1	<4.1
2.30		<5.0	NT	<5.0	4.6	<4.1	<4.1	<4.1	<4.1
2.31		<5.0	<5.0	<5.0	4.7	4.1	4.5	<4.1	<4.1
2.32		<5.0	<5.0	<5.0	4.5	<4.1	4.3	<4.1	4.2
2.33		<5.0	<5.0	<5.0	4.4	<4.1	<4.1	<4.1	<4.1
2.34		<5.0	<5.0	<5.0	4.3	<4.1	<4.1	<4.1	<4.1
2.35		<5.0	<5.0	<5.0	5.2	<4.0	4.8	4.6	4.5
2.36		<5.0	<5.0	<5.0	<4.1	<4.1	<4.1	<4.1	<4.1

It was hypothesised that anilines and tetrahydronaphthyridines lacked the flexibility, or the correct length, to reach the acidic residue; therefore, two compounds were designed with the amine homologated by one carbon. Based on molecular modelling, these compounds were further elaborated to target a nearby tyrosine within the binding pocket, Figure 2.20.
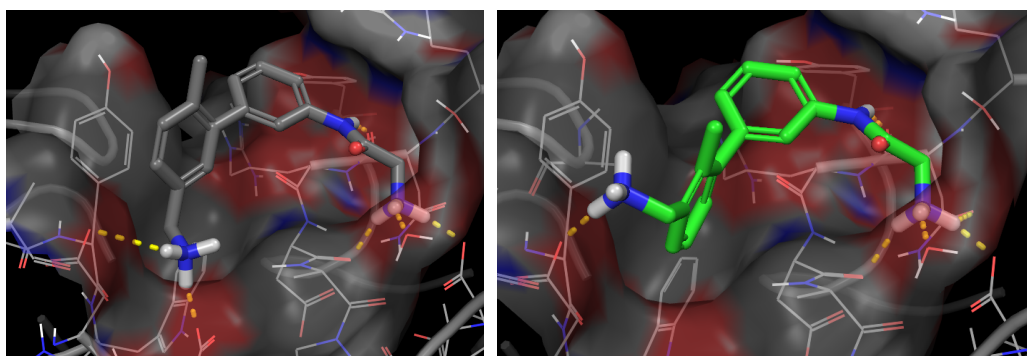
Figure 2.20 *In silico* study of **2.37** and **2.38**. Docked and visualised using LiveDesign.[140]

It was suggested that an *ortho* methyl group could increase the dihedral angle of the biphenyl bond and aid the potential π-π (face:face) interactions of the tolyl ring with Tyr178. A substructure search of the Cambridge Structural Database (CSD),[141] using the molecular geometry database Mogul,[142] demonstrates the effect of an *ortho* substituent on the torsion angle of a biphenyl bond. Figure 2.21 shows that in a biphenyl system without an *ortho* substituent there is a large population of near planar molecules with a torsion angle close to 0 ° or 180 °.
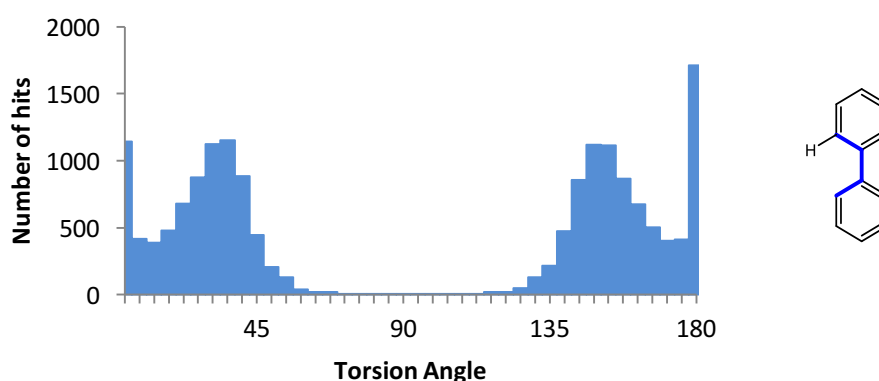
Figure 2.21. Torsion angle of biphenyl substructure, unsubstituted *ortho* positions.

Whereas if the biphenyl features an *ortho* substituent, for the CDS search a carbon based substituent was used, there is an effect on the torsion angle and the molecules no longer exist in a near planar geometry, Figure 2.22.
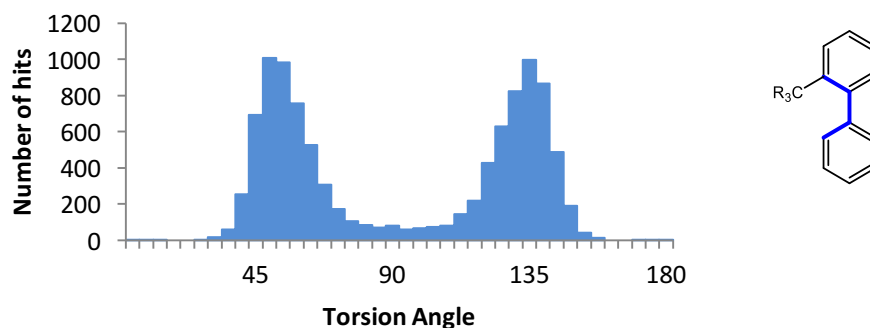
Figure 2.22. Torsion angle of biphenyl substructure with *ortho* carbon based substituent.

Two regioisomers with an *ortho* methyl were successfully synthesised (Table 2.5) and both analogues displayed inhibition of $\alpha_v\beta_3$.
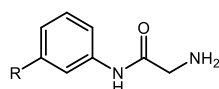
Table 2.5. Homologation of the amine.

Compound	R	Cell Assay			FP Assay				
		$\alpha_v\beta_1$	$\alpha_v\beta_3$	$\alpha_v\beta_6$	$\alpha_v\beta_1$	$\alpha_v\beta_3$	$\alpha_v\beta_5$	$\alpha_v\beta_6$	$\alpha v\beta_8$
2.37		5.2	<4.9	<4.9	6.3	5.5	5.8	<4.0	<4.0
2.38		<5.0	<5.0	5.2	5.7	4.9	5.2	4.5	4.8

Assay results from December 2015 and January 2016 testing.

Comparison of the activity profiles of compound **2.37** and **2.38** revealed that the regiochemistry had an effect on the selectivity observed between the five different integrins. Analogue **2.37**, with the 1,3,6-substitution pattern, had increased activity at

$\alpha_v\beta_3$ and was more selective over integrins $\alpha_v\beta_6$ and $\alpha_v\beta_8$ when compared to the 1,2,3-isomer **2.38**, Figure 2.23.
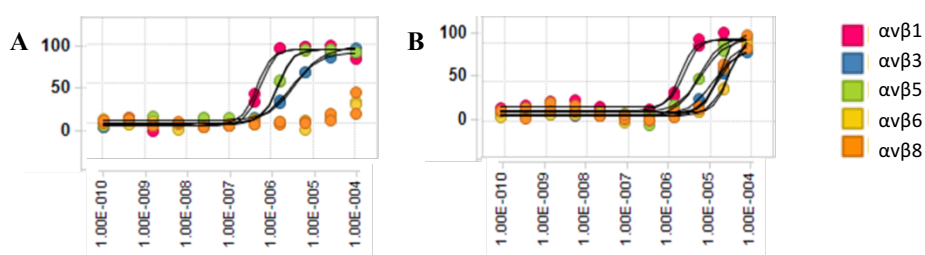
Figure 2.23. FP assay results for A: **2.37** and B: **2.38**. Plotted as % response vs. inhibitor concentration (M). Assay results from December 2015 and January 2016 testing. Data visualised using Spotfire.[143]

The initial hit compounds were investigated further with the synthesis of the compounds detailed in Table 2.6. The desmethyl analogue **2.39** showed that removal of the *ortho* group resulted in loss of activity at $\alpha_v\beta_3$, and further supported the hypothesis of the dihedral angle being important in the binding of these compounds. Removal of this substituent had no significant effect on the other four integrins, which suggested that this *ortho* position is important for targeting $\alpha_v\beta_3$ and could influence the selective profile as shown in analogues **2.37** and **2.38**. The amine was then homologated further to produce analogue **2.40**, however, this resulted in the loss of activity at all integrins in the assay screen. The effect of two *ortho* methyls was tested with compound **2.41**, but the assay results showed that this was not tolerated and no activity was observed at $\alpha_v\beta_3$. By introducing a pyridine ring, there were no significant changes to the activities observed with compound **2.42**. The ortho *N*-oxide of **2.43** was found to show similar activities as the *ortho* methyl analogue **2.38**, this demonstrated that an *ortho* substituent other than a methyl maybe used for activity at $\alpha_v\beta_3$. To explore the effect of the *ortho* substituent further, the amine was

moved to this position to give compound **2.44**. This resulted in a pIC$_{50}$ of 5.0 for

$\alpha_v\beta_3$, giving a similar activity to that of the *ortho* methyl compounds.
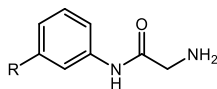
Table 2.6. SAR exploration of compounds **2.37** and **2.38**.

Compound	R	Cell Assay			FP Assay				
		$\alpha_v\beta_1$	$\alpha_v\beta_3$	$\alpha_v\beta_6$	$\alpha_v\beta_1$	$\alpha_v\beta_3$	$\alpha_v\beta_5$	$\alpha_v\beta_6$	$\alpha v\beta_8$
2.39		<5.0	<5.0	<5.0	5.2	<4.1	4.7	4.4	4.6
2.40		<5.0	<5.0	<5.0	<4.1	<4.1	<4.1	<4.1	<4.1
2.41		<5.0	<5.0	<5.0	4.4	<4.0	4.2	<4.0	<4.0
2.42		<5.0	<5.0	<5.0	5.0	<4.1	4.9	4.3	4.1
2.43		<5.0	<5.0	<5.0	5.2	4.1	5.0	4.3	4.2
2.44		<5.0	<5.0	<5.0	6.0	5.0	6.0	5.2	4.8

Based on the result of compound **2.44**, it appeared that the benzylic amine was not

targeting our desired acidic residues, and that the activity observed was a result of the

biphenyl orientation. Thus, a further series of analogues of the original hit compound

2.37 were designed to give insight into the binding of this compound and elucidate

which motifs were important for activity at $\alpha_v\beta_3$. Unsurprisingly, analogue **2.45** in which both amines were acylated resulted in loss of activity. By only acylating the benzylic amine (**2.48**), or by changing the same amine to an alcohol (**2.46**), we observed loss of activity. This showed that this molecule had little tolerance for changes to this region, a hypothesis which is further supported by analogues **2.49** and **2.50**. The *o*-tolyl analogue **2.51** was synthesised to determine whether the *ortho* methyl alone would provide potency, however, this compound and related analogues (**2.52** and **2.53**) were found to be inactive. The indanamine **2.54** was designed to explore the effect of tethering the amine to the *ortho* methyl; however, it was found that the constrained system was unfavourable for binding.

2.45
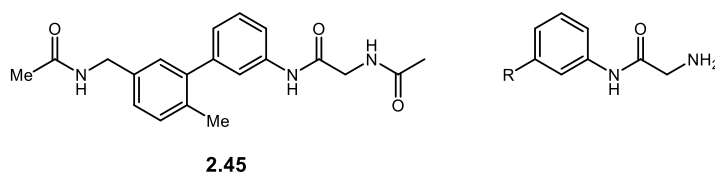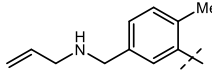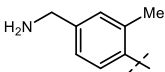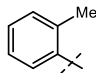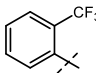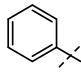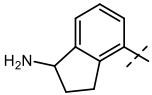
Table 2.7. Further SAR of compounds **2.37** and **2.38**. NT = not tested.

Compound	R	Cell Assay			FP Assay				
		$\alpha_v\beta_1$	$\alpha_v\beta_3$	$\alpha_v\beta_6$	$\alpha_v\beta_1$	$\alpha_v\beta_3$	$\alpha_v\beta_5$	$\alpha_v\beta_6$	$\alpha v\beta_8$
2.46		<5.0	NT	<5.0	<4.1	<4.1	<4.1	<4.1	<4.1
2.47		<5.0	NT	<5.0	<4.0	<4.0	<4.0	<4.0	<4.0
2.48		<5.0	NT	<5.0	<4.1	<4.1	<4.1	<4.1	<4.1

Table 2.7. *Continued.*

Compound	R	Cell Assay			FP Assay				
		$\alpha_v\beta_1$	$\alpha_v\beta_3$	$\alpha_v\beta_6$	$\alpha_v\beta_1$	$\alpha_v\beta_3$	$\alpha_v\beta_5$	$\alpha_v\beta_6$	$\alpha v\beta_8$
2.49		<5.0	NT	<5.0	<4.1	<4.1	<4.1	<4.1	<4.1
2.50		<5.0	NT	<5.0	<4.1	<4.1	<4.1	<4.1	<4.1
2.51		<5.0	NT	<5.0	<4.1	<4.1	<4.1	<4.1	<4.1
2.52		<5.0	NT	<5.0	<4.1	<4.1	<4.1	<4.1	<4.1
2.53		<4.9	NT	<4.9	<4.0	<4.0	<4.0	<4.0	<4.0
2.54		<5.0	NT	<5.0	<4.1	<4.1	<4.1	<4.1	<4.1

After no progress was made in the exploration of the initial hit compounds **2.37** and **2.38**, attentions were turned to the *ortho* amine analogue **2.44**. A set of nine compounds were designed and synthesised to investigate the scope for diversification in this region of the molecule. The alcohol **2.55** was designed to test whether the amine functionality of **2.44** was essential for activity, or if an alternative hydrogen bond donor would be suitable. Methylation of the amine to give analogue **2.56** was carried out to investigate the tolerance for alteration to this region of the molecule. The remaining six analogues were designed to give a diverse set of compounds to explore a range of different possible interactions. The initial hit compound **2.44** had been determined to have a pIC$_{50}$ of 5 against $\alpha_v\beta_3$ in the FP assay, but the series of

diverse analogues were all inactive, Table 2.8. This series of analogues suggested that any change to the amine, even a minor addition such as the methylation **2.56**, was unfavourable.
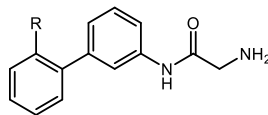
Table 2.8. Exploration of the *ortho* position. NT = not tested.

Compound	R	Cell Assay			FP Assay				
		$\alpha_v\beta_1$	$\alpha_v\beta_3$	$\alpha_v\beta_6$	$\alpha_v\beta_1$	$\alpha_v\beta_3$	$\alpha_v\beta_5$	$\alpha_v\beta_6$	$\alpha v\beta_8$
2.55	HO	<5.0	NT	<5.0	<4.1	<4.1	<4.1	<4.1	<4.1
2.56	Me, N	<5.0	NT	<5.0	<4.1	<4.1	<4.1	<4.1	<4.1
2.57		<5.0	NT	<5.0	<4.1	<4.1	<4.1	<4.1	<4.1
2.58		<5.0	NT	<5.0	<4.1	<4.1	<4.1	<4.1	<4.1
2.59	MeO	6.1[a]	NT	<5.0	<4.1	<4.1	<4.1	<4.1	<4.1
2.60		<5.0	NT	<5.0	<4.1	<4.1	<4.1	<4.1	<4.1
2.61	H_2N	<5.0	NT	<5.0	<4.1	<4.1	<4.1	<4.1	<4.1
2.62	HN	<5.0	NT	<5.0	<4.1	<4.1	<4.1	<4.1	<4.1

[a]Compound **2.59** was retested and found to be inactive in the $\alpha_v\beta_1$ cell assay. Further testing to obtain a correct value has not yet taken place.

After a series of inactive results, it was decided to retest two hit compounds to confirm that the activities observed previously were reproducible. Compound **2.37**

was resynthesised, retested, and found to be inactive, Table 2.9. This analogue was tested further as the HCl salt and also determined to be inactive. A retest of the original sample of **2.44** was attempted but could not be carried out due to solubility issues.[‡]
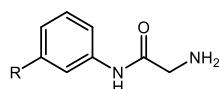
Table 2.9. Retest of hit compounds. NT = not tested.

Compound	R		Cell Assay			FP Assay				
			$\alpha_v\beta_1$	$\alpha_v\beta_3$	$\alpha_v\beta_6$	$\alpha_v\beta_1$	$\alpha_v\beta_3$	$\alpha_v\beta_5$	$\alpha_v\beta_6$	$\alpha v\beta_8$
2.37		1st screen[a]	5.2	<4.9	<4.9	6.3	5.5	5.8	<4.0	<4.0
		Retest[b]	<5.0	NT	<5.0	<4.1	<4.1	<4.1	<4.1	<4.1
2.44		1st screen[a]	<5.0	<5.0	<5.0	6.0	5.0	6.0	5.2	4.8
		Retest[c]	NT	NT	NT	NT	NT	NT	NT	NT

[a]Assay results from December 2015 and January 2016 testing. [b]Retest September 2016. [c]Retest not possible due to solubility issues.

These results were disappointing, but were consistent with the inactive results observed for the analogues described in Tables 2.7 and 2.8. Based on the retest results and the large number of inactive analogues, it was concluded that the initial assays results were false positives. It was unclear whether any of the pIC_{50} values obtained for the compounds synthesised throughout this project were correct, and therefore the synthetic work on this project ceased. As the biological evaluation of these compounds was carried out in house at GSK, it was not within the power of the author to investigate the assay issues.

[‡] Initially, compound **2.44** was tested in the assay without issue; however, upon retesting of the sample, it was observed that the compound had poor solubility in the assay medium.

2.3.3 Synthesis

In order to allow quick access to a range of structurally diverse compounds in the initial search for a hit compound, it was important to identify a key intermediate that was synthetically tractable and would allow synthetic divergence. Through the retrosynthetic analysis of the target chemotype, the boronic ester compound **2.64** was identified, Scheme 2.1. The formation of a biphenyl C-C bond using the Suzuki-Miyaura cross-coupling is a well precedented, robust reaction, and along with the vast availability of commercial coupling partners, this was the ideal intermediate to access compounds fitting the desired template.

Scheme 2.1. Retrosynthetic analysis.
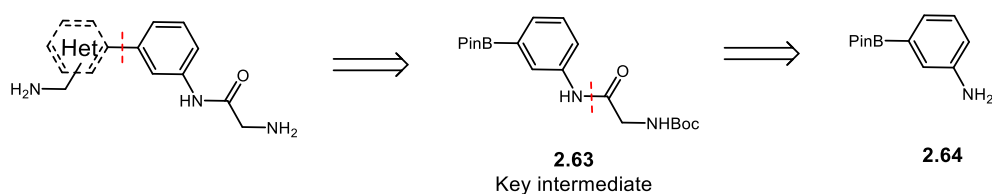
Intermediate **2.63** was easily accessed in two steps from the commercially available nitro **2.65**, Scheme 2.2. Starting with a hydrogenation to reduce the nitro group and afford the required aniline, followed by a subsequent amide coupling with *tert*-butyloxycarbonyl (Boc) protected glycine allowed for the key intermediate to be quickly and efficiently synthesised. Furthermore, this route was found to be amenable to gram scale, providing a robust route to larger quantities of **2.63**.

Scheme 2.2. Synthesis of key intermediate **2.63**.[a]
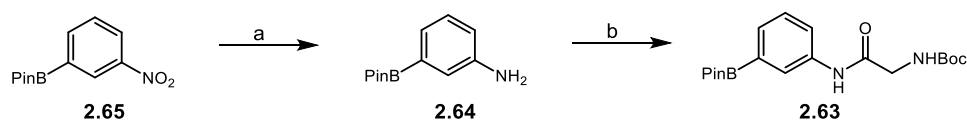
[a]Reagents and conditions: (a) 10 wt. % Pd-C, H_2, EtOH, RT, 16 h, 66%; (b) *N*-Boc glycine, HATU, DIPEA, DMF, RT, 16 h, 61%.

With the key intermediate **2.63** in hand, synthesis then focused on the formation of the biphenyl bond. Initial reactions involving the coupling of aryl halides (for example **2.66**) that featured the primary aniline were found to be unsuccessful. A number of different reaction protocols were trialled, but without success. It was found that by protecting the aniline with a Boc group, then carrying out the Suzuki-Miyaura cross-coupling at the reduced temperature of 50 °C, the reaction proceeded well with minimal deprotection of the aniline, Scheme 2.3. Once the cross-coupling was complete, the reaction mixtures were often telescoped into the final deprotection step to access the desired primary amines, for example compound **2.21**. This strategy was used to avoid any loss of product that had partially deprotected during the previous cross-coupling step.

Scheme 2.3. Synthesis of compound **2.21**.[a]
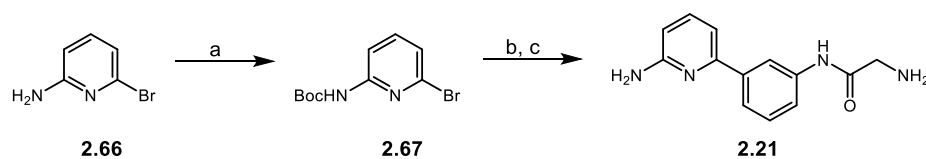
[a]Reagents and conditions: (a) Boc$_2$O, Et$_3$N, DMAP, DCM, RT, 16 h (b) **2.63**, K$_3$PO$_4$, 2′-(dimethylamino)-2-biphenylyl-palladium(II) chloride dinorbornylphosphine complex, 1,4-dioxane:H$_2$O (4:1), 50 °C, 16 h; (c) TFA, DCM, RT, 16 h, 6% over 3 steps.

The imidazopyridine amine heterocycle was synthesised from the commercially available diamine **2.68** and chloroacetal. This was followed by a Boc protection to afford the bromo coupling partner **2.69**, which was then coupled to the Bpin key intermediate **2.63** used previously; however, it was observed that the reaction did not proceed at 50 °C and required the elevated temperature of 90 °C, Scheme 2.4. A final deprotection then afforded the desired compound **2.28**.

Scheme 2.4. Synthesis of compound **2.28**.[a]

2.68   **2.69**   **2.28**
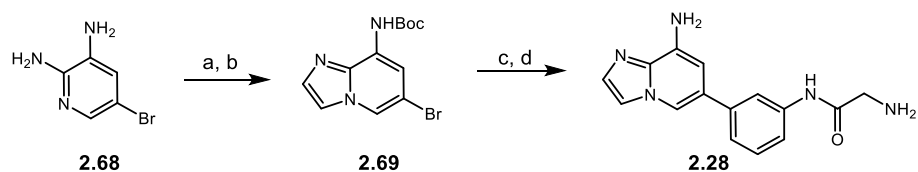
[a]Reagents and conditions: (a) chloroacetal, NaHCO$_3$, EtOH, reflux, 16 h, 55%; (b) Boc$_2$O, Et$_3$N, DMAP, DCM, RT, 16 h, 48%; (c) **2.63**, K$_3$PO$_4$, 2′-(dimethylamino)-2-biphenylyl-palladium(II) chloride dinorbornylphosphine complex, 1,4-dioxane:H$_2$O (4:1), 90 °C, 16 h; (d) TFA, DCM, RT, 16 h, 26% over 2 steps.

The saturated diamine analogue **2.31** was accessed using a Chan-Lam cross-coupling between the key intermediate **2.63** and Boc-protected piperazine, Scheme 2.5. Attempts were made to synthesis further saturated analogues; however, the cross-coupling of other diamines were not successful (data not shown). As analogue **2.31** was inactive in the biological evaluation, further saturated analogues were not pursued further. This decision was further supported by the *in silico* work, which suggested that it was beneficial to have a biphenyl structure that could form π-π interactions with the nearby aryl residues.

Scheme 2.5. Synthesis of compound **2.31**.[a]

2.70   **2.71**   **2.31**
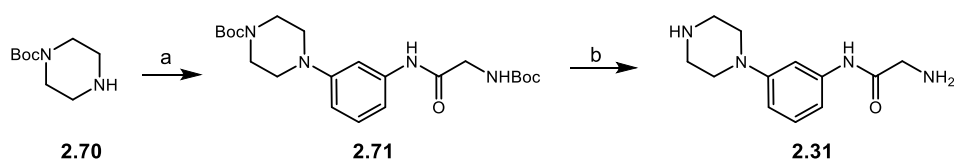
[a]Reagents and conditions: (a) **2.63**, Cu(OAc)$_2$, KOAc, MeCN, 60 °C, 16 h, 45% (b) TFA, DCM, 16 h, RT, 17%.

Tetrahydronapthyridine analogues were accessed using a hydrogenation of the naphthyridine motif. Reduction of the distal ring proceeded well under one atmosphere of hydrogen using Pd-C, Scheme 2.6.

Scheme 2.6. Synthesis of compound **2.35**.[a]
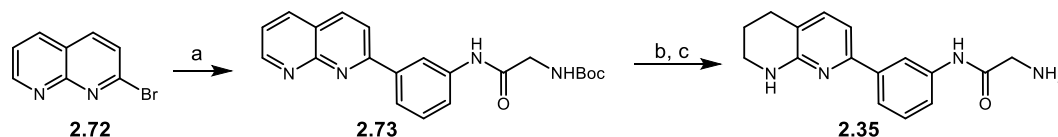
2.72 →(a) **2.73** →(b, c) **2.35**

[a]Reagents and conditions: (a) **2.63**, K$_3$PO$_4$, 2′-(dimethylamino)-2-biphenylyl-palladium(II) chloride dinorbornylphosphine complex, 1,4-dioxane:H$_2$O (4:1), 50 °C, 16 h; (b) 10 wt. % Pd-C, H$_2$, EtOH; (c) TFA, DCM, 39% over 2 steps.

During the *in silico* studies, it had been noted that a substituent *ortho* to the biphenyl bond could benefit binding by increasing the dihedral angle, positioning one aromatic ring to make π-π (face:face) interactions with a nearby tyrosine residue. One such analogue designed to fit this binding mode was compound **2.37**. This was synthesised from the commercially available nitrile in three steps, Scheme 2.7. The cross-coupling proceeded well to afford compound **2.75**, which was then used in a hydrogenation to reduce the nitrile and access the desired benzylic amine.

Scheme 2.7. Synthesis of compound **2.37**.[a]
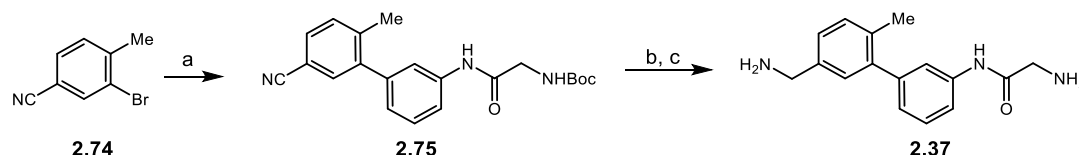
2.74 →(a) **2.75** →(b, c) **2.37**

[a]Reagents and conditions: (a) **2.63**, K$_3$PO$_4$, 2′-(dimethylamino)-2-biphenylyl-palladium(II) chloride dinorbornylphosphine complex, 1,4-dioxane:H$_2$O (4:1), 50 °C, 16 h, 58%; (b) H-cube, Raney-Ni, 2 M NH$_3$ MeOH, 0.02 M, 50 °C, 1 mL/min, two cycles; (c) TFA, DCM, RT, 16 h, 37% over 2 steps.

To test whether the *ortho* substituent in **2.37** was required, the desmethyl analogue **2.39** was also synthesised. The cross-coupling of **2.76** with **2.63** afforded the aldehyde intermediate **2.77**, from which the protected amine (**2.78**) was accessed by forming the *N*-sulfinyl imine, followed by a reduction using NaBH$_4$, Scheme 2.8.

This route provided a robust way to form the protected amine from the aldehyde and was used throughout this project. A final deprotection using TFA successfully removed both protecting groups to reveal the desired amines of compound **2.39**.

Scheme 2.8. Synthesis of compound **2.39**.[a]
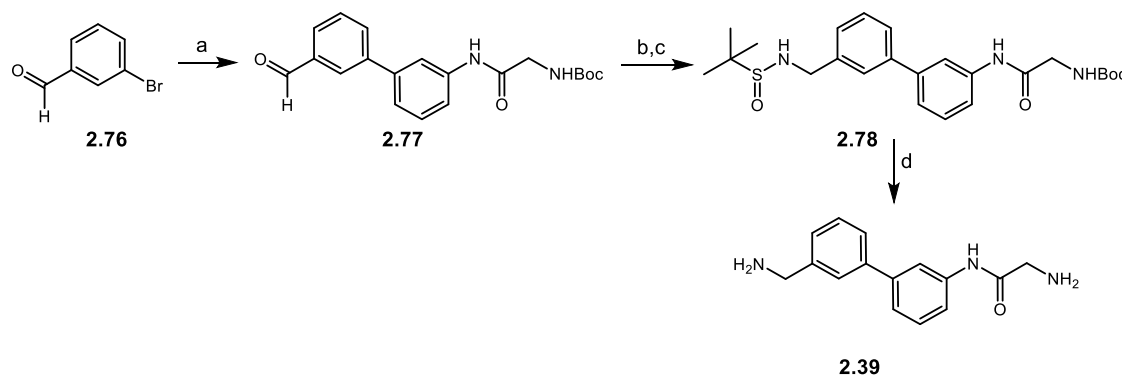
2.39

[a]Reagents and conditions: (a) **2.63**, K_3PO_4, 2′-(dimethylamino)-2-biphenylyl-palladium(II) chloride dinorbornylphosphine complex, 1,4-dioxane:H_2O (4:1), 50 °C, 16 h, 80%; (b) *tert*-butanesulfinamide, PPTS, $MgSO_4$, DCM, RT, 16 h; (c) $NaBH_4$, MeOH, RT, 2 h, 87% over 2 steps; (d) TFA, DCM, RT, 16 h, 78%.

An alternative approach was used to form the homologated analogue **2.40**, Scheme 2.9. Using a Mitsunobu reaction, alcohol **2.79** was successfully converted into the phthalimide protected amine **2.80**. Unfortunately, attempts to cross-couple **2.80** with the key intermediate **2.63** were unsuccessful. To mitigate this issue, the phthalimide protecting group was exchanged for a Boc group to form **2.81**. Using this alternative protecting group, the cross-coupling proceeded well and, following deprotection, the desired compound was accessed.

Scheme 2.9. Synthesis of compound **2.40**.[a]

2.79   **2.80**   **2.81**

2.40
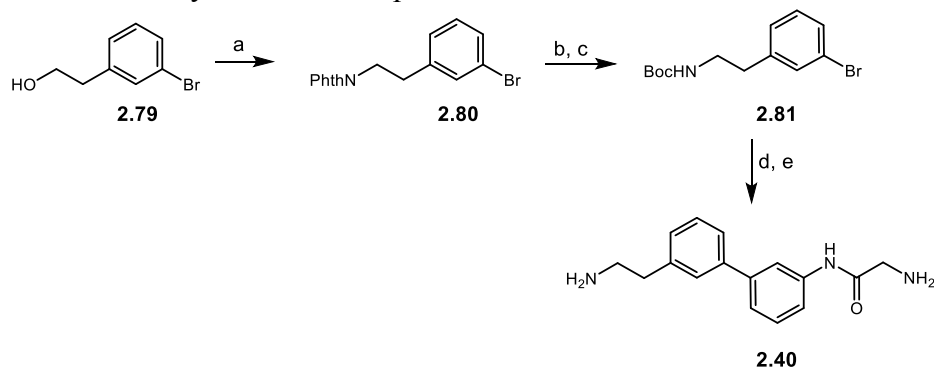
[a]Reagents and conditions: (a) DIAD, PPh₃, phthalimide, THF, 0 °C-RT, 16 h, 31%; (b) H₂NNH₂.H₂O, EtOH, 60 °C, 1 h, 99%; (c) Boc₂O, Et₃N, DMAP, DCM, RT, 16 h, 64%; (d) **2.63**, K₃PO₄, Pd(dppf)Cl₂·DCM, H₂O, THF, 50 °C, 16 h; (e) TFA, DCM, RT, 16 h, 89% over 2 steps.

The bis-methyl analogue was synthesised starting with a formylation of 2,6-dimethyl bromobenzene to form the required aldehyde **2.83**. This intermediate was successfully coupled and then converted to protected amine using the *N*-sulfinyl imine procedure discussed previously. From intermediate **2.85** a deprotection afforded the desired compound **2.41**, Scheme 2.10.

Scheme 2.10. Synthesis of compound **2.41**.[a]

2.82   **2.83**   **2.84**

2.41   **2.85**
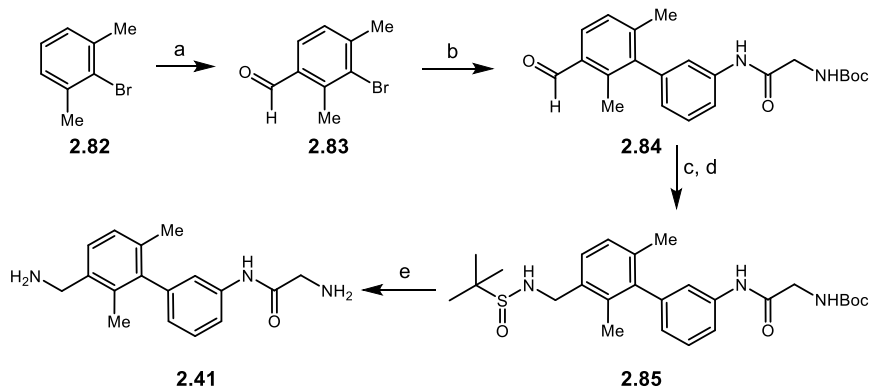
[a]Reagents and conditions: (a) TiCl₄, dichloro methyl ether, DCM, -78 °C-RT, 4 h, 73%; (b) **2.63**, K₃PO₄, 2′-(dimethylamino)-2-biphenylyl-palladium(II) chloride dinorbornylphosphine complex, 1,4-dioxane:H₂O (4:1), 50 °C, 16 h; (c) *tert*-butanesulfinamide, PPTS, MgSO₄, DCM, RT, 16 h; (d) NaBH₄, MeOH, RT, 2 h, 32% over 3 steps; (e) TFA, DCM, RT, 16 h, 44%.

Oxidation of the pyridine to form the *N*-oxide was achieved using *m*-CPBA, Scheme 2.11, during which the sulfinamide was also oxidised to the sulfonamide. In the final step, TFA was unsuccessful in the deprotection of both amines; therefore, trifluoromethane sulfonic acid was used to cleave the sulfonamide of **2.89** and reveal the desired amine.

Scheme 2.11. Synthesis of compound **2.43**.[a]
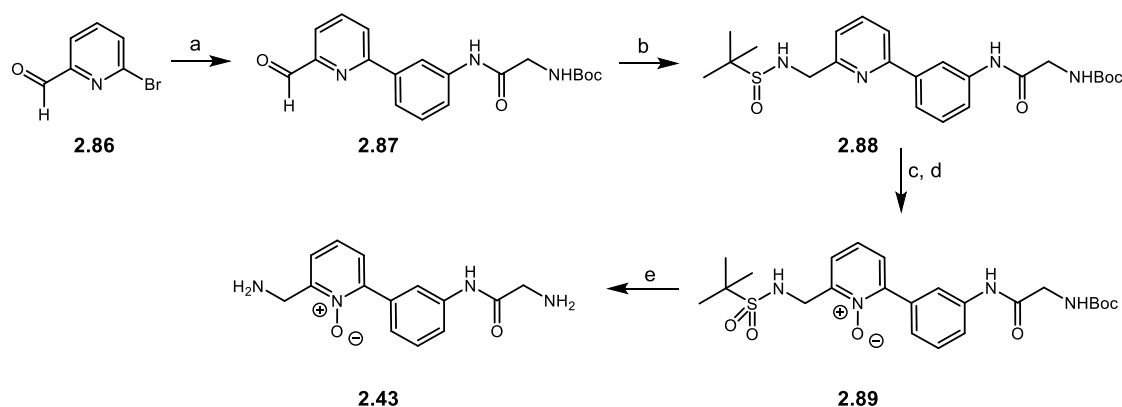
[a]Reagents and conditions: (a) **2.63**, K$_3$PO$_4$, Pd(dppf)Cl$_2$·DCM, H$_2$O, THF, 50 °C, 16 h 97%; (b) *tert*-butanesulfinamide, PPTS, MgSO$_4$, DCM, RT, 16 h; (c) NaBH$_4$, MeOH, RT, 2 h, 59% over 2 steps; (d) *m*-CPBA, DCM, RT 16 h; (e) TfOH, DCM, RT, 3 h, 20% over 2 steps.

In order to acylate the benzylic amine over the aliphatic amine, an orthogonal protecting group strategy was employed, Scheme 2.12. A reductive amination of aldehyde **2.92** with allylic amine afforded intermediate **2.93**, which allowed the benzylic amine to be deprotected with the Boc group remaining intact, **2.94**. This was followed by an acylation and final deprotection to access **2.48**. An additional analogue was also accessed using this route by removing the Boc group of **2.93** to afford the alkylated benzylic amine compound **2.49**.

Scheme 2.12. Synthesis of compounds **2.48** and **2.49**.[a]
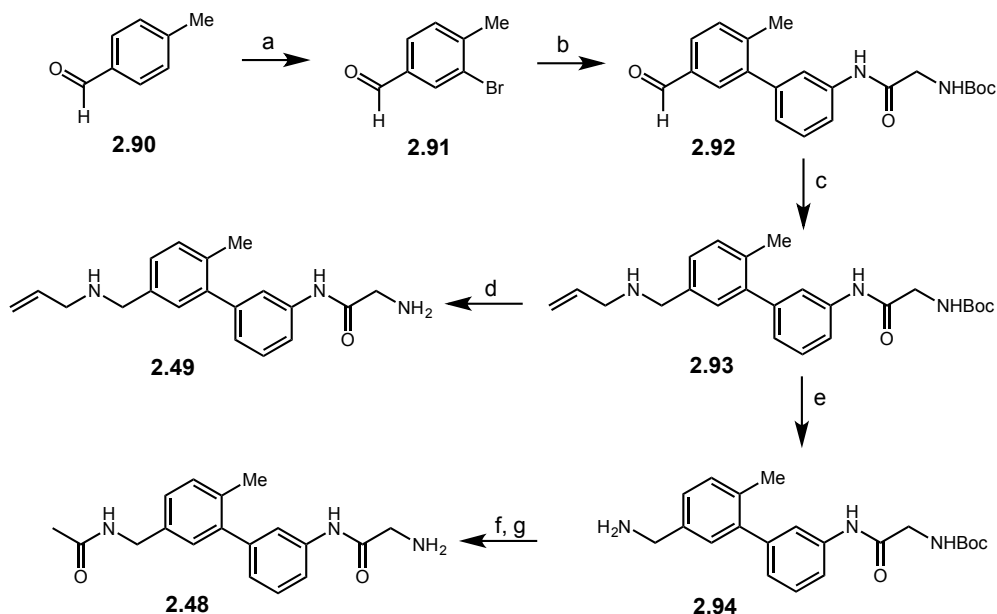
[a]Reagents and conditions: (a) AlCl$_3$, Br$_2$, DCM, 0-40 °C, 16 h, 47%; (b) **2.63**, K$_3$PO$_4$, Pd(dppf)Cl$_2$·DCM, H$_2$O, THF, 50 °C, 16 h, 94%; (c) prop-2-en-1-amine, MgSO$_4$, NaBH$_4$, THF, RT, 16 h, 37%; (d) TFA, DCM, RT 16 h, 85%; (e) Wilkinson's catalyst, MeCN:H$_2$O, (15:85), reflux, 1 h, 45%; (f) Ac$_2$O, pyridine, DCM, RT 16 h; (g) TFA, DCM, RT 16 h, 90% over 2 steps.

The indanamine analogue **2.54** was successfully synthesised from the 4-bromoindanone, Scheme 2.13.. The initial strategy towards **2.54** attempted to form the *N*-sulfinyl imine of **2.95** using Ti(O*i*Pr)$_4$, however, this was not successful and thus the alternative route via the oxime was employed. By converting the ketone to the oxime, followed by a reduction, the indanamine was afforded. This was subsequently Boc protected and coupled with intermediate **2.63**, followed by a global deprotection to afford the desired compound **2.54**.

Scheme 2.13. Synthesis of compound **2.54**.[a]

2.95   **2.96**   **2.97**   **2.54**
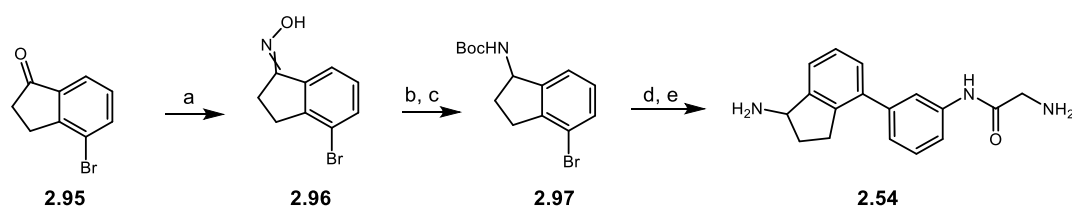
[a]Reagents and conditions: (a) H$_2$NOH.HCl, NaOAc, MeOH, RT, 16 h, 98%; (b) Zn, AcOH, RT, 16 h, 74%; (c) Boc$_2$O, Et$_3$N, DMAP, DCM, RT, 16 h, 81%; (d) **2.63**, K$_3$PO$_4$, Pd(dppf)Cl$_2$·DCM, H$_2$O, THF, 50 °C, 16 h; (e) TFA, DCM, RT, 16 h, 36% over 2 steps.

The last series of compounds to be synthesised explored the benzylic amine in the *ortho* position, Scheme 2.14. By carrying out a small reductive amination array using aldehyde **2.99**, seven diverse amines were successfully accessed, Table 2.10.
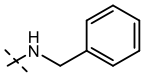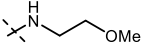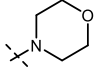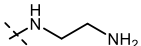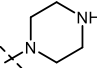
Scheme 2.14. Synthesis of compounds **2.56 – 2.62**.[a]

2.98   **2.99**   **2.56-2.62**
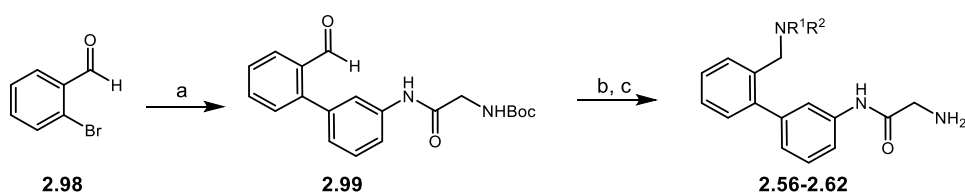
[a]Reagents and conditions: (a) **2.63**, K$_3$PO$_4$, Pd(dppf)Cl$_2$·DCM, H$_2$O, THF, 50 °C, 16 h, 98%; (b) amine, MgSO$_4$, NaBH$_4$, THF, RT, 16 h; (c) TFA, DCM, RT.
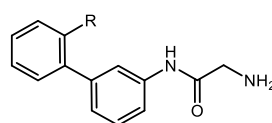
Table 2.10. Yields of compounds **2.56-2.62**.

R	Reductive amination	Deprotection
2.56	*Telescoped*	21% over 2 steps
2.57	82%	46%

136

Table 2.10. *Continued.*

R	Reductive amination	Deprotection
2.58	75%	35%
2.59	65%	60%
2.60	38%	81%
2.61	*Telescoped*	16% over 2 steps
2.62	*Telescoped*	2% over 2 steps

2.4 Conclusion

A series of non-RGD-mimetic compounds were designed and synthesised to target the RGD integrin $\alpha_v\beta_3$. *In silico* studies had suggested a simple biaryl scaffold with two primary amines: one to displace the Mg^{2+} ion and the second to interact with the target acidic residue. Two early hit compounds had proposed that the inclusion of a substituent *ortho* to the biphenyl bond favoured the binding, potentially through alternating the dihedral angle to aid π-π interactions with the residues within the binding site. Further exploration of the two initial hits led to the identification of a total of four promising lead-like inhibitors with pIC_{50} values ranging from 4.1-5.5 for the target integrin $\alpha_v\beta_3$, Table 2.11.
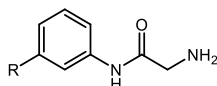
Table 2.11. Four potential $\alpha_v\beta_3$ inhibitors identified.

Compound	R	Cell Assay			FP Assay				
		$\alpha_v\beta_1$	$\alpha_v\beta_3$	$\alpha_v\beta_6$	$\alpha_v\beta_1$	$\alpha_v\beta_3$	$\alpha_v\beta_5$	$\alpha_v\beta_6$	$\alpha v\beta_8$
2.37		5.2	<5	<5	6.3	5.5	5.8	<4	<4
2.38		<5	<5	5.2	5.7	4.9	5.2	4.5	4.8
2.43		<5	<5	<5	5.2	4.1	5.0	4.3	4.2
2.44		<5	<5	<5	6.0	5.0	6.0	5.2	4.2

Assay results from December 2015 and January 2016 testing.

Unfortunately, the initial hit compound **2.37** (pIC$_{50}$ = 5.5), which had informed the subsequent compound design, was determined to be a false positive. After resynthesizing the original hit compound, the retest confirmed the false positive result, and thus work on the project ceased. At the time of this report, it was yet to be confirmed whether the other three α$_v$β$_3$ inhibitors (**2.38**, **2.43**, **2.44**) had also been false positives.

Robust biological screening is essential for any medicinal chemistry project, especially at the lead optimisation stage when the micromolar, or even millimolar, activities being measured are often at the limit of the assay concentration range. This project is an example of mis-led compound design due to false positive assay results. Although all testing was carried out in duplicate, the retest suggested that there was an issue in the FP assays ran during December 2015 and January 2016. As the issue did not come to light until some months later (August 2016), there was a significant amount of time and effort put into the design and synthesis of inactive compounds. The remaining time was used for retesting to confirm the false positives, thus the synthesis of new analogues was not possible.

This project has enabled the chemistry for the synthesis of a number of novel, valuable intermediates; furthermore, the diversity that can be achieved from these intermediates using a few simple synthetic steps has been demonstrated. Although the majority of compounds synthesised were inactive, these results provide information towards the development of non-RGD-mimetic inhibitors for the α$_v$β$_3$ receptor and other members of the RGD subfamily.

2.5   Future Work

Before any work can continue in this current project, it is imperative that reliable assays are set up for the evaluation of potential inhibitors. Once a robust assay is available, a full retest of the compounds detailed in this report should be carried out to determine whether any show antagonism of the $\alpha_v\beta_3$ receptor. If no hits were identified from the retesting of the compounds, then it would be the author's recommendation to start the compound design from the beginning with the known $\alpha_{IIb}\beta_3$ inhibitor **2.4**. This non-RGD-mimetic inhibitor has been shown to be inactive against the integrin $\alpha_v\beta_3$; nevertheless, through the synthesis and testing of a series of deletion analogues, valuable SAR for binding within the alpha domain could be determined, Figure 2.21. By exploring the heterocyclic portion of this molecule that has been shown to bind within the alpha domain, it may be possible to change the selectivity for $\alpha_{IIb}\beta_3$ to $\alpha_v\beta_3$.
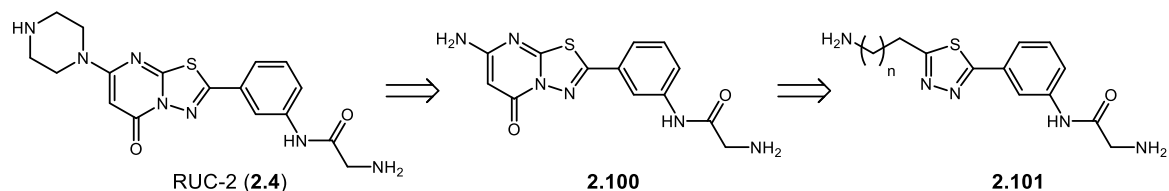
Figure 2.24. Deletion analogues of RUC-2 (**2.4**).

Perhaps a more logical strategy would be to start with a known non-RGD-mimetic inhibitor of the target integrin, $\alpha_v\beta_3$. To date there are no crystal structures of these compounds (a selection of these inhibitors is shown in Figure 2.25) in complex with the receptor reported, but these small molecules could provide excellent starting points for the development of novel non-RGD-mimetic inhibitors of $\alpha_v\beta_3$. For example, compound **2.13**, which has been shown to have an excellent subnanomolar IC_{50} of 0.03 nM, but the 2-imino rhodanine is a recognised PAINS motif. To

determine whether this activity is a false positive or due to the promiscuity of the PAINS, a series of compounds with the core of **2.13** changed to alternative heterocycles could be synthesised and tested. With an IC_{50} of 0.03 nM, there is room to lose some potency when searching for an analogue that avoids the use of the 2-imino rhodanine.

2.13	**2.15**	**2.17**
IC_{50} = 0.03 nM	IC_{50} = 33.5 ±3.1 μM	IC_{50} of 11 nM
MW: 433; clogP: 3.56; PSA: 91 Å	MW: 246; clogP: 1.93; PSA: 101 Å	MW: 394; clogP: 1.16; PSA: 133 Å
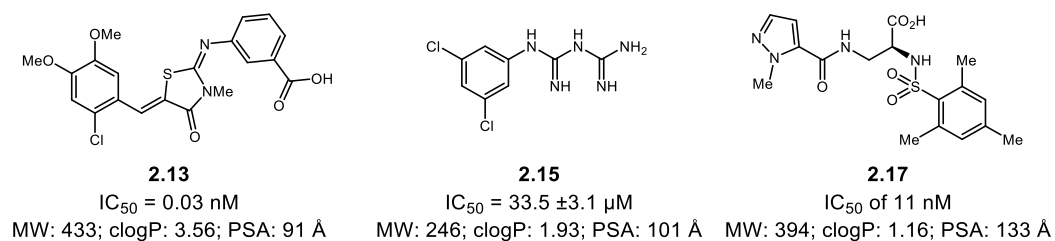
Figure 2.25. Non-RGD-mimetic inhibitors of $\alpha_v\beta_3$.

2.6   Experimental

2.6.1   General Techniques

All reagents and solvents were obtained from commercial suppliers and were used without further purification unless otherwise stated. Purification was carried out according to standard laboratory methods.[77]

2.6.2   Purification of Solvents

i)   All solvents used for dry reactions were obtained from a PureSolv SPS-400-5 solvent purification system. These solvents were transferred to and stored in a septum-sealed oven-dried flask over previously activated 4 Å molecular sieves and purged with and stored under nitrogen.

ii)   Dichloromethane (DCM), ethyl acetate (EtOAc), methanol (MeOH), petroleum ether 40-60°, methyl *tert*-butyl ether (MTBE), and cyclohexane for purification purposes were used as obtained from suppliers without further purification.

2.6.3   Experimental Details

i)   Air-sensitive reactions were carried out using conventional glassware. The glassware was oven-dried and purged with N_2 before use.

ii)   Purging refers to a vacuum/nitrogen-refilling procedure.

iii)   Reactions were carried out at -78 °C using dry ice/acetone baths.

iv)   Reactions were carried out at 0 °C using ice/water baths.

v)   Room temperature was generally ca. 18 °C.

vi)   Reactions were carried out at elevated temperatures using a temperature-regulated hotplate/stirrer.

2.6.4   Purification of Products

i)   Thin layer chromatography (TLC) was carried out using Merck silica plates coated with fluorescent indicator UV254. These were analysed

under 254 nm UV light or developed using potassium permanganate solution.

ii)   Silica chromatography was carried out using ZEOprep 60 HYD 40-63 μm silica gel or IST Isolute Flash silica cartridges.

iii)   Reverse-phase flash chromatography was carried out using IST Isolute C18 cartridges.

iv)   Reverse-phase HPLC purification was carried out using a Gilson 151 preparative HPLC using an Agilent Zorbax SB-C18 column at room temperature. Purification was performed using a gradient method, eluting with 5-80% MeCN/H_2O over 15 minutes at a flow rate of 10 mL/min. Fractions were collected automatically using a GX-271 liquid handler.

v)   Mass-directed automatic purification (MDAP) was carried out using a ZQ MS using alternate-scan positive and negative electrospray and a summed UV wavelength of 210-350 nm and an Xbridge C18 column (100 mm x 19 mm, 5 μm packing diameter, 20 mL/min flow rate) or Xbridge C18 column (150 mm x 30 mm, 5 μm packing diameter, 40 mL/min flow rate). Purification was performed using a gradient method at room temperature with the mobile phases as (A) 10 mM aqueous ammonium bicarbonate solution, adjusted to pH 10 with 0.88 M aqueous ammonia and (B) MeCN.

2.6.5   Analysis of Products

i)   Fourier Transformed Infra-Red (FTIR) spectra were obtained on one of three machines: (a) Shimadzu IRAffinity-1 machine; (b) A2 Technologies ATR spectrometer; (c) Agilent 5500a FTIR ATR.

ii) ^{1}H, ^{13}C, and ^{19}F NMR spectra were obtained on a one of four Bruker NMR spectrometers: (a) Advance III HD console, Ascend 500 MHz magnet, BBO smart probe; (b) Advance III console, 400 MHz Ultrashield magnet, Prodigy BBO probe, BB-H&F-D-05 Z; (c) Advance II console, 400 MHz 9.4 T Oxford unshielded magnet, BBFO-z-ATMA probe; (d) Advance III console, 600 MHz 14.1 T Bruker Ultrashield magnet, TBI-z probe. Chemical shifts are reported in ppm and coupling constants are reported in Hz with CDCl$_3$ referenced at 7.26 (^{1}H) and 77.16 ppm (^{13}C), CO(CD$_3$)$_2$ at 2.05 (^{1}H) and 29.84 ppm (^{13}C), CD$_3$OD at 3.31 (^{1}H) and 49.00 ppm (^{13}C), and DMSO-d_6 at 2.50 (^{1}H) and 39.52 ppm (^{13}C), respectively.

iii)   High-resolution mass spectra (HRMS) were obtained through analysis at the EPSRC National Mass Spectrometry Facility, University of Wales, Swansea or at the University of Glasgow using a Bruker Compass DataAnalysis 4.0.

2.7   General Experimental Procedures

2.64   **2.63**
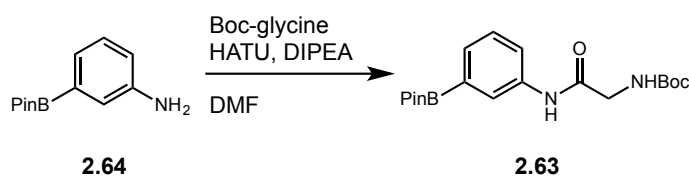
General Procedure A: Amidation, for example the preparation of *tert*-butyl (2-oxo-2-((3-(4,4,5,5-tetramethyl-1,3,2-dioxaborolan-2-yl)phenyl)amino)ethyl) carbamate (2.63). A solution of Boc-glycine (6.16 g, 35.1 mmol, 1.1 equiv.), DIPEA (11.16 mL, 63.9 mmol, 2 equiv.), and HATU (14.58 g, 38.3 mmol, 1.2 equiv.) in 50 mL DMF was stirred at room temperature for 10 min before the

addition of 3-(4,4,5,5-tetramethyl-1,3,2-dioxaborolan-2-yl)aniline (**2.64**) (7.00 g, 32.0 mmol, 1 equiv.) as a solution in 10 mL DMF to give a final DMF volume of 60 mL (0.5 M). The resulting solution was then stirred at room temperature for 16 h. The reaction mixture was diluted with 100 mL EtOAc and washed with sat. aq. NaHCO$_3$ (100 mL) then H$_2$O (2 x 100 mL). The organic layer was collected, dried (hydrophobic frit), and then concentrated under reduced pressure to afford a yellow oil. Purified using silica chromatography, eluting with 0-80% MTBE/cyclohexane, to afford the title compound as a cream solid (8.00 g, 61%).
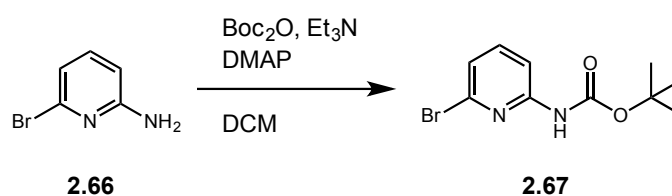
General Procedure B: Boc-protection of amine, for example the preparation of *tert*-butyl (6-bromopyridin-2-yl)carbamate (2.67). A solution of 6-bromopyridin-2-amine (**2.66**) (200 mg, 1.156 mmol, 1 equiv.), Boc$_2$O (295 µL, 1.272 mmol, 1.1 equiv.), Et$_3$N (193 µL, 1.387 mmol, 1.2 equiv.), and DMAP (28 mg, 0.231 mmol, 20 mol%) in 10 mL DCM (0.1 M) was stirred at room temperature overnight. The reaction mixture was diluted with 20 mL DCM and washed with brine (2 x 20 mL). The organic layer was collected, dried (hydrophobic frit), and then concentrated under reduced pressure to afford a yellow oil. The residue was loaded onto a plug of silica, eluted with 0-50% EtOAc/cyclohexane, to afford a colourless oil that was used in the next step without further purification (79 mg, 25%).
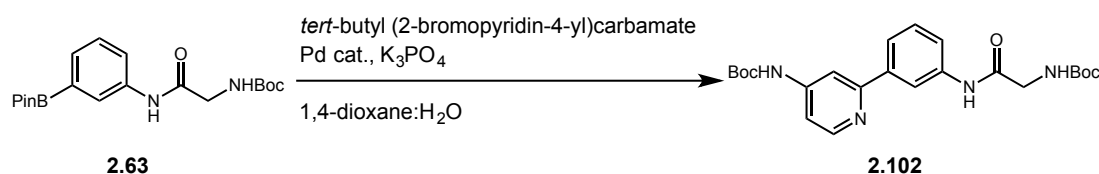
General Procedure C: Suzuki cross-coupling using 2′-(dimethylamino)-2-biphenylyl-palladium(II) chloride dinorbornylphosphine complex, for example the preparation of *tert*-butyl *N*-({[3-(4-{[(*tert*-butoxy)carbonyl]amino}pyridin-2-yl)phenyl] carbamoyl}methyl)carbamate (2.102). A reaction vial containing *tert*-butyl (2-bromopyridin-4-yl)carbamate (100 mg, 0.366 mmol, 1 equiv.), *tert*-butyl (2-oxo-2-((3-(4,4,5,5-tetramethyl-1,3,2-dioxaborolan-2-yl)phenyl)amino) ethyl) carbamate (**2.63**) (165 mg, 0.439 mmol, 1.2 equiv.), 2′-(dimethylamino)-2-biphenylyl-palladium(II) chloride dinorbornylphosphine complex (10 mg, 0.018 mmol, 5 mol%) and K_3PO_4 (311 mg, 1.465 mmol, 4 equiv.) was purged with nitrogen followed by the addition of 1.875 mL 1,4-dioxane:H_2O (4:1, 0.2 M). The reaction mixture was then heated at 50 °C for 16 h after which the reaction was allowed to return to RT, diluted with EtOAc (50 mL) and washed with sat. aq. $NaHCO_3$ (2 x 50 mL). The organic layer was collected, dried using a hydrophobic frit and concentrated under reduced pressure to a yellow oil. Purified using silica chromatography, eluting with 0-70% EtOAc/cyclohexane, to afford the title compound as a colourless oil (61 mg, 35%).
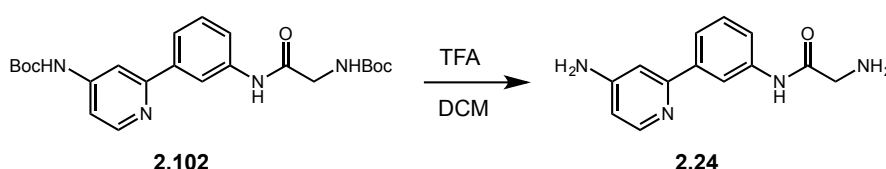
General Procedure D: Boc deprotection, for example the preparation of 2-amino-*N*-(3-(4-aminopyridin-2-yl)phenyl)acetamide (2.24). A solution of *tert*-

butyl   *N*-({[3-(4-{[(*tert*-butoxy)carbonyl]amino}pyridin-2-yl)phenyl]carbamoyl}

methyl)carbamate (**2.102**) (47 mg, 0.106 mmol, 1 equiv.) in 0.5 mL TFA and 1 mL

DCM was stirred at RT for 16 h. The reaction was then concentrated under

compressed air. Purified by revere-phase column chromatography, eluting with 5-

35% MeCN/H_2O (high pH method), to afford the title compound as a white solid (4

mg, 16%).

2.75   **2.103**
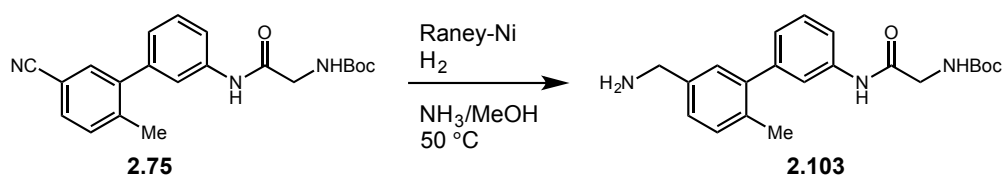
General Procedure E: Nitrile reduction, for example the preparation of *tert*-

butyl   (2-((5'-(aminomethyl)-2'-methyl-[1,1'-biphenyl]-3-yl)amino)-2-oxoethyl)

carbamate (2.103). A solution of *tert*-butyl (2-((5'-cyano-2'-methyl-[1,1'-biphenyl]-

3-yl)amino)-2-oxoethyl)carbamate (**2.75**) (100 mg, 0.274 mmol, 1 equiv.) in 2 M

NH_3 in MeOH (14 mL) was reduced using an H-cube fitted with a Raney Nickel

CatCart THS 01112 (750 mg, 8.75 mmol) CatCart. The solution was passed through

at 1 mL/min using full H mode and heating at 50 °C to afford approx. 50%

conversion by LCMS. The solution was then passed through a second time using the

same conditions to reach full conversion. The solution was then concentrated under

reduced pressure and used in the next step without further purification.

2.73   **2.104**
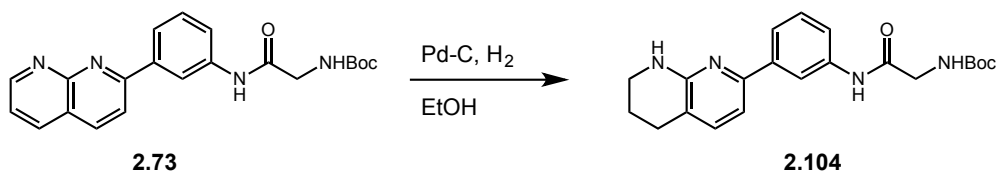
General Procedure F: Hydrogenation of naphthyridine distal ring, for example

the preparation of *tert*-butyl (2-oxo-2-((3-(5,6,7,8-tetrahydro-1,8-naphthyridin-

2-yl)phenyl)amino)ethyl)carbamate (2.104). A solution of *tert*-butyl (2-((3-(1,8-naphthyridin-2-yl)phenyl)amino)-2-oxoethyl)carbamate (**2.73**) (100 mg, 0.265 mmol, 1 equiv.) and 10 wt. % Pd-C (56 mg, 0.053 mmol, 20 mol%) in 2 mL EtOH (0.1 M) was stirred under 1 atmosphere of hydrogen for 16 h. The reaction mixture was then filtered through celite, eluting with MeOH, and the filtrate concentrated under reduced pressure to afford the title compound which was used in the next step without further purification.
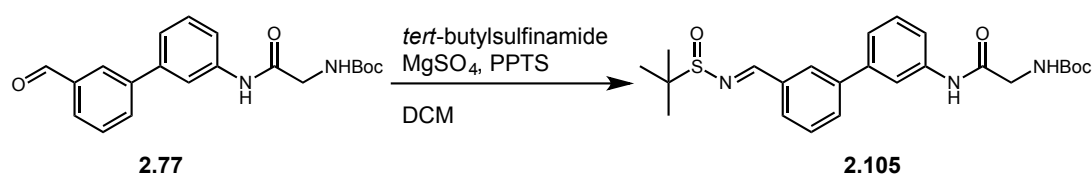
General Procedure G: *N*-Sulfinyl imine formation, for example the preparation of *tert*-butyl (*E*)-(2-((3'-((((*tert*-butylsulfinyl)imino)methyl)-[1,1'-biphenyl]-3-yl)amino)-2-oxoethyl)carbamate (2.105). A solution of *tert*-butyl (2-((3'-formyl-[1,1'-biphenyl]-3-yl)amino)-2-oxoethyl)carbamate (**2.77**) (228 mg, 0.644 mmol, 1.5 equiv.), *tert*-butanesulfinamide (52 mg, 0.429 mmol, 1 equiv), MgSO$_4$ (515 mg, 4.290 mmol, 10 equiv.), and pyridinium *p*-toluenesulfonate (PPTS) (5 mg, 0.002 mmol, 0.5 mol%) was stirred at room temperature. Once the imine formation was complete by TLC, the reaction mixture was filtered, and the filtrate concentrated under reduced pressure. The residue was washed through a plug of silica, eluting with 50% EtOAc/petroleum ether, to afford the title compound which was used without further purification.

2.105 → **2.78**
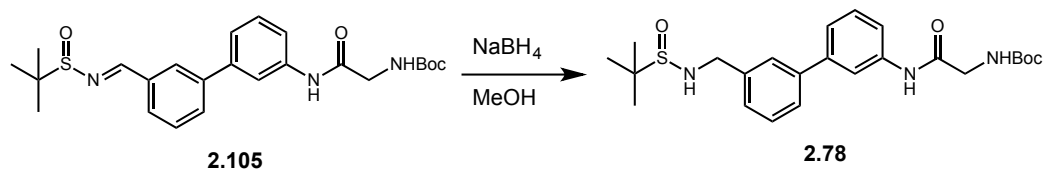
General Procedure H: Reduction using NaBH₄, for example the preparation of *tert*-butyl (2-((3'-(((*tert*-butylsulfinyl)amino)methyl)-[1,1'-biphenyl]-3-yl)amino)-2-oxoethyl)carbamate (2.78). NaBH₄ (49 mg, 1.287 mmol, 3 equiv.) was added slowly to a solution of *tert*-butyl (*E*)-(2-((3'-(((*tert*-butylsulfinyl)imino)methyl)-[1,1'-biphenyl]-3-yl)amino)-2-oxoethyl)carbamate (**2.105**) (196 mg, 0.429 mmol, 1 equiv.) in 5 mL MeOH (0.1 M). The reaction mixture was stirred at room temperature for 2 h and then diluted with 10 mL EtOAc and washed with H₂O (2 x 10 mL). The organic layer was dried using a hydrophobic frit and then concentrated under reduced pressure. The residue was purified by silica chromatography, eluting with 50-100% EtOAc/petroleum ether, to afford the title compound as a cream solid (171 mg, 87% over 2 steps).

2.63 → **2.106**
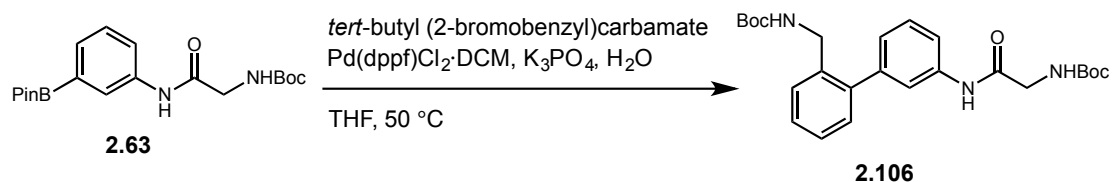
General Procedure I: Suzuki cross-coupling using Pd(dppf)Cl₂·DCM, for example the preparation of *tert*-butyl ((3'-(2-((*tert*-butoxycarbonyl)amino)acetamido)-[1,1'-biphenyl]-2-yl)methyl)carbamate (2.106). A round bottomed flask containing *tert*-butyl (2-bromobenzyl)carbamate (180 mg, 0.545 mmol, 1 equiv.), *tert*-butyl (2-oxo-2-((3-(4,4,5,5-tetramethyl-1,3,2-dioxaborolan-2-yl)phenyl)amino) ethyl) carbamate (**2.63**) (307 mg, 0.818 mmol, 1.5

149

equiv.), Pd(dppf)Cl$_2$·DCM (18 mg, 0.022 mmol, 4 mol%), and K$_3$PO$_4$ (347 mg, 1.635 mmol, 3 equiv.) was sealed with a suba seal, purged with nitrogen, followed by the addition of 3 mL THF (0.3 M) and H$_2$O (49 µL, 2.725 mmol, 5 equiv.). The reaction mixture was then heated at 50 °C for 16 h after which the reaction was allowed to return to RT, diluted with EtOAc (20 mL) and washed with sat. aq. NaHCO$_3$ (2 x 20 mL). The organic layer was collected, dried using a hydrophobic frit, and concentrated under reduced pressure. Purified using silica chromatography, eluting with 0-50% EtOAc/cyclohexane, to afford the title compound as a colourless oil (246 mg, 99%).

General Procedure J: Reductive amination, for example the preparation of *tert*-butyl (2-((5'-((allylamino)methyl)-2'-methyl-[1,1'-biphenyl]-3-yl)amino)-2-oxoethyl)carbamate (2.93). A flask containing *tert*-butyl (2-((5'-formyl-2'-methyl-[1,1'-biphenyl]-3-yl)amino)-2-oxoethyl)carbamate (**2.92**) (640 mg, 1.739 mmol, 1 equiv.), prop-2-en-1-amine (156 µL, 2.087 mmol, 1.2 equiv.), and MgSO$_4$ (2 g, 17.390 mmol, 10 equiv.) in 10 mL THF (0.2 M) was stirred at room temperature for 2 h. Once the aldehyde was consumed, NaBH$_4$ (198 mg, 5.217 mmol, 3 equiv.) was added and the reaction mixture was stirred at room temperature for a further 16 h. The reaction was then quenched with 20 mL H$_2$O, basified with sat. aq. NaHCO$_3$, and extracted using EtOAc (2 x 30 mL). The organics were collected, dried using a hydrophobic frit, then concentrated under reduced pressure. Purified by silica

chromatography, eluting with 40-100% EtOAc/petroleum ether, to afford the title compound as a cream solid (266 mg, 37%).
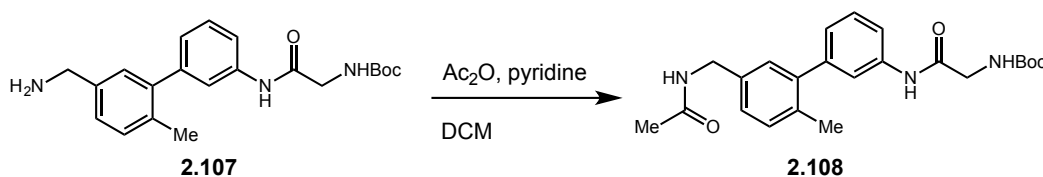
General Procedure K: Acylation of amine, for example the preparation of *tert*-butyl (2-((5'-(acetamidomethyl)-2'-methyl-[1,1'-biphenyl]-3-yl)amino)-2-oxoethyl)carbamate (2.108). A solution of *tert*-butyl (2-((5'-(aminomethyl)-2'-methyl-[1,1'-biphenyl]-3-yl)amino)-2-oxoethyl)carbamate (**2.107**) (37 mg, 0.100 mmol, 1 equiv.), Ac$_2$O (11 µL, 0.120 mmol, 1.2 equiv.), and pyridine (10 µL, 0.120 mmol, 1.2 equiv.) in 1 mL DCM (0.1 M) was stirred at room temperature for 16 h. The reaction mixture was then diluted with 10 mL DCM and washed with 1 M aq. HCl (2 x 10 mL). The organic layer was collected, dried using a hydrophobic frit, and concentrated under reduced pressure to afford the title compound which was used in the next step without further purification.

2.8   Synthesis of compounds 2.21-2.64, 2.69, 2.71, 2.73, 2.75, 2.77, 2.78, 2.80, 2.83, 2.85, 2.87, 2.88, 2.91-2.94, 2.98, 2.99, 2.102, 2.106, and 2.109-2.119.

Synthesis of 2-amino-*N*-(3-(6-aminopyridin-2-yl)phenyl)acetamide (2.21). *tert*-Butyl (6-bromopyridin-2-yl)carbamate was prepared according to general procedure B using 6-bromopyridin-2-amine (**2.66**) (200 mg, 1.156 mmol, 1 equiv.), Boc$_2$O (295 µL, 1.272 mmol, 1.1 equiv.), Et$_3$N (193 µL, 1.387 mmol, 1.2 equiv.), and DMAP (28 mg, 0.231 mmol, 20 mol%) in 10 mL DCM (0.1 M). The residue was loaded onto a plug of silica, eluted with 0-50% EtOAc/cyclohexane, to afford *tert*-butyl (6-

bromopyridin-2-yl)carbamate (**2.67**) as a colourless oil that was used in the next step without further purification. The next step was carried out according to General Procedure C using *tert*-butyl (2-oxo-2-((3-(4,4,5,5-tetramethyl-1,3,2-dioxaborolan-2-yl)phenyl)amino)ethyl) carbamate (**2.63**) (129 mg, 0.343 mmol, 1.2 equiv.), *tert*-butyl (6-bromopyridin-2-yl)carbamate (**2.67**) (78 mg, 0.286 mmol, 1 equiv.), K_3PO_4 (242 mg, 1.142 mmol, 4 equiv.), and 2′-(dimethylamino)-2-biphenylyl-palladium(II) chloride dinorbornylphosphine complex (8 mg, 0.014 mmol, 5 mol%) in 2.5 mL 1,4-dioxane:H_2O (4:1, 0.1 M). Following aqueous work-up, the residue obtained was used according to General Procedure D in 0.5 mL TFA and 1 mL DCM. Once the Boc deprotection was complete by TLC, the reaction mixture was concentrated under reduced pressure and purified using the MDAP, LpH method, to afford the title compound as a yellow oil (18 mg, 6% over 3 steps). ^{1}H NMR (400 MHz, CD_3OD): δ 8.34 (br. s, 2H), 8.07 (s, 1H), 7.69 – 7.53 (m, 3H), 7.42 (t, *J* = 7.9 Hz, 1H), 7.01 (d, *J* = 7.4 Hz, 1H), 6.60 (d, *J* = 8.3 Hz, 1H), 3.91 – 3.83 (m, 2H). CH_2NH_2 protons not observed. ^{13}C NMR (101 MHz, CD_3OD): δ 167.5, 160.5, 155.6, 141.2, 140.4, 139.5, 130.3, 124.2, 121.4, 119.6, 111.4, 109.5, 42.3. υ_{max} (neat): 3507, 3300, 3088, 1668, 1616, 1569 cm^{-1}. HRMS: exact mass calculated for $[M+H]^+$ ($C_{13}H_{15}N_4O$) *m/z* requires 243.1246, *m/z* found 243.1247.

Synthesis of 2-amino-*N*-(3-(2-aminopyridin-4-yl)phenyl)acetamide (2.22). Prepared according to General Procedure C using *tert*-butyl (2-oxo-2-((3-(4,4,5,5-tetramethyl-1,3,2-dioxaborolan-2-yl)phenyl)amino)ethyl)carbamate (**2.63**) (165 mg, 0.439 mmol, 1.2 equiv.), *tert*-butyl (4-bromopyridin-2-yl)carbamate (100 mg, 0.366 mmol, 1 equiv.), K_3PO_4 (311 mg, 1.465 mmol, 4 equiv.), and 2′-(dimethylamino)-2-biphenylyl-palladium(II) chloride dinorbornylphosphine complex (10 mg, 0.018

mmol, 5 mol%) in 2.5 mL 1,4-dioxane:H_2O (4:1, 0.1 M). Following aqueous work-up, the residue was used according to General Procedure D in 0.5 mL TFA and 1 mL DCM. Once the Boc deprotection was complete by TLC, the reaction mixture was concentrated under reduced pressure and purified using the MDAP, HpH method, to afford the title compound as a colourless oil (44 mg, 49% over 2 steps). ^{1}H NMR (400 MHz, CD_3OD): δ 7.98 − 7.88 (m, 2H), 7.62 − 7.55 (m, 1H), 7.45 − 7.33 (m, 2H), 6.85 (dd, J = 5.5, 1.6 Hz, 1H), 6.81 (s, 1H), 3.45 (s, 2H). Exchangeable protons not observed. ^{13}C NMR (101 MHz, CD_3OD): δ 173.5, 161.4, 151.7, 148.4, 140.7, 140.2, 130.5, 123.5, 121.4, 119.3, 112.5, 107.6, 45.6. υ_{max} (neat): 3386, 3325, 3204, 3081, 2915, 1688, 1647, 1606, 1539 cm^{-1}. HRMS: exact mass calculated for [M+H]$^+$ ($C_{13}H_{15}N_4O$) m/z requires 243.1240, m/z found 243.1243.

Synthesis of 2-amino-*N*-(3-(5-aminopyridin-3-yl)phenyl)acetamide (2.23). Prepared according to General Procedure D using *tert*-butyl *N*-({[3-(5-{[(*tert*-butoxy)carbonyl]amino}pyridin-3-yl)phenyl]carbamoyl}methyl)carbamate **(2.109)** (66 mg, 0.149 mmol, 1 equiv.) in 0.5 mL TFA and 1 mL DCM. Purified by revere-phase chromatography, eluting with 5-35% MeCN/H_2O (HpH method), to afford the title compound as a white solid (21 mg, 58%). ^{1}H NMR (400 MHz, CD_3OD): δ 8.02 (s, 1H), 7.95 (s, 1H), 7.88 (s, 1H), 7.57 (d, J = 8.0 Hz, 1H), 7.45 − 7.36 (m, 1H), 7.35 − 7.24 (m, 2H), 3.46 (s, 2H). Exchangeable protons not observed. ^{13}C NMR (101 MHz, CD_3OD): δ 173.4, 146.5, 140.2, 140.1, 138.6, 136.8, 136.2, 130.6, 123.8, 121.0, 120.6, 119.5, 45.6. υ_{max} (neat): 3417, 3359, 3302, 3205, 3026, 1680, 1630, 1612, 1597, 1561 cm^{-1}. HRMS: exact mass calculated for [M+H]$^+$ ($C_{13}H_{15}N4O$) m/z requires 243.1240, m/z found 243.1243.

Synthesis of 2-amino-*N*-(3-(4-aminopyridin-2-yl)phenyl)acetamide (2.24).

Prepared according to General Procedure D using *tert*-butyl *N*-({[3-(4-{[(*tert*-butoxy)carbonyl]amino}pyridin-2-yl)phenyl]carbamoyl}methyl)carbamate (**2.102**) (47 mg, 0.106 mmol, 1 equiv.) in 0.5 mL TFA and 1 mL DCM. Purified by revere-phase column chromatography, eluting with 5-35% MeCN/H_2O (HpH method), to afford the title compound as a white solid (4 mg, 16%). ^{1}H NMR (400 MHz, CD$_3$OD): δ 8.04 (d, *J* = 5.8 Hz, 1H), 7.98 (s, 1H), 7.65 (d, *J* = 8.1 Hz, 1H), 7.51 (d, *J* = 7.8 Hz, 1H), 7.40 (t, *J* = 7.9 Hz, 1H), 6.94 (d, *J* = 2.2 Hz, 1H), 6.56 (dd, *J* = 5.8, 2.2 Hz, 1H), 3.46 (s, 2H). Exchangeable protons not observed. ^{13}C NMR (101 MHz, CD$_3$OD): δ 173.2, 158.7, 157.7, 149.5, 141.8, 139.9, 130.1, 123.9, 121.4, 119.7, 109.2, 107.8, 45.6. υ_{max} (neat): 3445, 3376, 3307, 3233, 3194, 1649, 1641, 1597, 1558 cm^{-1}. HRMS: exact mass calculated for [M+H]$^+$ (C$_{13}$H$_{15}$N$_4$O) *m/z* requires 243.1246, *m/z* found 243.1249.

Synthesis of 2-amino-*N*-(3-(6-aminopyridin-3-yl)phenyl)acetamide (2.25).

Prepared according to General Procedure C using *tert*-butyl (2-oxo-2-((3-(4,4,5,5-tetramethyl-1,3,2-dioxaborolan-2-yl)phenyl)amino)ethyl)carbamate (**2.63**) (165 mg, 0.439 mmol, 1.2 equiv.), *tert*-butyl (5-bromopyridin-2-yl)carbamate (100 mg, 0.366 mmol, 1 equiv.), K$_3$PO$_4$ (311 mg, 1.465 mmol, 4 equiv.), and 2′-(dimethylamino)-2-biphenylyl-palladium(II) chloride dinorbornylphosphine complex (10 mg, 0.018 mmol, 5 mol%) in 2.5 mL 1,4-dioxane:H_2O (4:1, 0.1 M). Following aqueous work-up, the residue was used according to General Procedure D in 0.5 mL TFA and 1 mL DCM. Once the Boc deprotection was complete by TLC, the reaction mixture was concentrated under reduced pressure and purified by MDAP, HpH method, to afford the title compound as a yellow glass (29 mg, 33% over 2 steps). ^{1}H NMR (400 MHz,

CD$_3$OD): δ 8.15 (d, *J* = 2.4 Hz, 1H), 7.78 (s, 1H), 7.73 (dd, *J* = 8.7, 2.5 Hz, 1H), 7.49 (d, *J* = 8.0 Hz, 1H), 7.35 (app. t, *J* = 7.9 Hz, 1H), 7.30 – 7.21 (m, 1H), 6.66 (d, *J* = 8.7 Hz, 1H), 3.49 (s, 2H). Exchangeable protons not observed. ^{13}C NMR (101 MHz, CD$_3$OD): δ 172.7, 160.2, 145.9, 140.2, 140.1, 137.9, 130.5, 127.1, 122.8, 119.4, 118.5, 110.3, 45.3. υ$_{max}$ (neat): 3399, 3261, 3146, 2915, 1660, 1608, 1526 cm^{-1}. HRMS: exact mass calculated for [M+H]$^+$ (C$_{13}$H$_{15}$N$_4$O) *m/z* requires 243.1240, *m/z* found 243.1243.

Synthesis of 2-amino-*N*-(3-(2-aminopyrimidin-4-yl)phenyl)acetamide (2.26). Prepared according to General Procedure C using 4-bromopyrimidin-2-amine (100 mg, 0.575 mmol, 1 equiv.), *tert*-butyl (2-oxo-2-((3-(4,4,5,5-tetramethyl-1,3,2-dioxaborolan-2-yl)phenyl)amino)ethyl) carbamate (**2.63**) (259 mg, 0.690 mmol, 1.2 equiv.), 2′-(dimethylamino)-2-biphenylyl-palladium(II) chloride dinorbornylphosphine complex (16 mg, 0.029 mmol, 5 mol%), and K$_3$PO$_4$ (488 mg, 2.299 mmol, 4 equiv.) in 2.5 mL 1,4-dioxane:H$_2$O (4:1, 0.2 M) at the elevated temperature of 90 °C for 16 h. Following aqueous work-up, the residue was using according to General Procedure D using 0.5 mL TFA and 1 mL DCM. Once the Boc deprotection was complete by TLC, the reaction mixture was concentrated under reduced pressure and purified by MDAP, HpH method, to afford the title compound as a white solid (33 mg, 24% over 2 steps). ^{1}H NMR (400 MHz, CD$_3$OD): δ 8.28 – 8.23 (m, *J* = 3.9 Hz, 2H), 7.73 (dd, *J* = 7.8, 1.0 Hz, 1H), 7.68 (dd, *J* = 8.1, 1.2 Hz, 1H), 7.40 (app. t, *J* = 7.9 Hz, 1H), 7.05 (d, *J* = 5.3 Hz, 1H), 3.46 (s, 2H). Exchangeable protons not observed. ^{13}C NMR (101 MHz, CD$_3$OD): δ 173.2, 166.6, 164.9, 159.6, 140.1, 139.2, 130.3, 123.8, 123.1, 119.6, 107.9, 45.5. υ$_{max}$ (neat): 3352, 3298, 3207, 3138, 2911, 2437, 1658, 1612, 1556 cm^{-1}. HRMS: exact mass calculated

for [M+H]$^+$ (C$_{12}$H$_{14}$N$_5$O) m/z requires 244.1193, m/z found 244.1195.

Synthesis of 2-amino-N-(3'-amino-[1,1'-biphenyl]-3-yl)acetamide (2.27). Prepared according to General Procedure C using $tert$-butyl (3-bromophenyl)carbamate (100 mg, 0.367 mmol, 1 equiv.), $tert$-butyl (2-oxo-2-((3-(4,4,5,5-tetramethyl-1,3,2-dioxaborolan-2-yl)phenyl)amino) ethyl)carbamate (**2.63**) (166 mg, 0.441 mmol, 1.2 equiv.), 2'-(dimethylamino)-2-biphenylyl-palladium(II) chloride dinorbornylphosphine complex (10 mg, 0.018 mmol, 5 mol%), and K$_3$PO$_4$ (312 mg, 1.470 mmol, 4 equiv.) in 2.5 mL 1,4-dioxane:H$_2$O (4:1, 0.1 M). Following aqueous work-up, the residue was used according to General Procedure D in 0.5 mL TFA and 1 mL DCM. Once the Boc deprotection was complete by TLC, the reaction mixture was concentrated under reduced pressure and purified by MDAP, using the HpH method, to afford the title compound (64 mg, 72% over 2 steps). ^{1}H NMR (400 MHz, CD$_3$OD): δ 7.80 (s, 1H), 7.50 (dd, J = 5.6, 3.7 Hz, 1H), 7.36 − 7.25 (m, 2H), 7.14 (app. t, J = 7.8 Hz, 1H), 6.96 (s, 1H), 6.91 (ddd, J = 7.6, 1.7, 1.0 Hz, 1H), 6.70 (ddd, J = 7.9, 2.3, 0.9 Hz, 1H), 3.42 (s, 2H). Exchangeable protons not observed. ^{13}C NMR (101 MHz, CD$_3$OD): δ 173.4, 149.1, 143.7, 143.0, 139.8, 130.5, 130.1, 123.8, 119.7, 119.6, 118.0, 115.8, 115.0, 45.6. υ_{max} (neat): 3430, 3339, 2973, 2930, 1673, 1599, 1580, 1532 cm^{-1}. HRMS: exact mass calculated for [M+H]$^+$ (C$_{14}$H$_{16}$N$_3$O) m/z requires 242.1288, m/z found 242.1289.

Preparation of 2-amino-N-(3-(8-aminoimidazo[1,2-α]pyridin-6-yl)phenyl) acetamide (2.28). Prepared according to General Procedure C using $tert$-butyl (2-oxo-2-((3-(4,4,5,5-tetramethyl-1,3,2-dioxaborolan-2-yl)phenyl)amino)ethyl) carbamate (**2.63**) (130 mg, 0.346 mmol, 1.2 equiv.), $tert$-butyl (6-bromoimidazo[1,2-α]pyridin-8-yl)carbamate (**2.69**) (90 mg, 0.288 mmol, 1 equiv.), K$_3$PO$_4$ (245 mg,

1.153 mmol, 4 equiv.), and 2′-(dimethylamino)-2-biphenylyl-palladium(II) chloride dinorbornylphosphine complex (8 mg, 0.014 mmol, 5 mol%) in 2.5 mL 1,4-dioxane:H_2O (4:1, 0.1 M) at an elevated temperature of 90 °C for 16 h. Following aqueous work-up, the residue was used according to General Procedure D in 0.5 mL TFA and 1 mL DCM. Once the Boc deprotection was complete by TLC, the reaction was then concentrated under reduced pressure and purified by MDAP, HpH method, to afford the title compound as a yellow oil (21 mg, 26% over 2 steps). ^{1}H NMR (400 MHz, CD_3OD): δ 8.03 (d, J = 1.5 Hz, 1H), 7.88 (d, J = 10.3 Hz, 1H), 7.76 (d, J = 1.2 Hz, 1H), 7.58 − 7.49 (m, 1H), 7.47 (d, J = 1.2 Hz, 1H), 7.42 − 7.29 (m, 2H), 6.70 (d, J = 1.5 Hz, 1H), 3.46 (s, 2H). Exchangeable protons not observed. ^{13}C NMR (101 MHz, CD_3OD): δ 173.4, 142.9, 140.3, 140.1, 137.4, 132.1, 130.4, 129.6, 123.7, 120.2, 119.5, 115.5, 114.5, 104.2, 45.7. υ_{max} (neat): 3218, 2997, 2980, 1727, 1677, 1604, 1537 cm^{-1}. HRMS: exact mass calculated for [M+H]$^+$ ($C_{15}H_{16}N_5O$) m/z requires 282.1355, m/z found 282.1354.

Synthesis of 2-amino-*N*-(3-(2-methylpyridin-4-yl)phenyl)acetamide (2.29).
Prepared according to General Procedure D using *tert*-butyl (2-((3-(2-methylpyridin-4-yl)phenyl)amino)-2-oxoethyl)carbamate (**2.111**) (44 mg, 0.129 mmol, 1 equiv.) in 0.5 mL TFA and 1 mL DCM. Once the Boc deprotection was complete by TLC, the reaction mixture was concentrated under reduced pressure and purified by MDAP, using the HpH method, to afford the title compound as a colourless gum (16 mg, 50% yield). ^{1}H NMR (400 MHz, CD_3OD): δ 8.42 (d, J = 5.3 Hz, 1H), 8.02 (s, 1H), 7.64 − 7.57 (m, 1H), 7.53 (s, 1H), 7.48 − 7.42 (m, 3H), 3.47 (s, 2H), 2.58 (s, 3H). Exchangeable protons not observed. ^{13}C NMR (101 MHz, CD_3OD): δ 173.5, 159.8, 150.8, 149.8, 140.4, 139.8, 130.8, 123.7, 122.6, 121.7, 120.3, 119.4, 45.6, 23.9. υ_{max}

(neat): 3259, 3050, 2900, 1673, 1600, 1548, 1537 cm^{-1}. HRMS: exact mass calculated for [M+H]$^+$ (C$_{14}$H$_{16}$N$_3$O) *m/z* requires 242.1288, *m/z* found 242.1289.

Synthesis of 2-amino-*N*-(3-(pyridin-3-yl)phenyl)acetamide (2.30). Prepared according to General Procedure C using 3-bromopyridine (62 μL, 0.633 mmol, 1 equiv.), *tert*-butyl (2-oxo-2-((3-(4,4,5,5-tetramethyl-1,3,2-dioxaborolan-2-yl)phenyl)amino)ethyl)carbamate (**2.63**) (286 mg, 0.760 mmol, 1.2 equiv.), 2′-(dimethylamino)-2-biphenylyl-palladium(II) chloride dinorbornylphosphine complex (17.74 mg, 0.032 mmol, 5 mol%), and K$_3$PO$_4$ (537 mg, 2.53 mmol, 4 equiv.) in 2.5 mL 1,4-dioxane:H$_2$O (4:1, 0.2 M). Following aqueous work-up, the residue was used according to General Procedure D in 0.5 mL TFA and 1 mL DCM. Once the Boc deprotection was complete by TLC, the reaction mixture was concentrated under reduced pressure and purified by MDAP, HpH method, to afford the title compound as a white solid (71 mg, 49% over 2 steps). ^{1}H NMR (400 MHz, CD$_3$OD): δ 8.75 (dd, *J* = 2.3, 0.7 Hz, 1H), 8.49 (dd, *J* = 4.9, 1.6 Hz, 1H), 8.06 – 7.97 (m, 1H), 7.92 (s, 1H), 7.63 – 7.55 (m, 1H), 7.50 – 7.45 (m, 1H), 7.41 (app. t, *J* = 7.8 Hz, 1H), 7.37 – 7.32 (m, 1H), 3.46 (s, 2H). Exchangeable protons not observed. ^{13}C NMR (101 MHz, CD$_3$OD): δ 173.4, 148.9, 148.3, 140.4, 139.2, 138.2, 136.4, 130.8, 125.4, 123.7, 120.8, 119.4, 45.6. υ$_{max}$ (neat): 3356, 3302, 2963, 2932, 2908, 1686, 1673, 1606, 1598, 1566, 1530 cm^{-1}. HRMS: exact mass calculated for [M+H]$^+$ (C$_{13}$H$_{14}$N$_3$O) *m/z* requires 228.1131, *m/z* found 228.1133.

Synthesis of 2-amino-*N*-(3-(piperazin-1-yl)phenyl)acetamide (2.31). Prepared according to General Procedure D using *tert*-butyl 4-(3-(2-((*tert*-butoxycarbonyl)amino)acetamido)phenyl)piperazine-1-carboxylate (48 mg, 0.110 mmol, 1 equiv.) in 0.5 mL TFA and 1 mL DCM. Once the Boc deprotection was complete by TLC, the

reaction was concentrated under reduced pressure and purified by reverse phase column chromatography, eluting with 5-30% HpH method, to afford the title compound as a yellow oil (4 mg, 17% yield). ^{1}H NMR (400 MHz, CD$_3$OD): δ 7.30 (s, 1H), 7.18 (app. t, J = 8.1 Hz, 1H), 7.01 (d, J = 7.7 Hz, 1H), 6.73 (d, J = 8.6 Hz, 2H), 3.40 (s, 2H), 3.21 − 3.09 (m, 4H), 3.02 − 2.91 (m, 4H). Three exchangeable protons not observed. ^{13}C NMR (101 MHz, CD$_3$OD): δ 173.4, 153.8, 140.3, 130.3, 113.5, 112.8, 109.3, 51.1, 46.5, 45.7. υ$_{max}$ (neat): 3406, 3000, 2842, 1668, 1604, 1563, 1500 cm^{-1}. HRMS: exact mass calculated for [M+H]$^+$ (C$_{12}$H$_{19}$N$_4$O) m/z requires 235.1553, m/z found 235.1555.

Synthesis of 2-amino-*N*-(3-(5,6,7,8-tetrahydro-1,7-naphthyridin-2-yl)phenyl)acetamide (2.32). Prepared according to General Procedure C using *tert*-butyl 2-bromo-5,6-dihydro-1,7-naphthyridine-7(8*H*)-carboxylate (100 mg, 0.319 mmol, 1 equiv.), *tert*-butyl (2-oxo-2-((3-(4,4,5,5-tetramethyl-1,3,2-dioxaborolan-2-yl)phenyl)amino)ethyl)carbamate (**2.63**) (144 mg, 0.383 mmol, 1.2 equiv.), 2′-(dimethylamino)-2-biphenylyl-palladium(II) chloride dinorbornylphosphine complex (8.95 mg, 0.016 mmol, 5 mol%), and K$_3$PO$_4$ (271 mg, 1.277 mmol, 4 equiv.) in 2.5 mL 1,4-dioxane:H$_2$O (4:1, 0.1 M). Following aqueous work-up, the residue was used according to General Procedure D in 0.5 mL TFA and 1 mL DCM. Once the Boc deprotection was complete by TLC, the reaction mixture was concentrated under reduced pressure and purified by MDAP, HpH method, to afford the title compound as a colourless oil (18 mg, 20% over 2 steps). ^{1}H NMR (400 MHz, CD$_3$OD): δ 8.15 (s, 1H), 7.65 (d, J = 8.0 Hz, 2H), 7.58 (s, 2H), 7.40 (app. t, J = 7.9 Hz, 1H), 4.05 (s, 2H), 3.45 (s, 2H), 3.11 (t, J = 5.9 Hz, 2H), 2.88 (t, J = 5.9 Hz, 2H). Exchangeable protons not observed. ^{13}C NMR (101 MHz, CD$_3$OD): δ 173.4, 156.0, 155.9, 141.3,

140.0, 139.4, 130.6, 130.2, 123.7, 121.4, 120.2, 119.6, 50.9, 45.6, 43.8, 28.6. υ_{max} (neat): 3272, 2924, 2839, 1667, 1593, 1567, 1558, 1537 cm^{-1}. HRMS: exact mass calculated for [M+H]$^+$ ($C_{16}H_{19}N_4O$) *m/z* requires 283.1553, *m/z* found 283.1556.

Synthesis of *N*-(3-(1,8-naphthyridin-2-yl)phenyl)-2-aminoacetamide (2.33).
Prepared according to General Procedure D using *tert*-butyl (2-((3-(1,8-naphthyridin-2-yl)phenyl)amino)-2-oxoethyl)carbamate (**2.73**) (100 mg, 0.264 mmol, 1 equiv.) in 0.5 mL TFA and 1 mL DCM. Once the Boc deprotection was complete by TLC, the reaction was concentrated under reduced pressure and purified by MDAP, HpH method, to afford the title compound as a cream solid (35 mg, 47%). ^{1}H NMR (400 MHz, CD$_3$OD): δ 9.06 (br. s, 1H), 8.52 – 8.34 (m, 3H), 8.13 (d, *J* = 8.5 Hz, 1H), 8.01 (d, *J* = 7.8 Hz, 1H), 7.81 (d, *J* = 8.1 Hz, 1H), 7.66 – 7.56 (m, *J* = 7.9, 4.1 Hz, 1H), 7.50 (t, *J* = 7.9 Hz, 1H), 3.56 (br. s, 2H). Exchangeable protons not observed. ^{13}C NMR (101 MHz, CD$_3$OD): δ 172.4, 161.5, 156.6, 154.8, 140.5, 140.3, 139.8, 139.1, 130.5, 124.7, 123.6, 123.5, 122.8, 121.3, 120.3, 45.2. υ_{max} (neat): 3300, 3050, 1675, 1604, 1539 cm^{-1}. HRMS: exact mass calculated for [M+H]$^+$ ($C_{16}H_{15}N_4O$) *m/z* requires 279.1240, *m/z* found 279.1244.

Synthesis of 2-amino-*N*-(3-(2-methyl-1,8-naphthyridin-3-yl)phenyl)acetamide (2.34). Prepared according to General Procedure D using *tert*-butyl (2-((3-(2-methyl-1,8-naphthyridin-3-yl)phenyl)amino)-2-oxoethyl)carbamate (**2.112**) (100 mg, 0.255 mmol, 1 equiv.) in 0.5 mL TFA and 1 mL DCM. Once the Boc deprotection was complete by TLC, the reaction mixture was concentrated under reduced pressure and purified by MDAP, using the LpH method, to afford the title compound as a cream solid (20 mg, 26%). ^{1}H NMR (400 MHz, CD$_3$OD): δ 9.09 – 8.98 (m, 1H), 8.40 (dd, *J* = 8.1, 1.7 Hz, 1H), 8.33 (br. s, 2H), 8.19 (s, 1H), 7.78 (s, 1H), 7.68 – 7.56 (m, 2H),

7.48 (app. t, *J* = 7.9 Hz, 1H), 7.22 (d, *J* = 7.6 Hz, 1H), 3.92 (s, 2H), 2.67 (s, *J* = 8.6 Hz, 3H). One exchangeable proton not observed. ^{13}C NMR (101 MHz, CD$_3$OD): δ 166.2, 162.6, 155.6, 154.4, 140.9, 139.5, 139.0, 138.7, 138.2, 130.5, 126.4, 123.4, 122.9, 121.8, 120.6, 42.3, 24.7. υ$_{max}$ (neat): 2913, 2703, 1708, 1692, 1586, 1569 cm^{-1}. HRMS: exact mass calculated for [M+H]$^+$ (C$_{17}$H$_{17}$N$_4$O) *m/z* requires 293.1397, *m/z* found 293.1401.

Synthesis of 2-amino-*N*-(3-(5,6,7,8-tetrahydro-1,8-naphthyridin-2-yl)phenyl)acetamide (2.35). Prepared according to General Procedure F using *tert*-butyl (2-((3-(1,8-naphthyridin-2-yl)phenyl)amino)-2-oxoethyl)carbamate (**2.73**) (100 mg, 0.265 mmol, 1 equiv.) and 10 wt. % Pd-C (56 mg, 0.053 mmol, 20 mol%) in 2 mL EtOH (0.1 M). The residue was then used according to General Procedure D in 1 mL TFA and 1 mL DCM. Once the Boc deprotection was complete by TLC, the reaction mixture was concentrated under reduced pressure and purified by reverse-phase HPLC to afford the title compound as a cream solid (29 mg, 39% over 2 steps). ^{1}H NMR (400 MHz, CD$_3$OD): δ 8.06 (s, *J* = 1.8 Hz, 1H), 7.80 – 7.65 (m, 2H), 7.59 – 7.45 (m, 2H), 7.00 (d, *J* = 7.5 Hz, 1H), 3.92 (s, 2H), 3.65 – 3.48 (m, 2H), 2.89 (t, *J* = 6.1 Hz, 2H), 2.00 (dd, *J* = 6.4, 5.3 Hz, 2H). Exchangeable protons not observed. ^{13}C NMR (101 MHz, CD$_3$OD): δ 166.0, 153.2, 146.1, 142.7, 140.3, 134.3, 131.2, 124.0, 123.1, 122.3, 119.4, 111.4, 42.4, 42.2, 26.6, 20.4. υ$_{max}$ (neat): 3250, 3081, 2950, 1668, 1651, 1558 cm^{-1}. HRMS: exact mass calculated for [M+H]$^+$ (C$_{16}$H$_{19}$N$_4$O) *m/z* requires 283.1553, *m/z* found 283.1555.

Synthesis of 2-amino-*N*-(3-(2-methyl-5,6,7,8-tetrahydro-1,8-naphthyridin-3-yl)phenyl) acetamide (2.36). Prepared according to General Procedure F using *tert*-butyl (2-((3-(2-methyl-1,8-naphthyridin-3-yl)phenyl)amino)-2-oxoethyl)carbamate

(**2.112**) (91 mg, 0.232 mmol, 1 equiv.) and 10 wt. % Pd-C (49 mg, 0.046 mmol, 20 mol%) in 2 mL EtOH (0.1 M). The residue was then used according to General Procedure D in 1 mL TFA and 1 mL DCM. Once the Boc deprotection was complete by TLC, the reaction mixture was concentrated under reduced pressure and purified by reverse-phase HPLC to afford the title compound as a cream solid (30 mg, 43% over 2 steps). ^{1}H NMR (500 MHz, CD$_3$OD): δ 7.68 (s, 1H), 7.60 (s, 1H), 7.56 (dd, J = 8.2, 1.0 Hz, 1H), 7.45 (app. t, J = 7.9 Hz, 1H), 7.12 (d, J = 7.7 Hz, 1H), 3.88 (s, 2H), 3.58 – 3.49 (m, 2H), 2.86 (t, J = 6.1 Hz, 2H), 2.41 (s, 3H), 2.05 – 1.95 (m, 2H). Exchangeable protons not observed. ^{13}C NMR (101 MHz, CD$_3$OD): δ 165.8, 152.1, 143.9, 142.8, 139.7, 138.5, 130.6, 126.3, 125.9, 121.7, 120.7, 120.5, 42.2, 42.2, 26.3, 20.6, 17.5. υ_{max} (neat): 3071, 2950, 1662, 1565 cm^{-1}. HRMS: exact mass calculated for [M+H]$^{+}$ (C$_{17}$H$_{21}$N$_4$O) m/z requires 297.1710, m/z found 297.1711.

Synthesis of 2-amino-*N*-(5'-(aminomethyl)-2'-methyl-[1,1'-biphenyl]-3-yl)acetamide (2.37). Prepared according to General Procedure E using *tert*-butyl (2-((5'-cyano-2'-methyl-[1,1'-biphenyl]-3-yl)amino)-2-oxoethyl)carbamate (**2.75**) (100 mg, 0.274 mmol, 1 equiv.). After concentration under reduced pressure, the residue was then used according to General Procedure D in 0.5 mL TFA and 2 mL DCM. Once the Boc deprotection was complete by TLC, the reaction mixture was concentrated and purified by MDAP, HpH method, to afford the title compound as a yellow oil (27 mg, 37% over 2 steps). ^{1}H NMR (400 MHz, CD$_3$OD): δ 7.60 (s, 1H), 7.53 (d, J = 8.1 Hz, 1H), 7.37 (app. t, J = 7.9 Hz, 1H), 7.25 (s, 2H), 7.21 (s, 1H), 7.05 (d, J = 7.6 Hz, 1H), 3.85 (s, 2H), 3.44 (s, 2H), 2.24 (s, 3H). Exchangeable protons not observed. ^{13}C NMR (101 MHz, CD$_3$OD): δ 173.5, 143.9, 143.2, 139.4, 138.9, 135.6, 131.7, 130.0, 129.7, 127.8, 126.0, 121.8, 119.5, 45.8, 45.6, 20.2. υ_{max} (neat):

3284, 3051, 2993, 2902, 2839, 1682, 1667, 1606, 1587, 1558, 1539 cm^{-1}. HRMS: exact mass calculated for [M+H]$^{+}$ (C$_{16}$H$_{20}$N$_{3}$O) m/z requires 270.1601, m/z found 270.1605.

Synthesis of 2-amino-*N*-(3'-(aminomethyl)-2'-methyl-[1,1'-biphenyl]-3-yl)acetamide (2.38). Prepared according to General Procedure E using *tert*-butyl (2-((3'-cyano-2'-methyl-[1,1'-biphenyl]-3-yl)amino)-2-oxoethyl)carbamate (**2.113**) (100 mg, 0.274 mmol, 1 equiv.). After concentration under reduced pressure, the residue was then used according to General Procedure D in 0.5 mL TFA and 2 mL DCM. Once the Boc deprotection was complete by TLC, the reaction mixture was concentrated and purified by MDAP, HpH method, to afford the title compound as a colourless oil (21 mg, 29% over 2 steps). ^{1}H NMR (400 MHz, CD$_{3}$OD): δ 7.59 – 7.50 (m, 2H), 7.40 – 7.28 (m, 2H), 7.22 (app. t, J = 7.6 Hz, 1H), 7.11 (d, J = 7.6 Hz, 1H), 7.00 (d, J = 7.7 Hz, 1H), 3.90 (s, 2H), 3.43 (br. s, 2H), 2.21 (s, 3H). Exchangeable protons not observed. ^{13}C NMR (101 MHz, CD$_{3}$OD): δ 173.5, 144.4, 143.9, 141.0, 139.4, 134.2, 129.8, 129.6, 128.0, 126.8, 126.2, 122.0, 119.5, 45.7, 44.3, 16.2. υ$_{max}$ (neat): 3263, 2915, 1675, 1584, 1558, 1539 cm^{-1}. HRMS: exact mass calculated for [M+H]$^{+}$ (C$_{16}$H$_{20}$N$_{3}$O) m/z requires 270.1601, m/z found 270.1603.

Synthesis of 2-amino-*N*-(3'-(aminomethyl)-[1,1'-biphenyl]-3-yl)acetamide (2.39). Prepared according to General Procedure D using *tert*-butyl (2-((3'-(((*tert*-butylsulfinyl)amino)methyl)-[1,1'-biphenyl]-3-yl)amino)-2-oxoethyl) carbamate (**2.78**) (165 mg, 0.359 mmol, 1 equiv.) in 1 mL TFA and 1 mL DCM. Once the Boc deprotection was complete by TLC, the reaction mixture was concentrated under reduced pressure and purified by reverse-phase HPLC to afford the title compound as a colourless oil (71 mg, 78%). ^{1}H NMR (400 MHz, CD$_{3}$OD): δ 7.94 (s, 1H), 7.73 (s,

1H), 7.66 (d, J = 7.8 Hz, 1H), 7.63 − 7.56 (m, 1H), 7.53 (t, J = 7.7 Hz, 1H), 7.47 − 7.39 (m, 3H), 4.20 (s, 2H), 3.91 (s, 2H), 3.35 (s, 2H). Three exchangeable protons not observed. ^{13}C NMR (101 MHz, CD$_3$OD): δ 165.7, 143.0, 142.5, 139.8, 135.2, 130.8, 130.6, 129.1, 128.7, 128.7, 124.2, 120.2, 119.6, 44.3, 42.2. υ_{max} (neat): 3042, 1670, 1616, 1616, 1567, 1506 cm^{-1}. HRMS: exact mass calculated for [M+H]$^+$ (C$_{15}$H$_{18}$N$_3$O) m/z requires 256.1450, m/z found 256.1444.

Synthesis of 2-amino-*N*-(3'-(2-aminoethyl)-[1,1'-biphenyl]-3-yl)acetamide (2.40).
A solution of 2-(3-bromophenethyl)isoindoline-1,3-dione (**2.80**) (500 mg, 1.515 mmol, 1 equiv.) and H$_2$NNH$_2$.H$_2$O (440 μL, 9.091 mmol, 6 equiv.) in 6 mL EtOH (0.2 M) was stirred at 60 °C for 1 h then allowed to return to room temperature. The reaction mixture was filtered and the white precipitate washed with EtOH. The filtrate was then concentrated and purified by trituration in EtOH to afford 2-(3-bromophenyl)ethan-1-amine (901 mg, 99%), which was used in the next step without further purification. Prepared according to General Procedure B using 2-(3-bromophenyl)ethan-1-amine (296 mg, 1.48 mmol, 1 equiv.), Et$_3$N (206 μL, 1.48 mmol, 1 equiv.), and Boc$_2$O (323 mg, 1.48 mmol, 1 equiv.) in 5 mL THF (0.3 M). The reaction mixture was diluted with 20 mL EtOAc and washed with 1 M aq. HCl (2 x 20 mL). The organic layer was collected, dried using a hydrophobic frit, and concentrated under reduced pressure to afford *tert*-butyl (3-bromophenethyl)carbamate as a colourless oil (282 mg, 64%), which was used without further purification. The residue was used according to General Procedure I using *tert*-butyl (3-bromophenethyl)carbamate (106 mg, 0.355 mmol, 1 equiv.), *tert*-butyl (2-oxo-2-((3-(4,4,5,5-tetramethyl-1,3,2-dioxaborolan-2-yl)phenyl)amino) ethyl) carbamate (**2.63**) (200 mg, 0.532 mmol, 1.5 equiv.), Pd(dppf)Cl$_2$·DCM (11

mg, 0.014 mmol, 4 mol%), and K_3PO_4 (226 mg, 1.065 mmol, 3 equiv.) in 2 mL THF (0.2 M) and H_2O (32 μL, 1.775 mmol, 5 equiv.). The residue was loaded onto a plug of silica and eluted with 40% EtOAc/cyclohexane, then concentrated under reduced pressure. The residue was used according to General Procedure D in 1 mL TFA and 1 mL DCM. Once the Boc deprotection was complete by TLC, the reaction mixture was concentrated under reduced pressure and purified by reverse-phase HPLC to afford the title compound as a colourless oil (81 mg, 89% over 2 steps). ^{1}H NMR (400 MHz, CD_3OD): δ 7.81 (s, 1H), 7.50 (s, 1H), 7.43 (d, J = 7.9 Hz, 2H), 7.38 − 7.24 (m, 3H), 7.20 (d, J = 6.8 Hz, 1H), 3.86 (s, 2H), 3.21 − 3.08 (m, 2H), 2.97 (t, J = 7.0 Hz, 2H). Exchangeable protons not observed. ^{13}C NMR (101 MHz, CD_3OD): δ 165.7, 142.9, 142.6, 139.6, 138.6, 130.4, 128.9, 128.4, 126.8, 124.2, 120.0, 119.6, 42.1, 41.8, 34.5. One carbon not observed/coincident. $υ_{max}$ (neat): 3036, 1662, 1608, 1569 cm^{-1}. HRMS: exact mass calculated for [M+H]$^+$ ($C_{16}H_{20}N_3O$) m/z requires 270.1601, m/z found 270.1603.

Synthesis of 2-amino-*N*-(3'-(aminomethyl)-2',6'-dimethyl-[1,1'-biphenyl]-3-yl)acetamide (2.41). Prepared according to General Procedure D using *tert*-butyl (2-((3'-(((*tert*-butylsulfinyl)amino)methyl)-2',6'-dimethyl-[1,1'-biphenyl]-3-yl)amino)-2-oxoethyl)carbamate (**2.85**) (100 mg, 0.207 mmol, 1 equiv.) in 1 mL TFA and 1 mL DCM. Once the Boc deprotection was complete by TLC, the reaction mixture was concentrated under reduced pressure and purified by reverse-phase HPLC to afford the title compound as a yellow oil (26 mg, 44%). ^{1}H NMR (400 MHz, CD_3OD): δ 7.59 (dd, J = 8.2, 1.1 Hz, 1H), 7.49 − 7.39 (m, 2H), 7.30 (d, J = 7.8 Hz, 1H), 7.21 (d, J = 7.9 Hz, 1H), 6.87 (d, J = 7.5 Hz, 1H), 4.17 (s, 2H), 3.87 (s, 2H), 3.35 (br. s, 2H), 2.07 (s, 3H), 2.01 (s, 3H). Three exchangeable protons not observed. ^{13}C NMR (101

MHz, CD$_3$OD): δ 165.6, 144.0, 143.0, 139.8, 138.6, 135.9, 130.5, 130.4, 129.6, 128.9, 126.2, 121.4, 119.5, 42.2, 42.1, 21.1, 16.8. υ$_{max}$ (neat): 2980, 1664, 1623, 1567 cm^{-1}. HRMS: exact mass calculated for [M+Na]$^+$ (C$_{17}$H$_{21}$N$_3$ONa) *m/z* requires 306.1577, *m/z* found 306.1578.

Synthesis of 2-amino-*N*-(3-(6-(aminomethyl)pyridin-2-yl)phenyl)acetamide (2.42). Prepared according to General Procedure D using *tert*-butyl (2-((3-(6-(((*tert*-butylsulfinyl)amino)methyl)pyridin-2-yl)phenyl)amino)-2-oxoethyl)carbamate (**2.88**) (50 mg, 0.109 mmol, 1 equiv.) in 1 mL TFA and 1 mL DCM. Once the Boc deprotection was complete by TLC, the reaction mixture was concentrated under reduced pressure and purified by SCX to afford the title compound as a colourless oil (3 mg, 11%). ^{1}H NMR (500 MHz, CD$_3$OD): δ 8.34 (s, 1H), 7.85 (t, *J* = 7.6 Hz, 1H), 7.80 (d, *J* = 7.7 Hz, 1H), 7.76 (d, *J* = 7.9 Hz, 1H), 7.65 (d, *J* = 8.0 Hz, 1H), 7.44 (t, *J* = 7.9 Hz, 1H), 7.34 (d, *J* = 7.7 Hz, 1H), 4.06 (s, 2H), 3.47 (s, 2H). Exchangeable protons not observed. ^{13}C NMR (101 MHz, CD$_3$OD): δ 173.6, 160.0, 157.8, 141.2, 140.1, 139.2, 130.3, 123.8, 121.6, 121.5, 120.4, 119.6, 46.8, 45.7. υ$_{max}$ (neat): 3403, 3250, 3100, 1670, 1577 cm^{-1}. HRMS: exact mass calculated for [M+Na]$^+$ (C$_{14}$H$_{16}$N$_4$NaO) *m/z* requires 279.1216, *m/z* found 279.1207.

Synthesis of 2-(3-(2-aminoacetamido)phenyl)-6-(aminomethyl)pyridine 1-oxide (2.43). *m*-CPBA (47 mg, 0.272 mmol, 2.5 equiv.) was added to a solution of *tert*-butyl (*E*)-(2-((3-(6-(((*tert*-butylsulfinyl)imino)methyl)pyridin-2-yl)phenyl) amino)-2-oxoethyl)carbamate (**2.88**) (50 mg, 0.109 mmol, 1 equiv.) in 3 mL DCM (0.03 M) and the resulting solution stirred at room temperature for 16 h. The reaction mixture was diluted with 20 mL MeOH, silica added, and then concentrated under reduced pressure. The silica was loaded onto a column and eluted with 0-5% MeOH/DCM to

afford 2-(3-(2-((*tert*-butoxycarbonyl)amino)acetamido)phenyl)-6-(((1,1-dimethylethyl)sulfonamido)methyl)pyridine 1-oxide (**2.89**) which was used without further purification. The residue was used according to General Procedure D using 2-(3-(2-((*tert*-butoxycarbonyl)amino)acetamido)phenyl)-6-(((1,1-dimethylethyl) sulfonamido) methyl) pyridine 1-oxide (**2.89**) (54 mg, 0.109 mmol, 1 equiv.) in 1 mL TfOH and 1 mL DCM. Once the deprotection was complete by TLC, the reaction was concentrated under reduced pressure and purified by reverse-phase HPLC to afford the title compound as a colourless gum (6 mg, 20% over 2 steps). ^{1}H NMR (400 MHz, CD$_3$OD): δ 8.12 (t, *J* = 1.8 Hz, 1H), 7.74 (dd, *J* = 7.7, 2.3 Hz, 1H), 7.70 (ddd, *J* = 7.8, 3.5, 1.7 Hz, 2H), 7.64 (d, *J* = 7.7 Hz, 1H), 7.62 – 7.57 (m, 1H), 7.51 (app. t, *J* = 7.9 Hz, 1H), 4.40 (s, 2H), 3.89 (s, 2H). Exchangeable protons not observed. ^{13}C NMR (101 MHz, CD$_3$OD): δ 165.8, 150.8, 145.1, 139.4, 134.1, 130.2, 129.7, 129.2, 128.0, 126.6, 122.3, 121.8, 42.2, 41.2. υ$_{max}$ (neat): 3280, 3202, 3038, 1673, 1621, 1590, 1563, 1537 cm^{-1}. HRMS: exact mass calculated for [M+Na]$^+$ (C$_{14}$H$_{16}$N$_4$NaO$_2$) *m/z* requires 295.1165, *m/z* found 295.1161.

Synthesis of 2-amino-*N*-(2'-(aminomethyl)-[1,1'-biphenyl]-3-yl)acetamide bis(2,2,2-trifluoroacetate) (2.44). Prepared according to General Procedure D using *tert*-butyl ((3'-(2-((*tert*-butoxycarbonyl)amino)acetamido)-[1,1'-biphenyl]-2-yl)methyl)carbamate (**2.106**) (228 mg, 0.501 mmol, 1 equiv.) in 1 mL TFA and 1 mL DCM. Once the Boc deprotection was complete by TLC, the reaction mixture was concentrated under reduced pressure and purified by reverse-phase column chromatography, eluting with 100% H$_2$O, to afford the title compound as a colourless oil (213 mg, 88%). ^{1}H NMR (500 MHz, CD$_3$OD): δ 8.35 (br. s, 1H), 7.66 (s, 1H), 7.59 (dd, *J* = 11.6, 4.8 Hz, 2H), 7.51 – 7.42 (m, 3H), 7.38 – 7.32 (m, 1H),

7.13 (d, J = 7.6 Hz, 1H), 4.12 (s, 2H), 3.91 (s, 2H). Four exchangeable protons not observed. ^{13}C NMR (101 MHz, CD$_3$OD): δ 165.9, 143.3, 141.9, 139.4, 131.9, 131.6, 130.4, 130.0, 129.8, 129.5, 126.3, 122.0, 120.3, 42.2, 41.4. υ$_{max}$ (neat): 3354, 3271, 3057, 1670, 1590, 1558, 1534, 1496, 1478 cm^{-1}. HRMS: exact mass calculated for [M+H]$^+$ (C$_{15}$H$_{18}$N$_3$O) m/z requires 256.1444, m/z found 256.1441.

Synthesis of 2-acetamido-*N*-(5'-(acetamidomethyl)-2'-methyl-[1,1'-biphenyl]-3-yl)acetamide (2.45). Prepared according to General Procedure K using *N*-(5'-(acetamidomethyl)-2'-methyl-[1,1'-biphenyl]-3-yl)-2-aminoacetamide (**2.48**) (10 mg, 0.032 mmol, 1 equiv.), Ac$_2$O (5 μL, 0.048 mmol, 1.5 equiv.), and pyridine (4 μL, 0.048 mmol, 1.5 equiv.) in 0.5 mL DCM (0.1 M). The reaction mixture was diluted with DCM and washed with 1 M aq. HCl, the organic layer was dried using a hydrophobic frit and concentrated under reduced pressure to afford the title compound as a white solid (5 mg, 48%). ^{1}H NMR (500 MHz, CD$_3$OD): δ 7.57 – 7.48 (m, 2H), 7.36 (t, J = 8.0 Hz, 1H), 7.23 (d, J = 7.7 Hz, 1H), 7.17 (d, J = 7.8 Hz, 1H), 7.12 (s, 1H), 7.04 (s, 1H), 4.34 (s, 2H), 4.01 (s, 2H), 2.22 (s, 3H), 2.04 (s, 3H), 1.97 (s, 3H). Exchangeable protons not observed. ^{13}C NMR (126 MHz, CD$_3$OD): δ 173.9, 173.1, 169.8, 143.9, 143.1, 139.4, 137.4, 135.3, 131.6, 129.9, 129.7, 127.7, 126.0, 122.0, 119.8, 44.1, 43.9, 22.5, 22.4, 20.2. υ$_{max}$ (neat): 3412, 3325, 3289, 3066, 2924, 2880, 2408, 1634, 1591, 1539, 1504 cm^{-1}. HRMS: exact mass calculated for [M+Na]$^+$ (C$_{20}$H$_{23}$N$_3$NaO$_3$) m/z requires 376.1632, m/z found 376.1627.

Synthesis of 2-amino-*N*-(5'-(hydroxymethyl)-2'-methyl-[1,1'-biphenyl]-3-yl)acetamide (2.46). Prepared according to General Procedure D using *tert*-butyl (2-((5'-(hydroxymethyl)-2'-methyl-[1,1'-biphenyl]-3-yl)amino)-2-oxoethyl)carbamate (**2.114**) (87 mg, 0.235 mmol, 1 equiv.) in 1 mL TFA and 1 mL DCM. Once the Boc

deprotection was complete by TLC, the reaction mixture was concentrated under reduced pressure and purified by silica chromatography, eluting with 0-10% MeOH/DCM, to afford the title compound as a colourless oil (54 mg, 85%). ^{1}H NMR (500 MHz, CD$_3$OD): δ 7.61 – 7.52 (m, 2H), 7.37 (app. t, J = 7.8 Hz, 1H), 7.23 (s, 2H), 7.18 (s, 1H), 7.06 (d, J = 7.5 Hz, 1H), 4.59 (s, 2H), 3.72 (s, 2H), 2.22 (s, 3H). Exchangeable protons not observed. ^{13}C NMR (126 MHz, CD$_3$OD): δ 144.2, 142.8, 140.2, 139.1, 135.3, 131.4, 129.8, 129.3, 127.3, 126.3, 121.8, 119.5, 65.0, 49.8, 20.2. One carbon not observed/coincident. υ_{max} (neat): 3312, 2919, 2852, 1668, 1616, 1567 cm^{-1}. HRMS: exact mass calculated for [M+H]$^+$ (C$_{16}$H$_{19}$N$_2$O$_2$) m/z requires 271.1441, m/z found 271.1445.

Synthesis of 2-amino-N-(5'-cyano-2'-methyl-[1,1'-biphenyl]-3-yl)acetamide (2.47). Prepared according to General Procedure D using *tert*-butyl (2-((5'-cyano-2'-methyl-[1,1'-biphenyl]-3-yl)amino)-2-oxoethyl)carbamate (**2.75**) (150 mg, 0.411 mmol, 1 equiv.) in 1 mL TFA and 2 mL DCM. Once the Boc deprotection was complete by TLC, the reaction mixture was concentrated under reduced pressure and purified by silica chromatography, eluting with 0-10% MeOH/DCM, to afford the title compound as a cream solid (95 mg, 61%). ^{1}H NMR (400 MHz, CDCl$_3$): δ 9.51 (br. s, 1H), 7.62 (s, 1H), 7.58 (d, J = 8.1 Hz, 1H), 7.55 – 7.47 (m, 2H), 7.42 – 7.31 (m, 2H), 7.01 (d, J = 7.3 Hz, 1H), 3.51 (s, 2H), 2.33 (s, 3H). Two exchangeable protons not observed. ^{13}C NMR (101 MHz, CDCl$_3$): δ 171.0, 142.8, 141.6, 140.5, 137.9, 133.2, 131.2, 130.9, 129.2, 124.7, 120.0, 119.1, 118.8, 109.7, 45.2, 21.0. υ_{max} (neat): 3278, 3055, 2958, 2924, 2228, 1670, 1606, 1590, 1528 cm^{-1}. HRMS: exact mass calculated for [M+Na]$^+$ (C$_{16}$H$_{15}$N$_3$NaO) m/z requires 288.1107, m/z found 288.1098.

Synthesis of _N_-(5'-(acetamidomethyl)-2'-methyl-[1,1'-biphenyl]-3-yl)-2-aminoacetamide (2.48). Prepared according to General Procedure K using _tert_-butyl (2-((5'-(aminomethyl)-2'-methyl-[1,1'-biphenyl]-3-yl)amino)-2-oxoethyl)carbamate (**2.94**) (37 mg, 0.100 mmol, 1 equiv.), Ac₂O (11 μL, 0.120 mmol, 1.2 equiv.), and pyridine (10 μL, 0.120 mmol, 1.2 equiv.) in 1 mL DCM (0.1 M). Following aqueous work-up, the residue was used according to General procedure D in 1 mL TFA and 1 mL DCM. Once the Boc deprotection was complete by TLC, the reaction mixture was concentrated under reduced pressure and purified by silica chromatography, eluting with 0-10% MeOH/DCM, to afford the title compound as a brown oil (28 mg, 90% over 2 steps). ^{1}H NMR (400 MHz, CD₃OD): δ 7.62 – 7.52 (m, 2H), 7.38 (app. t, J = 8.1 Hz, 1H), 7.23 (d, J = 7.8 Hz, 1H), 7.17 (dd, J = 7.8, 1.7 Hz, 1H), 7.11 (s, 1H), 7.06 (d, J = 7.6 Hz, 1H), 4.34 (s, 2H), 3.87 (s, 2H), 2.21 (s, 3H), 1.97 (s, 3H). Exchangeable protons not observed. ^{13}C NMR (101 MHz, CD₃OD): δ 173.2, 165.6, 144.1, 142.9, 139.1, 137.5, 135.2, 131.6, 129.8, 129.8, 127.8, 126.3, 121.6, 119.4, 43.9, 42.2, 22.6, 20.2. υ_{max} (neat): 3278, 3088, 2956, 1763, 1675, 1565 cm^{-1}. HRMS: exact mass calculated for [M+H]$^+$ ($C_{18}H_{22}N_3O_2$) _m/z_ requires 312.1707, _m/z_ found 312.1709.

Synthesis of _N_-(5'-((allylamino)methyl)-2'-methyl-[1,1'-biphenyl]-3-yl)-2-aminoacetamide (2.49). Prepared according to General Procedure D using _tert_-butyl (2-((5'-((allylamino)methyl)-2'-methyl-[1,1'-biphenyl]-3-yl)amino)-2-oxoethyl)carbamate (**2.93**) (100 mg, 0.244 mmol, 1 equiv.) in 1 mL TFA and 1 mL DCM. Once the Boc deprotection was complete by TLC, the reaction mixture was concentrated under reduced pressure and purified by reverse-phase column chromatography, eluting with 100% H₂O, to afford the title compound as a yellow oil

(64 mg, 85%). ^{1}H NMR (400 MHz, CD$_3$OD): δ 7.62 – 7.51 (m, 2H), 7.35 (app. t, J = 7.9 Hz, 1H), 7.25 – 7.18 (m, 2H), 7.17 (s, 1H), 7.06 – 7.01 (m, 1H), 6.00 – 5.83 (m, 1H), 5.26 – 5.06 (m, 2H), 3.70 (br. s, 2H), 3.40 (d, J = 7.9 Hz, 2H), 3.22 (dt, J = 6.3, 1.3 Hz, 2H), 2.23 (s, 3H). Exchangeable protons not observed. ^{13}C NMR (101 MHz, CD$_3$OD): δ 173.6, 144.0, 143.0, 139.4, 138.0, 137.0, 135.2, 131.5, 130.9, 129.7, 128.7, 126.0, 121.8, 119.4, 117.5, 53.2, 52.2, 45.7, 20.3. υ$_{max}$ (neat): 3276, 3071, 2976, 2921, 1670, 1608, 1588, 1534 cm^{-1}. HRMS: exact mass calculated for [M+H]$^+$ (C$_{19}$H$_{24}$N$_3$O) m/z requires 310.1914, m/z found 310.1913.

Synthesis of 2-amino-*N*-(4'-(aminomethyl)-2'-methyl-[1,1'-biphenyl]-3-yl)acetamide (2.50). Prepared according to General Procedure B using (4-bromo-3-methylphenyl)methanamine (211 mg, 1.055 mmol, 1 equiv.), Boc$_2$O (253 mg, 1.160 mmol, 1.1 equiv.), and Et$_3$N (293 μL, 2.110 mmol, 2 equiv.) in 5 mL DCM (0.2 M). Following aqueous work-up, the residue was used in the next step according to General Procedure I using *tert*-butyl (4-bromo-3-methylbenzyl)carbamate (316 mg, 1.055 mmol, 1 equiv.), *tert*-butyl (2-oxo-2-((3-(4,4,5,5-tetramethyl-1,3,2-dioxaborolan-2-yl)phenyl)amino) ethyl) carbamate (**2.63**) (595 mg, 1.582 mmol, 1.5 equiv.), Pd(dppf)Cl$_2$·DCM (34 mg, 0.042 mmol, 4 mol%), and K$_3$PO$_4$ (671 mg, 3.165 mmol, 3 equiv.) in 4 mL THF (0.3 M) and H$_2$O (95 μL, 5.275 mmol, 5 equiv.). The crude material was loaded onto a plug of silica and eluted with 60% EtOAc/petroleum ether, to afford *tert*-butyl ((3'-(2-((*tert*-butoxycarbonyl)amino)acetamido)-2-methyl-[1,1'-biphenyl]-4-yl)methyl)carbamate which was used in the next step without further purification. The residue was then used according to General Procedure D in 1 mL TFA and 1 mL DCM. Once the Boc deprotection was complete by TLC, the reaction was concentrated and purified by

reverse-phase HPLC to afford the title compound as a cream solid (29 mg, 10% over 2 steps). ^{1}H NMR (400 MHz, CD$_3$OD): δ 7.62 (t, J = 1.8 Hz, 1H), 7.57 – 7.50 (m, 1H), 7.43 – 7.35 (m, 2H), 7.34 – 7.24 (m, 2H), 7.07 – 7.01 (m, 1H), 4.10 (s, 2H), 3.63 (s, 2H), 2.29 (s, 3H). Exchangeable protons not observed. ^{13}C NMR (101 MHz, CD$_3$OD): δ 170.1, 143.7, 143.3, 139.4, 137.4, 134.3, 131.8, 131.3, 129.9, 127.2, 126.0, 121.6, 119.7, 44.3, 44.1, 20.5. υ_{max} (neat): 2926, 1670, 1616, 1591, 1565, 1558 cm^{-1}. HRMS: exact mass calculated for [M+Na]$^+$ (C$_{16}$H$_{19}$N$_3$NaO) m/z requires 292.1420, m/z found 292.1413.

Synthesis of 2-amino-N-(2'-methyl-[1,1'-biphenyl]-3-yl)acetamide (2.51). Prepared according to General Procedure I using *tert*-butyl (2-((3-bromophenyl)amino)-2-oxoethyl)carbamate (**2.115**) (100 mg, 0.305 mmol, 1 equiv.), *o*-tolylboronic acid (62 mg, 0.457 mmol, 1.5 equiv.), Pd(dppf)Cl$_2$·DCM (10 mg, 0.012 mmol, 4 mol%), and K$_3$PO$_4$ (194 mg, 0.915 mmol, 3 equiv.) in 2 mL THF (0.2 M) and H$_2$O (27 μL, 1.525 mmol, 5 equiv.). The crude material was loaded onto a plug of silica and eluted with 40% EtOAc/cyclohexane, then concentrated under reduced pressure. The residue was used according to General Procedure D in 1 mL TFA and 1 mL DCM. Once the Boc deprotection was complete by TLC, the reaction mixture was concentrated under reduced pressure and purified by reverse-phase HPLC to afford the title compound as a white solid (50 mg, 68% over 2 steps). ^{1}H NMR (500 MHz, CD$_3$OD): δ 7.59 – 7.53 (m, 2H), 7.38 (t, J = 8.2 Hz, 1H), 7.28 – 7.18 (m, 3H), 7.16 (d, J = 7.0 Hz, 1H), 7.06 (d, J = 7.5 Hz, 1H), 3.87 (s, 2H), 2.23 (s, 3H). Exchangeable protons not observed. ^{13}C NMR (101 MHz, CD$_3$OD): δ 165.5, 144.3, 142.8, 139.0, 136.2, 131.3, 130.5, 129.8, 128.5, 126.8, 126.4, 121.7, 119.4, 42.2, 20.5. υ_{max} (neat): 3453, 3364, 3267, 3058, 2973, 2926, 1675, 1590, 1539 cm^{-1}.

HRMS: exact mass calculated for $[M+H]^+$ ($C_{15}H_{17}N_2O$) *m/z* requires 241.1335, *m/z* found 241.1336.

Synthesis of 2-amino-*N*-(2'-(trifluoromethyl)-[1,1'-biphenyl]-3-yl)acetamide (2.52). Prepared according to General Procedure I using *tert*-butyl (2-((3-bromophenyl)amino)-2-oxoethyl)carbamate (**2.115**) (100 mg, 0.305 mmol, 1 equiv.), 4,4,5,5-tetramethyl-2-(2-(trifluoromethyl)phenyl)-1,3,2-dioxaborolane (124 mg, 0.457 mmol, 1.5 equiv.), Pd(dppf)Cl$_2$·DCM (10 mg, 0.012 mmol, 4 mol%), and K$_3$PO$_4$ (194 mg, 0.915 mmol, 3 equiv.) in 2 mL THF (0.2 M) and H$_2$O (27 μL, 1.525 mmol, 5 equiv.). The crude material was loaded onto a plug of silica and eluted with 40% EtOAc/cyclohexane, then concentrated under reduced pressure. The residue was used according to General Procedure D in 1 mL TFA and 1 mL DCM. Once the Boc deprotection was complete by TLC, the reaction mixture was concentrated under reduced pressure and purified by reverse-phase HPLC to afford the title compound as a white solid (9 mg, 10% over 2 steps). ^{1}H NMR (500 MHz, CD$_3$OD): δ 7.77 (d, *J* = 7.9 Hz, 1H), 7.69 – 7.61 (m, 2H), 7.59 (s, 1H), 7.55 (app. t, *J* = 7.7 Hz, 1H), 7.41 – 7.32 (m, 2H), 7.07 (d, *J* = 7.6 Hz, 1H), 3.86 (s, 2H). Exchangeable protons not observed. ^{13}C NMR (101 MHz, CDCl$_3$): δ 170.6, 141.0, 140.8, 137.3, 132.2, 131.4, 128.6, 127.6, 126.2, 126.1, 125.0, 120.1, 118.8, 45.1. CF$_3$ carbon not observed. ^{19}F NMR (471 MHz, CD$_3$OD): δ -58.11. υ$_{max}$ (neat): 3429, 3362, 3274, 3071, 1670, 1606, 1591, 1565, 1539 cm^{-1}. HRMS: exact mass calculated for $[M+H]^+$ ($C_{15}H_{14}F_3N_2O$) *m/z* requires 295.1053, *m/z* found 295.1055.

Synthesis of *N*-([1,1'-biphenyl]-3-yl)-2-aminoacetamide (2.53). Prepared according to General Procedure I using *tert*-butyl (2-((3-bromophenyl)amino)-2-oxoethyl)carbamate (**2.115**) (100 mg, 0.305 mmol, 1 equiv.), phenylboronic acid

pinacol ester (93 mg, 0.457 mmol, 1.5 equiv.), Pd(dppf)Cl$_2$·DCM (10 mg, 0.012 mmol, 4 mol%), and K$_3$PO$_4$ (194 mg, 0.915 mmol, 3 equiv.) in 2 mL THF (0.2 M) and H$_2$O (27 μL, 1.525 mmol, 5 equiv.). The crude material was loaded onto a plug of silica and eluted with 40% EtOAc/cyclohexane, then concentrated under reduced pressure. The residue was used according to General Procedure D in 1 mL TFA and 1 mL DCM. Once the Boc deprotection was complete by TLC, the reaction mixture was concentrated under reduced pressure and purified by reverse-phase HPLC to afford the title compound as a white solid (30 mg, 44% over 2 steps). ^{1}H NMR (400 MHz, CDCl$_3$): δ 9.46 (br. s, 1H), 7.82 (s, 1H), 7.69 – 7.54 (m, 3H), 7.48 – 7.37 (m, 3H), 7.37 – 7.30 (m, 2H), 3.49 (s, 2H). Two exchangeable protons not observed. ^{13}C NMR (101 MHz, CDCl$_3$): δ 171.0, 142.2, 140.9, 138.2, 129.5, 128.9, 127.6, 127.3, 123.1, 118.5, 118.3, 45.3. υ_{max} (neat): 3380, 3297, 3055, 2924, 1658, 1601, 1526, 1508 cm^{-1}. HRMS: exact mass calculated for [M+H]$^+$ (C$_{14}$H$_{15}$N$_2$O) m/z requires 227.1179, m/z found 227.1177.

Synthesis of 2-amino-N-(3-(1-amino-2,3-dihydro-1H-inden-4-yl)phenyl)acetamide (2.54). Prepared according to General Procedure I using *tert*-butyl (4-bromo-2,3-dihydro-1H-inden-1-yl)carbamate (**2.97**) (180 mg, 0.577 mmol, 1 equiv.), *tert*-butyl (2-oxo-2-((3-(4,4,5,5-tetramethyl-1,3,2-dioxaborolan-2-yl)phenyl)amino) ethyl) carbamate (**2.63**) (325 mg, 0.865 mmol, 1.5 equiv.), Pd(dppf)Cl$_2$·DCM (19 mg, 0.023 mmol, 4 mol%), and K$_3$PO$_4$ (367 mg, 1.731 mmol, 3 equiv.) in 2 mL THF (0.3 M) and H$_2$O (52 μL, 2.885 mmol, 5 equiv.). The crude material was loaded onto a plug of silica and eluted with 60% EtOAc/petroleum ether, to afford *tert*-butyl (2-((3-(1-((*tert*-butoxycarbonyl)amino)-2,3-dihydro-1H-inden-4-yl)phenyl)amino)-2-oxoethyl)carbamate which was used in the next step

without further purification. The residue was then used according to General Procedure D in 1 mL TFA and 1 mL DCM. Once the Boc deprotection was complete by TLC, the reaction was concentrated and purified by reverse-phase HPLC to afford the title compound as a cream solid (58 mg, 36% over 2 steps). ^{1}H NMR (400 MHz, CD$_3$OD): δ 7.72 (s, 1H), 7.54 (ddd, J = 16.5, 7.8, 1.3 Hz, 1H), 7.41 − 7.32 (m, 2H), 7.28 (app. t, J = 7.5 Hz, 1H), 7.22 (d, J = 7.1 Hz, 1H), 7.15 (d, J = 7.6 Hz, 1H), 4.37 (t, J = 7.3 Hz, 1H), 3.42 (s, 2H), 3.04 − 2.94 (m, 1H), 2.94 − 2.79 (m, 1H), 2.52 − 2.36 (m, 1H), 1.76 − 1.63 (m, 1H). Exchangeable protons not observed. ^{13}C NMR (101 MHz, CD$_3$OD): δ 173.6, 148.3, 143.0, 142.0, 139.4, 130.3, 129.8, 128.7, 128.2, 125.3, 123.7, 121.2, 119.6, 57.9, 45.7, 36.8, 31.0. $υ_{max}$ (neat): 3347, 2919, 2852, 1675, 1584, 1558, 1539 cm^{-1}. HRMS: exact mass calculated for [M+Na]$^+$ (C$_{17}$H$_{19}$N$_3$NaO) m/z requires 304.1420, m/z found 304.1415.

Synthesis of 2-amino-N-(2'-(hydroxymethyl)-[1,1'-biphenyl]-3-yl)acetamide (2.55). Prepared according to General Procedure H using *tert*-butyl (2-((2'-formyl-[1,1'-biphenyl]-3-yl)amino)-2-oxoethyl)carbamate (**2.99**) (60 mg, 0.169 mmol, 1 equiv.) and NaBH$_4$ (19 mg, 0.508 mmol, 3 equiv.) in 2 mL MeOH (0.1 M).Following aqueous work-up, the residue was used according to General Procedure D in 0.5 mL TFA and 0.5 mL DCM. Once the Boc deprotection was complete by TLC, the reaction mixture was concentrated under reduced pressure and purified by silica chromatography, eluting with 10% MeOH/DCM, to afford the title compound as a cream solid (30 mg, 69% over 2 steps). ^{1}H NMR (500 MHz, CD$_3$OD): δ 7.62 − 7.55 (m, 3H), 7.40 − 7.35 (m, 2H), 7.32 (app. td, J = 7.5, 1.3 Hz, 1H), 7.24 (dd, J = 7.5, 1.2 Hz, 1H), 7.10 (d, J = 7.6 Hz, 1H), 4.53 (s, 2H), 3.43 (s, 2H). Exchangeable protons not observed. ^{13}C NMR (101 MHz, CD$_3$OD): δ 173.5, 143.0, 142.2, 139.6,

139.4, 130.7, 129.7, 129.4, 128.7, 128.3, 126.1, 121.9, 119.8, 62.8, 45.6. υ_{max} (neat): 3276, 2922, 2854, 1670, 1653, 1603, 1590, 1539 cm^{-1}. HRMS: exact mass calculated for [M+Na]$^+$ (C$_{15}$H$_{16}$NNaO$_2$) *m/z* requires 279.1104, *m/z* found 279.1103.

Synthesis of 2-amino-*N*-(2'-((methylamino)methyl)-[1,1'-biphenyl]-3-yl)acetamide bis(2,2,2-trifluoroacetate) (2.56). Prepared according to General Procedure J using *tert*-butyl (2-((2'-formyl-[1,1'-biphenyl]-3-yl)amino)-2-oxoethyl)carbamate (**2.99**) (300 mg, 0.847 mmol, 1 equiv.), 33 wt. % methylamine (95 mg, 1.017 mmol, 1.2 equiv.), MgSO$_4$ (305 mg, 2.541 mmol, 3 equiv.), and NaCNBH$_3$ (103 mg, 1.694 mmol, 2 equiv.) in 4 mL DCM (0.2 M). Following aqueous work-up, the residue was used according to General procedure D using 1 mL TFA and 1 mL DCM. Once the Boc deprotection was complete by TLC, the reaction mixture was concentrated under reduced pressure and purified by reverse-phase HPLC to afford the title compound as a colourless gum (89 mg, 21% over 2 steps). ^{1}H NMR (500 MHz, CD$_3$OD): δ 7.69 (s, *J* = 1.7 Hz, 1H), 7.62 – 7.59 (m, 1H), 7.56 – 7.44 (m, 4H), 7.41 – 7.36 (m, 1H), 7.13 (d, *J* = 7.6 Hz, 1H), 4.22 (s, 2H), 3.90 (s, 2H), 2.59 (s, 3H). Exchangeable protons not observed. ^{13}C NMR (101 MHz, CD$_3$OD): δ 166.0, 144.0, 141.8, 139.4, 131.8, 130.6, 130.1, 129.7, 126.5, 122.2, 120.5, 50.7, 42.2, 33.4. Two carbons not observed/coincident. υ_{max} (neat): 2991, 1779, 1668, 1617, 1565 cm^{-1}. HRMS: exact mass calculated for [M+H]$^+$ (C$_{16}$H$_{20}$N$_3$O) *m/z* requires 270.1601, *m/z* found 270.1594.

Synthesis of 2-amino-*N*-(2'-(((cyclohexylmethyl)amino)methyl)-[1,1'-biphenyl]-3-yl)acetamide (2.57). Prepared according to General Procedure D using *tert*-butyl (2-((2'-(((cyclohexylmethyl)amino)methyl)-[1,1'-biphenyl]-3-yl)amino)-2-

oxoethyl)carbamate (**2.116**) (84 mg, 0.186 mmol, 1 equiv.) in 0.5 mL TFA and 0.5 mL DCM. Purified by silica chromatography, eluting with 0-10% MeOH/DCM, to afford the title compound as a yellow oil (30 mg, 46%). ^{1}H NMR (400 MHz, CD$_3$OD): δ 7.71 (s, 1H), 7.57 – 7.50 (m, 2H), 7.47 – 7.36 (m, 3H), 7.33 – 7.27 (m, 1H), 7.10 (d, J = 7.6 Hz, 1H), 3.97 (s, 2H), 3.53 (s, 2H), 2.42 (d, J = 6.9 Hz, 2H), 1.76 – 1.58 (m, 3H), 1.58 – 1.48 (m, 2H), 1.49 – 1.31 (m, J = 14.8, 7.5, 3.6 Hz, 1H), 1.23 – 1.02 (m, 3H), 0.88 – 0.72 (m, 2H). Exchangeable protons not observed. ^{13}C NMR (101 MHz, CD$_3$OD): δ 172.0, 143.5, 142.5, 139.8, 134.4, 131.4, 130.9, 130.3, 129.4, 129.2, 126.0, 121.9, 120.0, 55.6, 50.8, 44.9, 37.0, 31.8, 27.3, 26.8. υ$_{max}$ (neat): 3276, 3058, 2924, 2852, 1670, 1591, 1558 cm^{-1}. HRMS: exact mass calculated for [M+H]$^+$ (C$_{22}$H$_{30}$N$_3$O) *m/z* requires 352.2383, *m/z* found 352.2370.

Synthesis of 2-amino-*N*-(2'-((benzylamino)methyl)-[1,1'-biphenyl]-3-yl)acetamide (2.58). Prepared according to General Procedure D using *tert*-butyl (2-((2'-((benzylamino)methyl)-[1,1'-biphenyl]-3-yl)amino)-2-oxoethyl)carbamate (**2.117**) (86 mg, 0.193 mmol, 1 equiv.) in 0.5 mL TFA and 0.5 mL DCM. Purified by silica chromatography, eluting with 0-10% MeOH/DCM, to afford the title compound as a yellow oil (23 mg, 35%). ^{1}H NMR (400 MHz, CD$_3$OD): δ 7.63 – 7.54 (m, 2H), 7.48 (dd, J = 7.4, 1.3 Hz, 1H), 7.39 – 7.28 (m, 3H), 7.27 – 7.15 (m, 4H), 7.12 – 7.08 (m, 2H), 7.03 (d, J = 7.6 Hz, 1H), 3.72 (s, 2H), 3.56 (s, 2H), 3.43 (s, 2H). Exchangeable protons not observed. ^{13}C NMR (101 MHz, CD$_3$OD): δ 173.5, 143.2, 143.1, 140.3, 139.7, 137.9, 131.0, 130.7, 130.0, 129.4, 128.8, 128.3, 128.1, 125.8, 121.6, 119.7, 53.8, 51.2, 45.6. One carbon not observed/coincident. υ$_{max}$ (neat): 3285, 3058, 3027, 2919, 2852, 1670, 1601, 1590, 1532 cm^{-1}. HRMS: exact

mass calculated for $[M+H]^+$ ($C_{22}H_{24}N_3O$) *m/z* requires 346.1914, *m/z* found 346.1910.

Synthesis of 2-amino-*N*-(2'-(((2-methoxyethyl)amino)methyl)-[1,1'-biphenyl]-3-yl)acetamide (2.59). Prepared according to General Procedure D using *tert*-butyl (2-((2'-(((2-methoxyethyl)amino)methyl)-[1,1'-biphenyl]-3-yl)amino)-2-oxoethyl)carbamate (**2.118**) (70 mg, 0.169 mmol, 1 equiv.) in 0.5 mL TFA and 0.5 mL DCM. Purified by silica chromatography eluting with 10% MeOH/DCM to afford the title compound as a colourless gum (32 mg, 60%). ^{1}H NMR (400 MHz, CDCl$_3$): δ 9.42 (br. s, 1H), 7.71 (ddd, *J* = 8.1, 2.1, 0.9 Hz, 1H), 7.53 (s, 1H), 7.46 (dd, *J* = 7.5, 1.1 Hz, 1H), 7.40 – 7.27 (m, 3H), 7.26 – 7.21 (m, 1H), 7.13 – 7.07 (m, 1H), 3.74 (s, 2H), 3.46 (s, 2H), 3.40 (d, *J* = 5.1 Hz, 2H), 3.28 (s, 3H), 2.67 (d, *J* = 5.3 Hz, 2H). Three exchangeable protons not observed. ^{13}C NMR (101 MHz, CDCl$_3$): δ 170.9, 142.1, 141.4, 137.6, 130.1, 129.2, 128.9, 127.7, 127.0, 125.0, 120.2, 118.3, 72.0, 58.8, 51.3, 48.7, 45.3. Once carbon not observed/coincident. υ_{max} (neat): 3280, 3058, 2919, 2854, 1670, 1610, 1590, 1532 cm^{-1}. HRMS: exact mass calculated for $[M+Na]^+$ ($C_{18}H_{23}N_3NaO_2$) *m/z* requires 336.1682, *m/z* found 336.1668.

Synthesis of 2-amino-*N*-(2'-(morpholinomethyl)-[1,1'-biphenyl]-3-yl)acetamide (2.60). Prepared according to General Procedure D using *tert*-butyl (2-((2'-(morpholinomethyl)-[1,1'-biphenyl]-3-yl)amino)-2-oxoethyl)carbamate (**2.119**) (38 mg, 0.089 mmol, 1 equiv.) in 0.5 mL TFA and 0.5 mL DCM. Purified by silica chromatography, eluting with 10-20% MeOH/DCM, to afford the title compound as a white solid (24 mg, 81%). ^{1}H NMR (400 MHz, CDCl$_3$): δ 9.43 (br s, 1H), 7.74 – 7.66 (m, 1H), 7.62 (app. t, *J* = 1.8 Hz, 1H), 7.52 – 7.46 (m, 1H), 7.36 (app. t, *J* = 7.9

Hz, 1H), 7.33 – 7.26 (m, 3H), 7.17 – 7.10 (m, 1H), 4.88 (br s, 1H), 3.69 – 3.59 (m, 4H), 3.49 (s, J = 1.5 Hz, 2H), 3.40 (s, 2H), 2.43 – 2.29 (m, 4H). One exchangeable proton not observed. ^{13}C NMR (101 MHz, CDCl$_3$): δ 170.8, 142.5, 142.4, 137.4, 135.4, 130.2, 130.2, 128.7, 127.3, 127.1, 125.5, 120.7, 118.1, 67.3, 60.4, 53.4, 45.3. υ_{max} (neat): 3375, 2956, 2932, 2855, 2813, 1668, 1584, 1558 cm^{-1}. HRMS: exact mass calculated for [M+H]$^+$ (C$_{19}$H$_{24}$N$_3$O$_2$) m/z requires 326.1863, m/z found 326.1849.

Synthesis of 2-amino-*N*-(2'-(((2-aminoethyl)amino)methyl)-[1,1'-biphenyl]-3-yl)acetamide tris(2,2,2-trifluoroacetate) (2.61). Prepared according to General Procedure J using *tert*-butyl (2-((2'-formyl-[1,1'-biphenyl]-3-yl)amino)-2-oxoethyl)carbamate (**2.99**) (300 mg, 0.847 mmol, 1 equiv.), ethane-1,2-diamine (68 μL, 1.017 mmol, 1.2 equiv.), MgSO$_4$ (305 mg, 2.541 mmol, 3 equiv.), and NaCNBH$_3$ (103 mg, 1.694 mmol, 2 equiv.) in 4 mL DCM (0.2 M). Following aqueous work-up, the residue was used according to General procedure D using 1 mL TFA and 1 mL DCM. Once the Boc deprotection was complete by TLC, the reaction mixture was concentrated under reduced pressure and purified by reverse-phase HPLC to afford the title compound as a colourless gum (85 mg, 16% over 2 steps). ^{1}H NMR (500 MHz, CD$_3$OD): δ 7.74 (s, 1H), 7.69 (m, 1H), 7.54 – 7.49 (m, 2H), 7.49 – 7.46 (m, 2H), 7.40 – 7.37 (m, 1H), 7.16 – 7.12 (m, 1H), 4.31 (s, 2H), 3.90 (s, 2H), 3.29 (s, 4H). Four exchangeable protons not observed. ^{13}C NMR (101 MHz, CD$_3$OD): δ 166.1, 144.0, 141.7, 139.2, 131.8, 130.9, 130.8, 130.7, 129.8, 129.7, 126.7, 122.4, 120.6, 45.5, 42.2, 36.7, 29.0. υ_{max} (neat): 3406, 3019, 1668, 1565, 1504 cm^{-1}. HRMS: exact mass calculated for [M+H]$^+$ (C$_{17}$H$_{23}$N$_4$O) m/z requires 299.1866, m/z found 299.1857.

Synthesis of 2-amino-*N*-(2'-(piperazin-1-ylmethyl)-[1,1'-biphenyl]-3-yl)acetamide bis(2,2,2-trifluoroacetate) (2.62). Prepared according to General Procedure J using *tert*-butyl (2-((2'-formyl-[1,1'-biphenyl]-3-yl)amino)-2-oxoethyl)carbamate (**2.99**) (300 mg, 0.847 mmol, 1 equiv.), *tert*-butyl piperazine-1-carboxylate (189 mg, 1.017 mmol, 1.2 equiv.), MgSO$_4$ (305 mg, 2.541 mmol, 3 equiv.), and NaCNBH$_3$ (103 mg, 1.694 mmol, 2 equiv.) in 4 mL DCM (0.2 M). Following aqueous work-up, the residue was used according to General procedure D using 1 mL TFA and 1 mL DCM. Once the Boc deprotection was complete by TLC, the reaction mixture was concentrated under reduced pressure and purified by reverse-phase HPLC to afford the title compound as a colourless gum (10 mg, 2% over 2 steps). ^{1}H NMR (500 MHz, CD$_3$OD): δ 7.67 (s, 1H), 7.60 − 7.55 (m, 1H), 7.50 (d, *J* = 8.2 Hz, 1H), 7.46 − 7.39 (m, 3H), 7.33 − 7.27 (m, 1H), 7.14 (d, *J* = 7.5 Hz, 1H), 3.93 − 3.81 (m, *J* = 5.4 Hz, 4H), 3.23 (br. s, 4H), 2.81 (br. s, 4H). Exchangeable protons not observed. ^{13}C NMR (101 MHz, CO(CH$_3$)$_2$): δ 163.6, 144.1, 142.8, 139.0, 131.5, 131.0, 129.5, 129.0, 128.7, 128.4, 125.7, 122.2, 119.2, 60.0, 50.9, 49.7, 43.8. υ_{max} (neat): 3397, 3313, 3017, 1670, 1567 cm^{-1}. HRMS: exact mass calculated for [M+H]$^+$ (C$_{19}$H$_{25}$N$_4$O) *m/z* requires 325.2023, *m/z* found 325.2012.

Synthesis of *tert*-butyl (2-oxo-2-((3-(4,4,5,5-tetramethyl-1,3,2-dioxaborolan-2-yl)phenyl) amino)ethyl)carbamate (2.63). Prepared according to General Procedure A using Boc-glycine (6.16 g, 35.1 mmol, 1.1 equiv.), DIPEA (11.16 mL, 63.9 mmol, 2 equiv.), and HATU (14.58 g, 38.3 mmol, 1.2 equiv.) in 50 mL DMF was stirred at room temperature for 10 min before the addition of 3-(4,4,5,5-tetramethyl-1,3,2-dioxaborolan-2-yl)aniline (**2.64**) (7.00 g, 32.0 mmol, 1 equiv.) as a solution in 10 mL

DMF to give a final DMF volume of 60 mL (0.5 M). Purified using silica chromatography, eluting with 0-80% MTBE/cyclohexane, to afford the title compound as a cream solid (8.00 g, 61%). ^{1}H NMR (400 MHz, CDCl$_3$): δ 8.28 (br. s, 1H), 7.84 (d, J = 8.0 Hz, 1H), 7.68 (s, 1H), 7.54 (d, J = 7.3 Hz, 1H), 7.33 (app. t, J = 7.7 Hz, 1H), 5.40 (s, 1H), 3.94 (d, J = 5.2 Hz, 2H), 1.46 (s, 9H), 1.32 (s, 12H). ^{13}C NMR (101 MHz, CDCl$_3$): δ 167.9, 156.4, 137.1, 131.0, 128.7, 126.1, 123.3, 84.1, 80.7, 45.4, 28.4, 25.0. One carbon not observed/coincident. ^{11}B NMR (128 MHz, CDCl$_3$): δ 31.33. υ_{max} (neat): 3419, 3337, 2978, 2924, 1706, 1679, 1613, 1558 cm^{-1}. HRMS: exact mass calculated for [M+H]$^+$ (C$_{19}$H$_{29}$BN$_2$O$_5$) m/z requires 399.2062, m/z found 399.2059.

Synthesis of 3-(4,4,5,5-tetramethyl-1,3,2-dioxaborolan-2-yl)aniline (2.64). A solution of 4,4,5,5-tetramethyl-2-(3-nitrophenyl)-1,3,2-dioxaborolane (**2.65**) (1 g, 4.010 mmol, 1 equiv.) and 10 wt. % Pd-C (427 mg, 0.401 mmol, 10 mol%) in 20 mL EtOH (0.2 M) was stirred under an atmosphere of hydrogen (excess) for 16 h. The resulting solution was then filtered through celite, eluting with DCM for 3 column volumes. The filtrate was collected and concentrated under reduced pressure to a colourless oil. Purified using silica chromatography, eluting with 0-50% MTBE/cyclohexane, to afford the title compound as a white solid (581 mg, 66%). ^{1}H NMR (400 MHz, CDCl$_3$): δ 7.37 – 7.31 (m, 1H), 7.31 – 7.24 (m, 2H), 6.92 (ddd, J = 7.9, 2.5, 1.2 Hz, 1H), 1.43 (s, 12H). NH$_2$ protons not observed. ^{13}C NMR (101 MHz, CDCl$_3$): δ 145.2, 128.9, 125.6, 121.6, 118.5, 83.9, 25.0. One carbon not observed/coincident. ^{11}B NMR (128 MHz, CDCl$_3$): δ 30.91. υ_{max} (neat): 3460, 3370, 2980, 1628, 1600, 1578 cm^{-1}. HRMS: exact mass calculated for [M+H]$^+$ (C$_{12}$H$_{19}$BNO$_2$) m/z requires 220.1503, m/z found 220.1501.

Synthesis of *tert*-butyl (6-bromoimidazo[1,2-α]pyridin-8-yl)carbamate (2.69).

Prepared according to General Procedure B using 6-bromoimidazo[1,2-α]pyridin-8-amine (**2.110**) (200 mg, 0.943 mmol, 1 equiv.), Boc$_2$O (241 μL, 1.038 mmol, 1.1 equiv.), DMAP (23 mg, 0.189 mmol, 20 mol%), and Et$_3$N (171 μL, 1.226 mmol, 1.3 equiv.) in 10 mL DCM (0.1 M). Purified by silica chromatography, eluting with 0-50% EtOAc/cyclohexane, to afford the title compound as a colourless oil (142 mg, 48%). ^{1}H NMR (400 MHz, CDCl$_3$): δ 7.92 – 7.87 (m, 3H), 7.48 (dd, J = 4.2, 1.2 Hz, 2H), 1.52 (s, 9H). ^{13}C NMR (101 MHz, CDCl$_3$): δ 152.4, 137.8, 132.5, 128.3, 119.2, 113.8, 111.5, 108.2, 81.7, 28.3. υ$_{max}$ (neat): 3181, 3118, 3043, 2980, 2930, 2772, 1725, 1627, 1537 cm^{-1}. HRMS: exact mass calculated for [M+H]$^+$ (C$_{12}$H$_{15}$BrN$_3$O$_2$) *m/z* requires 314.0322, *m/z* found 314.0324.

Synthesis of *tert*-butyl 4-(3-(2-((*tert*-butoxycarbonyl)amino)acetamido)phenyl) piperazine-1-carboxylate (2.71). A solution of *tert*-butyl piperazine-1-carboxylate (**2.70**) (99 mg, 0.532 mmol, 2 equiv.), *tert*-butyl (2-oxo-2-((3-(4,4,5,5-tetramethyl-1,3,2-dioxaborolan-2-yl)phenyl)amino)ethyl)carbamate (**2.63**) (100 mg, 0.266 mmol, 1 equiv.), copper (II) acetate (48 mg, 0.266 mmol, 1 equiv.), and KOAc (52.2 mg, 0.532 mmol, 2 equiv.) in 1 mL MeCN (0.3 M) was heated at 60 °C for 16 h. The reaction mixture was allowed to return to room temperature, diluted with 50 mL EtOAc and washed with sat. aq. NaHCO$_3$ (2 x 50 mL). The organic layer was collected, dried using a hydrophobic frit, and then concentrated under reduced pressure. Purified by reverse phase column chromatography, eluting with 40-95% HpH method, to afford the title compound as a grey solid (52 mg, 45%). ^{1}H NMR (400 MHz, CDCl$_3$): δ 8.29 (s, 1H), 7.29 (s, 1H), 7.17 (app. t, J = 8.1 Hz, 1H), 6.86 (d, J = 7.5 Hz, 1H), 6.65 (dd, J = 8.2, 1.7 Hz, 1H), 5.44 (br. s, 1H), 3.90 (d, J = 5.8

Hz, 2H), 3.62 – 3.49 (m, 4H), 3.17 – 3.05 (m, 4H), 1.47 (s, 9H), 1.46 (s, 9H). ^{13}C NMR (101 MHz, CDCl$_3$): δ 168.0, 156.6, 154.8, 152.0, 138.6, 129.6, 112.6, 111.7, 108.3, 80.8, 80.0, 49.3, 45.7, 43.6, 28.6, 28.4. υ$_{max}$ (neat): 3415, 3298, 3002, 2974, 2930, 2861, 1682, 1621, 1589, 1558 cm^{-1}. HRMS: exact mass calculated for [M+H]$^+$ (C$_{22}$H$_{35}$N$_4$O$_5$) *m/z* requires 435.2602, *m/z* found 435.2602.

Synthesis of *tert*-butyl (2-((3-(1,8-naphthyridin-2-yl)phenyl)amino)-2-oxoethyl) carbamate (2.73). Prepared according to General Procedure C using 2-bromo-1,8-naphthyridine (**2.72**) (93 mg, 0.443 mmol, 1 equiv.), *tert*-butyl (2-oxo-2-((3-(4,4,5,5-tetramethyl-1,3,2-dioxaborolan-2-yl)phenyl)amino)ethyl) carbamate (**2.63**) (200 mg, 0.532 mmol, 1.2 equiv.), 2′-(dimethylamino)-2-biphenylyl-palladium(II) chloride dinorbornylphosphine complex (12 mg, 0.022 mmol, 5 mol%), and K$_3$PO$_4$ (376 mg, 1.772 mmol, 4 equiv.) in 2.5 mL 1,4-dioxane:H$_2$O (4:1, 0.2 M). Purified using reverse-phase chromatography, eluting with 20-70% HpH method, to afford the title compound as a cream solid (134 mg, 78%). ^{1}H NMR (400 MHz, CDCl$_3$): δ 9.14 (dd, *J* = 4.2, 2.0 Hz, 1H), 8.47 (br. s, 1H), 8.38 (t, *J* = 1.8 Hz, 1H), 8.26 (d, *J* = 8.5 Hz, 1H), 8.21 (dd, *J* = 8.1, 2.0 Hz, 1H), 8.04 – 7.95 (m, 2H), 7.90 (d, *J* = 7.8 Hz, 1H), 7.53 – 7.42 (m, 2H), 5.56 (t, *J* = 5.8 Hz, 1H), 4.04 (d, *J* = 6.1 Hz, 2H), 1.50 (s, 9H). ^{13}C NMR (101 MHz, CDCl$_3$): δ 168.5, 159.8, 156.1, 154.0, 139.2, 138.5, 138.0, 137.0, 129.7, 123.8, 122.1, 122.0, 119.9, 119.4, 80.8, 45.6, 28.5. Two carbons not observed/coincident. υ$_{max}$ (neat): 3198, 360, 3012, 2969, 2924, 1711, 1670, 1604, 1539, 1506 cm^{-1}. HRMS: exact mass calculated for [M+H]$^+$ (C$_{21}$H$_{23}$N$_4$O$_3$) *m/z* requires 379.1765, *m/z* found 379.1763.

Synthesis of *tert*-butyl (2-((5'-cyano-2'-methyl-[1,1'-biphenyl]-3-yl)amino)-2-oxoethyl) carbamate (2.75). Prepared according to General Procedure C using 3-

bromo-4-methylbenzonitrile (**2.74**) (100 mg, 0.510 mmol, 1 equiv.), *tert*-butyl (2-oxo-2-((3-(4,4,5,5-tetramethyl-1,3,2-dioxaborolan-2-yl)phenyl)amino)ethyl) carbamate (**2.63**) (230 mg, 0.612 mmol, 1.2 equiv.), 2′-(dimethylamino)-2-biphenylyl-palladium(II) chloride dinorbornylphosphine complex (14 mg, 0.026 mmol, 5 mol%), and K_3PO_4 (433 mg, 2.040 mmol, 4 equiv.) in 2.5 mL 1,4-dioxane:H_2O (4:1, 0.2 M). Purified by reverse-phase column chromatography, eluting with 40-90% HpH method, to afford the title compound as a colourless oil (108 mg, 58%). ^1H NMR (400 MHz, CDCl$_3$): δ 8.58 (br. s, 1H), 7.57 − 7.41 (m, 4H), 7.35 (app. t, J = 8.2 Hz, 2H), 6.99 (d, J = 7.6 Hz, 1H), 5.47 (t, J = 5.7 Hz, 1H), 3.96 (d, J = 5.8 Hz, 2H), 2.30 (s, 3H), 1.45 (s, 9H). ^{13}C NMR (101 MHz, CDCl$_3$): δ 168.2, 156.7, 142.7, 141.6, 140.5, 137.9, 133.2, 131.3, 130.9, 129.2, 125.0, 120.6, 119.3, 119.0, 109.8, 80.9, 45.7, 28.4, 20.9. υ_{max} (neat): 3343, 3309, 2978, 2930, 2227, 1690, 1682, 1613, 1591, 1539, 1517, 1506 cm^{-1}. HRMS: exact mass calculated for [M+H]$^+$ (C$_{21}$H$_{24}$N$_3$O$_3$) *m/z* requires 366.1812, *m/z* found 366.1812.

Synthesis of *tert*-butyl (2-((3'-formyl-[1,1'-biphenyl]-3-yl)amino)-2-oxoethyl)carbamate (2.77). Prepared according to General Procedure C using 3-bromobenzaldehyde (**2.76**) (82 mg, 0.443 mmol, 1 equiv.), *tert*-butyl (2-oxo-2-((3-(4,4,5,5-tetramethyl-1,3,2-dioxaborolan-2-yl)phenyl)amino)ethyl)carbamate (**2.63**) (200 mg, 0.532 mmol, 1.2 equiv.), 2′-(dimethylamino)-2-biphenylyl-palladium(II) chloride dinorbornylphosphine complex (12 mg, 0.022 mmol, 5 mol%), and K_3PO_4 (376 mg, 1.772 mmol, 4 equiv.) in 2.5 mL 1,4-dioxane:H_2O (4:1, 0.2 M). Purified by silica chromatography, eluting with 10-40% EtOAc/petroleum ether, to afford the title compound as a brown oil (125 mg, 80%). ^1H NMR (400 MHz, CDCl$_3$): δ 10.08 (s, 1H), 8.30 (br. s, 1H), 8.08 (s, 1H), 7.92 − 7.80 (m, 3H), 7.60 (app. t, J = 7.7 Hz,

1H), 7.50 (d, J = 8.1 Hz, 1H), 7.45 – 7.35 (m, 2H), 5.27 (br. s, 1H), 3.96 (d, J = 6.0 Hz, 2H), 1.24 (s, 9H). ^{13}C NMR (101 MHz, CDCl$_3$): δ 192.4, 168.1, 141.8, 140.8, 138.3, 137.1, 133.3, 129.8, 129.7, 128.9, 128.5, 123.4, 119.6, 118.8, 45.9, 28.4. Two carbons not observed/coincident. υ_{max} (neat): 3310, 2978, 2934, 1683, 1599, 1539, 1521 cm^{-1}. HRMS: exact mass calculated for [M+Na]$^+$ (C$_{20}$H$_{22}$N$_2$NaO$_4$) m/z requires 377.1472, m/z found 377.1457.

tert-Butyl (2-((3'-((((tert-butylsulfinyl)amino)methyl)-[1,1'-biphenyl]-3-yl)amino)-2-oxoethyl) carbamate (2.78). Prepared according to General Procedure G using *tert*-butyl (2-((3'-formyl-[1,1'-biphenyl]-3-yl)amino)-2-oxoethyl)carbamate (**2.77**) (228 mg, 0.644 mmol, 1.5 equiv.), *tert*-butanesulfinamide (52 mg, 0.429 mmol, 1 equiv.), MgSO$_4$ (515 mg, 4.290 mmol, 10 equiv.), and PPTS (5 mg, 0.002 mmol, 0.5 mol%). The residue was washed through a plug of silica, eluting with 50% EtOAc/petroleum ether, to afford the desired imine which was used without further purification. The residue was used according to General Procedure H using NaBH$_4$ (49 mg, 1.287 mmol, 3 equiv.) in 5 mL MeOH (0.1 M). Purified by silica chromatography, eluting with 50-100% EtOAc/petroleum ether, to afford the title compound as a cream solid (171 mg, 87% over 2 steps). ^{1}H NMR (400 MHz, CDCl$_3$): δ 8.69 (br. s, 1H), 7.72 (s, 1H), 7.59 – 7.47 (m, 2H), 7.47 – 7.42 (m, 1H), 7.39 – 7.26 (m, 4H), 5.54 (s, 1H), 4.37 (dd, J = 13.8, 4.9 Hz, 1H), 4.27 (dd, J = 13.8, 7.4 Hz, 1H), 3.96 (d, J = 5.8 Hz, 2H), 3.78 (s, 1H), 1.44 (s, 9H), 1.25 (s, 9H). ^{13}C NMR (101 MHz, CDCl$_3$): δ 168.3, 141.7, 141.2, 139.1, 138.3, 129.5, 129.2, 127.4, 127.2, 126.6, 123.2, 119.1, 118.8, 80.7, 56.2, 49.7, 45.6, 28.4, 22.9. One carbon not observed/coincident. υ_{max} (neat): 3281, 2976, 2928, 2867, 1683, 1610, 1558, 1539,

1517 cm^{-1}. HRMS: exact mass calculated for [M+Na]$^+$ (C$_{24}$H$_{33}$N$_3$NaO$_4$S) *m/z* requires 482.2084, *m/z* found 482.2080.

Synthesis of 2-(3-bromophenethyl)isoindoline-1,3-dione (2.80). A Round bottomed flask containing 2-(3-bromophenyl)ethan-1-ol (**2.79**) (2.5 g, 12.438 mmol, 1 equiv.), PPh$_3$ (3.9 g, 14.925 mmol, 1.2 equiv.), and phthalimide (2.0 g, 13.682 mmol, 1.1 equiv.) in 60 mL THF (0.2 M) was cooled to 0 °C followed by the addition of DIAD (2.9 mL, 14.925 mmol, 1.2 equiv.). The reaction mixture was then allowed to return to room temperature and stirred for 16 h. The resulting solution was then diluted with 50 mL EtOAc and washed with sat. aq. NaCl (2 x 50 mL). The organic layer was collected, dried using a hydrophobic frit, and concentrated under reduced pressure. Purified by silica chromatography, eluting with 0-10% EtOAc/petroleum ether, followed by trituration from Et$_2$O to afford the title compound as a white solid (1.26 g, 31%). ^{1}H NMR (400 MHz, CDCl$_3$): δ 7.87 − 7.80 (m, 2H), 7.75 − 7.68 (m, 2H), 7.41 (s, 1H), 7.35 (dt, *J* = 7.5, 1.7 Hz, 1H), 7.22 − 7.12 (m, 2H), 3.96 − 3.86 (m, 2H), 3.02 − 2.88 (m, *J* = 8.6, 6.9 Hz, 2H). ^{13}C NMR (101 MHz, CDCl$_3$): δ 168.2, 140.4, 134.2, 132.2, 132.1, 130.3, 130.0, 127.6, 123.4, 122.7, 39.1, 34.4. υ_{max} (neat): 3462, 3055, 2988, 2949, 1768, 1705, 1619, 1597, 1569 cm^{-1}. HRMS: exact mass calculated for [M+Na]$^+$ (C$_{16}$H$_{12}$NNaO$_2$Br) *m/z* requires 351.9944, *m/z* found 351.9955.

Synthesis of 3-bromo-2,4-dimethylbenzaldehyde (2.83). A round bottomed flask containing TiCl$_4$ (1.20 mL, 10.811 mmol, 2 equiv.) and dichloromethyl methyl ether (0.54 mL, 5.946 mmol, 1.1 equiv.) in 10 mL DCM was cooled to -78 °C before the dropwise addition of 2-bromo-1,3-dimethylbenzene (**2.82**) (0.72 mL, 5.405 mmol, 1 equiv.). The red reaction mixture was allowed to warm to room temperature and the

resulting black solution was then stirred for a further 4 h at room temperature. The reaction mixture was then poured into 50 mL ice water and extracted with DCM (2 x 20 mL). The organic layers were combined, dried using a hydrophobic frit, and concentrated under reduced pressure. The residue was then purified by silica chromatography, eluting with 0-10% EtOAc/petroleum ether, to afford the title compound as a white solid (840 mg, 73%). ^{1}H NMR (500 MHz, CDCl$_3$): δ 10.22 (s, 1H), 7.67 (d, J = 7.8 Hz, 1H), 7.26 (d, J = 7.8 Hz, 1H), 2.78 (s, 3H), 2.50 (s, 3H). ^{13}C NMR (101 MHz, CDCl$_3$): δ 191.8, 145.1, 140.7, 133.8, 130.5, 130.3, 128.5, 25.1, 18.8. υ_{max} (neat): 3328, 2922, 2980, 2628, 1679, 1640, 1591, 1554 cm^{-1}. HRMS: *Unable to obtain exact mass due to instability of compound.*

Synthesis of *tert*-butyl (2-((3'-((((*tert*-butylsulfinyl)amino)methyl)-2',6'-dimethyl-[1,1'-biphenyl]-3-yl)amino)-2-oxoethyl)carbamate (2.85). Prepared according to General Procedure C using 3-bromo-2,4-dimethylbenzaldehyde (**2.83**) (142 mg, 0.665 mmol, 1 equiv.), *tert*-butyl (2-oxo-2-((3-(4,4,5,5-tetramethyl-1,3,2-dioxaborolan-2-yl)phenyl)amino)ethyl)carbamate (**2.63**) (300 mg, 0.798 mmol, 1.2 equiv.), 2′-(dimethylamino)-2-biphenylyl-palladium(II) chloride dinorbornylphosphine complex (18 mg, 0.033 mmol, 5 mol%), and K$_3$PO$_4$ (563 mg, 2.660 mmol, 4 equiv.) in 4.25 mL 1,4-dioxane:H$_2$O (4:1, 0.2 M). Purified by silica chromatography, eluting with 10-50% EtOAc/petroleum ether, to afford *tert*-butyl (2-((3'-formyl-2',6'-dimethyl-[1,1'-biphenyl]-3-yl)amino)-2-oxoethyl)carbamate (**2.84**) (130 mg, 0.340 mmol), which was used in the next step without further purification. The residue was used according to General Procedure G using *tert*-butanesulfinamide (27 mg, 0.227 mmol, 1 equiv.), MgSO$_4$ (408 mg, 3.400 mmol, 10 equiv.), and PPTS (3 mg, 0.011 mmol, 5 mol%) in 2 mL DCM (0.2 M). Once the

imine formation was complete by TLC, the reaction mixture was filtered and the filtrate concentrated under reduced pressure. The residue was then used according to General Procedure H using NaBH$_4$ (26 mg, 0.681 mmol, 3 equiv.) in 3 mL MeOH (0.1 M). Purified by silica chromatography, eluting with 50-100% EtOAc/petroleum ether, to afford the title compound as a yellow oil (104 mg, 32% over 3 steps). ^{1}H NMR (400 MHz, CDCl$_3$): δ 7.56 (dd, J = 13.4, 5.0 Hz, 1H), 7.34 − 7.25 (m, 2H), 7.19 − 7.12 (m, 1H), 7.02 (d, J = 7.8 Hz, 1H), 6.80 (app. t, J = 8.6 Hz, 1H), 5.71 (br. s, 1H), 4.34 − 4.26 (m, 1H), 4.21 − 4.10 (m, 1H), 4.00 (s, 2H), 3.92 (br. s, 2H), 1.95 (s, 6H), 1.20 (s, 9H), 1.18 (s, 9H). ^{13}C NMR (101 MHz, CDCl$_3$): δ 168.2, 156.5, 142.3, 141.9, 138.3, 136.0, 134.8, 133.7, 129.1, 128.2, 127.2, 124.9, 120.3, 118.2, 80.2, 56.0, 55.3, 48.1, 28.4, 22.8, 22.2, 21.0. υ_{max} (neat): 3235, 2960, 2926, 2868, 1688, 1614, 1590, 1558 cm^{-1}. HRMS: exact mass calculated for [M+Na]$^+$ (C$_{26}$H$_{37}$N$_3$NaO$_4$S) m/z requires 510.2397, m/z found 510.2379.

Synthesis of *tert*-butyl (2-((3-(6-formylpyridin-2-yl)phenyl)amino)-2-oxoethyl)carbamate (2.87). Prepared according to General Procedure I using 6-bromopicolinaldehyde (**2.86**) (88 mg, 0.472 mmol, 1 equiv.), *tert*-butyl (2-oxo-2-((3-(4,4,5,5-tetramethyl-1,3,2-dioxaborolan-2-yl)phenyl)amino) ethyl) carbamate (**2.63**) (266 mg, 0.707 mmol, 1.5 equiv.), Pd(dppf)Cl$_2$·DCM (15 mg, 0.019 mmol, 4 mol%), and K$_3$PO$_4$ (300 mg, 1.416 mmol, 3 equiv.) in 2 mL THF (0.2 M) and H$_2$O (43 µL, 2.360 mmol, 5 equiv.). Purified by silica chromatography, eluting with 20-80% EtOAc/petroleum ether, to afford the title compound as a colourless oil (163 mg, 97%). ^{1}H NMR (500 MHz, CDCl$_3$): δ 10.03 (s, 1H), 8.99 (br. s, 1H), 8.22 (s, 1H), 7.79 (br. s, 3H), 7.70 (d, J = 7.6 Hz, 1H), 7.60 (d, J = 7.3 Hz, 1H), 7.32 (app. t, J = 7.8 Hz, 1H), 5.83 (s, 1H), 4.01 (s, 2H), 1.43 (s, 9H). ^{13}C NMR (101 MHz, CDCl$_3$): δ

194.0, 168.3, 157.4, 152.8, 139.0, 138.4, 138.0, 129.8, 124.8, 123.1, 121.3, 120.2, 118.7, 81.0, 28.4, 25.0. One carbon not observed/coincident. υ_{max} (neat): 3312, 2978, 2934, 1707, 1675, 1612, 1590, 1550, 1539 cm^{-1}. HRMS: exact mass calculated for [M+Na]$^+$ (C$_{19}$H$_{21}$N$_3$NaO$_4$) m/z requires 378.1424, m/z found 378.1418.

Synthesis of *tert*-butyl (2-((3-(6-((((*tert*-butylsulfinyl)amino)methyl)pyridin-2-yl)phenyl)amino)-2-oxoethyl)carbamate (2.88). Prepared according to General Procedure G using *tert*-butyl (2-((3-(6-formylpyridin-2-yl)phenyl)amino)-2-oxoethyl)carbamate (**2.87**) (150 mg, 0.422 mmol, 1 equiv.), *tert*-butanesulfinamide (77 mg, 0.634 mmol, 1.5 equiv.), MgSO$_4$ (506 mg, 4.220 mmol, 10 equiv.), and PPTS (6 mg, 0.021 mmol, 5 mol%). Once the imine formation was complete by TLC, the reaction mixture was filtered, and the filtrate concentrated under reduced pressure. The residue was washed through a plug of silica, eluting with 50% EtOAc/petroleum ether, to afford *tert*-butyl (*E*)-(2-((3-(6-((((*tert*-butylsulfinyl)imino)methyl)pyridin-2-yl)phenyl)amino)-2-oxoethyl)carbamate which was used without further purification. The residue was used according to General Procedure H using *tert*-butyl (*E*)-(2-((3-(6-((((*tert*-butylsulfinyl)imino)methyl)pyridin-2-yl)phenyl)amino)-2-oxoethyl)carbamate (193 mg, 0.422 mmol, 1 equiv.) and NaBH$_4$ (48 mg, 1.266 mmol, 3 equiv.) in 2 mL MeOH (0.2 M). Purified by silica chromatography, eluting with 50-100% EtOAc/petroleum ether, to afford the title compound as a colourless oil (114 mg, 59% over 2 steps). ^{1}H NMR (400 MHz, CDCl$_3$): δ 8.87 (br. s, 1H), 8.04 (s, 1H), 7.74 – 7.58 (m, 3H), 7.54 (d, J = 7.7 Hz, 1H), 7.33 (app. t, J = 7.9 Hz, 1H), 7.22 (d, J = 7.5 Hz, 1H), 5.60 (s, 1H), 4.74 (t, J = 5.8 Hz, 1H), 4.53 – 4.36 (m, 2H), 3.95 (d, J = 4.1 Hz, 2H), 1.45 (s, 9H), 1.28 (s, 9H). ^{13}C NMR (101 MHz, CDCl$_3$): δ 168.2, 157.4,

156.2, 139.7, 138.4, 137.6, 129.4, 122.7, 120.8, 120.7, 119.3, 118.5, 80.5, 56.4, 49.9, 45.3, 28.5, 22.9. One carbon not observed/coincident. υ_{max} (neat): 3403, 3256, 2970, 2930, 1683, 1614, 1588, 1575, 1558 cm^{-1}. HRMS: exact mass calculated for [M+H]$^+$ (C$_{23}$H$_{32}$N$_4$NaO$_4$S) *m/z* requires 483.2036, *m/z* found 483.2020.

Synthesis of 3-bromo-4-methylbenzaldehyde (2.91). A solution of 4-methylbenzaldehyde (**2.90**) (4.9 g, 41.7 mmol, 1 equiv.) in 40 mL DCM (1 M) was cooled to 0 °C, followed by the slow addition of AlCl$_3$ (6.6 g, 50.0 mmol, 1.2 equiv.). The resulting solution was heated to 40 °C for 30 min, then allowed to return to room temperature before cooling to 0 °C followed by the slow addition of Br$_2$ (2.6 mL, 50.0 mmol, 1.2 equiv.). The reaction mixture was allowed to return to room temperature, stirred for 16 h, then quenched with 80 mL ice water. The reaction mixture was then basified using sat. aq. NaHCO$_3$ and extracted with DCM (2 x 50 mL). Purified by silica chromatography, eluting with 0-10% EtOAc/petroleum ether, to afford the title compound as a cream solid (3.9 g, 47%). ^{1}H NMR (400 MHz, CDCl$_3$): δ 9.90 (s, 1H), 8.02 (s, 1H), 7.70 (dd, *J* = 7.7, 1.5 Hz, 1H), 7.39 (d, *J* = 7.8 Hz, 1H), 2.47 (s, 3H). ^{13}C NMR (101 MHz, CDCl$_3$): δ 190.6, 145.3, 136.0, 133.6, 131.5, 128.5, 125.8, 23.6. υ_{max} (neat): 3084, 3064, 2978, 2956, 2922, 2848, 2654, 2584, 1675, 1603, 1563 cm^{-1}. HRMS: *Unable to obtain exact mass due to instability of compound.*

Synthesis of *tert*-butyl (2-((5'-formyl-2'-methyl-[1,1'-biphenyl]-3-yl)amino)-2-oxoethyl)carbamate (2.92). Prepared according to General Procedure I using 3-bromo-4-methylbenzaldehyde (**2.91**) (745.0 mg, 3.747 mmol, 1 equiv.), *tert*-butyl (2-oxo-2-((3-(4,4,5,5-tetramethyl-1,3,2-dioxaborolan-2-yl)phenyl)amino) ethyl) carbamate (**2.63**) (2.1 g, 5.620 mmol, 1.5 equiv.), Pd(dppf)Cl$_2$·DCM (122 mg, 0.150

mmol, 4 mol%), and K_3PO_4 (2.4 g, 11.241 mmol, 3 equiv.) in 20 mL THF (0.2 M) and H_2O (337 μL, 18.735 mmol, 5 equiv.). Purified by silica chromatography, eluting with 0-50% EtOAc/petroleum ether, to afford the title compound as a yellow oil (1.3 g, 94%). ^{1}H NMR (400 MHz, CDCl$_3$): δ 9.99 (s, 1H), 8.29 (br. s, 1H), 7.77 (dd, J = 7.8, 1.8 Hz, 1H), 7.71 (d, J = 1.7 Hz, 1H), 7.54 (s, 1H), 7.50 (d, J = 8.2 Hz, 1H), 7.44 – 7.33 (m, 2H), 7.07 (d, J = 7.6 Hz, 1H), 5.27 (s, 1H), 3.95 (d, J = 6.0 Hz, 2H), 2.35 (s, 3H), 1.47 (s, 9H). ^{13}C NMR (101 MHz, CDCl$_3$): δ 192.1, 168.0, 143.2, 142.3, 141.5, 137.7, 134.6, 131.4, 131.3, 129.2, 128.5, 125.3, 120.7, 119.0, 81.1, 45.9, 28.4, 21.1. One carbon not observed/coincident. υ_{max} (neat): 3405, 3312, 2978, 2932, 1683, 1606, 1591, 1550, 1539, 1517 cm^{-1}. HRMS: exact mass calculated for [M+Na]$^+$ (C$_{21}$H$_{24}$N$_2$NaO$_4$) m/z requires 391.1628, m/z found 391.1621.

Synthesis of *tert*-butyl (2-((5'-((allylamino)methyl)-2'-methyl-[1,1'-biphenyl]-3-yl)amino)-2-oxoethyl)carbamate (2.93). Prepared according to General Procedure J using *tert*-butyl (2-((5'-formyl-2'-methyl-[1,1'-biphenyl]-3-yl)amino)-2-oxoethyl)carbamate (**2.92**) (640 mg, 1.739 mmol, 1 equiv.), prop-2-en-1-amine (156 μL, 2.087 mmol, 1.2 equiv.), MgSO$_4$ (2 g, 17.390 mmol, 10 equiv.), and NaBH$_4$ (198 mg, 5.217 mmol, 3 equiv.) in 10 mL THF (0.2 M). Purified by silica chromatography, eluting with 40-100% EtOAc/petroleum ether, to afford the title compound as a cream solid (266 mg, 37%). ^{1}H NMR (400 MHz, CDCl$_3$): δ 8.65 (br. s, 1H), 7.52 (d, J = 8.0 Hz, 1H), 7.43 (s, 1H), 7.30 (app. t, J = 7.8 Hz, 1H), 7.24 – 7.17 (m, 2H), 7.15 (s, 1H), 7.04 (d, J = 7.6 Hz, 1H), 6.01 – 5.84 (m, 1H), 5.60 (t, J = 5.2 Hz, 1H), 5.25 – 5.08 (m, 2H), 3.93 (d, J = 5.6 Hz, 2H), 3.79 (s, 2H), 3.30 (d, J = 6.1 Hz, 2H), 2.45 (br. s, 1H), 2.22 (s, 3H), 1.44 (s, 9H). ^{13}C NMR (101 MHz, CDCl$_3$): δ 168.1, 156.7, 142.7, 141.5, 137.5, 136.9, 136.1, 134.4, 130.6, 129.8, 128.8,

127.5, 125.4, 120.9, 118.6, 116.9, 80.7, 52.7, 51.7, 45.5, 28.4, 20.2. υ_{max} (neat): 3405, 3297, 3073, 2978, 2926, 1675, 1612, 1591, 1554, 1539 cm^{-1}. HRMS: exact mass calculated for $[M+H]^+$ ($C_{24}H_{32}N_3O_3$) m/z requires 410.2438, m/z found 410.2427.

Synthesis of *tert*-butyl (2-((5'-(aminomethyl)-2'-methyl-[1,1'-biphenyl]-3-yl)amino)-2-oxoethyl)carbamate (2.94). A solution of *tert*-butyl (2-((5'-((allylamino)methyl)-2'-methyl-[1,1'-biphenyl]-3-yl)amino)-2-oxoethyl)carbamate (**2.93**) (100 mg, 0.244 mmol, 1 equiv.) and Wilkinson's catalyst (22 mg, 0.024 mmol, 10 mol%) in 4 mL MeCN:H$_2$O (15:85, 0.1 M) was refluxed for 1 h. The reaction was then allowed to return to room temperature, diluted with EtOAc, and washed with sat. aq. NaHCO$_3$. The organic layer was collected, dried using a hydrophobic frit, and concentrated under reduced pressure. Purified by silica chromatography, eluting with 0-20% MeOH/DCM, to afford the title compound as a yellow oil (41 mg, 45%). ^{1}H NMR (400 MHz, CDCl$_3$): δ 8.75 (br. s, 1H), 7.53 (d, J = 7.9 Hz, 1H), 7.42 (s, 1H), 7.31 − 7.27 (m, 1H), 7.21 − 7.14 (m, 2H), 7.12 (s, 1H), 7.01 (d, J = 7.6 Hz, 1H), 5.58 (s, 1H), 3.92 (d, J = 4.4 Hz, 2H), 3.84 (s, 2H), 3.14 (br. s, 2H), 2.20 (s, 3H), 1.42 (s, 9H). ^{13}C NMR (101 MHz, CDCl$_3$): δ 168.2, 156.7, 142.6, 141.7, 138.8, 137.6, 134.4, 130.8, 129.0, 128.8, 126.6, 125.3, 120.8, 118.6, 80.7, 45.6, 45.4, 28.4, 20.2. υ_{max} (neat): 3295, 2975, 2922, 2854, 1675, 1612, 1590, 1539, 1504 cm^{-1}. HRMS: exact mass calculated for $[M+Na]^+$ ($C_{21}H_{27}N_3NaO_3$) m/z requires 392.1945, m/z found 392.1927.

Synthesis of *tert*-butyl (4-bromo-2,3-dihydro-1*H*-inden-1-yl)carbamate (2.98). A round bottomed flask containing 4-bromo-2,3-dihydro-1*H*-inden-1-one (**2.95**) (400

mg, 1.914 mmol, 1 equiv.), H$_2$NOH.HCl (528 mg, 7.655 mmol, 4 equiv.), and NaOAc (628 mg, 7.655 mmol, 4 equiv.) in 10 mL MeOH (0.2 M) was stirred at room temperature for 16 h. The reaction mixture was then concentrated under reduced pressure, redissolved in 20 mL DCM, and washed with 20 mL sat. aq. NaHCO$_3$. The organic layer was collected, dried using a hydrophobic frit, and concentrated under reduced pressure to afford 4-bromo-2,3-dihydro-1*H*-inden-1-one oxime (**2.96**) as a white solid (426 mg, 98%) which was used in the next step without further purification. A round bottomed flask containing 4-bromo-2,3-dihydro-1*H*-inden-1-one oxime (**2.96**) (426 mg, 1.885 mmol, 1 equiv.) and Zn dust (429 mg, 6.5975 mmol, 3.5 equiv.) in 10 mL AcOH (0.2 M) was stirred at room temperature for 16 h. The resulting reaction mixture was then filtered through a plug of celite, washing with MeOH, and the filtrate was concentrated under reduced pressure to afford 4-bromo-2,3-dihydro-1*H*-inden-1-amine (157 mg, 74%) which was used in the next step without further purification. The residue was used according to General Procedure B using Boc$_2$O (178 mg, 0.818 mmol, 1.1 equiv.) and Et$_3$N (207 µL, 1.488 mmol, 2 equiv.) in 6 mL DCM (0.1 M). Purified by silica chromatography, eluting with 50% EtOAc/petroleum ether, to afford the title compound as a cream solid (189 mg, 81%). ^{1}H NMR (400 MHz, CO(CD$_3$)$_2$): δ 7.40 (d, J = 7.9 Hz, 1H), 7.27 (d, J = 7.4 Hz, 1H), 7.14 (app. t, J = 7.7 Hz, 1H), 6.33 (br. s, 1H), 5.28 – 5.15 (m, 1H), 3.04 – 2.93 (m, 1H), 2.88 – 2.72 (m, 1H), 2.56 – 2.44 (m, 1H), 1.98 – 1.86 (m, 1H), 1.44 (s, 9H). ^{13}C NMR (101 MHz, CO(CD$_3$)$_2$): δ 148.1, 144.0, 131.2, 129.6, 124.1, 120.4, 78.9, 57.5, 33.0, 32.0, 28.6. Once carbon not observed/coincident. υ$_{max}$ (neat): 2952, 2915, 2870, 1727, 1683, 1515, 1459 cm^{-1}. HRMS: exact mass calculated for [M+Na]$^+$ (C$_{14}$H$_{18}$NNaO$_2$Br) *m/z* requires 334.0413, *m/z* found 334.0408.

Synthesis of *tert*-butyl (2-((2'-formyl-[1,1'-biphenyl]-3-yl)amino)-2-oxoethyl)carbamate (2.99). Prepared according to General Procedure I using 2-bromobenzaldehyde (**2.98**) (1.0 g, 5.405 mmol, 1 equiv.), *tert*-butyl (2-oxo-2-((3-(4,4,5,5-tetramethyl-1,3,2-dioxaborolan-2-yl)phenyl)amino) ethyl) carbamate (**2.63**) (3.0 g, 8.108 mmol, 1.5 equiv.), Pd(dppf)Cl$_2$·DCM (176.0 mg, 0.216 mmol, 4 mol%), and K$_3$PO$_4$ (3.4 g, 16.215 mmol, 3 equiv.) in 30 mL THF (0.2 M) and H$_2$O (486 µL, 27.025 mmol, 5 equiv.). Purified by silica chromatography, eluting with 20-60% EtOAc/petroleum ether, to afford the title compound as a yellow oil (1.87 g, 98%). ^{1}H NMR (400 MHz, CDCl$_3$): δ 9.94 (s, *J* = 0.6 Hz, 1H), 8.76 (br. s, 1H), 7.98 (dd, *J* = 7.8, 1.2 Hz, 1H), 7.65 − 7.55 (m, *J* = 7.6, 1.5 Hz, 3H), 7.46 (app. t, *J* = 7.6 Hz, 1H), 7.41 − 7.32 (m, 2H), 7.07 (d, *J* = 7.6 Hz, 1H), 5.59 (t, *J* = 5.7 Hz, 1H), 3.97 (d, *J* = 5.6 Hz, 2H), 1.43 (s, 9H). ^{13}C NMR (101 MHz, CDCl$_3$): δ 192.5, 168.3, 156.8, 145.5, 138.7, 138.0, 133.8, 133.7, 130.8, 129.1, 128.0, 127.7, 126.3, 121.5, 119.7, 80.8, 45.5, 28.4. υ$_{max}$ (neat): 3306, 3060, 2978, 2934, 1690, 1681, 1593, 1550, 1517 cm^{-1}. HRMS: exact mass calculated for [M+Na]$^+$ (C$_{20}$H$_{22}$N$_2$NaO$_4$) *m/z* requires 377.1472, *m/z* found 377.1462.

Synthesis of *tert*-butyl *N*-({[3-(4-{[(*tert*-butoxy)carbonyl]amino}pyridin-2-yl)phenyl] carbamoyl}methyl)carbamate (2.102). Prepared according to General Procedure C using *tert*-butyl (2-bromopyridin-4-yl)carbamate (100 mg, 0.366 mmol, 1 equiv.), *tert*-butyl (2-oxo-2-((3-(4,4,5,5-tetramethyl-1,3,2-dioxaborolan-2-yl)phenyl)amino) ethyl) carbamate (**2.63**) (165 mg, 0.439 mmol, 1.2 equiv.), 2′-(dimethylamino)-2-biphenylyl-palladium(II) chloride dinorbornylphosphine complex (10.26 mg, 0.018 mmol, 5 mol%), and K$_3$PO$_4$ (311 mg, 1.465 mmol, 4 equiv.) in 1.875 mL 1,4-dioxane:H$_2$O (4:1, 0.2 M). Purified using silica chromatography,

eluting with 0-70% EtOAc/cyclohexane, to afford the title compound as a colourless oil (61 mg, 35%). ^{1}H NMR (400 MHz, CDCl$_3$): δ 8.47 (d, J = 5.6 Hz, 1H), 8.39 (br. s, 1H), 7.95 (s, 1H), 7.73 – 7.59 (m, 3H), 7.40 – 7.30 (m, 2H), 7.09 (s, 1H), 5.48 (br. s, 1H), 3.94 (d, J = 5.9 Hz, 2H), 1.54 (s, 9H), 1.47 (s, 9H). ^{13}C NMR (101 MHz, CDCl$_3$): δ 168.2, 157.9, 152.2, 150.5, 146.7, 140.3, 138.0, 129.5, 123.3, 120.9, 118.6, 111.4, 109.6, 81.8, 80.9, 45.6, 28.5, 28.4. One carbon not observed/coincident. υ$_{max}$ (neat): 3283, 2974, 2930, 1680, 1582, 1515 cm^{-1}. HRMS: exact mass calculated for [M+H]$^+$ (C$_{23}$H$_{31}$N$_4$O$_5$) m/z requires 443.2289, m/z found 443.2283.

Synthesis of *tert*-butyl ((3'-(2-((*tert*-butoxycarbonyl)amino)acetamido)-[1,1'-biphenyl]-2-yl)methyl)carbamate (2.106). Prepared according to General Procedure I using *tert*-butyl (2-bromobenzyl)carbamate (180 mg, 0.545 mmol, 1 equiv.), *tert*-butyl (2-oxo-2-((3-(4,4,5,5-tetramethyl-1,3,2-dioxaborolan-2-yl)phenyl)amino) ethyl) carbamate (**2.63**) (307 mg, 0.818 mmol, 1.5 equiv.), Pd(dppf)Cl$_2$·DCM (18 mg, 0.022 mmol, 4 mol%), and K$_3$PO$_4$ (347 mg, 1.635 mmol, 3 equiv.) in 3 mL THF (0.3 M) and H$_2$O (49 μL, 2.725 mmol, 5 equiv.). Purified using silica chromatography, eluting with 0-50% EtOAc/cyclohexane, to afford the title compound as a colourless oil (246 mg, 99%). ^{1}H NMR (400 MHz, CDCl$_3$): δ 8.52 (br. s, 1H), 7.52 – 7.39 (m, 3H), 7.37 – 7.28 (m, 3H), 7.20 (dd, J = 7.4, 1.3 Hz, 1H), 7.02 (d, J = 7.5 Hz, 1H), 5.46 (s, 1H), 4.93 (s, 1H), 4.24 (d, J = 5.3 Hz, 2H), 3.94 (d, J = 4.8 Hz, 2H), 1.45 (s, 9H), 1.42 (s, 9H). ^{13}C NMR (101 MHz, CDCl$_3$): δ 168.1, 156.1, 141.7, 141.0, 137.5, 136.4, 130.1, 129.1, 128.5, 128.0, 127.3, 125.3, 120.9, 118.9, 80.8, 79.5, 45.5, 42.5, 28.5, 28.4. One carbon not observed/coincident. υ$_{max}$ (neat): 3312, 2978, 2932, 1681, 1614, 1591, 1513 cm^{-1}. HRMS: exact mass calculated for [M+Na]$^+$ (C$_{25}$H$_{33}$N$_3$NaO$_5$) m/z requires 478.2312, m/z found 478.2293.

Synthesis of *tert*-butyl *N*-({[3-(5-{[(*tert*-butoxy) carbonyl]amino}pyridin-3-yl)phenyl] carbamoyl}methyl)carbamate (2.109). Prepared according to General Procedure C using *tert*-butyl (5-bromopyridin-3-yl)carbamate (100 mg, 0.366 mmol, 1 equiv.), *tert*-butyl (2-oxo-2-((3-(4,4,5,5-tetramethyl-1,3,2-dioxaborolan-2-yl)phenyl)amino)ethyl)carbamate (**2.63**) (165 mg, 0.439 mmol, 1.2 equiv.), 2′-(dimethylamino)-2-biphenylyl-palladium(II) chloride dinorbornylphosphine complex (10 mg, 0.018 mmol, 5 mol%), and K_3PO_4 (311 mg, 1.465 mmol, 4 equiv.) in 1.875 mL 1,4-dioxane:H_2O (4:1, 0.2 M). Purified on using silica chromatography, eluting with 0-70% EtOAc/cyclohexane, to afford the title compound as a white solid (93 mg, 53%). ^{1}H NMR (400 MHz, CD$_3$OD): δ 8.55 (d, *J* = 2.2 Hz, 1H), 8.40 (d, *J* = 1.9 Hz, 1H), 8.20 (s, 1H), 7.87 (s, 1H), 7.61 (d, *J* = 7.9 Hz, 1H), 7.44 (t, *J* = 7.8 Hz, 1H), 7.37 (d, *J* = 7.7 Hz, 1H), 3.89 (s, 2H), 1.54 (s, 9H), 1.47 (s, 9H). Three exchangeable protons not observed. ^{13}C NMR (101 MHz, CD$_3$OD): δ 170.8, 155.0, 142.0, 140.4, 139.4, 139.3, 138.4, 138.3, 130.7, 125.3, 123.9, 121.1, 119.8, 81.7, 80.8, 45.1, 28.7, 28.6. One carbon not observed/coincident. υ_{max} (neat): 3283, 2974, 2930, 1686, 1677, 1593, 1543, 1535 cm^{-1}. HRMS: exact mass calculated for $[M+H]^+$ (C$_{23}$H$_{31}$N$_4$O$_5$) *m/z* requires 443.2289, *m/z* found 443.2281.

Synthesis of 6-bromoimidazo[1,2-α]pyridin-8-amine (2.110). Prepared according to the literature procedure.[144] A solution of 5-bromopyridine-2,3-diamine (**2.68**) (1 g, 5.32 mmol, 1 equiv.), sodium bicarbonate (894 mg, 10.64 mmol, 2 equiv.), and chloroacetal (844 μL, 13.30 mmol, 2.5 equiv.) in 20 mL EtOH (0.3 M) was heated at reflux for 16 h. The reaction mixture was allowed to return to room temperature and then concentrated under reduced pressure. The residue was dissolved in 50 mL DCM and washed with H_2O (2 x 50 mL). The organic layer was dried using a hydrophobic

frit and then concentrated under reduced pressure. Precipitation from DCM afforded 462 mg of the desired product. The filtrated was purified by column chromatography, eluting with 0-50% EtOAc/cyclohexane, to afford a further 162 mg of the desired product. The two batches were combined to give a total yield of 624 mg (55%) of the title compound as a cream solid. ^{1}H NMR (400 MHz, CDCl$_3$): δ 7.73 (d, J = 1.6 Hz, 1H), 7.49 (d, J = 1.2 Hz, 1H), 7.46 (d, J = 1.2 Hz, 1H), 6.40 (d, J = 1.6 Hz, 1H), 4.62 (br. s, 2H). ^{13}C NMR (101 MHz, CDCl$_3$): δ 138.3, 136.3, 132.4, 115.9, 113.7, 108.4, 105.5. υ$_{max}$ (neat): 3401, 3295, 3161, 3092, 3047, 1644 cm^{-1}. HRMS: exact mass calculated for [M+H]$^{+}$ (C$_7$H$_7$BrN$_3$) m/z requires 213.9797, m/z found 213.9796.

Synthesis of *tert*-butyl (2-((3-(2-methylpyridin-4-yl)phenyl)amino)-2-oxoethyl) carbamate (2.111). Prepared according to General Procedure C using 4-bromo-2-methylpyridine (69 μL, 0.581 mmol, 1 equiv.), *tert*-butyl (2-oxo-2-((3-(4,4,5,5-tetramethyl-1,3,2-dioxaborolan-2-yl)phenyl)amino)ethyl)carbamate (**2.63**) (262 mg, 0.698 mmol, 1.2 equiv.), 2′-(dimethylamino)-2-biphenylyl-palladium(II) chloride dinorbornylphosphine complex (16 mg, 0.029 mmol, 5 mol%), and K$_3$PO$_4$ (494 mg, 2.325 mmol, 4 equiv.) in 2.5 mL 1,4-dioxane:H$_2$O (4:1, 0.2 M). Purified by reverse-phase column chromatography, eluting with 10-55% HpH method, to afford the title compound as a colourless oil (134 mg, 67%). ^{1}H NMR (400 MHz, CDCl$_3$): δ 8.88 (br. s, 1H), 8.47 (d, J = 5.2 Hz, 1H), 7.86 (s, 1H), 7.49 (d, J = 7.7 Hz, 1H), 7.38 – 7.27 (m, 3H), 7.23 (dd, J = 5.2, 1.5 Hz, 1H), 5.66 (s, 1H), 3.98 (d, J = 5.8 Hz, 2H), 2.56 (s, 3H), 1.46 (s, 9H). ^{13}C NMR (101 MHz, CDCl$_3$): δ 168.4, 158.9, 156.8, 149.5, 148.4, 139.3, 138.6, 129.7, 123.0, 121.3, 120.4, 119.0, 118.6, 80.8, 45.6, 28.4, 24.5. υ$_{max}$ (neat): 3285, 3002, 2974, 2928, 1686, 1677, 1602, 1547, 1535 cm^{-1}.

HRMS: exact mass calculated for [M+Na]$^+$ (C$_{19}$H$_{23}$N$_3$NaO$_3$) *m/z* requires 364.1632, *m/z* found 364.1620.

Synthesis of *tert*-butyl (2-((3-(2-methyl-1,8-naphthyridin-3-yl)phenyl)amino)-2-oxoethyl)carbamate (2.112). Prepared according to General Procedure C using 3-bromo-2-methyl-1,8-naphthyridine (99 mg, 0.443 mmol, 1 equiv.), *tert*-butyl (2-oxo-2-((3-(4,4,5,5-tetramethyl-1,3,2-dioxaborolan-2-yl)phenyl)amino)ethyl)carbamate (**2.63**) (200 mg, 0.532 mmol, 1.2 equiv.), 2′-(dimethylamino)-2-biphenylyl-palladium(II) chloride dinorbornylphosphine complex (12 mg, 0.022 mmol, 5 mol%), and K$_3$PO$_4$ (376 mg, 1.772 mmol, 4 equiv.) in 2.5 mL 1,4-dioxane:H$_2$O (4:1, 0.2 M). Purified by reverse-phase column chromatography, eluting with 20-70% HpH method, to afford the title compound as a colourless glass (142 mg, 82% yield). ^{1}H NMR (400 MHz, CDCl$_3$): δ 9.08 (dd, *J* = 4.3, 2.0 Hz, 1H), 8.58 (br. s, 1H), 8.15 (dd, *J* = 8.1, 1.9 Hz, 1H), 7.97 (s, 1H), 7.64 (s, 1H), 7.57 (d, *J* = 8.1 Hz, 1H), 7.48 – 7.37 (m, 2H), 7.14 (d, *J* = 7.6 Hz, 1H), 5.40 (br. s, 1H), 3.99 (d, *J* = 6.0 Hz, 2H), 2.69 (s, 3H), 1.47 (s, 9H). ^{13}C NMR (101 MHz, CDCl$_3$): δ 168.5, 161.5, 156.7, 155.1, 153.4, 139.8, 138.3, 137.0, 136.7, 129.3, 125.1, 122.0, 121.3, 120.8, 120.2, 119.7, 80.6, 45.6, 28.4, 24.9. υ$_{max}$ (neat): 3278, 2976, 2930, 1681, 1614, 1591, 1554 cm^{-1}. HRMS: exact mass calculated for [M+H]$^+$ (C$_{22}$H$_{25}$N$_4$O$_3$) *m/z* requires 393.1921, *m/z* found 393.1914.

Synthesis of *tert*-butyl (2-((3′-cyano-2′-methyl-[1,1′-biphenyl]-3-yl)amino)-2-oxoethyl)carbamate (2.113). Prepared according to General Procedure C using 3-bromo-2-methylbenzonitrile (100 mg, 0.510 mmol, 1 equiv.), *tert*-butyl (2-oxo-2-((3-(4,4,5,5-tetramethyl-1,3,2-dioxaborolan-2-yl)phenyl)amino)ethyl)carbamate (**2.63**) (230 mg, 0.612 mmol, 1.2 equiv.), 2′-(dimethylamino)-2-biphenylyl-palladium(II)

chloride dinorbornylphosphine complex (14 mg, 0.026 mmol, 5 mol%), and K_3PO_4 (433 mg, 2.040 mmol, 4 equiv.) in 2.5 mL 1,4-dioxane:H_2O (4:1, 0.2 M). Purified by reverse-phase column chromatography, eluting with 40-90% HpH method, to afford the title compound as a colourless oil (111 mg, 60%). ^{1}H NMR (400 MHz, CDCl$_3$): δ 8.67 (br. s, 1H), 7.59 (dd, J = 7.7, 1.3 Hz, 1H), 7.55 − 7.45 (m, 2H), 7.39 (dd, J = 7.7, 1.3 Hz, 1H), 7.33 (app. t, J = 7.9 Hz, 1H), 7.29 (d, J = 7.5 Hz, 1H), 6.98 (d, J = 7.6 Hz, 1H), 5.54 (t, J = 5.7 Hz, 1H), 3.96 (d, J = 5.8 Hz, 2H), 2.41 (s, 3H), 1.44 (s, 9H). ^{13}C NMR (101 MHz, CDCl$_3$): δ 168.2, 156.7, 142.9, 140.9, 139.5, 137.9, 134.1, 131.9, 129.1, 126.3, 125.1, 120.6, 119.2, 118.5, 113.8, 80.8, 45.6, 28.4, 19.0. υ$_{max}$ (neat): 3304, 2973, 2928, 2223, 1719, 1686, 1671, 1612, 1591, 1543, 1509 cm^{-1}. HRMS: exact mass calculated for [M+H]$^+$ (C$_{21}$H$_{24}$N$_3$O$_3$) m/z requires 366.1812, m/z found 366.1812.

Synthesis of *tert*-butyl (2-((5'-(hydroxymethyl)-2'-methyl-[1,1'-biphenyl]-3-yl)amino)-2-oxoethyl)carbamate (2.114). Prepared according to General Procedure H using *tert*-butyl (2-((5'-formyl-2'-methyl-[1,1'-biphenyl]-3-yl)amino)-2-oxoethyl)carbamate (**2.92**) (110 mg, 0.299 mmol, 1 equiv.) and NaBH$_4$ (34 mg, 0.897 mmol, 3 equiv.) in 4 mL MeOH (0.1 M). Purified by silica chromatography, eluting with 20-60% EtOAc/petroleum ether, to afford the title compound as a colourless oil (106 mg, 96%). ^{1}H NMR (500 MHz, CDCl$_3$): δ 8.62 (br. s, 1H), 7.46 (d, J = 7.8 Hz, 1H), 7.39 (s, 1H), 7.27 (app. t, J = 7.7 Hz, 1H), 7.23 − 7.16 (m, 2H), 7.15 (s, 1H), 7.01 (d, J = 7.4 Hz, 1H), 5.55 (t, J = 5.2 Hz, 1H), 4.63 (s, 2H), 3.90 (d, J = 3.4 Hz, 2H), 2.61 (br. s, J = 7.9 Hz, 1H), 2.21 (s, 3H), 1.43 (s, 9H). ^{13}C NMR (126 MHz, CDCl$_3$): δ 168.2, 156.7, 142.6, 141.5, 138.6, 137.5, 134.8, 130.6, 128.8, 128.6, 126.3, 125.4, 120.9, 118.6, 80.8, 65.1, 45.4, 28.4, 20.2. υ$_{max}$ (neat): 3405, 3297,

2976, 2926, 1673, 1612, 1591 cm^{-1}. HRMS: exact mass calculated for [M+Na]$^+$ (C$_{21}$H$_{26}$N$_2$NaO$_4$) m/z requires 393.1785, m/z found 393.1777.

Synthesis of *tert*-butyl (2-((3-bromophenyl)amino)-2-oxoethyl)carbamate (2.115). Prepared according to General Procedure A using Boc-glycine (2.2 g, 12.791 mmol, 1.1 equiv.), DIPEA (4.1 mL, 23.256 mmol, 2 equiv.), HATU (5.3 g, 13.953 mmol, 1.2 equiv.), and 3-bromoaniline (1.3 mL, 11.628 mmol, 1 equiv.) in 25 mL DMF (0.5 M). Purified using silica chromatography, eluting with 0-40% EtOAc/petroleum ether, to afford the title compound as a white solid (3.8 g, 98%). ^{1}H NMR (500 MHz, CDCl$_3$): δ 8.29 (br. s, 1H), 7.77 (s, 1H), 7.41 (d, J = 8.0 Hz, 1H), 7.24 (d, J = 8.2 Hz, 1H), 7.18 (app. t, J = 8.0 Hz, 1H), 5.24 (br. s, 1H), 3.92 (d, J = 6.0 Hz, 2H), 1.49 (s, 9H). ^{13}C NMR (101 MHz, CDCl$_3$): δ 167.4, 138.2, 129.8, 127.0, 122.3, 122.2, 117.8, 80.6, 45.3, 27.8. One carbon not observed/coincident. υ$_{max}$ (neat): 3250, 3194, 3131, 3062, 2973, 2939, 1709, 1668, 1608, 1591, 1541 cm^{-1}. HRMS: exact mass calculated for [M+Na]$^+$ (C$_{13}$H$_{17}$N$_2$NaO$_3$Br) m/z requires 351.0315, m/z found 351.0298.

Synthesis of *tert*-butyl (2-((2'-((((cyclohexylmethyl)amino)methyl)-[1,1'-biphenyl]-3-yl)amino)-2-oxoethyl)carbamate (2.116). Prepared according to General Procedure J using *tert*-butyl (2-((2'-formyl-[1,1'-biphenyl]-3-yl)amino)-2-oxoethyl)carbamate (**2.99**) (100 mg, 0.282 mmol, 1 equiv.), cyclohexylmethanamine (44 μL, 0.338 mmol, 1.2 equiv.), MgSO$_4$ (102 mg, 0.846 mmol, 3 equiv.), and NaCNBH$_3$ (36 mg, 0.564 mmol, 2 equiv.) in 2 mL DCM (0.2 M). Purified by silica chromatography, eluting with 50-100% EtOAc/petroleum ether, to afford the title compound as a cream solid (104 mg, 82%). ^{1}H NMR (400 MHz, CDCl$_3$): δ 8.32 (br. s, 1H), 7.57 (d, J = 8.1 Hz, 1H), 7.51 – 7.42 (m, 2H), 7.38 – 7.27 (m, 3H), 7.21 (dd, J

= 7.4, 1.5 Hz, 1H), 7.13 (d, J = 7.6 Hz, 1H), 5.34 (br. s, 1H), 3.93 (d, J = 5.9 Hz, 2H), 3.70 (s, 2H), 2.31 (d, J = 6.6 Hz, 2H), 1.70 – 1.57 (m, 6H), 1.47 (s, 9H), 1.22 – 1.06 (m, 3H), 0.89 – 0.71 (m, 2H). One exchangeable proton not observed. ^{13}C NMR (101 MHz, CDCl$_3$): δ 167.9, 142.3, 141.3, 137.9, 137.5, 130.1, 129.3, 129.0, 127.8, 127.6, 127.0, 125.4, 120.6, 118.7, 81.0, 56.4, 51.8, 45.8, 37.9, 31.5, 28.4, 26.8, 26.2. υ_{max} (neat): 3304, 3060, 3004, 2978, 2922, 2852, 1675, 1614, 1591, 1554 cm^{-1}. HRMS: exact mass calculated for [M+H]$^+$ (C$_{27}$H$_{38}$N$_3$O$_3$) m/z requires 452.2908, m/z found 452.2899.

Synthesis of *tert*-butyl (2-((2'-((benzylamino)methyl)-[1,1'-biphenyl]-3-yl)amino)-2-oxoethyl)carbamate (2.117). Prepared according to General Procedure J using *tert*-butyl (2-((2'-formyl-[1,1'-biphenyl]-3-yl)amino)-2-oxoethyl)carbamate (**2.99**) (100 mg, 0.282 mmol, 1 equiv.), benzylamine (37 µL, 0.338 mmol, 1.2 equiv.), MgSO$_4$ (102 mg, 0.846 mmol, 3 equiv.), and NaCNBH$_3$ (36 mg, 0.564 mmol, 2 equiv.) in 2 mL DCM (0.2 M). Purified by silica chromatography, eluting with 50-70% EtOAc/petroleum ether, to afford the title compound as a cream solid (94 mg, 75%). ^{1}H NMR (400 MHz, CDCl$_3$): δ 8.24 (br. s, 1H), 7.59 (d, J = 8.0 Hz, 1H), 7.53 – 7.45 (m, 2H), 7.41 – 7.29 (m, 4H), 7.28 – 7.20 (m, 5H), 7.13 (d, J = 7.6 Hz, 1H), 5.30 (br. s, 1H), 3.94 (d, J = 5.9 Hz, 2H), 3.78 (s, 2H), 3.71 (s, 2H), 1.49 (s, 9H). ^{13}C NMR (101 MHz, CDCl$_3$): δ 167.9, 142.1, 141.5, 139.8, 137.5, 137.1, 130.2, 129.6, 129.1, 128.5, 128.3, 127.8, 127.3, 127.1, 125.4, 120.7, 118.8, 80.9, 53.3, 50.8, 45.7, 28.4. One carbon not observed/coincident. υ_{max} (neat): 3299, 3060, 3027, 2976, 2854, 1675, 1614, 1591 cm^{-1}. HRMS: exact mass calculated for [M+H]$^+$ (C$_{27}$H$_{32}$N$_3$O$_3$) m/z requires 446.2438, m/z found 446.2425.

Synthesis of *tert*-butyl (2-((2'-(((2-methoxyethyl)amino)methyl)-[1,1'-biphenyl]-3-yl)amino)-2-oxoethyl)carbamate (2.118). Prepared according to General Procedure J using *tert*-butyl (2-((2'-formyl-[1,1'-biphenyl]-3-yl)amino)-2-oxoethyl)carbamate (**2.99**) (100 mg, 0.282 mmol, 1 equiv.), 2-methoxyethan-1-amine (25 mg, 0.339 mmol, 1.2 equiv.), MgSO$_4$ (101 mg, 0.846 mmol, 3 equiv.), and NaCNBH$_3$ (35 mg, 0.564 mmol, 2 equiv.) in 1 mL DCM (0.3 M). Purified by silica chromatography, eluting with 0-10% MeOH/DCM, to afford the title compound as a colourless oil (76 mg, 65%). ^{1}H NMR (400 MHz, CDCl$_3$): δ 8.67 (br. s, 1H), 7.66 (d, *J* = 8.1 Hz, 1H), 7.49 (s, 1H), 7.45 (dd, *J* = 7.5, 1.3 Hz, 1H), 7.38 − 7.19 (m, 4H), 7.08 (d, *J* = 7.6 Hz, 1H), 5.54 (t, *J* = 5.5 Hz, 1H), 3.92 (d, *J* = 5.4 Hz, 2H), 3.72 (s, 2H), 3.51 − 3.35 (m, 2H), 3.29 (s, 3H), 2.76 − 2.63 (m, 2H), 2.25 (br. s, 1H), 1.45 (s, 9H). ^{13}C NMR (101 MHz, CDCl$_3$): δ 168.0, 156.6, 141.9, 141.4, 137.7, 137.1, 130.1, 129.4, 129.0, 127.8, 127.2, 125.2, 120.7, 118.8, 80.6, 71.7, 58.7, 51.2, 48.5, 45.3, 28.4. υ$_{max}$ (neat): 3312, 3058, 2976, 2930, 2889, 2822, 1679, 1614, 1591, 1543, 1524 cm^{-1}. HRMS: exact mass calculated for [M+H]$^+$ (C$_{18}$H$_{24}$N$_3$O$_2$) *m/z* requires 314.1863, *m/z* found 314.1849.

Synthesis of *tert*-butyl (2-((2'-(morpholinomethyl)-[1,1'-biphenyl]-3-yl)amino)-2-oxoethyl)carbamate (2.119). Prepared according to General Procedure J using *tert*-butyl (2-((2'-formyl-[1,1'-biphenyl]-3-yl)amino)-2-oxoethyl)carbamate (**2.99**) (100 mg, 0.282 mmol, 1 equiv.), morpholine (29 μL, 0.338 mmol, 1.2 equiv.), MgSO$_4$ (102 mg, 0.846 mmol, 3 equiv.), and NaCNBH$_3$ (36 mg, 0.564 mmol, 2 equiv.) in 2 mL DCM (0.2 M). Purified by silica chromatography, eluting with 50-80% EtOAc/petroleum ether, to afford the title compound as a colourless oil (45 mg, 38%). ^{1}H NMR (400 MHz, CDCl$_3$): δ 8.17 (br. s, 1H), 7.58 − 7.48 (m, 3H), 7.39 −

7.27 (m, 3H), 7.25 – 7.22 (m, 1H), 7.15 (d, J = 7.5 Hz, 1H), 5.22 (br. s, 1H), 3.93 (d, J = 6.0 Hz, 2H), 3.65 (br. s, 4H), 3.42 (s, 2H), 2.36 (br. s, 4H), 1.47 (s, 9H). ^{13}C NMR (101 MHz, CDCl$_3$): δ 167.9, 142.5, 142.3, 137.2, 130.2, 128.7, 127.5, 127.1, 125.9, 121.1, 118.6, 67.1, 60.3, 53.4, 45.9, 29.8, 28.4. Two carbons not observed/coincident. υ_{max} (neat): 3395, 3295, 2960, 2926, 2854, 2811, 1675, 1614, 1591, 1539 cm^{-1}. HRMS: exact mass calculated for [M+H]$^+$ (C$_{24}$H$_{32}$N$_3$O$_4$) m/z requires 426.2387, m/z found 426.2367.

3 References

1. Wynn, T. A. Fibrotic disease and the T(H)1/T(H)2 paradigm. *Nat. Rev. Immunol.* **2004**, *4* (8), 583-594.

2. Wynn, T. A.; Ramalingam, T. R. Mechanisms of fibrosis: therapeutic translation for fibrotic disease. *Nat. Med.* **2012**, *18* (7), 1028-1040.

3. Gabbiani, G. The myofibroblast in wound healing and fibrocontractive diseases. *J. Pathol.* **2003**, *200* (4), 500-503.

4. Prasse, A. [Idiopathic Pulmonary Fibrosis]. *Pneumologie* **2015**, *69* (10), 608-614.

5. Pardo, A.; Selman, M. Idiopathic pulmonary fibrosis: new insights in its pathogenesis. *Int. J. Biochem. Cell Biol.* **2002**, *34* (12), 1534-1538.

6. Navaratnam, V.; Fleming, K. M.; West, J.; Smith, C. J.; Jenkins, R. G.; Fogarty, A.; Hubbard, R. B. The rising incidence of idiopathic pulmonary fibrosis in the U.K. *Thorax* **2011**, *66* (6), 462-467.

7. Stracke, M. L.; Krutzsch, H. C.; Unsworth, E. J.; Arestad, A.; Cioce, V.; Schiffmann, E.; Liotta, L. A. Identification, purification, and partial sequence analysis of autotaxin, a novel motility-stimulating protein. *J. Biol. Chem.* **1992**, *267* (4), 2524-2529.

8. Tokumura, A.; Majima, E.; Kariya, Y.; Tominaga, K.; Kogure, K.; Yasuda, K.; Fukuzawa, K. Identification of human plasma lysophospholipase D, a lysophosphatidic acid-producing enzyme, as autotaxin, a multifunctional phosphodiesterase. *J. Biol. Chem.* **2002**, *277* (42), 39436-39442.

9.   Yokoyama, K.; Baker, D. L.; Virag, T.; Liliom, K.; Byun, H. S.; Tigyi, G.; Bittman, R. Stereochemical properties of lysophosphatidic acid receptor activation and metabolism. *Biochim. Biophys. Acta* **2002**, *1582* (1-3), 295-308.

10.   Yung, Y. C.; Stoddard, N. C.; Chun, J. LPA receptor signaling: pharmacology, physiology, and pathophysiology. *J. Lipid. Res.* **2014**, *55* (7), 1192-1214.

11.   Mutoh, T.; Rivera, R.; Chun, J. Insights into the pharmacological relevance of lysophospholipid receptors. *Br. J. Pharmacol.* **2012**, *165* (4), 829-844.

12.   Tager, A. M.; LaCamera, P.; Shea, B. S.; Campanella, G. S.; Selman, M.; Zhao, Z.; Polosukhin, V.; Wain, J.; Karimi-Shah, B. A.; Kim, N. D.; Hart, W. K.; Pardo, A.; Blackwell, T. S.; Xu, Y.; Chun, J.; Luster, A. D. The lysophosphatidic acid receptor LPA1 links pulmonary fibrosis to lung injury by mediating fibroblast recruitment and vascular leak. *Nat. Med.* **2008**, *14* (1), 45-54.

13.   Nam, S. W.; Clair, T.; Kim, Y. S.; McMarlin, A.; Schiffmann, E.; Liotta, L. A.; Stracke, M. L. Autotaxin (NPP-2), a metastasis-enhancing motogen, is an angiogenic factor. *Cancer Res.* **2001**, *61* (18), 6938-6944.

14.   Gotoh, M.; Fujiwara, Y.; Yue, J.; Liu, J.; Lee, S.; Fells, J.; Uchiyama, A.; Murakami-Murofushi, K.; Kennel, S.; Wall, J.; Patil, R.; Gupte, R.; Balazs, L.; Miller, D. D.; Tigyi, G. J. Controlling cancer through the autotaxin-lysophosphatidic acid receptor axis. *Biochem. Soc. Trans.* **2012**, *40* (1), 31-36.

15.   Zahednasab, H.; Balood, M.; Harirchian, M. H.; Mesbah-Namin, S. A.; Rahimian, N.; Siroos, B. Increased autotaxin activity in multiple sclerosis. *J Neuroimmunol.* **2014**, *273* (1-2), 120-123.

16.   Kanda, H.; Newton, R.; Klein, R.; Morita, Y.; Gunn, M. D.; Rosen, S. D. Autotaxin, an ectoenzyme that produces lysophosphatidic acid, promotes the entry of lymphocytes into secondary lymphoid organs. *Nat. Immunol.* **2008**, *9* (4), 415-423.

17.   Awada, R.; Rondeau, P.; Grès, S.; Saulnier-Blache, J. S.; Lefebvre d'Hellencourt, C.; Bourdon, E. Autotaxin protects microglial cells against oxidative stress. *Free Radic. Biol. Med.* **2012**, *52* (2), 516-526.

18.   Castagna, D.; Budd, D. C.; Macdonald, S. J.; Jamieson, C.; Watson, A. J. B. Development of Autotaxin Inhibitors: An Overview of the Patent and Primary Literature. *J. Med. Chem.* **2016**, *59* (12), 5604-5621.

19.   Gijsbers, R.; Aoki, J.; Arai, H.; Bollen, M. The hydrolysis of lysophospholipids and nucleotides by autotaxin (NPP2) involves a single catalytic site. *FEBS Lett.* **2003**, *538* (1-3), 60-64.

20.   Nishimasu, H.; Okudaira, S.; Hama, K.; Mihara, E.; Dohmae, N.; Inoue, A.; Ishitani, R.; Takagi, J.; Aoki, J.; Nureki, O. Crystal structure of autotaxin and insight into GPCR activation by lipid mediators. *Nat. Struct. Mol. Biol.* **2011**, *18* (2), 205-212.

21.   Hausmann, J.; Kamtekar, S.; Christodoulou, E.; Day, J. E.; Wu, T.; Fulkerson, Z.; Albers, H. M.; van Meeteren, L. A.; Houben, A. J.; van Zeijl, L.; Jansen, S.; Andries, M.; Hall, T.; Pegg, L. E.; Benson, T. E.; Kasiem, M.; Harlos, K.; Kooi, C. W.; Smyth, S. S.; Ovaa, H.; Bollen, M.; Morris, A. J.; Moolenaar, W. H.; Perrakis, A. Structural basis of substrate discrimination and integrin binding by autotaxin. *Nat. Struct. Mol. Biol.* **2011**, *18* (2), 198-204.

22.   Tabchy, A.; Tigyi, G.; Mills, G. B. Location, location, location: a crystal-clear view of autotaxin saturating LPA receptors. *Nat. Struct. Mol. Biol.* **2011**, *18* (2), 117-118.

23.   Stefan, C.; Jansen, S.; Bollen, M. NPP-type ectophosphodiesterases: unity in diversity. *Trends Biochem. Sci.* **2005**, *30* (10), 542-550.

24.   Nishimasu, H.; Ishitani, R.; Aoki, J.; Nureki, O. A 3D view of autotaxin. *Trends Pharmacol. Sci.* **2012**, *33* (3), 138-145.

25.   Dassault Systèmes BIOVIA*,* Discovery Studio Modeling Environment, Release 2017*,* San Diego: Dassault Systèmes, 2016.

26.   Murph, M.; Tanaka, T.; Pang, J.; Felix, E.; Liu, S.; Trost, R.; Godwin, A. K.; Newman, R.; Mills, G. Liquid chromatography mass spectrometry for quantifying plasma lysophospholipids: potential biomarkers for cancer diagnosis. *Methods Enzymol.* **2007**, *433*, 1-25.

27.   Umezu-Goto, M.; Kishi, Y.; Taira, A.; Hama, K.; Dohmae, N.; Takio, K.; Yamori, T.; Mills, G. B.; Inoue, K.; Aoki, J.; Arai, H. Autotaxin has lysophospholipase D activity leading to tumor cell growth and motility by lysophosphatidic acid production. *J. Cell. Biol.* **2002**, *158* (2), 227-233.

28.   Imamura, S.; Horiuti, Y. Enzymatic determination of phospholipase D activity with choline oxidase. *J. Biochem.* **1978**, *83* (3), 677-680.

29.   Tokumura, A.; Miyake, M.; Yoshimoto, O.; Shimizu, M.; Fukuzawa, K. Metal-ion stimulation and inhibition of lysophospholipase D which generates bioactive lysophosphatidic acid in rat plasma. *Lipids* **1998**, *33* (10), 1009-1015.

30.   Scherer, M.; Schmitz, G.; Liebisch, G. High-throughput analysis of sphingosine 1-phosphate, sphinganine 1-phosphate, and lysophosphatidic acid in

plasma samples by liquid chromatography-tandem mass spectrometry. *Clin. Chem.* **2009**, *55* (6), 1218-1222.

31.   North, E. J.; Howard, A. L.; Wanjala, I. W.; Pham, T. C.; Baker, D. L.; Parrill, A. L. Pharmacophore development and application toward the identification of novel, small-molecule autotaxin inhibitors. *J. Med. Chem.* **2010**, *53* (8), 3095-3105.

32.   Takakusa, H.; Kikuchi, K.; Urano, Y.; Sakamoto, S.; Yamaguchi, K.; Nagano, T. Design and synthesis of an enzyme-cleavable sensor molecule for phosphodiesterase activity based on fluorescence resonance energy transfer. *J. Am. Chem. Soc.* **2002**, *124* (8), 1653-1657.

33.   Ferguson, C. G.; Bigman, C. S.; Richardson, R. D.; van Meeteren, L. A.; Moolenaar, W. H.; Prestwich, G. D. Fluorogenic phospholipid substrate to detect lysophospholipase D/autotaxin activity. *Org. Lett.* **2006**, *8* (10), 2023-2026.

34.   Kawaguchi, M.; Okabe, T.; Okudaira, S.; Nishimasu, H.; Ishitani, R.; Kojima, H.; Nureki, O.; Aoki, J.; Nagano, T. Screening and X-ray crystal structure-based optimization of autotaxin (ENPP2) inhibitors, using a newly developed fluorescence probe. *ACS Chem. Biol.* **2013**, *8* (8), 1713-1721.

35.   Albers, H. M.; van Meeteren, L. A.; Egan, D. A.; van Tilburg, E. W.; Moolenaar, W. H.; Ovaa, H. Discovery and optimization of boronic acid based inhibitors of autotaxin. *J. Med. Chem.* **2010**, *53* (13), 4958-4967.

36.   Miller, D.; Tigyi, G.; Gududuru, V.; Fujiwara, Y.; Baker, D.; Walker, M.; Durgam, G. Acetal phosphate-derived LPA mimics, PPARgamma activators, and autotaxin inhibitors. US 20060270634, 2006.

37.   Zhang, H.; Xu, X.; Gajewiak, J.; Tsukahara, R.; Fujiwara, Y.; Liu, J.; Fells, J. I.; Perygin, D.; Parrill, A. L.; Tigyi, G.; Prestwich, G. D. Dual activity lysophosphatidic acid receptor pan-antagonist/autotaxin inhibitor reduces breast cancer cell migration in vitro and causes tumor regression in vivo. *Cancer Res.* **2009**, *69* (13), 5441-5449.

38.   Ferry, G.; Moulharat, N.; Pradère, J. P.; Desos, P.; Try, A.; Genton, A.; Giganti, A.; Beucher-Gaudin, M.; Lonchampt, M.; Bertrand, M.; Saulnier-Blache, J. S.; Tucker, G. C.; Cordi, A.; Boutin, J. A. S32826, a nanomolar inhibitor of autotaxin: discovery, synthesis and applications as a pharmacological tool. *J. Pharmacol. Exp. Ther.* **2008**, *327* (3), 809-819.

39.   Jiang, G.; Madan, D.; Prestwich, G. D. Aromatic phosphonates inhibit the lysophospholipase D activity of autotaxin. *Bioorg. Med. Chem. Lett.* **2011**, *21* (17), 5098-5101.

40.   Gierse, J.; Thorarensen, A.; Beltey, K.; Bradshaw-Pierce, E.; Cortes-Burgos, L.; Hall, T.; Johnston, A.; Murphy, M.; Nemirovskiy, O.; Ogawa, S.; Pegg, L.; Pelc, M.; Prinsen, M.; Schnute, M.; Wendling, J.; Wene, S.; Weinberg, R.; Wittwer, A.; Zweifel, B.; Masferrer, J. A novel autotaxin inhibitor reduces lysophosphatidic acid levels in plasma and the site of inflammation. *J. Pharmacol. Exp. Ther.* **2010**, *334* (1), 310-317.

41.   Staehle, W.; Schiemann, K.; Schultz, M. Heterocyclische verbindungen als autotaxin-inhibitoren. WO 2010112116 A1, 2010.

42.   Schultz, M.; Schiemann, K.; Staehle, W. Autotaxin inhibitors. WO 2010112124 A1, 2010.

43.   Albers, H. M.; Ovaa, H., Chemical evolution of autotaxin inhibitors. *Chem. Rev.* **2012**, *112* (5), 2593-2603.

44.   Hutchinson, J. H.; Lonergan, D.; Huang, F.; Rowbottom, M.; Calderon, I. Autotaxin inhibitor compounds. WO 2015048301 A1, 2015.

45.   Stein, A. J.; Bain, G.; Prodanovich, P.; Santini, A. M.; Darlington, J.; Stelzer, N. M.; Sidhu, R. S.; Schaub, J.; Goulet, L.; Lonergan, D.; Calderon, I.; Evans, J. F.; Hutchinson, J. H. Structural Basis for Inhibition of Human Autotaxin by Four Potent Compounds with Distinct Modes of Binding. *Mol. Pharmacol.* **2015**, *88* (6), 982-992.

46.   Jones, S. B.; Pfeifer, L. A.; Bleisch, T. J.; Beauchamp, T. J.; Durbin, J. D.; Klimkowski, V. J.; Hughes, N. E.; Rito, C. J.; Dao, Y.; Gruber, J. M.; Bui, H.; Chambers, M. G.; Chandrasekhar, S.; Lin, C.; McCann, D. J.; Mudra, D. R.; Oskins, J. L.; Swearingen, C. A.; Thirunavukkarasu, K.; Norman, B. H. Novel Autotaxin Inhibitors for the Treatment of Osteoarthritis Pain: Lead Optimization via Structure-Based Drug Design. *ACS Med. Chem. Lett.* **2016**, DOI: 10.1021/acsmedchemlett.6b00207.

47.   Hutchinson, J. H.; Parr, T. A.; Roppe, J. R.; Stock, N. S.; Volkots, D. Autotaxin inhibitors and uses thereof. WO 2012024620 A2, 2012.

48.   Roppe, J. R.; Parr, T. A.; Hutchinson, J. H. Heterocyclic autotaxin inhibitors and uses thereof. WO 2012166415 A1, 2012.

49.   Roppe, J. R.; Parr, T. A.; Hutchinson, J. H. Heterocyclic autotaxin inhibitors and uses thereof. US 20130029948 A1, 2013.

50.   Desroy, N.; Heckmann, B.; Brys, R. C. X.; Joncour, A.; Peixoto, C.; Bock, X. Compounds and pharmaceutical compositions thereof for the treatment of inflammatory disorders. WO 2014139882 A1, 2014.

51.   Desroy, N.; Heckmann, B.; Brys, R. C. X.; Joncour, A. M.; Peixoto, C.; Bock, X. M.; Houssme, C. G. Novel compounds and pharmaceutical compositions thereof for the treatment of inflammatory disorders. WO 2014202458 A1, 2014.

52.   Lipinski, C. A.; Lombardo, F.; Dominy, B. W.; Feeney, P. J., Experimental and computational approaches to estimate solubility and permeability in drug discovery and development settings. *Adv. Drug Deliv. Rev.* **2001**, *46* (1-3), 3-26.

53.   Leeson, P. D.; Davis, A. M. Time-related differences in the physical property profiles of oral drugs. *J. Med. Chem.* **2004**, *47* (25), 6338-6348.

54.   JChem for Office (Excel) 16.3.2100.656, 2008-2016, ChemAxon (http://www.chemaxon.com).

55.   Gleeson, M. P., Generation of a set of simple, interpretable ADMET rules of thumb. *J. Med. Chem.* **2008**, *51* (4), 817-834.

56.   Hughes, J. D.; Blagg, J.; Price, D. A.; Bailey, S.; Decrescenzo, G. A.; Devraj, R. V.; Ellsworth, E.; Fobian, Y. M.; Gibbs, M. E.; Gilles, R. W.; Greene, N.; Huang, E.; Krieger-Burke, T.; Loesel, J.; Wager, T.; Whiteley, L.; Zhang, Y. Physiochemical drug properties associated with in vivo toxicological outcomes. *Bioorg. Med. Chem. Lett.* **2008**, *18* (17), 4872-4875.

57.   Ritchie, T. J.; Macdonald, S. J., The impact of aromatic ring count on compound developability--are too many aromatic rings a liability in drug design? *Drug. Discov. Today* **2009**, *14* (21-22), 1011-1020.

58.   Hill, A. P.; Young, R. J. Getting physical in drug discovery: a contemporary perspective on solubility and hydrophobicity. *Drug Discov. Today.* **2010**, *15* (15-16), 648-655.

59.   Bickerton, G. R.; Paolini, G. V.; Besnard, J.; Muresan, S.; Hopkins, A. L. Quantifying the chemical beauty of drugs. *Nat. Chem.* **2012**, *4* (2), 90-98.

60.   Blake, J. F. Examination of the computed molecular properties of compounds selected for clinical development. *Biotechniques* **2003**, *Suppl*, 16-20.

61.   Oprea, T. I.; Davis, A. M.; Teague, S. J.; Leeson, P. D. Is there a difference between leads and drugs? A historical perspective. *J. Chem. Inf. Comput. Sci.* **2001**, *41* (5), 1308-1315.

62.   Hopkins, A. L.; Keserü, G. M.; Leeson, P. D.; Rees, D. C.; Reynolds, C. H. The role of ligand efficiency metrics in drug discovery. *Nat. Rev. Drug Discov.* **2014**, *13* (2), 105-121.

63.   Leach, A. R.; Hann, M. M.; Burrows, J. N.; Griffen, E. J. Fragment screening: an introduction. Molecular BioSystems, 2006, Vol. 2, 429-446.

64.   Hopkins, A. L.; Groom, C. R.; Alex, A. Ligand efficiency: a useful metric for lead selection. *Drug Discov. Today* **2004**, *9* (10), 430-431.

65.   Hajduk, P. J. Fragment-based drug design: how big is too big? *J. Med. Chem.* **2006**, *49* (24), 6972-6976.

66.   Fells, J. I.; Lee, S. C.; Fujiwara, Y.; Norman, D. D.; Lim, K. G.; Tsukahara, R.; Liu, J.; Patil, R.; Miller, D. D.; Kirby, R. J.; Nelson, S.; Seibel, W.; Papoian, R.; Parrill, A. L.; Baker, D. L.; Bittman, R.; Tigyi, G. Hits of a high-throughput screen identify the hydrophobic pocket of autotaxin/lysophospholipase D as an inhibitory surface. *Mol. Pharmacol.* **2013**, *84* (3), 415-424.

67.   Fells, J. I.; Lee, S. C.; Norman, D. D.; Tsukahara, R.; Kirby, J. R.; Nelson, S.; Seibel, W.; Papoian, R.; Patil, R.; Miller, D. D.; Parrill, A. L.; Pham, T. C.; Baker, D. L.; Bittman, R.; Tigyi, G. Targeting the hydrophobic pocket of autotaxin with virtual screening of inhibitors identifies a common aromatic sulfonamide structural motif. *FEBS J.* **2014**, *281* (4), 1017-1028.

68.   Keune, W. J.; Hausmann, J.; Bolier, R.; Tolenaars, D.; Kremer, A.; Heidebrecht, T.; Joosten, R. P.; Sunkara, M.; Morris, A. J.; Matas-Rico, E.; Moolenaar, W. H.; Oude Elferink, R. P.; Perrakis, A. Steroid binding to Autotaxin links bile salts and lysophosphatidic acid signalling. *Nat. Commun.* **2016**, *7*, article 11248.

69.   Jones, G.; Willett, P.; Glen, R. C.; Leach, A. R.; Taylor, R. Development and validation of a genetic algorithm for flexible docking. *J. Mol. Biol.* **1997**, *267* (3), 727-748.

70.   Copeland, R. A., Evaluation of enzyme inhibitors in drug discovery : a guide for medicinal chemists and pharmacologists. John Wiley: Hoboken, N.J. Chichester, 2005.

71.   Emsley, P.; Lohkamp, B.; Scott, W. G.; Cowtan, K. Features and development of Coot. *Acta Crystallogr. D. Biol. Crystallogr.* **2010**, *66* (Pt 4), 486-501.

72.   Potterton, L.; McNicholas, S.; Krissinel, E.; Gruber, J.; Cowtan, K.; Emsley, P.; Murshudov, G. N.; Cohen, S.; Perrakis, A.; Noble, M. Developments in the CCP4 molecular-graphics project. *Acta Crystallogr. D. Biol. Crystallogr.* **2004**, *60* (Pt 12 Pt 1), 2288-2294.

73. Miller, L. M.; Keune, W. J.; Castagna, D.; Young, L. C.; Duffy, E. L.; Potjewyd, F.; Salgado-Polo, F.; Garcia, P. E.; Semaan, D.; Pritchard, J. M.; Perrakis, A.; Macdonald, S. J. F.; Jamieson, C.; Watson, A. J. B. Structure-activity Relationships of Small Molecule Autotaxin Inhibitors with a Discrete Binding Mode. *Submitted*.

74. Ma, W.; Ackermann, L. Ruthenium(II)-catalyzed C-H alkenylations of phenols with removable directing groups. *Chemistry* **2013**, *19* (41), 13925-13928.

75. Maiti, D.; Buchwald, S. L. Cu-catalyzed arylation of phenols: synthesis of sterically hindered and heteroaryl diaryl ethers. *J. Org. Chem.* **2010**, *75* (5), 1791-1794.

76. Moolenaar, W. H.; Perrakis, A. Insights into autotaxin: how to produce and present a lipid mediator. *Nat. Rev. Mol. Cell Biol.* **2011**, *12* (10), 674-679.

77. Perrin, D. D.; Armarego, W. L. F. Purification of laboratory chemicals. 3rd ed. Pergamon: Oxford, 1988.

78. Huang, W. H.; Jia, W. L.; Wang, S., 7-Azaindolyl- and indolyl-functionalized starburst molecules with a 1,3,5-triazine or a benzene core - Syntheses and luminescence. *Can. J. Chem.* **2006**, *84*, 477–485.

79. Barczyk, M.; Carracedo, S.; Gullberg, D., Integrins. *Cell Tissue Res.* **2010**, *339* (1), 269-280.

80. Tamkun, J. W.; DeSimone, D. W.; Fonda, D.; Patel, R. S.; Buck, C.; Horwitz, A. F.; Hynes, R. O. Structure of integrin, a glycoprotein involved in the transmembrane linkage between fibronectin and actin. *Cell* **1986**, *46* (2), 271-282.

81. Santala, P.; Heino, J., Regulation of integrin-type cell adhesion receptors by cytokines. *J. Biol. Chem.* **1991**, *266* (34), 23505-23509.

82. Zhang, K.; Chen, J. The regulation of integrin function by divalent cations. *Cell Adh. Migr.* **2012**, *6* (1), 20-29.

83. Springer, T. A.; Dustin, M. L. Integrin inside-out signaling and the immunological synapse. *Curr. Opin. Cell Biol.* **2012**, *24* (1), 107-115.

84. Shen, B.; Delaney, M. K.; Du, X., Inside-out, outside-in, and inside-outside-in: G protein signaling in integrin-mediated cell adhesion, spreading, and retraction. *Curr. Opin. Cell. Biol.* **2012**, *24* (5), 600-606.

85. Arnaout, M. A.; Goodman, S. L.; Xiong, J. P. Structure and mechanics of integrin-based cell adhesion. *Curr. Opin. Cell Biol.* **2007**, *19* (5), 495-507.

86. Zhu, J.; Luo, B. H.; Xiao, T.; Zhang, C.; Nishida, N.; Springer, T. A. Structure of a complete integrin ectodomain in a physiologic resting state and activation and deactivation by applied forces. *Mol. Cell* **2008**, *32* (6), 849-861.

87. Van Agthoven, J. F.; Xiong, J. P.; Alonso, J. L.; Rui, X.; Adair, B. D.; Goodman, S. L.; Arnaout, M. A. Structural basis for pure antagonism of integrin αVβ3 by a high-affinity form of fibronectin. *Nat. Struct. Mol. Biol.* **2014**, *21* (4), 383-388.

88. Cox, D.; Brennan, M.; Moran, N. Integrins as therapeutic targets: lessons and opportunities. *Nat. Rev. Drug Discov.* **2010**, *9* (10), 804-820.

89. Bonaca, M. P.; Steg, P. G.; Feldman, L. J.; Canales, J. F.; Ferguson, J. J.; Wallentin, L.; Califf, R. M.; Harrington, R. A.; Giugliano, R. P. Antithrombotics in Acute Coronary Syndromes. *Journal of the American College of Cardiology* **2009**, *54* (11), 969-984.

90. Coller, B. S. αIIbβ3: structure and function. *J. Thromb. Haemost.* **2015**, *13* (Suppl 1), S17-25.

91.   Ndrepepa, G.; Kastrati, A.; Mehilli, J.; Neumann, F. J.; ten Berg, J.; Bruskina, O.; Dotzer, F.; Seyfarth, M.; Pache, J.; Dirschinger, J.; Berger, P. B.; Schömig, A. One-year clinical outcomes with abciximab vs. placebo in patients with non-ST-segment elevation acute coronary syndromes undergoing percutaneous coronary intervention after pre-treatment with clopidogrel: results of the ISAR-REACT 2 randomized trial. *Eur. Heart J.* **2008**, *29* (4), 455-461.

92.   Usta, C.; Turgut, N. T.; Bedel, A. How abciximab might be clinically useful. *Int. J. Cardiol.* **2016**, *222*, 1074-1078.

93.   Bhatt, D. L.; Lee, B. I.; Casterella, P. J.; Pulsipher, M.; Rogers, M.; Cohen, M.; Corrigan, V. E.; Ryan, T. J.; Breall, J. A.; Moses, J. W.; Eaton, G. M.; Sklar, M. A.; Lincoff, A. M. Safety of concomitant therapy with eptifibatide and enoxaparin in patients undergoing percutaneous coronary intervention: results of the Coronary Revascularization Using Integrilin and Single bolus Enoxaparin Study. *J. Am. Coll. Cardiol.* **2003**, *41* (1), 20-25.

94.   Sherwood, M. W.; Tcheng, J. E. Eptifibatide in coronary intervention: past time for the next chapter. *Circ. Cardiovasc. Interv.* **2015**, *8* (2), e002340.

95.   Egbertson, M. S.; Chang, C. T.; Duggan, M. E.; Gould, R. J.; Halczenko, W.; Hartman, G. D.; Laswell, W. L.; Lynch, J. J.; Lynch, R. J.; Manno, P. D., Non-peptide fibrinogen receptor antagonists. 2. Optimization of a tyrosine template as a mimic for Arg-Gly-Asp. *J. Med. Chem.* **1994**, *37* (16), 2537-2551.

96.   Lang, S. H.; Manning, N.; Armstrong, N.; Misso, K.; Allen, A.; Di Nisio, M.; Kleijnen, J. Treatment with tirofiban for acute coronary syndrome (ACS): a systematic review and network analysis. *Curr. Med. Res. Opin.* **2012**, *28* (3), 351-370.

97.   King, S.; Short, M.; Harmon, C. Glycoprotein IIb/IIIa inhibitors: The resurgence of tirofiban. *Vascul. Pharmacol.* **2016**, *78*, 10-16.

98.   Cox, D. Oral GPIIb/IIIa antagonists: what went wrong? *Curr. Pharm. Des.* **2004**, *10* (14), 1587-1596.

99.   Chew, D. P.; Bhatt, D. L.; Topol, E. J. Oral glycoprotein IIb/IIIa inhibitors: why don't they work? *Am. J. Cardiovasc. Drugs* **2001**, *1* (6), 421-428.

100.   Coller, B. S. Translating from the rivers of Babylon to the coronary bloodstream. *J. Clin. Invest.* **2012**, *122* (11), 4293-4299.

101.   Ley, K.; Rivera-Nieves, J.; Sandborn, W. J.; Shattil, S. Integrin-based therapeutics: biological basis, clinical use and new drugs. *Nat. Rev. Drug Discov.* **2016**, *15* (3), 173-183.

102.   Hersey, P.; Sosman, J.; O'Day, S.; Richards, J.; Bedikian, A.; Gonzalez, R.; Sharfman, W.; Weber, R.; Logan, T.; Buzoianu, M.; Hammershaimb, L.; Kirkwood, J. M.; Group, E. M. S. A randomized phase 2 study of etaracizumab, a monoclonal antibody against integrin alpha(v)beta(3), + or - dacarbazine in patients with stage IV metastatic melanoma. *Cancer* **2010**, *116* (6), 1526-1534.

103.   Delbaldo, C.; Raymond, E.; Vera, K.; Hammershaimb, L.; Kaucic, K.; Lozahic, S.; Marty, M.; Faivre, S. Phase I and pharmacokinetic study of etaracizumab (Abegrin), a humanized monoclonal antibody against alphavbeta3 integrin receptor, in patients with advanced solid tumors. *Invest. New Drugs* **2008**, *26* (1), 35-43.

104.   Pickarski, M.; Gleason, A.; Bednar, B.; Duong, L. T. Orally active αvβ3 integrin inhibitor MK-0429 reduces melanoma metastasis. *Oncol. Rep.* **2015**, *33* (6), 2737-2745.

105.   Murphy, M. G.; Cerchio, K.; Stoch, S. A.; Gottesdiener, K.; Wu, M.; Recker, R.; Group, L.-S. Effect of L-000845704, an alphaVbeta3 integrin antagonist, on markers of bone turnover and bone mineral density in postmenopausal osteoporotic women. *J. Clin. Endocrinol. Metab.* **2005**, *90* (4), 2022-2028.

106.   Rosenthal, M. A.; Davidson, P.; Rolland, F.; Campone, M.; Xue, L.; Han, T. H.; Mehta, A.; Berd, Y.; He, W.; Lombardi, A. Evaluation of the safety, pharmacokinetics and treatment effects of an alpha(nu)beta(3) integrin inhibitor on bone turnover and disease activity in men with hormone-refractory prostate cancer and bone metastases. *Asia Pac. J. Clin. Oncol.* **2010**, *6* (1), 42-48.

107.   Mas-Moruno, C.; Rechenmacher, F.; Kessler, H. Cilengitide: the first anti-angiogenic small molecule drug candidate design, synthesis and clinical evaluation. *Anticancer Agents Med. Chem.* **2010**, *10* (10), 753-768.

108.   Gerstner, E. R.; Ye, X.; Duda, D. G.; Levine, M. A.; Mikkelsen, T.; Kaley, T. J.; Olson, J. J.; Nabors, B. L.; Ahluwalia, M. S.; Wen, P. Y.; Jain, R. K.; Batchelor, T. T.; Grossman, S. A phase I study of cediranib in combination with cilengitide in patients with recurrent glioblastoma. *Neuro. Oncol.* **2015**, *17* (10), 1386-1392.

109.   Weller, M.; Nabors, L. B.; Gorlia, T.; Leske, H.; Rushing, E.; Bady, P.; Hicking, C.; Perry, J.; Hong, Y. K.; Roth, P.; Wick, W.; Goodman, S. L.; Hegi, M. E.; Picard, M.; Moch, H.; Straub, J.; Stupp, R. Cilengitide in newly diagnosed glioblastoma: biomarker expression and outcome. *Oncotarget* **2016**, *7* (12), 15018-15032.

110.   Zahn, G.; Volk, K.; Lewis, G. P.; Vossmeyer, D.; Stragies, R.; Heier, J. S.; Daniel, P. E.; Adamis, A. P.; Chapin, E. A.; Fisher, S. K.; Holz, F. G.; Löffler, K. U.; Knolle, J. Assessment of the integrin alpha5beta1 antagonist JSM6427 in

proliferative vitreoretinopathy using in vitro assays and a rabbit model of retinal detachment. *Invest. Ophthalmol. Vis. Sci.* **2010**, *51* (2), 1028-1035.

111. Bell-McGuinn, K. M.; Matthews, C. M.; Ho, S. N.; Barve, M.; Gilbert, L.; Penson, R. T.; Lengyel, E.; Palaparthy, R.; Gilder, K.; Vassos, A.; McAuliffe, W.; Weymer, S.; Barton, J.; Schilder, R. J. A phase II, single-arm study of the anti-α5β1 integrin antibody volociximab as monotherapy in patients with platinum-resistant advanced epithelial ovarian or primary peritoneal cancer. *Gynecol. Oncol.* **2011**, *121* (2), 273-279.

112. Almokadem, S.; Belani, C. P. Volociximab in cancer. *Expert Opin. Biol. Ther.* **2012**, *12* (2), 251-257.

113. Xiong, J. P.; Stehle, T.; Zhang, R.; Joachimiak, A.; Frech, M.; Goodman, S. L.; Arnaout, M. A. Crystal structure of the extracellular segment of integrin alpha Vbeta3 in complex with an Arg-Gly-Asp ligand. *Science* **2002**, *296* (5565), 151-155.

114. Du, X. P.; Plow, E. F.; Frelinger, A. L.; O'Toole, T. E.; Loftus, J. C.; Ginsberg, M. H. Ligands "activate" integrin alpha IIb beta 3 (platelet GPIIb-IIIa). *Cell* **1991**, *65* (3), 409-416.

115. Bassler, N.; Loeffler, C.; Mangin, P.; Yuan, Y.; Schwarz, M.; Hagemeyer, C. E.; Eisenhardt, S. U.; Ahrens, I.; Bode, C.; Jackson, S. P.; Peter, K. A mechanistic model for paradoxical platelet activation by ligand-mimetic alphaIIb beta3 (GPIIb/IIIa) antagonists. *Arterioscler Thromb. Vasc. Biol.* **2007**, *27* (3), e9-15.

116. Hantgan, R. R.; Stahle, M. C. Integrin priming dynamics: mechanisms of integrin antagonist-promoted alphaIIbbeta3:PAC-1 molecular recognition. *Biochemistry* **2009**, *48* (35), 8355-8365.

117.   Reynolds, A. R.; Hart, I. R.; Watson, A. R.; Welti, J. C.; Silva, R. G.; Robinson, S. D.; Da Violante, G.; Gourlaouen, M.; Salih, M.; Jones, M. C.; Jones, D. T.; Saunders, G.; Kostourou, V.; Perron-Sierra, F.; Norman, J. C.; Tucker, G. C.; Hodivala-Dilke, K. M. Stimulation of tumor growth and angiogenesis by low concentrations of RGD-mimetic integrin inhibitors. *Nat. Med.* **2009**, *15* (4), 392-400.

118.   Weller, M.; Reardon, D.; Nabors, B.; Stupp, R., Will integrin inhibitors have proangiogenic effects in the clinic? *Nat. Med.* **2009**, *15* (7), 726; author reply 727.

119.   Baba, K.; Aga, Y.; Nakanishi, T.; Motoyama, T.; Ueno, H. UR-3216: a manageable oral GPIIb/IIIa antagonist. *Cardiovasc. Drug Rev.* **2001**, *19* (1), 25-40.

120.   Aga, Y.; Baba, K.; Tam, S.; Nakanishi, T.; Yoneda, K.; Kita, J.; Ueno, H., UR-3216: a new generation oral platelet GPIIb/IIIa antagonist. *Curr. Pharm. Des.* **2004**, *10* (14), 1597-1601.

121.   Blue, R.; Murcia, M.; Karan, C.; Jirousková, M.; Coller, B. S. Application of high-throughput screening to identify a novel alphaIIb-specific small- molecule inhibitor of alphaIIbbeta3-mediated platelet interaction with fibrinogen. *Blood* **2008**, *111* (3), 1248-1256.

122.   Blue, R.; Kowalska, M. A.; Hirsch, J.; Murcia, M.; Janczak, C. A.; Harrington, A.; Jirouskova, M.; Li, J.; Fuentes, R.; Thornton, M. A.; Filizola, M.; Poncz, M.; Coller, B. S. Structural and therapeutic insights from the species specificity and in vivo antithrombotic activity of a novel alphaIIb-specific alphaIIbbeta3 antagonist. *Blood* **2009**, *114* (1), 195-201.

123.   Zhu, J.; Negri, A.; Provasi, D.; Filizola, M.; Coller, B. S.; Springer, T. A. Closed headpiece of integrin αIIbβ3 and its complex with an αIIbβ3-specific antagonist that does not induce opening. *Blood* **2010**, *116* (23), 5050-5059.

124.   Zhu, J.; Choi, W. S.; McCoy, J. G.; Negri, A.; Naini, S.; Li, J.; Shen, M.; Huang, W.; Bougie, D.; Rasmussen, M.; Aster, R.; Thomas, C. J.; Filizola, M.; Springer, T. A.; Coller, B. S. Structure-guided design of a high-affinity platelet integrin αIIbβ3 receptor antagonist that disrupts Mg^{2+} binding to the MIDAS. *Sci. Transl. Med.* **2012**, *4* (125), 125ra32.

125.   Jiang, J. K.; McCoy, J. G.; Shen, M.; LeClair, C. A.; Huang, W.; Negri, A.; Li, J.; Blue, R.; Harrington, A. W.; Naini, S.; David, G.; Choi, W. S.; Volpi, E.; Fernandez, J.; Babayeva, M.; Nedelman, M. A.; Filizola, M.; Coller, B. S.; Thomas, C. J. A novel class of ion displacement ligands as antagonists of the αIIbβ3 receptor that limit conformational reorganization of the receptor. *Bioorg. Med. Chem. Lett.* **2014**, *24* (4), 1148-1153.

126.   Coller, B. S.; Thomas, C.; Filizola, M.; Mccoy; J.; Huang, W.; Shen, M.; K., J. J. 7-(Piperazin-1-yl)-5H-[1,3,4]thiadiazolo[3,2-A]pyrimidin-5-ones for the Treatment of Thrombotic Disorders. US 9303044 B2, 2016.

127.   Li, J.; Vootukuri, S.; Shang, Y.; Negri, A.; Jiang, J. K.; Nedelman, M.; Diacovo, T. G.; Filizola, M.; Thomas, C. J.; Coller, B. S. RUC-4: a novel αIIbβ3 antagonist for prehospital therapy of myocardial infarction. *Arterioscler Thromb. Vasc. Biol.* **2014**, *34* (10), 2321-2329.

128.   Negri, A.; Li, J.; Naini, S.; Coller, B. S.; Filizola, M. Structure-based virtual screening of small-molecule antagonists of platelet integrin αIIbβ3 that do not prime the receptor to bind ligand. *J. Comput. Aided Mol. Des.* **2012**, *26* (9), 1005-1015.

129.   Irwin, J. J.; Shoichet, B. K. ZINC--a free database of commercially available compounds for virtual screening. *J. Chem. Inf. Model.* **2005**, *45* (1), 177-182.

130.   Wang, Y.; Zhao, Y.; Sun, R.; Kong, W.; Wang, B.; Yang, G.; Li, Y. Discovery of novel antagonists of glycoprotein IIb/IIIa-mediated platelet aggregation through virtual screening. *Bioorg. Med. Chem. Lett.* **2015**, *25* (6), 1249-1253.

131.   Polishchuk, P. G.; Samoylenko, G. V.; Khristova, T. M.; Krysko, O. L.; Kabanova, T. A.; Kabanov, V. M.; Kornylov, A. Y.; Klimchuk, O.; Langer, T.; Andronati, S. A.; Kuz'min, V. E.; Krysko, A. A.; Varnek, A. Design, Virtual Screening, and Synthesis of Antagonists of αIIbβ3 as Antiplatelet Agents. *J. Med. Chem.* **2015**, *58* (19), 7681-7694.

132.   Krysko, A. A.; Kornylov, A. Y.; Polishchuk, P. G.; Samoylenko, G. V.; Krysko, O. L.; Kabanova, T. A.; Kravtsov, V. C. h.; Kabanov, V. M.; Wicher, B.; Andronati, S. A. Synthesis, biological evaluation and molecular docking studies of 2-piperazin-1-yl-quinazolines as platelet aggregation inhibitors and ligands of integrin αIIbβ3. *Bioorg. Med. Chem. Lett.* **2016**, *26* (7), 1839-1843.

133.   Dayam, R.; Aiello, F.; Deng, J.; Wu, Y.; Garofalo, A.; Chen, X.; Neamati, N. Discovery of small molecule integrin alphavbeta3 antagonists as novel anticancer agents. *J. Med. Chem.* **2006**, *49* (15), 4526-4534.

134.   Baell, J. B.; Holloway, G. A. New substructure filters for removal of pan assay interference compounds (PAINS) from screening libraries and for their exclusion in bioassays. *J. Med. Chem.* **2010**, *53* (7), 2719-2740.

135.   Zhou, Y.; Peng, H.; Ji, Q.; Qi, J.; Zhu, Z.; Yang, C. Discovery of small molecule inhibitors of integrin alphavbeta3 through structure-based virtual screening. *Bioorg. Med. Chem. Lett.* **2006**, *16* (22), 5878-5882.

136.   Elliot, D.; Henshaw, E.; MacFaul, P. A.; Morley, A. D.; Newham, P.; Oldham, K.; Page, K.; Rankine, N.; Sharpe, P.; Ting, A.; Wood, C. M. Novel

inhibitors of the alphavbeta3 integrin--lead identification strategy. *Bioorg. Med. Chem. Lett.* **2009**, *19* (16), 4832-4835.

137.   Arnould; C., J.; Delouvrie, B.; Kettle, J. G. Chemical Compounds. WO091046 A1, 2007.

138.   Kim, M.; Kang, I. Anti-angiogenic Mechanism of IPS-05002, a Novel Antagonist Against Integrin a5β1, Determined by ProteoChip-based Antibody Array. *BioChip J.* **2016,** *10*, 174-181.

139.   Adams, J.; Anderson, E. C.; Blackham, E. E.; Chiu, Y. W.; Clarke, T.; Eccles, N.; Gill, L. A.; Haye, J. J.; Haywood, H. T.; Hoenig, C. R.; Kausas, M.; Le, J.; Russell, H. L.; Smedley, C.; Tipping, W. J.; Tongue, T.; Wood, C. C.; Yeung, J.; Rowedder, J. E.; Fray, M. J.; McInally, T.; Macdonald, S. J. Structure Activity Relationships of αv Integrin Antagonists for Pulmonary Fibrosis by Variation in Aryl Substituents. *ACS Med. Chem. Lett.* **2014**, *5* (11), 1207-1212.

140.   Discovery Informatics Suite 2016-3, Schrödinger, LLC, New York, NY, 2016.

141.   Groom, C. R.; Bruno, I. J.; Lightfoot, M. P.; Ward, S. C., The Cambridge Structural Database. *Acta Crystallogr. B. Struct. Sci. Cryst. Eng. Mater.* **2016**, *72* (Pt 2), 171-179.

142.   Bruno, I. J.; Cole, J. C.; Kessler, M.; Luo, J.; Motherwell, W. D.; Purkis, L. H.; Smith, B. R.; Taylor, R.; Cooper, R. I.; Harris, S. E.; Orpen, A. G. Retrieval of crystallographically-derived molecular geometry information. *J. Chem. Inf. Comput. Sci.* **2004**, *44* (6), 2133-2144.

143.   Spotfire Platform, 2016 TIBCO Software Inc.

144.   Burgey, C. S.; Deng, Z. J.; Nguyen, D. N.; Paone, D. V.; Potteiger, C. M.; Stauffer, S. R.; Segerdell, C.; Nomland, A.; Lim, J. J. P2x3, receptor antagonists for treatment of pain. WO2010111058 A1, 2010.